STRINGQFT

String-Theoretic Construction
of Quantum Field Theory

VOLUME III

Brane Preliminaries

Xingyang Yu

StringQFT v1.0 / Source build candidate

Drafted with AI assistance under the supervision of the author.
Manuscript free to read. All rights reserved.

Contents

III.1 Boundary conditions and Chan–Paton factors **1**

III.1.1 An endpoint turns a string into a brane probe 1
III.1.2 Neumann and Dirichlet data 2
III.1.3 Light states on one brane 5
III.1.4 Chan–Paton endpoints 7
III.1.5 Coincidence and enhancement 9
III.1.6 From flat branes to a projection 11
III.1.7 Exercises 13
III.1.8 Take-home message 14
Status and sources 15

III.2 The boundary-state formalism **17**

III.2.1 A boundary viewed from the other channel 17
III.2.2 Boundary conditions as a closed-channel state 17
III.2.3 Zero modes and localization 20
III.2.4 The cylinder in two channels 22
III.2.5 NSNS and RR sectors 24
III.2.6 Orbifold boundary states 27
III.2.7 Exercises 29
Status and sources 30

III.3 D-brane effective actions: DBI and Chern–Simons/WZ couplings **32**

III.3.1 One brane, two responses 32
III.3.2 Pullback geometry and the gauge-invariant field 33
III.3.3 DBI at quadratic order 35
III.3.4 The trace normalization 36
III.3.5 WZ couplings and lower charge 38
III.3.6 Wrapped and interval reductions 40
III.3.7 Exercises 43
Status and sources 44

III.4 Multiple branes: non-abelian worldvolume structure **46**

III.4.1 From endpoints to a matrix field 46
III.4.2 Ordered endpoints and the gauge algebra 47

III.4.3 Reducing the leading ten-dimensional action . . . 49
III.4.4 Positive energy and classical positions . . . 52
III.4.5 Separation and the massive spatial vector . . . 54
III.4.6 A dielectric D0 example and its boundary . . . 58
III.4.7 Exercises . . . 61
Status and sources . . . 62

III.5 Branes within branes: dissolved charges, instanton numbers, K-theory (light) 64
III.5.1 A smooth field can carry a lower charge . . . 64
III.5.2 Charge from the WZ exponential . . . 65
III.5.3 Instanton number as dissolved branes . . . 67
III.5.4 Bundles and charge bookkeeping . . . 69
III.5.5 Nonspin cycles and half flux . . . 71
III.5.6 Page, source and Maxwell charges . . . 74
III.5.7 Exercises . . . 76
Status and sources . . . 77

III.6 Branes at angles and magnetized branes: chiral spectra at intersections 79
III.6.1 A string joining two directions . . . 79
III.6.2 Intersecting boundary conditions . . . 80
III.6.3 Fractional moding and light states . . . 82
III.6.4 Chirality from oriented intersections . . . 85
III.6.5 Magnetic dual description . . . 89
III.6.6 Supersymmetric angle choices . . . 92
III.6.7 Exercises . . . 95
III.6.8 Take-home message . . . 96
Status and sources . . . 96

III.7 Branes ending on branes: boundary conditions and BIons 99
III.7.1 What an endpoint asks of a field . . . 99
III.7.2 Boundary variation of a gauge theory . . . 100
III.7.3 Electric spikes . . . 102
III.7.4 Flux measures string charge . . . 105
III.7.5 Nonabelian endpoint data . . . 108
III.7.6 Interval zero modes . . . 111
III.7.7 Exercises . . . 114
Status and sources . . . 116

III.8 T-duality on D-branes: the brane dictionary 118
III.8.1 An endpoint loses a direction . . . 118
III.8.2 Boundary conditions and oscillators . . . 119
III.8.3 Wilson lines become positions . . . 122
III.8.4 Wrapped brane energies and gauge couplings . . . 125
III.8.5 Two dualities and a tiling . . . 128

III.8.6 Circle fibrations and localization . . . 131
III.8.7 Exercises . . . 136
III.8.8 Take-home message . . . 138
Status and sources . . . 138

III.9 Kappa symmetry and supersymmetric branes 141
III.9.1 A supersymmetric brane is a compatible object . . . 141
III.9.2 A local fermionic redundancy . . . 142
III.9.3 The real spinor space . . . 144
III.9.4 Compatible intersections . . . 146
III.9.5 The signed magnetic projector . . . 149
III.9.6 Local energy and dissolved charge . . . 151
III.9.7 The membrane action . . . 153
III.9.8 Tangent planes and calibration . . . 155
III.9.9 From local planes to global states . . . 158
III.9.10 Exercises . . . 160
III.9.11 Take-home message . . . 161
Status and sources . . . 161

III.10 NS5-brane worldvolume theories and little strings 164
III.10.1 The worldvolume question . . . 164
III.10.2 Fields on separated fivebranes . . . 165
III.10.3 Strings between fivebranes . . . 168
III.10.4 Keeping a finite string scale . . . 172
III.10.5 A circle along the fivebrane . . . 175
III.10.6 Beyond the local description . . . 178
III.10.7 Exercises . . . 179
III.10.8 Take-home message . . . 180

Chapter III.1

Boundary conditions and Chan–Paton factors

III.1.1 An endpoint turns a string into a brane probe

A closed string has no distinguished point at which it can be attached to a surface. An open string has two such points. If they may move along some spacetime directions but must remain at specified positions in the others, the surface they sweep out is a D-brane worldvolume. The same boundary data that locate the brane also decide which string vibrations can move on it. They will eventually give a vector field along the worldvolume and scalars that record motion normal to it.

There is a second piece of information at each end: which brane receives it. For a stack, the ordered pair of endpoint labels is a matrix index. A string from brane 1 to brane 2 is then a different state from one going from 2 to 1. When the branes meet, the states that had to span the gap become light and complete a larger matrix algebra. We will follow that chain through five concrete operations: solve the boundary problem, count the first physical oscillators, multiply endpoint matrices, compare stretched-string and quadratic field-theory masses, and impose one geometric projection.

The setting is a flat ten-dimensional type-II background with parallel, oriented Dp-branes of the same kind. Both endpoints have matching Neumann and Dirichlet directions. There is no background B field, flux, Wilson line, compact winding or mixed ND coordinate. Time is Neumann. For ordinary BPS branes, p is odd in type IIB and even in type IIA. The massless spectrum below uses the sourced GSO projection; solving a classical wave equation alone does not derive that projection.

After this chapter one should be able to solve an unequal fixed-endpoint coordinate, obtain the position-scalar normalization, count the eight first-level bosonic modes for D1, D3 and D9, construct an oriented $U(2)$ endpoint algebra, and calculate a local $\mathbb{Z}_2$ invariant matrix spectrum. Volume II, Chapter 1 supplied the free strip normalization, and Volume II, Chapter 4 supplies the RNS origin of the GSO premise. Chapter 2 will treat boundary states, while Chapters 3 and 4 will give brane effective actions and nonabelian field dynamics. The orbifold example points ahead to Volume VI, Chapter 2.

III.1.2 Neumann and Dirichlet data

Which boundary condition lets a string endpoint travel along a hypersurface while holding its normal coordinate fixed? In conformal gauge take $0 \le \sigma \le \pi$, $\eta_{ab} = \mathrm{diag}(-1,+1)$, and $T = 1/(2\pi\alpha')$. A dot and a prime mean ∂_τ and ∂_σ. For the free coordinate action,

$$S_X = \frac{1}{4\pi\alpha'}\int d\tau \int_0^\pi d\sigma\,(\dot X^\mu \dot X_\mu - X'^\mu X'_\mu), \qquad \eta_{\mu\nu} = \mathrm{diag}(-1,+1,\dots,+1). \tag{III.1.1}$$

Varying X and integrating by parts in both coordinates gives a bulk wave equation and a spatial boundary term. We fix the temporal end slices in the variation, so their terms vanish:

$$\delta S_X = -\frac{1}{2\pi\alpha'}\int d\tau \int_0^\pi d\sigma\,\delta X_\mu(\ddot X^\mu - X''^\mu) - \frac{1}{2\pi\alpha'}\int d\tau\,[\delta X_\mu X'^\mu]_{\sigma=0}^{\sigma=\pi}. \tag{III.1.2}$$

The first term sets $\ddot X - X'' = 0$. At either spatial end the second term can vanish in two different ways. A freely varied endpoint coordinate has $X' = 0$, called Neumann or NN when imposed at both ends. A fixed coordinate has $\delta X = 0$, called Dirichlet or DD at both ends. The choice applies to each target coordinate separately:

$$\partial_\sigma X^a\big|_{0,\pi} = 0 \quad (a = 0,\dots,p), \qquad X^I(\tau,0) = Y_0^I, \quad X^I(\tau,\pi) = Y_1^I \quad (I = p{+}1,\dots,9). \tag{III.1.3}$$

The $p+1$ tangent coordinates include time. The $9-p$ normal positions Y_0^I, Y_1^I specify the two branes on which the endpoints lie. Figure III.1.1 keeps their identities fixed while changing only the separation.

To see why these conditions produce different oscillator bases, solve one spatial eigenvalue problem before assembling the full wave. Put $X(\tau,\sigma) = q(\tau)f(\sigma)$ for a nonzero frequency n. The bulk equation separates into $\ddot q + n^2 q = 0$ and $f'' + n^2 f = 0$, with general spatial solution $A\cos(n\sigma) + B\sin(n\sigma)$. At $\sigma = 0$, NN requires $B = 0$ while DD fluctuations require $A = 0$. The second endpoint then quantizes n to a positive integer in either case:

$$f_{\mathrm{NN,n}}(\sigma) = \cos(n\sigma), \qquad f_{\mathrm{DD,n}}(\sigma) = \sin(n\sigma), \qquad n = 1,2,\dots. \tag{III.1.4}$$

The zero-frequency equation is different: $f'' = 0$ gives $A + B\sigma$. NN sets $B = 0$ and leaves a freely moving constant coordinate; fixed DD data determine both $A = Y_0$ and $B = (Y_1 - Y_0)/\pi$. This limiting calculation explains why the DD affine piece must be written separately from its positive-frequency sine series. It is not the $n \to 0$ value of $\sin(n\sigma)$ with an arbitrary free coefficient.

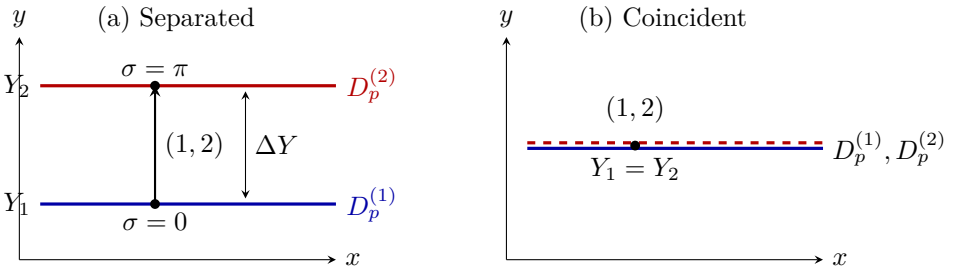


Figure III.1.1: Two parallel branes $D_p^{(1)}$ and $D_p^{(2)}$ with the same worldvolume x direction and normal y direction. Panel (a) has $\Delta Y = Y_2 - Y_1 \neq 0$; the oriented $(1,2)$ string runs from $\sigma = 0$ to $\sigma = \pi$. Panel (b) moves the same two branes to $Y_1 = Y_2$. Dashed overlap distinguishes their labels, even though the geometric gap vanishes. This drawing fixes endpoint order and geometry; the mass calculation follows below.

The bulk equation is linear, so solve it by separating the endpoint profile from the oscillations. A Neumann coordinate admits the constant spatial mode and the cosine harmonics. Their time-dependent coefficients yield

$$X^a(\tau,\sigma) = x^a + 2\alpha' p^a \tau + i\sqrt{2\alpha'} \sum_{n\neq 0} \frac{\alpha_n^a}{n} e^{-in\tau} \cos(n\sigma), \qquad \alpha_{-n}^a = (\alpha_n^a)^\dagger. \tag{III.1.5}$$

Indeed $\partial_\sigma \cos(n\sigma) = -n \sin(n\sigma)$ vanishes at $0, \pi$, whereas the spatial constant is the only zero-frequency Neumann solution with unconstrained temporal drift. Its normalization is fixed by the conserved tangent momentum. With $\Pi^a = \dot{X}^a/(2\pi\alpha')$, orthogonality of the cosine modes gives

$$P^a = \int_0^\pi d\sigma\, \Pi^a = \frac{1}{2\pi\alpha'} \int_0^\pi d\sigma\, (2\alpha' p^a) = p^a. \tag{III.1.6}$$

Thus the coefficient $2\alpha' p^a$ is a physical normalization, not a choice that can be halved when the interval is $[0, \pi]$.

For a normal DD coordinate, the spatial zero-frequency solution is instead an affine segment. A convenient real sine expansion writes

$$X^I(\tau,\sigma) = Y_0^I + \frac{Y_1^I - Y_0^I}{\pi}\sigma + \sum_{n=1}^{\infty} q_n^I(\tau) \sin(n\sigma), \qquad \ddot{q}_n^I + n^2 q_n^I = 0. \tag{III.1.7}$$

The sine terms vanish at both ends. The affine piece satisfies $X'' = 0$ and fixes both positions. A term $c^I \tau$ would change the endpoint positions and is therefore forbidden by the fixed DD data. In particular, there is no independent normal momentum zero mode. Integrated normal oscillator momentum can still be nonzero at an instant: fixed endpoints exert a force and break normal translation invariance. The affine slope on a noncompact normal line is a physical stretch, not winding around a circle.

Take the explicit one-coordinate data $\alpha' = 2$, $Y_0 = -\pi$ and $Y_1 = 4\pi$. The unique zero-frequency normal profile is

$$X_{\rm cl}(\sigma) = -\pi + \frac{4\pi - (-\pi)}{\pi}\sigma = -\pi + 5\sigma, \quad X_{\rm cl}(0) = -\pi, \quad X_{\rm cl}(\pi) = 4\pi. \tag{III.1.8}$$

Its derivative is five and its physical length is 5π. The classical string tension therefore contributes the rest energy

$$E_{\text{stretch}} = T|Y_1 - Y_0| = \frac{|Y_1 - Y_0|}{2\pi\alpha'} = \frac{5\pi}{4\pi} = \frac{5}{4}. \tag{III.1.9}$$

Squaring gives 25/16 for the corresponding classical contribution to M^2. The worldsheet constraint gives the same coefficient: the affine piece enters the spatial integral as

$$\frac{1}{4\pi\alpha'}\int_0^\pi d\sigma\,(X'_{\text{cl}})^2 = \frac{|Y_1 - Y_0|^2}{4\pi^2\alpha'}, \qquad \Delta M^2 = \frac{|Y_1 - Y_0|^2}{(2\pi\alpha')^2}. \tag{III.1.10}$$

The first quantity is the L_0 contribution in these strip conventions; its conversion to M^2 divides by α'. This result describes parallel matching NN/DD ends. A coordinate with one N and one D end has different oscillators and belongs to another chapter. The distinction between NN drift and DD stretch will also matter when the separation is read as a scalar expectation value.

For more than one normal coordinate, the classical profile is a straight segment in the normal Euclidean space. If two endpoints differ by $\Delta Y^{p+1} = 3\ell$ and $\Delta Y^{p+2} = 4\ell$, with all other normal differences zero, the string length is 5ℓ, not 7ℓ. Both normal slopes enter the constraint quadratically:

$$|\Delta Y|^2 = (3\ell)^2 + (4\ell)^2 = 25\ell^2, \qquad \Delta M^2 = \frac{25\ell^2}{(2\pi\alpha')^2}. \tag{III.1.11}$$

This geometric check is useful later when several scalar expectation values differ. A vector of displacements produces one stretch mass through its norm. It does not create a separate additive mass for each coordinate before squaring.

The boundary conditions also control how worldsheet energy and target momentum cross an endpoint. In the free theory the momentum density and its normal flux obey a local continuity equation,

$$\Pi^\tau_\mu = \frac{\dot{X}_\mu}{2\pi\alpha'}, \qquad \Pi^\sigma_\mu = -\frac{X'_\mu}{2\pi\alpha'}, \qquad \partial_\tau\Pi^\tau_\mu + \partial_\sigma\Pi^\sigma_\mu = 0. \tag{III.1.12}$$

Integrating the last equation shows exactly why tangent momentum is conserved: the NN endpoint condition sets both tangent fluxes to zero. In a DD direction the slope can exert a force on each fixed endpoint, so the string alone need not conserve its integrated normal momentum,

$$\frac{d}{d\tau}\int_0^\pi d\sigma\,\Pi^\tau_I = -\left[\Pi^\sigma_I\right]_0^\pi = \frac{X'_I(\pi) - X'_I(0)}{2\pi\alpha'}. \tag{III.1.13}$$

For the static affine profile both endpoint slopes coincide, making the net force on the string zero, while the individual endpoint forces are opposite and nonzero. An oscillator can make the two slopes unequal and transfer normal momentum to the branes. This is why absence of a DD *zero-mode charge* is stronger than the false statement that every normal momentum integral must vanish instantaneously.

One can also check the energy result directly without naming a mode operator. The static Hamiltonian density is $T(X')^2/2$ in conformal gauge, but a static stretched string satisfying the constraints also has a target-time contribution. With static gauge $X^0 = \ell\tau/\pi$ and $X^I = \Delta Y^I \sigma/\pi$, the Virasoro constraint fixes $\ell = |\Delta Y|$. Integrating the target-time momentum then yields

$$E = \frac{1}{2\pi\alpha'}\int_0^\pi d\sigma\, \dot{X}^0 = \frac{|\Delta Y|}{2\pi\alpha'} = T|\Delta Y|. \tag{III.1.14}$$

Thus the tension argument and the constrained strip solution agree. The chosen target-time gauge is a check on the static classical string, not a new condition imposed on the quantum oscillators.

III.1.3 Light states on one brane

Which of these open-string vibrations becomes a field living on the brane? In the critical type-II NS sector the zero-point energy is $E_{\rm NS} = -\frac{1}{2}$. We use a positive intercept $a_{\rm NS} = -E_{\rm NS} = +\frac{1}{2}$ in a *subtractive* mass formula. For equal endpoints, the sourced GSO projection removes the NS vacuum and retains the first state made by one $\psi_{-1/2}$ oscillator:

$$\alpha' M^2 = N_{\rm NS} - a_{\rm NS}, \qquad N_{\rm NS}(\psi^\mu_{-1/2}|0;k\rangle) = \frac{1}{2}, \qquad M^2 = 0. \tag{III.1.15}$$

The eight transverse bosonic polarizations at this level are a physical spectrum premise of the type-II theory. The finite calculation here is the way those eight modes split under the brane's tangent and normal rotations. It does not supply a derivation of the GSO projection or the consistency of the complete open/closed theory. The bosonic-string intercept $a = 1$ of Volume II, Chapter 1 cannot be substituted into this NS formula.

For $p \geq 1$ choose a nonzero null momentum tangent to the brane. Transversality and the gauge equivalence of a massless vector remove the longitudinal and temporal components of A_a. The tangent vector has $(p+1) - 2 = p - 1$ local propagating polarizations. Every normal coordinate provides one scalar polarization. Consequently

$$\underbrace{8}_{SO(8)\ \text{transverse}} = \underbrace{(p-1)}_{A_a\ \text{local modes}} + \underbrace{(9-p)}_{\Phi^I\ \text{normal modes}}, \qquad 1 \leq p \leq 9, \qquad k_a k^a = 0, \qquad k_a \neq 0. \tag{III.1.16}$$

The hypothesis of nonzero null worldvolume momentum is essential to this light-cone count. It applies to the massless self-endpoint or coincident sector. The separated off-diagonal vector in Section III.1.5 is massive and obtains a longitudinal mode from a scalar; applying $p - 1$ to it would count the wrong representation.

The two subtractions in $p + 1 - 2$ have different origins. Choose a null worldvolume momentum with $k^a = (\omega, \omega, 0, \ldots, 0)$ in a local Lorentz frame. The massless vector polarization obeys $k_a \epsilon^a = 0$; the gauge shift $\epsilon^a \sim \epsilon^a + c k^a$ removes its remaining component in the lightlike plane. Only $\epsilon^2, \ldots, \epsilon^p$ remain, giving $p - 1$ independent

directions:

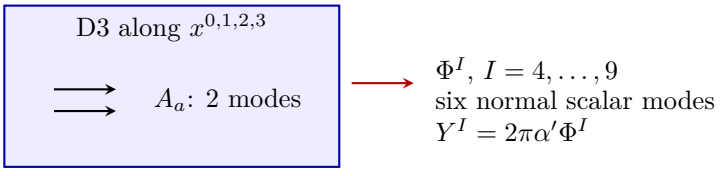
$$\epsilon^a \in \mathbb{C}^{p+1}, \qquad k \cdot \epsilon = 0, \qquad \epsilon \sim \epsilon + ck \quad \Longrightarrow \quad \dim_{\mathbb{C}} \mathcal{P}_A = (p+1) - 1 - 1 = p - 1. \tag{III.1.17}$$

For $p = 1$ there are no indices between 2 and p. This is the concrete reason a D1 connection can influence charges and holonomies while carrying no local photon wave. It is not a declaration that the connection itself vanishes.

The D3 example makes the geometry visible. A D3 spans $x^{0,1,2,3}$ and has six real normal coordinates $x^4, \ldots, x^9$. Its gauge field has two local polarizations and its six scalars have one each:

$$p = 3 : \qquad (p - 1, 9 - p) = (2, 6), \qquad 2 + 6 = 8. \tag{III.1.18}$$

Figure III.1.2 labels those directions. Its arrows only record the field split, not an additional dynamical equation.



Schematic mode count at nonzero null brane momentum

Figure III.1.2: The D3 tangent and normal split for the first GSO-surviving NS level at nonzero null worldvolume momentum. The two arrows on the sheet count local vector polarizations, while $I = 4, \ldots, 9$ lists six scalar polarizations. The normal arrow represents the position-scalar dictionary; it is schematic mode bookkeeping rather than a proof of interactions.

The edge cases sharpen the meaning of "local." A D1 has a gauge connection A_a but no propagating photon in two-dimensional Maxwell theory; its eight physical bosonic modes are transverse scalars. A D9 has no normal coordinate and eight vector polarizations. In the theories in which these ordinary branes occur, the same arithmetic reads

$$p = 1 : \ (0, 8), \qquad p = 3 : \ (2, 6), \qquad p = 9 : \ (8, 0), \qquad N_A + N_\Phi = 8 \text{ in each case.} \tag{III.1.19}$$

This is a kinematic count. D0 and D(-1) require different treatment of a worldvolume null momentum and are not covered by this equation. The oriented D9 vector statement by itself also does not construct a globally consistent space-filling ten-dimensional vacuum.

A constant transverse scalar has a direct geometric measurement: it moves the brane. The normalization is fixed by the physical separation of endpoint positions, equivalently by the T-dual Wilson-line dictionary. If Y^I is a position with units of length, then

$$Y^I = 2\pi\alpha' \Phi^I, \qquad [\alpha'] = L^2, \quad [Y^I] = L, \quad [\Phi^I] = L^{-1}. \tag{III.1.20}$$

Fix a reference length ℓ_0, hence an inverse-length unit ℓ_0^{-1}. A D3 at $Y^4 = 3\pi\alpha'/\ell_0$ has $\Phi^4 = 3/(2\ell_0)$; moving it to $5\pi\alpha'/\ell_0$ shifts Φ^4 by $1/\ell_0$. It is the *difference* of such diagonal values that a stretched string measures. This is the field content from which Chapter 4 will build a leading Yang–Mills worldvolume action; this chapter fixes neither that action's complete nonlinear extension nor a numerical Yang–Mills coupling.

The position map can be tested against a directly measurable gap. Move one D3 from $3\pi\alpha'/\ell_0$ to $5\pi\alpha'/\ell_0$ while leaving another at the first position. The gap is $2\pi\alpha'/\ell_0$, so the scalar difference and first-level mass are $1/\ell_0$ at tension $T = 1/(2\pi\alpha')$:

$$|\Delta\Phi^4| = \frac{2\pi\alpha'/\ell_0}{2\pi\alpha'} = \frac{1}{\ell_0}, \qquad T|\Delta Y^4| = \frac{1}{\ell_0} = M. \tag{III.1.21}$$

This agreement tests a normalization with units, not a choice of symbol. It also explains why the scalar expectation value is naturally measured in inverse length even though the brane displacement is measured in length. Multiple normal scalar differences combine by their Euclidean norm in the free flat background.

III.1.4 Chan–Paton endpoints

How can one oscillator carry several distinct brane fields? Label the two ends of an *oriented* open string by i at $\sigma = 0$ and j at $\sigma = \pi$. If there are N available same-kind branes, its state has an oscillator factor and an ordered matrix factor:

$$|\mathrm{osc}; i, j\rangle = |\mathrm{osc}\rangle \otimes E_{ij}, \qquad E_{ij} = |i\rangle\langle j| \in \mathrm{End}(\mathbb{C}^N). \tag{III.1.22}$$

The first index is the row, the second the column. This convention also fixes the later quiver arrow: the component E_{ij} is drawn from i to j. An endpoint label is not an extra target-space direction; it specifies which open-string sector is being quantized.

The algebra records joining. Compose a string $i \to j$ with a string $k \to l$. The intermediate end must match, since

$$E_{ij}E_{kl} = |i\rangle\langle j|k\rangle\langle l| = \delta_{jk}E_{il}. \tag{III.1.23}$$

For a cyclically ordered disc boundary, the CP factors multiply in that order and the boundary closes with a trace:

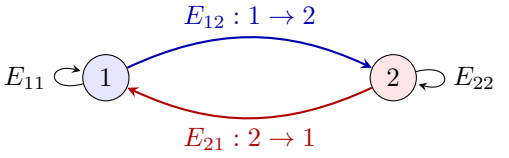
$$\mathrm{Tr}(E_{i_1j_1}E_{i_2j_2}\cdots E_{i_rj_r}) = \delta_{j_1i_2}\delta_{j_2i_3}\cdots\delta_{j_ri_1}. \tag{III.1.24}$$

This trace is a sourced rule for oriented disc interactions, beyond the bare fact that vector spaces carry matrices. It is compatible with cyclicity: the starting point around the boundary is arbitrary. It does not determine every interaction coefficient or the global form of a gauge group.

A two-brane example displays every orientation. The four matrix units are

$$E_{11} = \begin{pmatrix} 1 & 0 \\ 0 & 0 \end{pmatrix}, \quad E_{12} = \begin{pmatrix} 0 & 1 \\ 0 & 0 \end{pmatrix}, \quad E_{21} = \begin{pmatrix} 0 & 0 \\ 1 & 0 \end{pmatrix}, \quad E_{22} = \begin{pmatrix} 0 & 0 \\ 0 & 1 \end{pmatrix}. \tag{III.1.25}$$

For example $E_{12}E_{21} = E_{11}$ and its trace is one, while $E_{12}E_{11} = 0$. Also $E_{12}E_{21}E_{11} = E_{11}$, so a three-factor closed chain has trace one. Figure III.1.3 displays the same four sectors and their joining condition.



$$E_{ij}E_{kl} = \delta_{jk}E_{il}$$
$$\mathrm{Tr}(E_{12}E_{21}) = 1$$

Figure III.1.3: The four oriented endpoint sectors for the same two rank-one brane labels used in Figure III.1.1. A loop is a same-brane sector; the arrows $1 \to 2$ and $2 \to 1$ are distinct. The matrix product on the right implements endpoint matching, and its trace closes an oriented disc boundary.

A unitary change of endpoint basis acts by $|i\rangle \mapsto U|i\rangle$, so a matrix-valued field transforms as

$$M \longmapsto UMU^{-1}, \qquad U \in U(N). \tag{III.1.26}$$

For the massless vector on coincident oriented branes, Hermitian matrix fields span the Lie algebra $\mathfrak{u}(N)$ in the physicist's Hermitian generator convention. A single E_{12} is *not* Hermitian. Its conjugate $E_{21} = E_{12}^\dagger$ pairs with it. One possible Hermitian basis is

$$T^0 = \frac{E_{11} + E_{22}}{2}, \quad T^3 = \frac{E_{11} - E_{22}}{2},$$
$$T^1 = \frac{E_{12} + E_{21}}{2}, \quad T^2 = \frac{-iE_{12} + iE_{21}}{2}, \qquad \mathrm{Tr}_f(T^aT^b) = \frac{\delta^{ab}}{2}. \tag{III.1.27}$$

For the relative diagonal matrix $H = E_{11} - E_{22}$,

$$[H, E_{12}] = 2E_{12}, \qquad [H, E_{21}] = -2E_{21}, \qquad [H, E_{11}] = [H, E_{22}] = 0. \tag{III.1.28}$$

The opposite charges remember the opposite string orientations. When the branes are separated, the diagonal sectors remain self-endpoint states; the off-diagonal sectors must span the gap. The next section converts that geometric statement into an exact first-level mass in this flat setup.

The action of a finite diagonal basis change makes these relative charges transparent. Let $U = \mathrm{diag}(e^{i\theta_1}, e^{i\theta_2})$. Conjugation gives the two opposite phases

$$UE_{12}U^{-1} = e^{i(\theta_1 - \theta_2)}E_{12}, \qquad UE_{21}U^{-1} = e^{-i(\theta_1 - \theta_2)}E_{21}. \tag{III.1.29}$$

If $\theta_1 = \theta_2$, both phases are one: the common center acts trivially on this adjoint pair. Taking $\theta_1 = \vartheta, \theta_2 = -\vartheta$ instead reproduces the ± 2 eigenvalues of H by differentiating at $\vartheta = 0$. The integer two reflects the normalization $H = \mathrm{diag}(1, -1)$; halving H would give charges ± 1 without changing the strings.

Joining also knows about order. The product $E_{12}E_{21}E_{12} = E_{12}$ is an open chain, and its trace vanishes; attaching E_{21} closes it and gives trace one. By contrast, $E_{12}E_{12} = 0$

because its middle endpoints cannot meet. These are small calculations, but they prevent a common mistake in quiver drawings: an arrow is not an unoriented adjacency line. The ordered matrix product and a later gauge-invariant cycle both use the same row-to-column orientation.

The rule works without restricting us to two labels. With three labels, $E_{12}E_{23}E_{31} = E_{11}$ and the trace is one. Reordering the second and third factors gives $E_{12}E_{31} = 0$ before any trace is taken. A unitary basis change preserves the nonzero cyclic product because adjacent inverse matrices cancel:

$$\begin{aligned}\mathrm{Tr}(UM_1U^{-1}UM_2U^{-1}\cdots UM_rU^{-1}) &= \mathrm{Tr}(UM_1M_2\cdots M_rU^{-1})\\ &= \mathrm{Tr}(M_1M_2\cdots M_r).\end{aligned} \tag{III.1.30}$$

This is the elementary compatibility between the endpoint-basis action and a disc boundary trace. A trace can also vanish for reasons beyond endpoint mismatch, such as a matrix coefficient cancellation; the Kronecker product in (III.1.24) isolates the simple matrix-unit case.

The familiar oriented local $U(N)$ algebra should not be confused with the $SO(32)$ algebra of the separately orientation-projected type-I construction. A D9 stack in the oriented calculation illustrates the local CP algebra, while its global RR tadpole question is a further condition. Counting matrices alone settles neither orientifold projection nor a complete vacuum.

III.1.5 Coincidence and enhancement

Why does moving two parallel branes together add light vectors? For an (i, j) string let $\Delta Y^I = Y_j^I - Y_i^I$ and let M be the mass measured from conserved momentum along the common worldvolume. The affine DD contribution from Section III.1.2 adds to the NS level. In the same type-II GSO sector as Section III.1.3,

$$M_{ij}^2 = \frac{|\Delta Y|^2}{(2\pi\alpha')^2} + \frac{N_{\mathrm{NS}} - \frac{1}{2}}{\alpha'}, \qquad |\Delta Y|^2 = \sum_{I=p+1}^{9} (Y_j^I - Y_i^I)^2. \tag{III.1.31}$$

This formula assumes the same flat parallel boundary conditions on both ends and no additional Wilson-line or background contribution. The first GSO-surviving level has $N_{\mathrm{NS}} = \frac{1}{2}$, so

$$M_{ij,\mathrm{first}}^2 = \frac{|Y_j - Y_i|^2}{(2\pi\alpha')^2} = |\Phi_j - \Phi_i|^2, \qquad \Phi_i^I = \frac{Y_i^I}{2\pi\alpha'}. \tag{III.1.32}$$

The second equality uses the physical position-scalar normalization. The first equality is a free-string statement; the rightmost expression makes contact with a leading worldvolume field theory. A higher NS level still carries its oscillator term and does not become massless merely because the branes coincide.

For a numerical case, take $\alpha' = 3/2$ and $|\Delta Y| = 9\pi$. Then $2\pi\alpha' = 3\pi$ and the stretch contribution is

$$\frac{|\Delta Y|^2}{(2\pi\alpha')^2} = \frac{(9\pi)^2}{(3\pi)^2} = 9. \tag{III.1.33}$$

At $N_{\rm NS}=\frac{1}{2}$ the mass squared is nine. At the next listed NS level $N_{\rm NS}=\frac{3}{2}$ the oscillator term is $(\frac{3}{2}-\frac{1}{2})/(\frac{3}{2})=2/3$, hence

$$M_{1/2}^2=9,\qquad M_{3/2}^2=9+\frac{2}{3}=\frac{29}{3},\qquad M_{1/2}^2\big|_{\Delta Y=0}=0. \tag{III.1.34}$$

The first string and the next oscillator level answer different questions; subtracting the bosonic intercept would give a false threshold. The particular 9π example is an algebraic comparison, not an assertion that a low-energy field theory controls physics at that separation.

We can independently see the same quadratic mass in the leading reduced Yang–Mills description. This comparison needs its own sign and trace conventions. Use Hermitian matrices, $D_a=\partial_a-i[A_a,\cdot\,]$, $F_{ab}=\partial_aA_b-\partial_bA_a-i[A_a,A_b]$ and the fundamental trace Tr_f with the generator normalization of (III.1.27). Write only the terms needed for the quadratic mass:

$$S_{\rm quad}\subset-\kappa\int d^{p+1}x\ \mathrm{Tr}_f\left(\frac{1}{4}F_{ab}F^{ab}+\frac{1}{2}D_a\Phi^ID^a\Phi^I\right),\qquad \kappa>0. \tag{III.1.35}$$

The trace and D_a sign here are book conventions. A source convention with $D_a^{\rm src}=\partial_a+i[A_a^{\rm src},\cdot\,]$ translates by $A_a=-A_a^{\rm src}$ and $\Phi^I=\Phi^I_{\rm src}$. Changing its Hermitian generator trace from $\mathrm{Tr}(T_nT_m)=N\delta_{nm}$ to $\mathrm{Tr}_f(T^aT^b)=\delta^{ab}/2$ also rescales the *component coefficients* of a fixed matrix. We compare matrix expressions, not same-named components in inequivalent bases. Neither translation nor a squared-mass match fixes κ or a numerical $g_{\rm YM}$.

Set a constant diagonal background $\bar\Phi^I=\mathrm{diag}(\phi_1^I,\phi_2^I)$ and expand the off-diagonal vector as $A_a^{\rm off}=W_aE_{12}+W_a^*E_{21}$. The matrix commutator gives the mass directly:

$$[\bar\Phi^I,E_{12}]=(\phi_1^I-\phi_2^I)E_{12},\qquad [\bar\Phi^I,E_{21}]=-(\phi_1^I-\phi_2^I)E_{21}. \tag{III.1.36}$$

After the scalar fluctuation supplying the longitudinal mode is put in unitary gauge, the background part of $D_a\Phi^I$ is $-i[A_a^{\rm off},\bar\Phi^I]$. Taking the trace and retaining terms quadratic in W gives

$$\mathrm{Tr}_f\big((D_a\Phi^I)(D^a\Phi^I)\big)_{W^2}=2\sum_I|\phi_1^I-\phi_2^I|^2W_a^*W^a,\quad \mathrm{Tr}_f(F_{ab}F^{ab})_{W^2}=2f_{ab}^*f^{ab}, \tag{III.1.37}$$

where $f_{ab}=\partial_aW_b-\partial_bW_a$. Thus the common coefficient κ multiplies both the kinetic and mass terms,

$$\mathcal{L}_{W^2}=-\frac{\kappa}{2}f_{ab}^*f^{ab}-\kappa\sum_I|\phi_1^I-\phi_2^I|^2W_a^*W^a,\qquad m_W^2=\sum_I|\phi_1^I-\phi_2^I|^2. \tag{III.1.38}$$

The ratio is the standard complex Proca mass normalization. Substituting $\phi_i^I=Y_i^I/(2\pi\alpha')$ reproduces (III.1.32), including the numerical example $m_W^2=9$. A squared mass cannot determine the signed covariant derivative, which is why the source-to-book sign translation was stated before this comparison.

The scalar fluctuation mentioned in the calculation deserves a closer look. If $\Phi^I = \bar{\Phi}^I + \varphi^I$, then at linear order the off-diagonal derivative is

$$(D_a\Phi^I)_{12} = \partial_a\varphi^I_{12} + i(\phi^I_1 - \phi^I_2)W_a + O(\text{quadratic fluctuations}). \tag{III.1.39}$$

The combination of φ^I_{12} parallel to $\phi^I_1 - \phi^I_2$ is the mode absorbed into the massive vector; scalar directions orthogonal to the displacement are not its longitudinal polarization. For a single nonzero separation component $\Delta\phi$, the quadratic term is proportional to $|\partial_a\varphi_{12} + i\Delta\phi W_a|^2$. An off-diagonal infinitesimal gauge transformation shifts the scalar by the background commutator, so a unitary-gauge choice removes precisely that parallel mode. The remaining vector then has the mass read from (III.1.38).

This also reconciles the polarization statements. At nonzero null momentum a massless vector in $p+1$ dimensions has $p-1$ local modes. Moving off coincidence, one scalar direction becomes longitudinal and the massive vector has p modes, as expected for a nonzero mass in the same dimension. The total number of physical bosonic modes in the first-level multiplet is preserved by this rearrangement:

$$(p{-}1){+}(9{-}p) = 8 \quad (1 \le p \le 9), \qquad p{+}(8{-}p) = 8 \quad (1 \le p \le 8,\ |\Delta Y| > 0). \tag{III.1.40}$$

This count is a bookkeeping comparison under the same first-level spectrum premise. It does not turn the separated vector into an extra massless polarization.

At $Y_1 = Y_2$ the four E_{ij} first-level sectors all have zero stretch mass. Their Hermitian vector components span T^0, T^1, T^2, T^3:

$$\Delta Y \neq 0: \quad E_{11}, E_{22} \text{ massless},\ E_{12}, E_{21} \text{ massive}; \qquad \Delta Y = 0: \quad \dim_{\mathbb{R}} \mathfrak{u}(2) = 4. \tag{III.1.41}$$

The two off-diagonal complex orientations are conjugate pieces of Hermitian fields, not two unrelated Hermitian generators per E_{ij}. For separated branes their massive vectors include longitudinal modes from normal scalar components. At coincidence the massless vector and scalar split of Section III.1.3 applies again. This is the local enhancement mechanism illustrated in Figure III.1.1. Chapter 4 will treat the interacting reduced theory; no complete nonabelian brane action is deduced from this one quadratic comparison.

III.1.6 From flat branes to a projection

How does a geometric quotient act on the matrix fields just constructed? Consider a flat type-IIB D3 spanning unaffected $\mathbb{R}^{1,3}$, with three complex transverse coordinates in $\mathbb{C}^2/\mathbb{Z}_2 \times \mathbb{C}$. Its generator acts by

$$g : (z_1, z_2, z_3) \longmapsto (-z_1, -z_2, z_3). \tag{III.1.42}$$

The first two signs have product $+1$, so the action on $\mathbb{C}^2$ lies in $SU(2)$. This is not the reflection of only one complex normal coordinate. The D3 has six real normals, grouped into three complex scalar fields Φ_1, Φ_2, Φ_3. The third is a spectator under g.

Give the two-dimensional CP space one regular representation of $\mathbb{Z}_2$:

$$\gamma(g) = \begin{pmatrix} 1 & 0 \\ 0 & -1 \end{pmatrix}, \qquad \gamma(g)^2 = \mathbf{1}, \qquad \chi(1) = 2, \quad \chi(g) = 0. \tag{III.1.43}$$

Here $\chi(h) = \operatorname{Tr}\gamma(h)$ is the character of this CP representation; $\gamma(1) = \mathbf{1}$. The two CP labels here are the two irreducible character sectors of *one* regular representation. They should not be read as two arbitrary regular bulk branes. The source projection algebra initially uses D5 branes with four orbifold-normal real coordinates. We apply that algebra to this explicitly different D3 probe and its three complex normal fields; a D9 would not possess these normal scalars.

A vector tangent to the unaffected D3 has geometric sign $+1$. The normal complex fields have signs $r_1 = r_2 = -1$ and $r_3 = +1$. Invariance of an open state combines the geometric action with conjugation on its CP factor:

$$A_a = \gamma(g) A_a \gamma(g)^{-1}, \qquad \Phi_\alpha = r_\alpha \gamma(g) \Phi_\alpha \gamma(g)^{-1}, \qquad (r_1, r_2, r_3) = (-1, -1, +1). \tag{III.1.44}$$

To evaluate this rather than merely name a projection, write a generic 2×2 matrix $M = (m_{ij})$ and CP eigenvalues $(\lambda_0, \lambda_1) = (+1, -1)$. The (i, j) component acquires the factor $r\lambda_i \lambda_j^{-1}$. Its entry survives exactly when this factor equals one:

$$(r\gamma M \gamma^{-1})_{ij} = r\lambda_i \lambda_j^{-1} m_{ij}, \qquad m_{ij} \neq 0 \implies r\lambda_i \lambda_j^{-1} = 1. \tag{III.1.45}$$

For $r = +1$, the two diagonal factors are $+1$ and the two off-diagonal factors are -1; for $r = -1$ the retained entries exchange places. The four invariant binary masks, in the row/column order $(0, 1)$, are

$$\mathcal{M}_A = \mathcal{M}_{\Phi_3} = \begin{pmatrix} 1 & 0 \\ 0 & 1 \end{pmatrix}, \qquad \mathcal{M}_{\Phi_1} = \mathcal{M}_{\Phi_2} = \begin{pmatrix} 0 & 1 \\ 1 & 0 \end{pmatrix}. \tag{III.1.46}$$

A one means that the corresponding complex matrix entry remains a field; a zero means that invariance sets it to zero. For example, A_{01} is odd under CP conjugation and is removed, whereas $(\Phi_1)_{01}$ gets one minus sign from geometry and one from CP, so it survives. The spectator $(\Phi_3)_{00}$ survives because both signs are positive.

There is a direct way to recover every mask without guessing which entries are even. Since $g^2 = 1$ and $r^2 = 1$, the linear operator $Q_r(M) = r\gamma M \gamma^{-1}$ obeys $Q_r^2 = 1$. Its invariant projector is therefore

$$\mathcal{P}_r(M) = \frac{1}{2}\left(M + r\gamma M \gamma^{-1}\right), \qquad \mathcal{P}_r^2 = \mathcal{P}_r. \tag{III.1.47}$$

Apply it to an arbitrary matrix and carry the entries through:

$$M = \begin{pmatrix} a & b \\ c & d \end{pmatrix}, \quad \gamma M \gamma^{-1} = \begin{pmatrix} a & -b \\ -c & d \end{pmatrix}, \quad \mathcal{P}_+(M) = \begin{pmatrix} a & 0 \\ 0 & d \end{pmatrix}, \quad \mathcal{P}_-(M) = \begin{pmatrix} 0 & b \\ c & 0 \end{pmatrix}. \tag{III.1.48}$$

The vector and spectator scalar use $\mathcal{P}_+$; the two flipped scalars use $\mathcal{P}_-$. The computation explains the four masks as two instances of one idempotent map. It also shows why the representation matters: changing γ changes the invariant subspaces even if the geometric signs remain fixed.

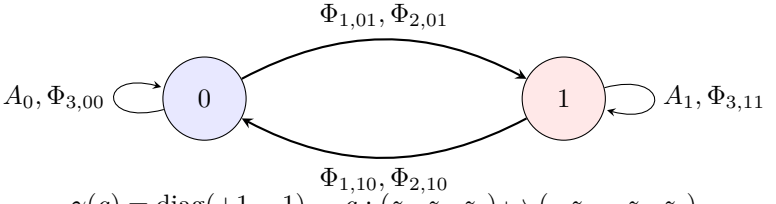
The surviving spaces also behave correctly under ordinary matrix multiplication. Multiplying two off-diagonal matrices of the form $\mathcal{P}_-(M)$ produces a diagonal matrix,

while a diagonal matrix times an off-diagonal matrix remains off-diagonal. In terms of geometric signs this is simply $(-1)(-1) = +1$ and $(+1)(-1) = -1$:

$$\begin{pmatrix} 0 & b \\ c & 0 \end{pmatrix} \begin{pmatrix} 0 & b' \\ c' & 0 \end{pmatrix} = \begin{pmatrix} bc' & 0 \\ 0 & cb' \end{pmatrix}, \qquad \begin{pmatrix} a & 0 \\ 0 & d \end{pmatrix} \begin{pmatrix} 0 & b \\ c & 0 \end{pmatrix} = \begin{pmatrix} 0 & ab \\ dc & 0 \end{pmatrix}. \tag{III.1.49}$$

These identities make the projected node-and-arrow drawing consistent with the CP joining rule. They are an algebraic closure check, not a calculation of a superpotential or an orbifold scattering amplitude.

The invariant Hermitian vector matrices are diagonal, giving the local Lie algebra $\mathfrak{u}(1) \oplus \mathfrak{u}(1)$. The two flipped complex scalars supply oppositely oriented off-diagonal entries for each $\alpha = 1, 2$; the spectator has two diagonal entries. Figure III.1.4 records that matrix information as a projected two-node diagram using the arrow convention of Section III.1.4.



$$\gamma(g) = \mathrm{diag}(+1, -1), \quad g : (z_1, z_2, z_3) \mapsto (-z_1, -z_2, z_3)$$

Figure III.1.4: The local $\mathbb{Z}_2$ invariant mask for one regular CP representation on the stated flat D3 probe. Loops denote diagonal vector and spectator-scalar entries. The vector labels A_0, A_1 use node indices $0, 1$; the Lorentz index a of A_a is suppressed. Each direction has two complex scalar entries, one from Φ_1 and one from Φ_2. An arrow $i \to j$ means row i, column j. The diagram records invariant open fields; it is not a complete orbifold vacuum or a catalogue of all quiver data.

Three operations should remain separate. The geometric quotient specifies g on target coordinates. The equation (III.1.44) projects open-string states. A quotient of vacua by gauge transformations is a later dynamical and geometric question. The local masks alone establish neither an orbifold boundary CFT nor RR tadpole cancellation, anomaly freedom or a global gauge-group form. Chapter 6 of Volume II develops the closed orbifold setting, Chapter 2 studies boundary states, and Volume VI, Chapter 2 constructs the fuller quiver theory. Here the point is the explicit bridge from an endpoint matrix to a projected matrix field.

III.1.7 Exercises

For each exercise submit the stated exact answer through the chapter's reader interface and accompany it with written working. The bounded checker evaluates the requested numerical or matrix fields; the explanations require a reader or instructor.

1. **Endpoint modes (E1).** Take $\alpha' = 2$, tangent momentum $p = 3/2$, and $y(0) = -\pi$, $y(\pi) = 4\pi$. Submit the NN coefficient multiplying τ and the DD coefficient multiplying σ. Show both endpoint substitutions and explain why the DD coordinate cannot carry an independent momentum zero mode. Use the fields `nn_drift` and `dd_slope`.

2. **Spectrum and quadratic comparison (E2).** For two parallel same-kind branes with $\alpha' = 3/2$ and $|\Delta Y| = 9\pi$, compute M^2 for $N_{\rm NS} = 1/2$ and $3/2$, the first-level value at coincidence, and the leading reduced-SYM off-diagonal quadratic mass squared. Show the stretch and oscillator terms separately. Explain the scope of comparing the last quantity at finite separation. Submit the four mass-squared values in the named fields `first_mass_squared`, `next_mass_squared`, `coincident_mass_squared`, and `ym_offdiagonal_mass_squared`, in that order.

3. **Ordered CP states (E3).** Write the four exact 2×2 E_{ij} matrices for $(1,1), (1,2), (2,1), (2,2)$, and compute the commutator eigenvalues of E_{12} and E_{21} under $H = \mathrm{diag}(1, -1)$. Explain the sign reversal by string orientation. Submit `basis` and `relative_charges`.

4. **Polarizations (E4).** At the first ten-dimensional type-II NS level with nonzero null worldvolume momentum, submit for D1, D3 and D9 the local vector count, normal scalar count and total. Explain why the D1 connection exists even though its local vector count vanishes. Submit objects `D1`, `D3`, `D9`, each with `vector`, `scalars`, `total`.

5. **One open-state projection (E5).** For the D3 probe of Section III.1.6, use $g : (z_1, z_2, z_3) \mapsto (-z_1, -z_2, z_3)$ and $\gamma(g) = \mathrm{diag}(1, -1)$. Submit binary 2×2 masks for vector, Φ_1, Φ_2 and Φ_3 entries. Explain why these masks are an open-state projection rather than a quotient of the vacuum space. Submit `vector`, `phi1`, `phi2`, `phi3`.

III.1.8 Take-home message

Take-home message

A free open string has NN momentum drift along a D-brane and a fixed DD stretch between branes. The first GSO-surviving type-II NS level gives a worldvolume vector and normal position scalars with $Y^I = 2\pi\alpha'\Phi^I$. Oriented endpoints supply matrix units whose joining is matrix multiplication. For parallel branes their off-diagonal first-level mass is $|\Delta Y|/(2\pi\alpha')$, so coincidence restores the full local $U(N)$ adjoint spectrum. A geometric orbifold acts on that spectrum together with a CP representation; its invariant matrix entries are an open-state calculation, while the complete orbifold theory needs further input.

Status and sources

The flat boundary action, NN/DD conditions, modes and fixed-endpoint stretch in Section III.1.2 follow Tong (2009, physical PDF pp. 57–60, 66, eqs. (3.1)–(3.5)) and the type-II Dp endpoint premise in Polchinski (1995, physical PDF p. 3, eq. (4)). The boundary variation, explicit affine example, tension and L_0 mass translation are algebraic [WS] and [MATH] statements under flat matching boundary conditions. Tong's following bosonic tachyon discussion is not imported into the type-II NS spectrum. The absence of a normal momentum zero mode does not mean that the spatial integral of every normal oscillator momentum vanishes.

The sourced GSO projection and eight first-level NS polarizations in Section III.1.3 are [WS] premises from Johnson (2000, physical PDF pp. 87–88, eqs. (231)–(234)). The source's physical p. 87 prose assigns $a = -1/2$ immediately before a subtractive mass equation, in conflict with its p. 88 massless level. We use $E_{\mathrm{NS}} = -1/2$ and $a_{\mathrm{NS}} = -E_{\mathrm{NS}} = +1/2$. The $(p-1)+(9-p)$ split is [MATH] under nonzero null brane momentum and the sourced massless state, not a separated massive-vector count. The position normalization follows Johnson (2000, physical PDF p. 63, eq. (172)) in its T-dual setting and Myers (1999, physical PDF pp. 2, 6) for physical transverse displacement. GSO, RR identification and complete open/closed consistency are cited premises, not proofs supplied by this chapter.

The oriented endpoint factors and cyclic disc trace of Section III.1.4 follow Johnson (2000, physical PDF pp. 33–34, eqs. (88)–(90)); E_{ij} multiplication, the $U(2)$ matrices and commutator charges are [MATH]. The local enhancement in Section III.1.5 uses Johnson (2000, physical PDF pp. 65–67, eqs. (174)–(175)) and Myers (1999, physical PDF p. 3). The type-II NS intercept replaces the bosonic intercept of the former pages. The leading reduced Yang–Mills derivative and scalar commutator premise are Myers (1999, physical PDF pp. 6–8, eqs. (13)–(14), (18), (20), (23)). Our Hermitian $D = \partial - i[A, \cdot]$ uses $A_{\mathrm{book}} = -A_{\mathrm{Myers}}$ and $\Phi_{\mathrm{book}} = \Phi_{\mathrm{Myers}}$; component coefficients change with generator normalization. The quadratic trace ratio is [MATH] under that leading-action premise. It fixes no numerical coupling and makes no large-separation EFT claim. The oriented D9 statement is local; the distinct type-I projection and space-filling consistency issue are described in Polchinski (1995, physical PDF p. 8).

The combined geometric and CP projection in Section III.1.6 follows the algebra of Douglas and Moore (1996, physical PDF pp. 8–9, 11, eqs. (3.1)–(3.3), (3.8)). That source begins with D5 branes and four orbifold-normal real directions; our stated flat IIB D3 with six real normals is a specialization of the projection rule, not an identification of their full setups. The four masks and $SU(2)$ sign product are [MATH] in this local setup. No full orbifold boundary CFT, vacuum quotient, RR charge proof, tadpole or anomaly claim follows from them. The metric, tension, orbifold and gauge-group conventions are as stated in the chapter.

References

Douglas, M. R. and G. Moore (1996). *D-branes, Quivers, and ALE Instantons*. arXiv: `hep-th/9603167`.

Johnson, C. V. (2000). *D-Brane Primer*. DOI: 10.1142/9789812799630_0002. arXiv: hep-th/0007170.

Myers, R. C. (1999). "Dielectric-Branes". In: *JHEP* 12, p. 022. DOI: 10.1088/1126-6708/1999/12/022. arXiv: hep-th/9910053.

Polchinski, J. (1995). "Dirichlet-Branes and Ramond-Ramond Charges". In: *Phys. Rev. Lett.* 75, pp. 4724–4727. DOI: 10.1103/PhysRevLett.75.4724. arXiv: hep-th/9510017.

Tong, D. (2009). *String Theory*. arXiv: 0908.0333.

Chapter III.2

The boundary-state formalism

III.2.1 A boundary viewed from the other channel

Put an open string between two parallel D-branes and join its initial and final time slices. The resulting worldsheet is a cylinder. Its two rims are open-string endpoints if time runs around the cylinder. If time instead runs from one rim to the other, each rim prepares a closed-string state. The closed string then propagates between two brane sources. This change of time direction is the central move of this chapter.

The boundary-state description answers two related questions. Which closed-string state imposes the same Neumann and Dirichlet data as the open endpoint? With what normalization does exchange between two such states reproduce an open-string loop? The oscillator equations answer the first question, but the full cylinder, including its zero modes, ghosts, measure and endpoint multiplicities, answers the second. Figure III.2.1 displays the two readings of the same surface.

We work first in the free critical bosonic source theory, where all normalization factors can be followed explicitly. We then use the sourced flat type-II completion and a local $\mathbb{C}^2/\mathbb{Z}_2$ example. Time is a Neumann direction throughout. The bosonic cylinder has a tachyon, so its open/closed equality is an identity of formal integrands; it does not define a generally convergent static force. Chapter 1 supplied the endpoint data, and Volume II, Chapters 2 and 4 supplied the cylinder oscillators and RNS sectors. The present construction will supply the boundary source needed for the brane actions of Chapter 3 and for later fractional-brane and twisted-tadpole examples.

III.2.2 Boundary conditions as a closed-channel state

How does an endpoint condition become a condition on a closed-string state? On the open strip, a brane extends along coordinates X^a, $a = 0, \dots, p$, and sits at $X^I = y^I$, $I = p+1, \dots, d-1$. The open boundary has $\partial_\sigma X^a = 0$ and $X^I = y^I$. Rotate the cylinder so the boundary is at closed-channel time $\tau = 0$. With the orientation shown

in Figure III.2.1, its conditions are

$$\partial_\tau X^a(0,\sigma)|B_X\rangle = 0, \qquad \big(X^I(0,\sigma) - y^I\big)|B_X\rangle = 0. \tag{III.2.1}$$

The derivative changes its worldsheet role under rotation. Reversing the normal to this homogeneous boundary condition multiplies $\partial_\tau X^a = 0$ by -1 and leaves its solution space unchanged. The relative oscillator sign below is fixed by the mode expansion and the chosen ket convention, not by a choice of normal.

Use the closed-string oscillators of Volume II with $[\alpha_m^\mu, \alpha_n^\nu] = m\eta^{\mu\nu}\delta_{m+n,0}$ and the analogous independent tilded algebra. The source's $\alpha, \widetilde{\alpha}$ families are kept in that order. Define the mixed tensor $S^\mu{}_\nu$ by $+1$ on every Neumann direction, including time, and -1 on every Dirichlet direction. Lower its first index with the Minkowski metric:

$$S^\mu{}_\nu = \mathrm{diag}(\underbrace{+1,\ldots,+1}_{p+1 \text{ NN}}, \underbrace{-1,\ldots,-1}_{d-p-1 \text{ DD}}), \qquad S_{\mu\nu} = \eta_{\mu\rho}S^\rho{}_\nu. \tag{III.2.2}$$

In the source's closed mode expansion, the α_n wave depends on $\tau - \sigma$ and the $\widetilde{\alpha}_n$ wave on $\tau + \sigma$. At $\tau = 0$, the coefficient of $e^{in\sigma}$ in $\partial_\tau X^a$ pairs α_n^a with $\widetilde{\alpha}_{-n}^a$, giving their sum; the coefficient in $X^I - y^I$ gives their difference. Thus the nonzero Fourier coefficients of (III.2.1) become

$$\big(\alpha_n^\mu + S^\mu{}_\nu \widetilde{\alpha}_{-n}^\nu\big)|B_X\rangle = 0, \qquad n \in \mathbb{Z} \setminus \{0\}. \tag{III.2.3}$$

For a positive n, this relates an annihilator in one family to a creator in the other. The conjugate bra obeys $\langle B_X|(\alpha_{-n}^\mu + S^\mu{}_\nu \widetilde{\alpha}_n^\nu) = 0$: its mode indices change, but the relative sign does not. Changing the plus to a minus with the oscillator basis fixed would exchange NN and DD gluing. The state is a coherent pair source, not an ordinary one-oscillator eigenstate.

Write the nonzero-mode exponent as

$$A = -\sum_{n=1}^{\infty} \frac{1}{n}\, \alpha_{-n}^\mu S_{\mu\nu} \widetilde{\alpha}_{-n}^\nu, \qquad |B_X\rangle_{\mathrm{osc}} = e^A|0\rangle. \tag{III.2.4}$$

The algebra gives a short, complete check. Tilded creation operators commute with α_n^μ, while the untilded commutator selects one term of the sum:

$$[\alpha_n^\mu, A] = -\eta^{\mu\rho}S_{\rho\nu}\widetilde{\alpha}_{-n}^\nu = -S^\mu{}_\nu \widetilde{\alpha}_{-n}^\nu, \qquad [[\alpha_n^\mu, A], A] = 0. \tag{III.2.5}$$

Hence $e^{-A}\alpha_n^\mu e^A = \alpha_n^\mu + [\alpha_n^\mu, A]$. Acting on the vacuum makes $(\alpha_n^\mu + S^\mu{}_\nu \widetilde{\alpha}_{-n}^\nu)e^A|0\rangle$ zero. The condition for $n < 0$ follows by the analogous tilded commutation. This calculation constructs only the matter oscillator factor; the ghost and physical-state completion enters below as additional input.

A one-mode example exposes the signs. For a spacelike diagonal direction, set $A_n = c\alpha_{-n}\widetilde{\alpha}_{-n}$. The residual of the gluing operator on $e^{A_n}|0\rangle$ is

$$(\alpha_n + S\widetilde{\alpha}_{-n})e^{A_n}|0\rangle = (nc + S)\widetilde{\alpha}_{-n}e^{A_n}|0\rangle. \tag{III.2.6}$$

At $n = 2$, a spacelike NN mode has $c = -1/2$, while a spacelike DD mode has $c = +1/2$. Swapping either sign leaves a nonzero residual of magnitude 2 in these units.

Time is different because the metric enters twice. It remains NN, so $S^0{}_0 = +1$, but $S_{00} = -1$, and the coefficient of $\alpha^0_{-2}\widetilde{\alpha}^0_{-2}$ is $+1/2$. Indeed its commutator residual is $-2(+1/2) + 1 = 0$. Treating the time component with the positive-metric scalar rule would give the wrong state.

The pair $\alpha_{-n}\widetilde{\alpha}_{-n}$ creates equal left and right levels, as required at a stationary boundary. A boundary state is distributional and not a normalizable one-particle state. Its normalization will be determined by the cylinder rather than by setting its norm to one. That distinction also explains why solving (III.2.3) alone cannot fix the multiplicity of open strings between two branes.

It is useful to see why the exponential, rather than just its first pair, is required. In one positive-metric direction with fixed n, let $a^\dagger = \alpha_{-n}$ and $b^\dagger = \widetilde{\alpha}_{-n}$. Both creation operators have commutators of magnitude n with their annihilators. The proposed state has the series

$$e^{ca^\dagger b^\dagger}|0\rangle = \sum_{k=0}^{\infty} \frac{c^k}{k!}(a^\dagger)^k(b^\dagger)^k|0\rangle. \tag{III.2.7}$$

Act with $a + Sb^\dagger$ on its k-pair term. The annihilator lowers k to $k-1$ and supplies nk; the $Sb^\dagger$ term raises the neighboring $(k-1)$-pair term. At every $k \geq 1$, cancellation requires the same recurrence

$$\frac{nkc^k}{k!} + \frac{Sc^{k-1}}{(k-1)!} = 0 \quad \Longleftrightarrow \quad nc + S = 0. \tag{III.2.8}$$

For $n = 2$ NN, the first three terms are $|0\rangle - \frac{1}{2}a^\dagger b^\dagger|0\rangle + \frac{1}{8}(a^\dagger b^\dagger)^2|0\rangle$. The coefficient of $a^\dagger(b^\dagger)^2$ in the gluing residual receives $+1/2$ from the annihilator acting on the two-pair term and $-1/2$ from the gluing creator acting on the one-pair term. This neighboring-level cancellation is why a truncated state can pass at one pair number and fail at the next. The all-mode BCH statement above is stronger than checking a finite Fock truncation.

The oscillator gluing also has a geometric interpretation. At the closed rim, left and right traveling waves are reflected into one another. A tangent displacement is allowed, so its reflected derivative carries the NN sign; a normal displacement is fixed, so its coordinate carries the DD sign. Lowering S in the exponent is essential because the oscillators there both have upper target indices. This distinction is the same one that prevented the time oscillator from being treated as a positive-metric NN scalar.

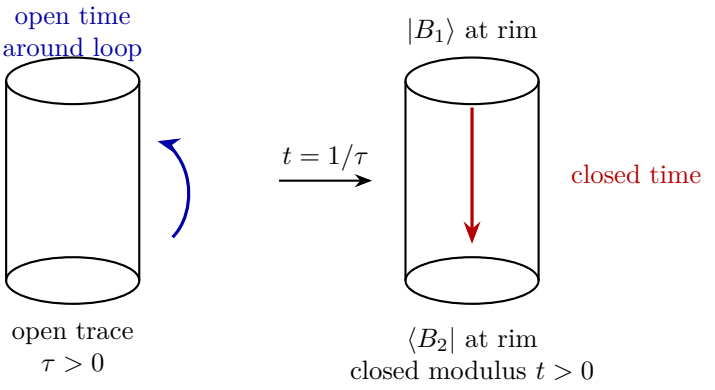


Figure III.2.1: One cylinder read in two directions. The open trace evolves around the loop with modulus $\tau > 0$; the closed state propagates between its two rims with modulus $t = 1/\tau$ for the periods used in this chapter. The arrows mark worldsheet time, and each closed rim imposes the rotated boundary conditions.

III.2.3 Zero modes and localization

What part of the boundary state tells the exchanged closed string where the brane sits? The $n = 0$ equations must be separated from (III.2.3). Along the brane, the rotated Neumann condition kills the closed zero-mode momentum. In a normal direction, the fixed-position condition localizes the coordinate:

$$p^a|B_X\rangle_0 = 0, \qquad (q^I - y^I)|B_X\rangle_0 = 0. \tag{III.2.9}$$

Thus a convenient symbolic zero-mode state is

$$|B_X(y)\rangle_0 = C_0 \prod_{a=0}^{p} \delta(p^a) \prod_{I=p+1}^{d-1} \delta(q^I - y^I). \tag{III.2.10}$$

Here C_0 is absorbed into the eventual source normalization. The formula states support, not a finite Hilbert-space norm. The position delta function is equivalently a superposition of all normal momenta:

$$\delta^{d_\perp}(q - y) = \int \frac{d^{d_\perp}Q}{(2\pi)^{d_\perp}} e^{iQ\cdot(q-y)}, \qquad d_\perp = d - p - 1. \tag{III.2.11}$$

There is therefore no condition $p^I = 0$. Closed exchange between two localized sources carries normal momentum Q.

Let the two branes be separated by the normal vector $\Delta y = y_1 - y_2$. In the source cylinder, the normal zero-mode Hamiltonian contributes $e^{-\pi\alpha' t Q^2/2}$. The Fourier integral is elementary once its measure is retained:

$$\int \frac{d^{d_\perp}Q}{(2\pi)^{d_\perp}} e^{-\frac{\pi\alpha' t}{2}Q^2 + iQ\cdot\Delta y} = (2\pi^2\alpha' t)^{-d_\perp/2} e^{-|\Delta y|^2/(2\pi\alpha' t)}. \tag{III.2.12}$$

For one normal coordinate this follows from $\int dQ\, e^{-aQ^2+iQy}/(2\pi) = (4\pi a)^{-1/2} e^{-y^2/(4a)}$ with $a = \pi\alpha' t/2$. Raising that factor to $d_\perp$ gives the full result. The $\delta(p^a)$ support instead produces the common longitudinal volume V_{p+1}, which is suppressed when we quote an amplitude per worldvolume.

For a concrete two-normal-coordinate slice, take $\Delta y = (3/2, -5/3)$, with both entries measured in the same length units. Its squared length is

$$|\Delta y|^2 = (3/2)^2 + (-5/3)^2 = \frac{9}{4} + \frac{25}{9} = \frac{181}{36}, \qquad e^{-|\Delta y|^2/(2\pi\alpha' t)} = e^{-181/(72\pi\alpha' t)}. \tag{III.2.13}$$

At coincidence the last factor is one. At fixed separation it suppresses short closed propagation $t \to 0^+$, just as a stretched open string acquires an energy cost. The normal oscillator modes remain present in either case; localization has altered the zero-mode integral, not deleted the normal coordinates. Figure III.2.2 keeps these two kinds of support apart. This is the factor we will carry into the complete cylinder, and twisted closed fields later use the same idea of a source tied to a fixed locus.

One can carry the two-normal-coordinate example through the integral instead of substituting only its distance at the end. With $a = \pi\alpha' t/2$, the two integrals factor:

$$\prod_{J=1}^{2} \int \frac{dQ_J}{2\pi} e^{-aQ_J^2 + iQ_J \Delta y_J} = \frac{1}{4\pi a} e^{-[(3/2)^2 + (-5/3)^2]/(4a)}. \tag{III.2.14}$$

The prefactor equals $(2\pi^2\alpha' t)^{-1}$, which is the $d_\perp = 2$ case of (III.2.12). Had we imposed normal momentum $Q_J = 0$, both the t^{-1} and the dependence on the separation would have disappeared. Neither loss is compatible with a localized pair of sources.

The sign of the Fourier phase can be reversed by exchanging the two boundary labels; the final Gaussian depends only on $|y_1 - y_2|^2$. This is a useful orientation check, but it does not make the individual boundary states position independent. Each source still carries its own $\delta(q - y_i)$. Translation of both branes together leaves their exchange invariant because only their difference enters the cylinder.

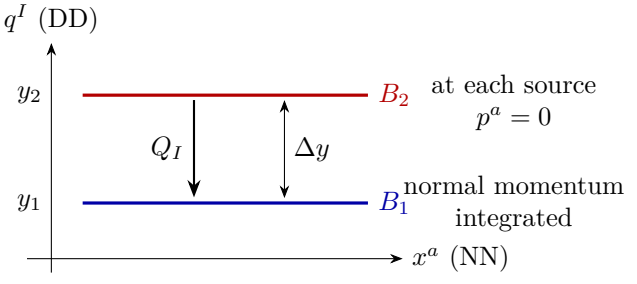


Figure III.2.2: The brane is homogeneous in a Neumann coordinate x^a and fixed at $q^I = y^I$ in a normal coordinate. Closed exchange has $p^a = 0$ at each source but integrates over normal momentum Q_I; the separation $y_1 - y_2$ supplies its Fourier phase.

III.2.4 The cylinder in two channels

Which factors make the open loop equal to closed exchange, including its normalization? Use the critical bosonic theory with $d = 26$, $d_\perp = 25 - p$, two parallel Dp-branes, and the source's periods. The oscillator contraction of the matter state first yields $\prod_{n\geq 1}(1 - e^{-2\pi t n})^{-26}$. The ghost contribution replaces the exponent 26 by 24. Define the source's function

$$f_1(q) = q^{1/12}\prod_{n=1}^{\infty}(1 - q^{2n}), \qquad q = e^{-\pi t}. \tag{III.2.15}$$

The q prefactor carries the bosonic zero-point energy, and $[f_1(e^{-\pi t})]^{-24}$ packages that factor with the 24 effective oscillators. We need the zero-mode Gaussian (III.2.12) and the propagator measure as well.

The single bosonic number-operator trace is a geometric series. If $u = e^{-2\pi t n}$ for mode n, then $\mathrm{Tr}\, u^{N_n} = \sum_{m\geq 0} u^m = (1-u)^{-1}$. Multiplying over modes and 24 effective coordinates gives

$$\prod_{n=1}^{\infty}\left(\sum_{m=0}^{\infty} e^{-2\pi t n m}\right)^{24} = \prod_{n=1}^{\infty}(1 - e^{-2\pi t n})^{-24}. \tag{III.2.16}$$

The zero-point factor in f_1^{-24} is not generated by that geometric series; it comes from the normal-ordering constant. In the critical source its value is $q^{-2} = e^{2\pi t}$, as the definition of f_1 shows. Calling the product alone the entire annulus would therefore lose the intercept and its tachyonic large-t behavior.

Write N_p for the normalization of the source's bosonic matter boundary state. Its propagator supplies $\alpha'/(4\pi)$; the radial substitution $|z| = e^{-\pi t}$ supplies π; the angular integration supplies 2π. Their product is

$$\frac{\alpha'}{4\pi}\,\pi\,(2\pi) = \frac{\pi\alpha'}{2}. \tag{III.2.17}$$

After factoring out V_{p+1}, the complete closed expression in this source frame is

$$\frac{\mathcal{A}_{\mathrm{cl}}}{V_{p+1}} = N_p^2\frac{\pi\alpha'}{2}(2\pi^2\alpha')^{-d_\perp/2}\int_0^\infty dt\, t^{-d_\perp/2}e^{-y^2/(2\pi\alpha' t)}[f_1(e^{-\pi t})]^{-24}. \tag{III.2.18}$$

Every piece has a different origin: N_p^2 comes from the two boundaries, the power of t from normal momentum, and the product from oscillator and ghost contraction. Replacing any one of them by a convenient convention after the calculation would alter the open string multiplicity.

In the open channel, a real-field one-loop trace starts with 1/2. For the oriented string stretched between the two branes, interchanging the two endpoint orderings contributes 2. The factors cancel. After Wick rotating loop energy and worldvolume time, let k_E^2 be positive Euclidean momentum squared. We use the correspondingly continued V_{p+1} in this formal amplitude and may continue back after matching. The

separation $y^2 = |\Delta y|^2$ is a transverse spatial norm. The longitudinal momentum trace is

$$\int \frac{d^{p+1}k_E}{(2\pi)^{p+1}} e^{-2\pi\alpha'\tau k_E^2} = (8\pi^2\alpha'\tau)^{-(p+1)/2}. \tag{III.2.19}$$

The open stretch contributes $\exp[-y^2\tau/(2\pi\alpha')]$. With the same 24 effective oscillator factors, the open result per worldvolume is

$$\frac{\mathcal{A}_{\rm op}}{V_{p+1}} = (8\pi^2\alpha')^{-(p+1)/2} \int_0^\infty \frac{d\tau}{\tau}\, \tau^{-(p+1)/2} e^{-y^2\tau/(2\pi\alpha')} [f_1(e^{-\pi\tau})]^{-24}. \tag{III.2.20}$$

The first coefficient already remembers the endpoint count. The change of channel must preserve it.

The open expression can be reconstructed directly from its mass operator, which helps keep the stretch and loop momentum distinct. In these conventions,

$$L_0 = \alpha' k_E^2 + \frac{y^2}{(2\pi)^2\alpha'} + \sum_{n\geq 1} \alpha_{-n}\cdot\alpha_n. \tag{III.2.21}$$

The trace contains $\exp[-2\pi\tau(L_0 - 1)]$. Multiplying its three displayed terms by $-2\pi\tau$ produces, in order, the momentum Gaussian of (III.2.19), the stretch factor $e^{-y^2\tau/(2\pi\alpha')}$, and the oscillator trace; the -1 supplies $e^{2\pi\tau}$, the intercept factor in $f_1(e^{-\pi\tau})^{-24}$. The normal separation is an open-string classical energy, whereas the same variable is a Fourier phase in the closed zero-mode integral. Their equality after $t = 1/\tau$ is a concrete form of open/closed duality.

For these periods the modular relation is $f_1(e^{-\pi/t}) = \sqrt{t}\, f_1(e^{-\pi t})$. Set $t = 1/\tau$. Reversing the integration bounds restores the positive measure $d\tau/\tau = dt/t$. The longitudinal factor becomes $t^{(p+1)/2}$, while the 24 oscillator factors yield t^{-12}:

$$\tau^{-(p+1)/2} \longmapsto t^{(p+1)/2}, \quad [f_1(e^{-\pi/t})]^{-24} = t^{-12}[f_1(e^{-\pi t})]^{-24}. \tag{III.2.22}$$

Thus the transformed open expression is

$$\frac{\mathcal{A}_{\rm op}}{V_{p+1}} = (8\pi^2\alpha')^{-(p+1)/2} \int_0^\infty \frac{dt}{t}\, t^{(p+1)/2-12} e^{-y^2/(2\pi\alpha' t)} [f_1(e^{-\pi t})]^{-24}. \tag{III.2.23}$$

The two powers really match: since $d_\perp = 25 - p$, $t^{-d_\perp/2}dt = t^{(p+1)/2-12}dt/t$. This equality is the useful modular check, but it says nothing yet about the overall coefficient.

The individual powers also diagnose common slips. If the modular square root were inverted, the oscillator factor would contribute t^{+12}, missing the closed Gaussian power by 24. If the open integration measure were treated as $d\tau$ without its $1/\tau$, the exponent inside dt/t would shift by one. Figure III.2.1 uses the particular source periods that make $t = 1/\tau$; a cylinder with another circumference convention needs its own modular map. The equality we use is not a universal statement that every quantity called t is the reciprocal of every quantity called τ.

Equating (III.2.18) with (III.2.23) fixes

$$N_p^2 \frac{\pi\alpha'}{2} (2\pi^2\alpha')^{-(25-p)/2} = (8\pi^2\alpha')^{-(p+1)/2}. \tag{III.2.24}$$

Solving the positive-phase branch and using the source's critical-bosonic tension symbol gives

$$T_p^{\mathrm{bos,src}} = \frac{\sqrt{\pi}}{16}(2\pi\sqrt{\alpha'})^{11-p}, \qquad N_p^{\mathrm{bos,src}} = \frac{1}{2}T_p^{\mathrm{bos,src}}. \tag{III.2.25}$$

The ratio is not an independent convention. Inserting the source $T_p^{\mathrm{bos,src}}$ and $N_p = T_p/2$ into the left side of (III.2.24) gives the full coefficient check:

$$N_p^2 \frac{\pi\alpha'}{2}(2\pi^2\alpha')^{-(25-p)/2} = 2^{-3(p+1)/2}\pi^{-(p+1)}(\alpha')^{-(p+1)/2} = (8\pi^2\alpha')^{-(p+1)/2}. \tag{III.2.26}$$

The transverse count $25-p$ and longitudinal count $p+1$ sum to 26. The equality checks all powers of 2, π and α'. At $p = 25$, the closed prefactor still includes the propagator measure, while its transverse Gaussian is empty.

At $p = 3$, the power inside dt/t is $(3+1)/2 - 12 = -10$. If $a = y^2/(2\pi\alpha') = 3/2$, the separation factor in the closed channel is $e^{-3/(2t)}$; this particular exponential is an interpretation exercise rather than a submitted numerical answer. At $p = 25$, $d_\perp = 0$, the Gaussian integral is absent and the inner power is $+1$. These two limits test different ingredients. The source's $T_p^{\mathrm{bos,src}}$ and $N_p^{\mathrm{bos,src}}$ must remain distinct from the book's physical type-II tension τ_p. An absolute RR charge also depends on the normalization of the free RR kinetic term. Chapter 3 will need that spacetime convention before turning a source coefficient into a physical Wess–Zumino coupling.

Matching modular weight alone fixes only the power of the modulus. The Gaussian, propagator measure and endpoint count determine the overall coefficient and hence the intended integral open-string multiplicity.

III.2.5 NSNS and RR sectors

How can two identical charged branes exchange closed strings without exerting a net force? The bosonic cylinder does not answer this question. For a flat type-II Dp-brane, the closed source has matter fermions, reparametrization ghosts and superghosts as well as X^μ. The distinction between the NSNS and RR sectors changes both the oscillator product and its zero modes. The source frame fixes the fermionic gluing sign through a label $\eta = \pm 1$:

$$\big(\psi_r^\mu - i\eta S^\mu{}_\nu \widetilde{\psi}_{-r}^\nu\big)|B_\psi, \eta\rangle = 0, \qquad r \in \mathbb{Z} + \tfrac{1}{2}\ (\mathrm{NSNS}),\ r \in \mathbb{Z}\ (\mathrm{RR}). \tag{III.2.27}$$

The source uses the same coordinate families for ψ and $\widetilde{\psi}$ as for α and $\widetilde{\alpha}$. Here S is still the tensor defined in (III.2.2), with time Neumann. The nonzero-mode fermion factor has exponent

$$A_\psi(\eta) = i\eta \sum_{r>0} \psi_{-r}^\mu S_{\mu\nu} \widetilde{\psi}_{-r}^\nu. \tag{III.2.28}$$

With the source's choice of vacuum phases the NSNS matter factor is $-ie^{A_\psi}|0\rangle_{\mathrm{NSNS}}$, whereas the RR factor is $-e^{A_\psi}|B_\psi, \eta\rangle_{\mathrm{RR}}^{(0)}$. These overall phases can disappear from a self-overlap but matter when one records the state itself. The RR zero-mode spinor must separately obey the $r = 0$ equation; the exponent in (III.2.28) does not solve it.

In NSNS the first pair has $r = 1/2$; in RR the integer-moded oscillators sit above a separate Clifford zero-mode state. The source phases above belong to these states and cannot be inferred from the nonzero-mode equation alone.

The superghost state also has an ordered left/right picture. For NSNS, both ket and bra use $(-1,-1)$. With (β,γ) and $(\widetilde{\beta},\widetilde{\gamma})$ denoting the two superghost families, its ket factor is

$$|B_{\rm sgh},\eta\rangle_{\rm NS} = \exp\left[i\eta\sum_{r>0}(\gamma_{-r}\widetilde{\beta}_{-r} - \beta_{-r}\widetilde{\gamma}_{-r})\right]|-1\rangle|\widetilde{-1}\rangle. \tag{III.2.29}$$

The RR ket instead uses $(-1/2,-3/2)$. Its chosen vacuum is annihilated by β_0 and $\widetilde{\gamma}_0$; the zero-mode factor is $e^{i\eta\gamma_0\widetilde{\beta}_0}$. The conjugate RR bra uses $(-3/2,-1/2)$ and has the zero-mode factor $e^{-i\eta\beta_0\widetilde{\gamma}_0}$. Displaying their order matters because the overlap pairs these different pictures:

$$\begin{aligned} |B_{\rm sgh},\eta\rangle^{(0)}_{\rm RR} &= e^{i\eta\gamma_0\widetilde{\beta}_0}|-\tfrac{1}{2}\rangle|\widetilde{-\tfrac{3}{2}}\rangle, \qquad \beta_0|0\rangle = \widetilde{\gamma}_0|0\rangle = 0, \\ {}^{(0)}_{\rm RR}\langle B_{\rm sgh},\eta| &= \langle-\tfrac{3}{2}|\langle\widetilde{-\tfrac{1}{2}}|e^{-i\eta\beta_0\widetilde{\gamma}_0}. \end{aligned} \tag{III.2.30}$$

The vacuum symbols in the annihilation relation refer to the ordered RR ket vacuum in the first line. This is a stated source prescription for this cylinder, not a derivation of general picture changing.

The flat type-II GSO-invariant source uses opposite combinations of the two η labels:

$$|B\rangle_{\rm NSNS} = \frac{1}{2}\big(|B,+\rangle_{\rm NSNS} - |B,-\rangle_{\rm NSNS}\big), \qquad |B\rangle_{\rm RR} = \frac{1}{2}\big(|B,+\rangle_{\rm RR} + |B,-\rangle_{\rm RR}\big). \tag{III.2.31}$$

The sourced completion allows even p in type IIA and odd p in type IIB. BRST invariance and these GSO projections are physical inputs to the complete source. The free bosonic commutator calculation cannot derive them. In particular, the plus sign in the RR sum must not be changed simply to make a partial oscillator expression look symmetric. The source projector acts on total worldsheet parity $(-1)^{F+G}$, where F counts matter fermions and G superghosts. In NSNS its convention includes a -1 vacuum shift in F: $(-1)^F|B_\psi,\eta\rangle = -|B_\psi,-\eta\rangle$, while $(-1)^G|B_{\rm sgh},\eta\rangle = |B_{\rm sgh},-\eta\rangle$. These actions give the NSNS difference above; the RR vacuum and parity actions give the RR sum. The orbifold trace below uses its own source symbol F and vacuum convention. We do not identify those two operators.

The effect of the GSO signs can be displayed before performing any spin-sector trace. In the ordered $(+,-)$ basis, the NSNS coefficient vector is $(1,-1)/2$, and the RR vector is $(1,1)/2$. If $A_{\eta\eta'}$ and $R_{\eta\eta'}$ denote the corresponding *complete* overlaps, including ghosts, then the two quadratic forms are

$$\begin{aligned} \mathcal{A}_{\rm NSNS} &= \tfrac{1}{4}(A_{++} + A_{--} - A_{+-} - A_{-+}), \\ \mathcal{A}_{\rm RR} &= \tfrac{1}{4}(R_{++} + R_{--} + R_{+-} + R_{-+}). \end{aligned} \tag{III.2.32}$$

This expansion shows exactly where a changed η sign would enter the amplitude. It does not determine any of the A or R entries, and in particular it does not regularize RR zero modes. The sector combination and the sector overlap are separate operations.

There is a further zero-mode qualification. For zero mixed ND directions, the regulated RR result belongs to the *combined* matter and superghost zero-mode state $|B,\eta\rangle^{(0)}_{\rm RR} = |B_\psi,\eta\rangle^{(0)}_{\rm RR}|B_{\rm sgh},\eta\rangle^{(0)}_{\rm RR}$. The source prescription gives

$$\mathcal{Z}^{(0)}_{\rm RR}(\eta_1,\eta_2) = -16\,\delta_{\eta_1\eta_2,\,1} \qquad \text{(zero ND directions)}. \tag{III.2.33}$$

Neither factor is assigned -16 on its own. Trying to normalize the fermionic zero modes separately and multiplying by an independently regularized superghost result is not this prescription. The sign and factor in (III.2.33) enter the sector comparison represented in Figure III.2.3.

For identical parallel branes there are no mixed ND directions. Specializing the sourced spin-sector amplitudes to this case, define the common measure and zero-mode factor by

$$K(t) = V_{p+1}(8\pi^2\alpha')^{-(p+1)/2}t^{-(9-p)/2}e^{-y^2/(2\pi\alpha' t)}, \qquad q = e^{-\pi t}, \quad y^2 = |\Delta y|^2. \tag{III.2.34}$$

The dt integrands, including the common GSO factor $1/2$ and oscillator denominator, are

$$\frac{d\mathcal{A}_{\rm NSNS}}{dt} = K(t)\frac{f_3(q)^8 - f_4(q)^8}{2f_1(q)^8}, \qquad \frac{d\mathcal{A}_{\rm RR}}{dt} = -K(t)\frac{f_2(q)^8}{2f_1(q)^8}. \tag{III.2.35}$$

The two NSNS numerator terms come from the uninserted and $(-1)^{F+G}$-inserted source sectors. The regulated combined RR zero modes supply the displayed relative sign. These are the source's zero-ND integrands, not a book-unit RR charge.

Define the source products before expanding them:

$$\begin{aligned} f_3(q) &= q^{-1/24}\prod_{n\geq 1}(1+q^{2n-1}),\\ f_4(q) &= q^{-1/24}\prod_{n\geq 1}(1-q^{2n-1}),\\ f_2(q) &= \sqrt{2}\,q^{1/12}\prod_{n\geq 1}(1+q^{2n}). \end{aligned} \tag{III.2.36}$$

The leading oscillator arithmetic can be seen without claiming the whole cancellation. Put $q = e^{-\pi t}$. The standard products have small-q behavior

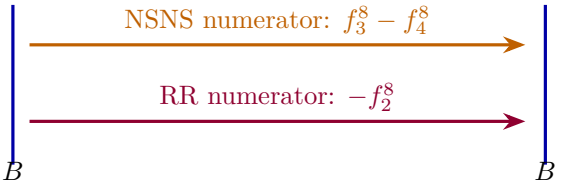
$$\begin{aligned} &f_3(q) = q^{-1/24}(1+q+O(q^3)), \qquad f_4(q) = q^{-1/24}(1-q+O(q^3)), \\ &f_2(q) = \sqrt{2}\,q^{1/12}(1+O(q^2)). \end{aligned} \tag{III.2.37}$$

Expand the two eighth powers before subtracting. Their constant terms cancel; their linear terms add:

$$f_3^8 - f_4^8 = q^{-1/3}\big[(1+8q+\cdots)-(1-8q+\cdots)\big] = 16q^{2/3}+\cdots, \qquad f_2^8 = 16q^{2/3}+\cdots. \tag{III.2.38}$$

These are numerator coefficients, not complete exchange amplitudes: both terms in (III.2.35) also contain $K(t)/(2f_1^8)$. Their first signed difference is $16-16=0$. For

identical parallel BPS sources, the cited all-level Jacobi identity $f_3^8 - f_4^8 - f_2^8 = 0$, together with the stated GSO, zero-mode and physical BPS premises, gives the full cancellation. The leading calculation is a useful control on relative signs, not a proof of the identity or of spacetime supersymmetry. Reversing the RR source orientation for a brane and an antibrane changes the relative exchange sign, so this particular cancellation no longer follows.



identical orientation; full cancellation uses GSO,
combined RR zero modes and the Jacobi identity

Figure III.2.3: The identical-brane cylinder receives NSNS and RR closed exchange with opposite signed contributions. The two displayed numerator functions share $K(t)/(2f_1^8)$; their equal leading coefficients 16 are oscillator arithmetic. The all-level cancellation uses the sourced GSO, combined RR zero-mode prescription and Jacobi identity. Reversing the RR source orientation changes this relative sign.

An absolute RR source coefficient is another question. A free spacetime kinetic action can contain a convention-dependent coefficient α_p, and factorization then fixes a combination such as μ_p^2/α_p, not μ_p without a field normalization. The source bosonic T_p, its N_p, the book's τ_p, and a source RR coefficient cannot be identified by renaming them. The comparison with a physical brane action in Chapter 3 begins after the dilaton and RR field normalizations are specified. This separation also matters for twisted fields, whose kinetic terms need their own normalization.

III.2.6 Orbifold boundary states

How does a brane at an orbifold fixed locus source a twisted closed string? Consider $\mathbb{C}^2/\mathbb{Z}_2$, with generator $g : (z_1, z_2) \mapsto (-z_1, -z_2)$. A third complex coordinate, when present in a $\mathbb{C}^3$ embedding, is a spectator. There are two one-dimensional Chan–Paton representations, $\chi_+(g) = +1$ and $\chi_-(g) = -1$, both with $\chi_\pm(1) = 1$. The brane lies at the fixed locus, so untwisted and twisted closed sectors can both couple to it.

Call the source-defined sector states $|T_1\rangle$ and $|T_g\rangle$. These symbols are not unit-normalized vectors. Each is fixed through a separate NSNS and RR comparison to a g-inserted open trace. In the source's oriented convention the schematic equality, with the source factors displayed, is

$$2\int_0^\infty \frac{dt}{2t}\,\mathrm{Tr}_{\mathrm{NS-R}}\left[\frac{g}{|\Gamma|}\,\frac{1+(-1)^F}{2}\,e^{-2\pi t H_o}\right] = \langle T_g|\Delta|T_g\rangle, \qquad |\Gamma| = 2. \tag{III.2.39}$$

Here H_o is the open Hamiltonian, F the open worldsheet fermion number, and the trace includes zero modes and oscillators. The displayed 2 counts oriented endpoint orderings; the $|\Gamma|^{-1}$ is the orbifold average; the last $1/2$ is GSO. The $\mathrm{NS}-\mathrm{R}$ notation means a signed spin-sector combination, not a single unprojected trace. The source propagator and its closed modulus l are

$$\Delta = \pi\alpha' \int_0^\infty dl\, e^{-2\pi l H_c}. \tag{III.2.40}$$

These periods differ from the bosonic calculation above. In the source's D0 illustration, the explicit Appendix matching uses $t = 1/(2l)$. We do not transfer that D0 absolute coefficient or modulus to a D3 example.

The three factors outside the spin trace in (III.2.39) have separate origins. The orbifold average is $1/2$, the oriented endpoint count is 2, and the GSO projector contributes $1/2$. Their product is $1/2$ before the remaining trace and propagator are evaluated. Dropping the orientation factor would halve a sector overlap even though its character signs would be unchanged. A vanishing supersymmetric sum would conceal precisely this normalization error. This is why the source compares NSNS and RR terms individually.

Why keep the spin pieces separate if a supersymmetric total self-overlap can vanish? If $\langle T_g|\Delta|T_g\rangle = 0$, replacing $|T_g\rangle$ by $\lambda|T_g\rangle$ still gives zero for any λ. The vanishing sum cannot fix a sector normalization. The source fixes the separate NSNS and RR pieces by their separate open/closed terms, including the factors in (III.2.39). In the source's $\mathbb{Z}_N$ notation, N is the group order and k labels the twisted sector. Its special $k = N/2$ sector uses an *η-plus* NSNS combination. Here $N = 2$ and $k = 1$, so importing the flat NSNS minus sign of (III.2.31) would change the source state.

The open string from a brane of type a to one of type b has a Chan–Paton matrix Λ_{ab}. The group acts on it by $\gamma_a(g)\Lambda_{ab}\gamma_b(g)^{-1}$, while g also acts on its oscillators. Thus its physical projector is

$$P_{ab} = \frac{1}{2}\left(1 + \gamma_a(g)(\,\cdot\,)\gamma_b(g)^{-1} g_{\mathrm{osc}}\right). \tag{III.2.41}$$

For $a = +$, $b = -$, the CP factor is -1; on an oscillator eigenstate of parity $\epsilon = \pm 1$,

$$P_{+-}\big|_\epsilon = \frac{1}{2}(1-\epsilon), \qquad \dim_{\text{projected}}(\text{even}) = 0, \quad \dim_{\text{projected}}(\text{odd}) = 1 \tag{III.2.42}$$

per one-dimensional oscillator eigenspace. This integer test depends on the actual CP action, not merely on a diagram of two fractional sources. The reverse $-+$ string has the same character product. For $++$ or $--$, the CP product is $+1$, so even oscillator parity survives instead.

The regular Chan–Paton representation gives an independent matrix check. In the ordered $(+,-)$ basis choose $\gamma_{\mathrm{reg}}(g) = \mathrm{diag}(1,-1)$. Conjugation on its four matrix units gives

$$g_{\mathrm{CP}} : (E_{++}, E_{+-}, E_{-+}, E_{--}) \longmapsto (+E_{++}, -E_{+-}, -E_{-+}, +E_{--}). \tag{III.2.43}$$

The endpoint representation has $\mathrm{Tr}\,\gamma_{\mathrm{reg}}(1,g) = (2,0)$. The displayed conjugation action on $\mathrm{End}(\mathbb{C}^2)$ instead has character $(4,0)$. Even oscillator parity keeps the two

diagonal units, while odd parity keeps the two off-diagonal units. These are integer open multiplicities. The same regular character has no twisted closed component in (III.2.45), connecting the open matrix projection to the closed source sum.

In the spin-resolved sector basis just defined, the character formula for fractional sources is

$$|B_a\rangle = \sum_{h\in\{1,g\}} \chi_a(h)|T_h\rangle, \qquad |B_+\rangle = |T_1\rangle + |T_g\rangle, \quad |B_-\rangle = |T_1\rangle - |T_g\rangle. \tag{III.2.44}$$

Their sum is the regular source,

$$|B_{\rm reg}\rangle = |B_+\rangle + |B_-\rangle = 2|T_1\rangle + 0|T_g\rangle. \tag{III.2.45}$$

The two fractional branes have opposite twisted components, so the regular representation has no twisted source in this basis. Figure III.2.4 shows the cancellation. The numbers $1, \pm 1$ are relative character coefficients after the sector states have been normalized by their individual overlaps; they are not an extra $1/\sqrt{2}$ convention and do not fix an absolute twisted RR charge or geometric tension.

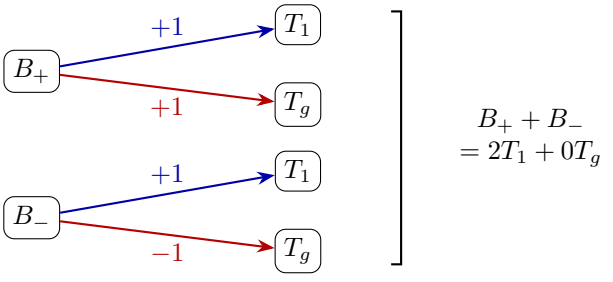


Figure III.2.4: The two $\mathbb{Z}_2$ characters weight the same untwisted sector equally and the twisted sector with opposite signs. Adding the two sources gives the regular representation and removes its twisted component. Sector widths are schematic and imply no absolute charge normalization.

This construction is the local source ingredient for twisted RR tadpoles and fractional-brane quivers in Volume V. It establishes relative sector components and the finite CP projector. A complete spacetime RR charge needs the twisted-field kinetic normalization, and a general boundary-CFT classification requires further hypotheses. The finite open/closed consistency condition here is the spin-resolved overlap (III.2.39) and the projector (III.2.41).

III.2.7 Exercises

The five numbered tasks have submitted-answer fields in the companion question file. Work the algebra before submitting the fields. The explanations requested after each calculation are written exercises; they are not part of the exact-answer grade.

1. **E1, spacelike gluing.** At mode $n = 2$, solve for the coefficient of $\alpha_{-2}\widetilde{\alpha}_{-2}$ separately for one positive-metric NN and one positive-metric DD direction. Use (III.2.6) and submit `nn_coefficient` and `dd_coefficient`. Explain in writing why the two-upper-index time coefficient is different although time remains NN.

2. **E2, zero-mode support.** Take two NN coordinates and two DD coordinates with normal brane position $y = (3/2, -5/3)$. Submit their ordered zero-mode support in the `neumann_momentum` and `dirichlet_position` fields of the public schema. Explain why the DD momenta are integrated in a closed exchange rather than set to zero.

3. **E3, the bosonic cylinder.** For parallel bosonic D3-branes, transform the open expression with $t = 1/\tau$ and $f_1(e^{-\pi/t}) = \sqrt{t} f_1(e^{-\pi t})$. Submit the power inside dt/t, the source ratio N_p/T_p, and the oriented endpoint factor. Explain separately how the longitudinal Gaussian, oscillator modular weight and measure produce your power. If $a = 3/2$, write the transformed separation exponential and explain its short-t behavior; this exponential and explanation are not submitted fields.

4. **E4, $\mathbb{Z}_2$ sources and projector.** With $\chi_+(g) = 1$, $\chi_-(g) = -1$, submit the ordered untwisted/twisted components of both fractional sources and their regular sum. For a $+-$ open string, submit the surviving even and odd multiplicities per one-dimensional oscillator eigenspace. Explain why the zero total supersymmetric self-overlap would not have determined these normalizations.

5. **E5, first no-force coefficient.** Expand $f_3^8 - f_4^8$ and f_2^8 to their first $q^{2/3}$ terms. Submit their coefficients and the signed difference. State in writing which physical and all-level inputs are still required to conclude no force.

Take-home message

A brane endpoint becomes a closed-string pair source when the cylinder is read across its rims. Oscillator gluing determines its form; zero-mode support localizes it; matching the complete two-channel amplitude fixes its normalization. In type II, the NSNS and RR pieces require their own GSO, picture and combined zero-mode prescriptions. At an orbifold fixed locus, characters weight spin-resolved untwisted and twisted sources, and the regular sum removes the twisted component. A reader should now be able to solve one-mode gluing, evaluate the transverse Gaussian, track the cylinder prefactor, check a leading NSNS/RR coefficient, and compute a $\mathbb{Z}_2$ CP projection.

Status and sources

The rotated boundary conditions, oscillator gluing and support in Sections III.2.2 and III.2.3 follow Di Vecchia and Liccardo (1999, physical PDF pp. 30–34, eqs. (6.169)–(6.190)). The BCH residual, metric-lowered timelike example and Fourier Gaussian are algebraic [MATH] calculations in that source frame. The ghost and BRST completion of the boundary state are sourced worldsheet inputs [WS], not consequences of the scalar commutator. The support equations are distributional.

Section III.2.4 uses Di Vecchia and Liccardo (1999, physical PDF pp. 34–37, eqs. (6.190), (6.196), (6.202)–(6.205)). The transverse Gaussian, propagator/radial/angular factors, oriented endpoint 2, modular power and coefficient equality are displayed explicitly above [MATH]. The source's $N_p = T_p/2$ is a positive-phase critical-bosonic result. The bosonic tachyon limits the integrated-force interpretation. Neither that T_p nor its N_p is the book's type-II τ_p, with the physical tension normalized separately.

The flat type-II fermion and superghost states, their phases, ordered pictures and GSO signs in Section III.2.5 follow Di Vecchia and Liccardo (1999, physical PDF p. 8, eqs. (2.42)–(2.43), pp. 41, 44–46, eqs. (7.230)–(7.265)). The regulated *combined* RR zero-mode overlap and identical-brane cancellation follow Di Vecchia and Liccardo (1999, physical PDF pp. 49–50, eqs. (9.282)–(9.290)). The leading $16 - 16$ coefficient is a bounded algebraic [MATH] check. GSO, BRST, the regulator, the full Jacobi identity and BPS interpretation remain sourced [WS] and [DEC] premises. The dependence of RR charge on its kinetic normalization, and the unresolved historical comparison, are explicit in Polchinski (1995, physical PDF pp. 6–7, eqs. (12)–(16)). No numerical book RR charge follows from this cylinder.

The spin-resolved $\mathbb{C}^2/\mathbb{Z}_2$ sector overlap, source propagator, character formula and CP projector in Section III.2.6 follow Takayanagi (1999, physical PDF pp. 4–5, eqs. (3.1)–(3.7), pp. 15–18, eqs. (A.10)–(A.20)). Its $k = N/2$ twisted NSNS sign is plus, including $\mathbb{Z}_2$; the flat NSNS sign is not transferred. The Appendix's absolute D0 example and its $t = 1/(2l)$ map remain source-local. Character addition and the mixed CP projector are exact finite [MATH] statements. Twisted-field kinetic normalization, general Cardy classification, orientifold amplitudes and full disk interactions are outside this chapter. The original Cardy article was identified bibliographically but was not read or used as a scientific anchor. The metric, tension, orbifold and gauge-group conventions are as stated in the chapter.

References

Di Vecchia, P. and A. Liccardo (1999). *D Branes in String Theory, I.* arXiv: `hep-th/9912161`.

Polchinski, J. (1995). *Dirichlet-Branes and Ramond-Ramond Charges.* arXiv: `hep-th/9510017`.

Takayanagi, T. (1999). *String Creation and Monodromy from Fractional D-branes on ALE spaces.* arXiv: `hep-th/9912157`.

Chapter III.3

D-brane effective actions: DBI and Chern–Simons/WZ couplings

III.3.1 One brane, two responses

Imagine bending a D-brane and threading a compact part of it with magnetic flux. The bend changes its proper area. The flux changes both its energy and the Ramond–Ramond (RR) fields to which it couples. These are two distinct responses of the same worldvolume. The Dirac–Born–Infeld (DBI) action measures the local cost of the induced geometry and gauge field; the Wess–Zumino (WZ) action measures oriented RR source charge. A later brane construction may use a gauge coupling, a dissolved lower brane charge, or a three-dimensional Chern–Simons level. This chapter shows which part of the worldvolume action supplies each quantity and tracks the factors that make the answers comparable.

We use mostly-plus spacetime signature and write $\lambda = 2\pi\alpha'$. A Dp-brane has spatial dimension p and a $(p+1)$-dimensional worldvolume. The string coupling is the constant asymptotic value $g_s = e^{\Phi}$ where a constant-dilaton calculation is made. Orientations and the choice of gauge-field coordinate will be stated where they affect an answer. Chapter 1 introduced the endpoint gauge field and transverse massless scalars; Chapter 2 described a brane as a source for closed strings. Here those data become coefficients in a low-energy action. Chapter 5 will revisit the global meaning of the charge read from flux.

The disk-derived abelian action and its RR normalization are inputs. We derive the consequences that can be obtained by expanding a determinant, integrating a normalized form, or reducing a leading local term. We use the abelian action for slowly varying field strength and slowly varying scalar gradients; the quadratic approximation also requires small fields. These conditions matter whenever a seemingly simple coefficient is exported to a brane construction.

III.3.2 Pullback geometry and the gauge-invariant field

What metric does a bent brane feel? Let ξ^a, $a = 0, \ldots, p$, be worldvolume coordinates and $X^M(\xi)$ its embedding into spacetime. For the string-frame bulk metric G_{MN}, the induced tensor is the pullback

$$P[G]_{ab} = G_{MN}(X)\, \partial_a X^M \partial_b X^N. \tag{III.3.1}$$

The same operation applies to the bulk two-form B: $P[B]_{ab} = B_{MN}(X)\partial_a X^M \partial_b X^N$. The notation is geometric rather than cosmetic. The bulk fields are evaluated on the moving brane, and their indices are contracted with its tangent vectors. Figure III.3.1 keeps these two maps visible.

Choose local static gauge $X^a = \xi^a$, and denote the physical transverse coordinates by $X^i = \lambda\Phi^i$. The endpoint scalar Φ^i is therefore a position divided by a length squared. Splitting the bulk indices into tangent and normal directions gives the expansion

$$P[G]_{ab} = G_{ab} + G_{ai}\partial_b X^i + G_{ib}\partial_a X^i + G_{ij}\partial_a X^i \partial_b X^j. \tag{III.3.2}$$

In orthogonal flat coordinates $G_{ai} = 0$ and $G_{ij} = \delta_{ij}$, so the familiar metric becomes

$$P[G]_{ab} = \eta_{ab} + \partial_a X^i \partial_b X_i = \eta_{ab} + \lambda^2 \partial_a \Phi^i \partial_b \Phi_i. \tag{III.3.3}$$

Thus the kinetic term of a transverse scalar will arise from proper worldvolume area. It is not a separate geometrical guess.

For example, take a flat 1+1 portion of the brane and one transverse coordinate $X = u\xi^1$. The tangent along ξ^1 has squared length $1+u^2$, and a coordinate segment $d\xi^1$ has proper length $\sqrt{1+u^2}\, d\xi^1$. If instead $X = v\xi^0$, then $P[G]_{00} = -1 + v^2$, giving the proper-time factor $\sqrt{1-v^2}$ for $|v| < 1$. These are different signs from the same pullback rule. Both slopes are dimensionless derivatives of a physical coordinate; replacing X by Φ without the factor λ would spoil the kinetic normalization.

The slope and motion can be combined without assuming that the induced metric stays diagonal. For $X = v\xi^0 + u\xi^1$, its mixed component is $P[G]_{01} = uv$. Keeping it gives

$$P[G]_{ab} = \begin{pmatrix} -1+v^2 & uv \\ uv & 1+u^2 \end{pmatrix}, \qquad -\det P[G] = 1 + u^2 - v^2. \tag{III.3.4}$$

The two u^2v^2 terms cancel between the diagonal product and the square of the mixed entry. Dropping $P[G]_{01}$ would leave a spurious quartic term. At $u = 3/4$, $v = 1/2$, the proper area density is $\sqrt{1 + 9/16 - 1/4} = \sqrt{21}/4$. A spatial slope increases area; temporal motion decreases proper time. Both effects will appear in one DBI square root.

The endpoint also carries an abelian connection one-form A, with $F = dA$. Why does a bulk B-field enter with this endpoint field? Under a local bulk gauge transformation $\delta B = d\zeta$, the open-string boundary term changes by the pullback of ζ. Its cancellation requires the boundary connection to transform as

$$\delta A = -\frac{P[\zeta]}{\lambda}, \qquad \delta F = -\frac{dP[\zeta]}{\lambda}. \tag{III.3.5}$$

Pullback commutes with the exterior derivative. Consequently the worldvolume two-form entering the action is

$$\mathcal{F} = P[B] + \lambda F, \qquad \delta\mathcal{F} = P[d\zeta] - dP[\zeta] = 0. \tag{III.3.6}$$

This is a local gauge statement. On overlapping patches, the potentials have transition data, and a bare integral of F need not by itself be a complete global charge. We return to the restricted charge calculation below and leave the global completion to Chapter 5.

The cancellation can also be seen directly in coordinates. On a planar patch let $\zeta = h\xi^1 d\xi^2$, with constant h. Then $d\zeta = h\, d\xi^1 \wedge d\xi^2$. The boundary shift $\delta A = -(h/\lambda)\xi^1 d\xi^2$ has curvature $\lambda d(\delta A) = -h\, d\xi^1 \wedge d\xi^2$. The local B-component rises by h and the local λF-component falls by h. This is a calculation with potentials on a patch. It does not assert that one ζ or A exists over a compact flux cycle.

There is a simple numerical check of the transformation. On a flat (ξ^1, ξ^2) patch take $B_{12} = b_0$ and $\lambda F_{12} = f_0$. A gauge shift that changes the local B_{12} component by Δ changes λF_{12} by $-\Delta$. The two entries separately depend on the potential choice, while $\mathcal{F}_{12} = b_0 + f_0$ does not. For example, $(b_0, f_0) = (3/5, -1/5)$ and a shift $\Delta = 2/5$ give $(1, -3/5)$; both have $\mathcal{F}_{12} = 2/5$. This small example will prevent us from treating F as the sole observable when we later restore B.

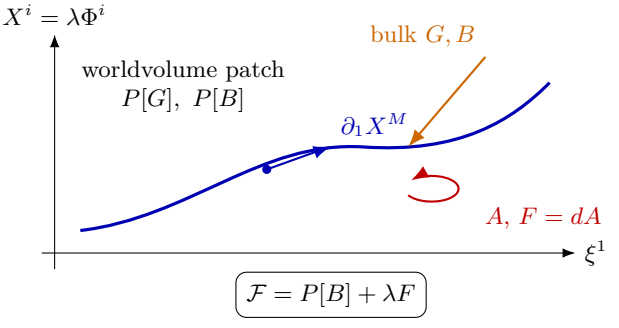


Figure III.3.1: A worldvolume coordinate patch bends into a transverse physical coordinate $X^i = \lambda\Phi^i$. Tangent vectors $\partial_a X^M$ pull bulk tensors onto the brane. The endpoint connection contributes λF to the local invariant two-form $P[B] + \lambda F$; the drawing fixes no global flux quantization.

The pullback, rather than a flat metric inserted by hand, is what the DBI square root must contain. In a curved or time-dependent background every tensor in the next section is evaluated on the embedding. Our explicit determinants use the flat local frame, where the role of each sign can be seen without concealing it in coordinates.

III.3.3 DBI at quadratic order

How does a single action produce the scalar and Maxwell kinetic terms? In the book RR charge frame define

$$\mu_p = \frac{1}{(2\pi)^p(\alpha')^{(p+1)/2}}, \qquad \tau_p = \frac{\mu_p}{g_s}, \qquad \lambda = 2\pi\alpha'. \tag{III.3.7}$$

Here μ_p is the RR source coefficient and τ_p the physical tension at constant dilaton. The sourced slowly varying abelian DBI action uses this string-frame metric and is

$$S_{\rm DBI} = -\mu_p \int d^{p+1}\xi\, e^{-\Phi}\sqrt{-\det\bigl(P[G]_{ab} + \mathcal{F}_{ab}\bigr)}. \tag{III.3.8}$$

At $e^{\Phi} = g_s$, its prefactor is τ_p. Multiplying τ_p by another $e^{-\Phi}$ would count the same asymptotic dilaton twice. Equation (III.3.8) is a disk-level worldvolume premise, not a theorem obtained from the determinant algebra that follows. In particular, slowly varying means that derivative corrections in F and second derivatives of the embedding are being set aside.

Set $B = 0$ and use the flat static-gauge metric from (III.3.3). Write $H_{ab} = \partial_a X^i \partial_b X_i$ and $M^a{}_b = \eta^{ac}(H_{cb} + \lambda F_{cb})$. Then

$$\sqrt{-\det(\eta + H + \lambda F)} = \sqrt{\det(1+M)} = 1 + \frac{1}{2}\operatorname{tr} M + \frac{1}{8}(\operatorname{tr} M)^2 - \frac{1}{4}\operatorname{tr}(M^2) + \cdots . \tag{III.3.9}$$

The tensor H is already quadratic in scalar first derivatives. The antisymmetry of F gives $\operatorname{tr}(\eta^{-1}F) = 0$, while contraction with the mostly-plus metric gives $\operatorname{tr}[(\eta^{-1}F)^2] = -F_{ab}F^{ab}$. Keeping only terms quadratic in ∂X or λF therefore yields

$$\sqrt{-\det(\eta + H + \lambda F)} = 1 + \frac{1}{2}\partial_a X^i \partial^a X_i + \frac{\lambda^2}{4} F_{ab}F^{ab} + O\bigl((\partial X)^4, F^4, (\partial X)^2 F^2\bigr). \tag{III.3.10}$$

Odd powers of a lone antisymmetric F cannot contribute to this quadratic result; the scalar term first enters through $\operatorname{tr} H$. When this square root is multiplied by $-\tau_p$, a time derivative of a scalar has positive kinetic energy, as does an electric field.

The determinant formula can be reconstructed without memorizing a square-root identity. Write $\det(1+M) = \exp\{\operatorname{tr}\log(1+M)\}$, expand $\log(1+M) = M - M^2/2 + O(M^3)$, and expand the outer exponential. This gives

$$\begin{aligned} \log\sqrt{\det(1+M)} &= \frac{1}{2}\operatorname{tr} M - \frac{1}{4}\operatorname{tr} M^2 + O(M^3), \\ \sqrt{\det(1+M)} &= 1 + \frac{1}{2}\operatorname{tr} M + \frac{1}{8}(\operatorname{tr} M)^2 \\ &\quad - \frac{1}{4}\operatorname{tr} M^2 + O(M^3). \end{aligned} \tag{III.3.11}$$

Now count H as second order in ∂X and λF as first order in field strength. At the required order, $\operatorname{tr} M = \operatorname{tr}(\eta^{-1}H)$ and $\operatorname{tr} M^2 = \lambda^2 \operatorname{tr}[(\eta^{-1}F)^2]$. A cross term with one H and one F is cubic in these small quantities and also vanishes as the contraction of

symmetric and antisymmetric tensors. This order counting explains the scalar one-half and gauge one-quarter coefficients even though the fields enter the same square root. At higher order the gauge and induced-metric terms do mix.

An exact small-block calculation tests both signs and shows what the series omitted. Put $u = \partial_1 X$ and $e = \lambda F_{01}$ on a 1+1 subspace. The two-form has $F_{10} = -F_{01}$, so

$$\big(P[G] + \lambda F\big)_{0,1} = \begin{pmatrix} -1 & e \\ -e & 1+u^2 \end{pmatrix}, \qquad \det\big(P[G] + \lambda F\big) = -(1 + u^2 - e^2). \quad \text{(III.3.12)}$$

At the deliberately nonunit values $u = 3/5$, $e = 2/5$, the quantity under the square root is $1 + 9/25 - 4/25 = 6/5$. The quadratic series instead gives $1 + u^2/2 - e^2/2 = 11/10$; the exact value is $\sqrt{6/5}$. The difference is a higher-field correction, not a failed electric sign. Since $F_{ab}F^{ab} = -2F_{01}^2$ here, (III.3.10) indeed contributes $-e^2/2$ inside the square root.

The exact block also explains the signs in the action. At fixed $u = 0$, $\sqrt{1 - e^2} = 1 - e^2/2 + O(e^4)$. Multiplication by $-\tau_p$ gives $+\tau_p e^2/2$ in the Lagrangian, as expected from $-F^2/(4g^2)$. At fixed $e = 0$, $\sqrt{1 + u^2} = 1 + u^2/2 + O(u^4)$, so the Lagrangian contains $-\tau_p u^2/2$, the spatial-gradient part of scalar kinetics. The sign of energy cannot be read from one square-root coefficient without the overall negative action and Lorentzian contraction.

A magnetic component checks the other sign without appealing to analytic continuation. On a flat 2+1 block set $b = \lambda F_{12}$ as well as the preceding u, e. Direct expansion along the first row gives

$$\det \begin{pmatrix} -1 & e & 0 \\ -e & 1+u^2 & b \\ 0 & -b & 1 \end{pmatrix} = -(1 + u^2 + b^2 - e^2), \qquad \sqrt{-\det} = 1 + \frac{u^2 + b^2 - e^2}{2} + O(4). \quad \text{(III.3.13)}$$

For $(u, e, b) = (3/5, 2/5, 4/5)$, the exact radicand is $1 + 9/25 + 16/25 - 4/25 = 46/25$, positive and larger than the pure-slope result. The b^2 contribution is the local magnetic energy. Figure III.3.2 displays the tensor entries whose relative signs produce it.

The square root also has a domain visible in this elementary example: for the static slope block it is real only while $e^2 \le 1 + u^2 + b^2$. We use the expansion strictly near zero fields, not as an exact effective description at a critical electric field. The next question is which gauge coupling its Maxwell term defines.

III.3.4 The trace normalization

Why do two familiar D3 gauge couplings differ by a factor of two? For one brane, take A to be the connection to which a unit-charge endpoint couples. Its field strength is $F = dA$. The gauge term of (III.3.10) is

$$S_{U(1),2} = -\frac{\tau_p \lambda^2}{4} \int d^{p+1}\xi \, F_{ab}F^{ab} = -\frac{1}{4g^2_{U(1),\mathrm{int}}} \int F_{ab}F^{ab}, \quad g^2_{U(1),\mathrm{int}} = \frac{1}{\tau_p \lambda^2}. \quad \text{(III.3.14)}$$

$a, b \in \{0, 1, 2\}$: row and column indices

$$P[G] + \lambda F = \begin{pmatrix} -1 & e & 0 \\ -e & 1+u^2 & b \\ 0 & -b & 1 \end{pmatrix}$$

time $-$ $\qquad F_{ab} = -F_{ba}$ $\qquad$ slope u^2

$$-\det(P[G] + \lambda F) = 1 + u^2 + b^2 - e^2$$

Figure III.3.2: The flat $(0, 1, 2)$ block used in (III.3.13). A physical transverse slope raises the 11 metric entry, while electric and magnetic two-form entries occur in antisymmetric pairs. Its determinant is $-[1 + u^2 + b^2 - e^2]$; the picture is a sign guide, not an independent action derivation.

The subscript "int" recalls that periods of this connection are normalized for integer endpoint charge. It is a coordinate choice with physical content when flux is integrated; we will not silently replace it by a rescaled generator component.

For a stack, only the leading quadratic matrix kinetic term is needed here. Write a Hermitian matrix connection $A = A^a T^a$, where a is a gauge-generator index, with $\mathrm{Tr}_f(T^a T^b) = \delta^{ab}/2$. The book component convention is $S_{\mathrm{YM}} = -\int F^a_{\mu\nu} F^{a\,\mu\nu}/(4g^2_{\mathrm{book}})$. Here $\mu, \nu = 0, \ldots, p$ are worldvolume indices, distinct from the generator index a. At this order the disk coefficient is

$$-\frac{\tau_p \lambda^2}{4}\,\mathrm{Tr}_f\, F_{\mu\nu} F^{\mu\nu} = -\frac{\tau_p \lambda^2}{8} F^a_{\mu\nu} F^{a\,\mu\nu}, \qquad \frac{1}{g^2_{\mathrm{book}}} = \frac{\tau_p \lambda^2}{2}. \tag{III.3.15}$$

The factor of one half comes entirely from the fundamental trace, before any dimensional reduction or duality. Substituting (III.3.7) gives

$$g^2_{\mathrm{book}} = \frac{2}{\tau_p \lambda^2} = 2(2\pi)^{p-2} g_s (\alpha')^{(p-3)/2}, \qquad g^2_{U(1),\mathrm{int}} = \frac{g^2_{\mathrm{book}}}{2}. \tag{III.3.16}$$

This leading trace statement is sufficient to compare kinetic coefficients. It does not postulate an exact nonabelian DBI determinant with a particular trace prescription.

Dimensions provide a second check. Since $\tau_p \sim (\alpha')^{-(p+1)/2}$ and $\lambda^2 \sim (\alpha')^2$, the coupling has

$$[g^2_{\mathrm{book}}] = [\tau_p^{-1} \lambda^{-2}] = \mathrm{length}^{p+1-4} = \mathrm{length}^{p-3}. \tag{III.3.17}$$

The D3 coupling is dimensionless; the D6 coupling has dimension length^3. Integrating a D6 zero mode across a physical length will give a six-dimensional coupling of dimension length^2. This catches a common indexing error: seven worldvolume dimensions come from $p = 6$, not $p = 7$. Dimensions do not fix the numerical factor of two; the trace does.

For a rank-one matrix, the normalized Lie-algebra generator is $T = 1/\sqrt{2}$. If a is the integer-charge identity connection, write $A = A^0 T = a\mathbf{1}$; hence $A^0 = \sqrt{2}\, a$ and

$F^0 = \sqrt{2}\, f$. Indeed,

$$-\frac{(F^0)^2}{4g^2_{\text{book}}} = -\frac{2f^2}{4g^2_{\text{book}}} = -\frac{f^2}{4g^2_{U(1),\text{int}}}. \tag{III.3.18}$$

The two displayed couplings refer to different coordinates on the same quadratic action. A unit-charged endpoint couples to a, and $\int f/(2\pi)$, rather than $\int F^0/(2\pi)$, is the integer period used in the WZ example.

Check the conversion backward. Begin with the integer connection a and set $A^0 = \sqrt{2}a$. Its component action becomes $-2f^2/(4g^2_{\text{book}})$. Equality with the single-brane disk term $-\tau_p\lambda^2 f^2/4$ requires $2/g^2_{\text{book}} = \tau_p\lambda^2$, exactly (III.3.15). Starting from the connection whose holonomy and flux are specified makes the factor of two transparent. It prevents a generator normalization from turning an integer period into $\sqrt{2}$ times an integer.

At $p = 3$, $g^2_{\text{book}} = 4\pi g_s$ and $g^2_{U(1),\text{int}} = 2\pi g_s$. Choose the nonunit $g_s = 3/2$: the two values are 6π and 3π, and their ratio is two. A reader who obtains 3π for the book component coupling has likely omitted the half-trace, while a reader who obtains 6π for the unit-charge connection has silently changed the flux coordinate. This distinction is particularly important when Chapters 4 and 5 use the same field both in a Yang–Mills term and in a charge integral.

Different primary accounts distribute the asymptotic dilaton among symbols differently. In the book frame, μ_p is the RR charge coefficient and $\tau_p = \mu_p/g_s$. A convention with shifted dilaton $\phi_\infty = 0$ and rescaled RR potentials $C_{\text{source}} = g_s C_{\text{book}}$ can write equal-looking source tension and charge coefficients $T_{p,\text{source}} = \mu_{p,\text{source}} = \mu_{p,\text{book}}/g_s$. Myers states the string-frame metric and dilaton profile before this normalization, and gives the equal tension/charge coefficients later. The WZ product $\mu_{p,\text{source}} C_{\text{source}}$ then equals $\mu_{p,\text{book}} C_{\text{book}}$. This algebra translates the restricted RR-potential units; it does not change a physical RR charge. Likewise, if a printed final expression drops g_s while the same source has $\tau_p = \mu_p/g_s$, the dimensional identity $g^2 = 1/(\tau_p\lambda^2)$ and the explicit tension fix the comparison. The cylinder discussion of Chapter 2 fixes a source in its own RR kinetic frame, not an unqualified absolute μ_p.

III.3.5 WZ couplings and lower charge

How can a Dp-brane become a source for a lower RR potential without ceasing to be a Dp-brane? Let $C = \sum_q C_q$ denote the RR potential polyform in the book charge frame. The sourced leading abelian WZ term selects the worldvolume top-form from

$$S_{\text{WZ}} = \mu_p \int_{W_{p+1}} \big[P[C] \wedge e^{\mathcal{F}}\big]_{p+1}, \qquad \mathcal{F} = P[B] + \lambda F. \tag{III.3.19}$$

The orientation of W_{p+1} is part of this integral. Expanding the exponential by degree makes the first three source channels clear:

$$\big[P[C]e^{\mathcal{F}}\big]_{p+1} = P[C_{p+1}] + P[C_{p-1}] \wedge \mathcal{F} + \frac{1}{2}P[C_{p-3}] \wedge \mathcal{F} \wedge \mathcal{F} + \cdots. \tag{III.3.20}$$

Each factor of a two-form lowers the potential degree by two, so every term remains a $(p+1)$-form on the same brane. The one-half in the third term is the exponential

coefficient; it will matter for the D4 Chern–Simons reduction. Figure III.3.3 shows the degree count and the selected orientation, rather than depicting actual separated lower branes.

For $p = 4$, the first three degrees are concrete: C_5, $C_3 \wedge \mathcal{F}$, and $C_1 \wedge \mathcal{F}^2/2$. They couple, respectively, to a five-form potential, a three-form with one two-form insertion, and a one-form with two insertions. The last is the term later reduced on $M_3 \times C$. Form-degree counting alone does not assign an integer lower charge. That also needs μ_p, the period of the connection, and the product orientation. In the restricted $B = 0$ frame, the D4 terms can be written with their coefficients exposed:

$$S_{\mathrm{D4,WZ}} = \mu_4 \int_{W_5} \left[C_5 + \lambda C_3 \wedge F + \frac{\lambda^2}{2} C_1 \wedge F \wedge F + \cdots \right]. \tag{III.3.21}$$

The first flux term is linear in the integer-charge connection; the second is quadratic and carries the factor that will survive the wrapped reduction.

Set $B = 0$ and take an oriented compact two-cycle Σ inside the brane. Suppose the unit-charge connection has integral period $\int_\Sigma F/(2\pi) = n$. From the charge units in (III.3.7),

$$\frac{\mu_p \lambda}{\mu_{p-2}} = \frac{(2\pi\alpha')(2\pi)^{p-2}(\alpha')^{(p-1)/2}}{(2\pi)^p(\alpha')^{(p+1)/2}} = \frac{1}{2\pi}. \tag{III.3.22}$$

Suppose $W_{p+1} = W_{p-1} \times \Sigma$ with the indicated product orientation. For the factorized action below, the external RR potential pulled back to the brane is itself pulled back from W_{p-1}, or we extract its compact zero-mode coupling; the contributing F has its two legs on Σ. Integrating that internal flux over the stated product fiber gives

$$\mu_p \lambda \int_{W_{p-1}\times\Sigma} P[C_{p-1}] \wedge F = \mu_{p-2} \left(\frac{1}{2\pi} \int_\Sigma F \right) \int_{W_{p-1}} P[C_{p-1}] = n\mu_{p-2} \int_{W_{p-1}} P[C_{p-1}]. \tag{III.3.23}$$

The lower charge is a worldvolume flux source. The computation identifies its RR coupling, not a new localized geometric position for n lower branes. It also shows why the charge coefficient has no extra g_s^{-1}: the WZ coefficient is μ_p, whereas the constant-dilaton DBI tension is μ_p/g_s. A nonuniform external test potential along Σ instead weights the local flux distribution: two flux profiles with the same integral n can have different couplings to that probe. Their total integrated lower charge remains n.

The ratio is independent of p, provided $p \geq 2$ so the lower potential exists in this sequence of WZ form degrees. For D2, $\mu_2\lambda/\mu_0 = 1/(2\pi)$: one oriented unit of flux gives one D0 source unit. For D4, the same arithmetic gives D2 source charge from $C_3 \wedge F$. Its next term has a different coefficient because two factors of F bring the exponential factor $1/2!$. This is why the exponential must be expanded before comparing a D4 term to a normalized Chern–Simons action. The mnemonic that each flux lowers the RR potential degree by two does not determine all coefficients.

For example, take $n = -3$ on a positively oriented parent Dp-brane. Its induced D$(p-2)$ source is -3 in μ_{p-2} units. Reverse the parent brane orientation while holding the two-cycle and the displayed flux-coordinate convention fixed. The WZ integral changes sign, giving $+3$. Reversing the cycle orientation at the same time would also

change the written period; therefore sign statements need the orientation data, not just a bare integer.

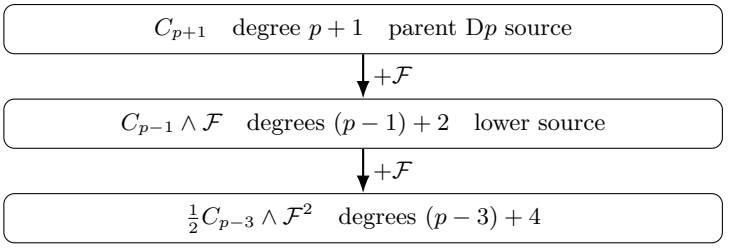


Figure III.3.3: The first three top-form channels in the oriented WZ integral. Every step adds one worldvolume two-form and drops the RR potential degree by two. The coefficient 1/2 in the third row comes from the exponential. For the lower-charge computation the two-form is λF with $B = 0$, and the cycle orientation defines $n = \int_\Sigma F/(2\pi)$.

The preceding integral has a precise boundary. With nonzero B, the action uses $P[B] + \lambda F$. Curvature terms and the global restriction on allowed flux can also alter how a lower charge is assigned. The formula n is therefore a local, restricted flux/Chern-character statement in the source frame, not a universal Page-charge or K-theory classification. Chapter 5 will supply the global distinctions. The RR normalization may be checked against closed-string source calculations, but a cylinder charge product alone does not replace the explicit μ_p convention used here.

III.3.6 Wrapped and interval reductions

The two action pieces now answer two different engineering questions. What kinetic coupling remains when a D6 gauge field is constant along an interval? What topological coefficient remains when a D4 wraps a two-cycle carrying RR flux? Both are integrations, but the first integrates a positive physical length and the second an oriented period. Figure III.3.4 separates the geometries.

For the interval calculation, take a flat unwarped D6 worldvolume $M_6 \times I$, constant dilaton, and physical interval coordinate $s \in [0, L]$. The physical length L is measured with the same constant-dilaton string-frame metric used in (III.3.8); the stretched D2 below uses that same length. Let the seven-dimensional gauge zero mode be independent of s, with no mixed field-strength component in the term being reduced. The leading book-trace kinetic term is

$$S_{7,2} = -\frac{1}{4g_7^2} \int_{M_6} d^6x \int_0^L ds\, F^a_{\mu\nu} F^{a\,\mu\nu} = -\frac{1}{4g_6^2} \int_{M_6} d^6x\, F^a_{\mu\nu} F^{a\,\mu\nu}, \quad \frac{1}{g_6^2} = \frac{L}{g_7^2}. \tag{III.3.24}$$

Here g_7 labels the coupling in seven worldvolume dimensions, while g_6 labels that of the six-dimensional zero mode; neither subscript is a brane value of p. For D6, set $p = 6$ in (III.3.16), obtaining

$$g_7^2 = 2(2\pi)^4 g_s(\alpha')^{3/2}, \qquad g_6^2 = \frac{2(2\pi)^4 g_s(\alpha')^{3/2}}{L}. \tag{III.3.25}$$

If $L = 5/2$ in the chosen length units, then $g_6^2/g_7^2 = 1/L = 2/5$. A shorter interval raises the six-dimensional coupling because less seven-dimensional kinetic volume is integrated. The formula says nothing by itself about warping, varying dilaton, endpoints, or the ultraviolet completion at $L = 0$.

The zero-mode assumption is doing work. If the gauge field depends on s, the coefficient in (III.3.24) does not by itself give the kinetic coefficient of an arbitrary six-dimensional field. One must decompose the seven-dimensional field into profiles along the interval and integrate each profile with the physical metric and dilaton measure. For the constant profile in the flat frame, that integral is exactly L. This bulk coefficient alone supplies neither a boundary condition nor a localized degree of freedom at the two ends. It is the piece of a D6 interval construction that leading DBI can determine without specifying junction dynamics.

There is a useful tension check using a different brane. A D2 stretched along the same physical interval has energy per unit unwrapped spatial length, or action coefficient per 1+1 worldsheet volume,

$$T_{\mathrm{D2},I} = L\tau_2 = \frac{L}{(2\pi)^2 g_s(\alpha')^{3/2}}. \tag{III.3.26}$$

Combining this actual D2 tension with (III.3.25) and (III.3.24) cancels the interval and string units:

$$T_{\mathrm{D2},I}\, g_6^2 = \frac{L}{(2\pi)^2 g_s(\alpha')^{3/2}} \frac{2(2\pi)^4 g_s(\alpha')^{3/2}}{L} = 2(2\pi)^2 = 8\pi^2. \tag{III.3.27}$$

At $L = 5/2$, dividing by π^2 still gives eight. This equality is a leading flat-space DBI relation between the specified D2 object and the zero-mode coupling. It is not an exact statement about an arbitrarily curved six-dimensional theory.

For the second reduction, take a positively oriented D4 worldvolume $M_3 \times C$, where C is an oriented two-cycle and the product fixes the M_3 orientation. We now use a Hermitian matrix connection A pulled back from M_3, independent of the point on C, with

$$F = dA + iA \wedge A, \qquad \omega_3(A) = \mathrm{Tr}_f \left(A \wedge dA + \frac{2i}{3} A \wedge A \wedge A \right), \qquad d\omega_3 = \mathrm{Tr}_f\, F \wedge F. \tag{III.3.28}$$

This is the convention for the Chern–Simons form in the present reduction. Chapter 1's endpoint matrix convention is $D_{\mathrm{III.1}} = d - i[A_{\mathrm{III.1}}, \cdot]$, whereas the matrix coordinate here has $D = d + i[A, \cdot]$. They describe the same adjoint derivative when $A = -A_{\mathrm{III.1}}$; the corresponding curvature coordinate changes sign as well. The sign in ω_3 cannot be copied between these coordinates while keeping $F = dA + iA^2$ fixed. For the rank-one

case the cubic term vanishes, but the sign choice remains essential for the matrix expression.

Define the normalized RR one-form and its curvature by $\mathcal{C}_1 = \mu_0 C_1$ and $\mathcal{F}_2 = d\mathcal{C}_1$. The quadratic WZ term of the D4 is

$$S_{\mathrm{D4},F^2} = \frac{\mu_4 \lambda^2}{2} \int_{M_3 \times C} C_1 \wedge \mathrm{Tr}_f\, F \wedge F = \frac{1}{8\pi^2} \int_{M_3 \times C} \mathcal{C}_1 \wedge \mathrm{Tr}_f\, F \wedge F. \tag{III.3.29}$$

To see the half-factor rather than simply memorize it, insert the charge units:

$$\frac{\mu_4 \lambda^2}{2\mu_0} = \frac{1}{(2\pi)^4 (\alpha')^{5/2}} \frac{(2\pi\alpha')^2}{2} (\alpha')^{1/2} = \frac{1}{2(2\pi)^2} = \frac{1}{8\pi^2}. \tag{III.3.30}$$

Omitting the exponential's $1/2$ would double the eventual bare Chern–Simons level.

Assume the restricted RR curvature class has the integral oriented period $K = \int_C \mathcal{F}_2/(2\pi) \in \mathbb{Z}$. With the connection pulled back from M_3, its ω_3 is also independent of C, as required by the displayed product reduction. For nonzero K, $\mathcal{C}_1$ is generally a collection of local potentials on patches of C, not a globally defined one-form. The inherited patch or extension descent pairs this RR flux with the local Chern–Simons form. With the positive D4 wrapping orientation fixed above, the resulting three-dimensional term is

$$S_{\mathrm{CS}} = \frac{1}{8\pi^2} \left(\int_C \mathcal{F}_2 \right) \int_{M_3} \omega_3 = \frac{K}{4\pi} \int_{M_3} \omega_3. \tag{III.3.31}$$

This descent equation specifies the restricted orientation and normalization used in later brane constructions. It should not be obtained by a global integration by parts in (III.3.29): a global $\mathcal{C}_1$ would contradict a nonzero flux period on closed C. Patch transitions or an extension supply the missing data. The chapter uses that descent input; it does not prove a general global pairing theorem.

To locate the missing step, cover the oriented cycle by patches U_N, U_S on which one-form potentials $\mathcal{C}_{1,N}, \mathcal{C}_{1,S}$ exist. Each satisfies $d\mathcal{C}_{1,N} = d\mathcal{C}_{1,S} = \mathcal{F}_2$ locally, but their difference on the overlap is transition data. The integral $\int_C \mathcal{F}_2$ measures the obstruction to choosing a single potential on the whole closed cycle. The formal identity

$$\mathcal{C}_1 \wedge d\omega_3 = \mathcal{F}_2 \wedge \omega_3 - d(\mathcal{C}_1 \wedge \omega_3) \tag{III.3.32}$$

holds on one patch, where both forms exist. Adding patch integrals also adds overlap or extension terms. Discarding the local total derivatives alone would not establish a global sign. The adopted descent statement fixes that sign with positive wrapped orientation; this patch picture explains the qualification and is not a new proof of the global descent.

For a concrete oriented period $K = -2$, a positive wrapped D4 produces bare level -2 in (III.3.31). Reverse the wrapped D4 charge while keeping the orientation of M_3, the cycle convention, and the RR flux fixed: the WZ source changes sign, and the bare level is $+2$. This discrete sign contrasts with the positive length L, which changes the continuous inverse gauge coupling in (III.3.24). The interval relation feeds the D6 constructions of X.4; the flux descent feeds the M2-brane and three-dimensional gauge-theory examples of Volume VIII, Chapter 5. The dynamics of those constructions requires their additional ingredients.

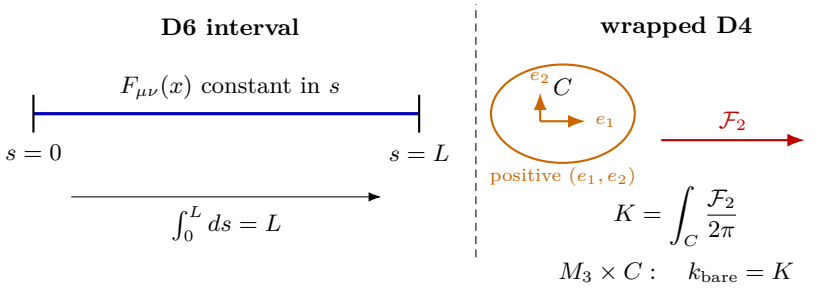


Figure III.3.4: Two independent reductions. Left: a flat D6 has a gauge zero mode constant along the physical interval $0 \le s \le L$, so integrating its kinetic density multiplies $1/g_7^2$ by L. Right: a positively oriented D4 wraps $M_3 \times C$, and the oriented RR period $K = \int_C \mathcal{F}_2/(2\pi)$ fixes the bare level. The ordered local tangent basis (e_1, e_2) marks the positive orientation of the two-cycle C; together with the stated M_3 orientation it gives the positive D4 product orientation. Reversing D4 charge reverses the level while holding the M_3 orientation fixed.

III.3.7 Exercises

The first five exercises ask for exact submitted coefficients or integers as well as written reasoning. The public companion supplies the JSON field names and grades those submitted values. The last exercise is a written interpretation question.

1. **E1, determinant signs.** On a flat 2+1 worldvolume take one physical slope $u = \partial_1 X$, $e = \lambda F_{01}$, and $b = \lambda F_{12}$. Compute the determinant of $P[G] + \lambda F$ and submit the coefficients of u^2, e^2, b^2 in its square root through quadratic order. Explain why the electric coefficient has its sign.

2. **E2, two gauge coordinates.** For D3 at $g_s = 3/2$, submit g^2_{book}/π, $g^2_{U(1),\text{int}}/\pi$, and their ratio. Use $\text{Tr}_f(T^a T^b) = \delta^{ab}/2$, and explain in writing how $A^0 T = a\mathbf{1}$ preserves the integer-charge connection.

3. **E3, orientation.** With $B = 0$, take a positively oriented Dp-brane and an oriented two-cycle with $\int_\Sigma F/(2\pi) = -3$. Submit the induced D$(p-2)$ charge in μ_{p-2} units, then the charge after reversing parent-brane orientation while holding the flux-coordinate convention fixed. Show the charge-ratio step.

4. **E4, interval and tension.** A flat D6 has an interval-constant gauge zero mode on a physical interval of length $L = 5/2$. Submit g_6^2/g_7^2 and $T_{\text{D2},I} g_6^2/\pi^2$ in the book trace convention. Calculate the actual stretched D2 tension before canceling units.

5. **E5, flux descent.** A positive D4 wraps $M_3 \times C$ with $K = -2$ in the oriented RR convention of (III.3.31). Submit the bare Chern–Simons level, then the level after reversing wrapped charge with M_3's orientation held fixed. Identify the factor of one-half in the WZ exponential.

6. **E6, written interpretation.** Explain why a nonzero B-field, curvature terms, or restrictions on allowed worldvolume flux can change a naive lower-charge interpretation. Explain also why a nontrivial RR period requires patch or extension descent instead of a global $\mathcal{C}_1$ integration by parts. No detailed global charge formula is requested.

Take-home message

DBI turns the pullback metric and invariant two-form into local scalar and gauge kinetic terms. WZ turns oriented worldvolume flux into RR source charge. With $\lambda = 2\pi\alpha'$, an integer-charge single-brane connection and a half-trace matrix component differ by a factor of two in their displayed couplings. A flat D6 interval gives $1/g_6^2 = L/g_7^2$ and a stretched D2 tension $8\pi^2/g_6^2$; an oriented D4 RR period gives a bare three-dimensional Chern–Simons level. A reader should now be able to expand an induced determinant, translate the two gauge coordinates, integrate a restricted lower-charge flux, and track the orientation of a flux descent.

Status and sources

The pullback, local B-gauge compensation and abelian DBI premise in Sections III.3.2 and III.3.3 follow Johnson (2000, physical PDF pp. 78–80, eqs. (199), (204)–(207)) and Myers (1999, physical PDF p. 2, eqs. (1)–(2)). The determinant series, nonunit electric/magnetic blocks and signs are [MATH] deductions under their flat, slowly varying premises. The original full Dirichlet sigma-model derivation is identified by Leigh (1989) as a proof pointer, but its primary text was not used as an exact equation anchor here. The Born–Infeld analysis Callan and Maldacena (1997, physical PDF pp. 2–3) supplies abelian context in its $\alpha' = 1$ units, not the present normalization.

The RR charge and physical tension in (III.3.7) follow Johnson (2000, physical PDF p. 109, eqs. (274)–(275)) (cited physical input). The first equality of that source's equation (276) gives the single-brane abelian kinetic coefficient; its printed final expression omits g_s relative to equation (275). The book half-trace component translation in Section III.3.4 is explicit [MATH] algebra using the stated tension and trace conventions. Myers' string-frame metric and dilaton/kinetic convention on physical PDF pp. 4–5, and his equal tension/charge units on physical PDF p. 7, are source-local physical inputs. The algebraic conversion $C_{\text{source}} = g_s C_{\text{book}}$ above relates those RR-potential units; it is not itself a further source declaration. The cylinder and minimal RR charge product in Polchinski (1995, physical PDF pp. 5–6, eqs. (9)–(15)) provide an independent RR context but do not by themselves fix the book's absolute μ_p.

The WZ exponential and first lower-source terms in Section III.3.5 follow Johnson (2000, physical PDF pp. 112–113, eqs. (284)–(287)) and Myers (1999, physical PDF p. 2, eq. (3)) (cited physical input). The charge ratio and oriented integral are [MATH] under the stated $B = 0$, integral-period and product-orientation conditions. They are not a full global charge classification.

The flat constant-mode interval algebra and actual D2 tension in Section III.3.6 are [MATH] consequences of the displayed tension and dimensional-reduction conventions. The D4 term uses the same WZ source, while its oriented flux-to-Chern–Simons descent is

restricted to the stated patch and extension. Its Hermitian connection has $F = dA + iA^2$ and $\omega_3 = \mathrm{Tr}_f(A\,dA + 2iA^3/3)$. Chapter 1's separate endpoint connection coordinate uses the opposite commutator sign and must be translated before comparison. The nonzero RR period prevents a global-potential integration by parts. Global Freed–Witten, curvature and K-theory refinements, a full disk proof, exact nonabelian DBI, derivative corrections, and warped interval dynamics are outside the results established here. No universal global descent follows from this local calculation.

The cited physical inputs in this apparatus retain their stated source and regime and are cited physical inputs. The mathematical checks do not establish those physical premises.

References

Callan Jr., C. G. and J. M. Maldacena (1997). *Brane Dynamics From the Born-Infeld Action*. arXiv: hep-th/9708147.

Johnson, C. V. (2000). *D-Brane Primer*. arXiv: hep-th/0007170.

Leigh, R. G. (1989). "Dirac-Born-Infeld Action from Dirichlet Sigma-Model". In: *Modern Physics Letters A* 4, pp. 2767–2772. DOI: 10.1142/S0217732389003099.

Myers, R. C. (1999). *Dielectric-Branes*. arXiv: hep-th/9910053.

Polchinski, J. (1995). *Dirichlet-Branes and Ramond-Ramond Charges*. arXiv: hep-th/9510017.

Chapter III.4

Multiple branes: non-abelian worldvolume structure

III.4.1 From endpoints to a matrix field

Put two parallel D-branes on top of each other. An open string can start and end on either one. Its endpoints therefore have more information than the endpoints of the single-brane strings in Chapter 1. In particular, the string that goes from brane 1 to brane 2 cannot be described by a second copy of the abelian gauge field. It supplies an off-diagonal component. At coincidence these components are light, and the leading low-energy fields assemble into a Hermitian matrix connection and Hermitian transverse scalar matrices.

This chapter asks three linked questions. How do endpoint labels produce matrix multiplication? Why does the leading action force static flat-space scalar vacua to commute? How does a physical separation then give a mass to an off-diagonal worldvolume vector? The first two questions lead to the classical configuration space used in later brane-probe constructions. The last connects that field theory to the energy of a stretched string. A separate D0 example shows how a background Ramond–Ramond (RR) field changes the leading scalar energy.

Through the spatial-vector calculation take identical parallel type-II Dp-branes in flat noncompact space, with no background B-field or RR flux. The low-energy spectrum and its maximally supersymmetric $U(N)$ Yang–Mills interaction are string-theoretic inputs. They have sixteen real supercharges. We derive the bosonic consequences of that leading action. Its fermions are needed for supersymmetry but are not derived here. Chapter 3 supplied the single-brane kinetic normalization; the matrix theory below uses the book's fundamental trace normalization. The result is a leading field theory, not a formula for the complete nonabelian Born–Infeld action.

III.4.2 Ordered endpoints and the gauge algebra

Why is the extra endpoint information an algebra rather than merely a list of N^2 particles? Label an oriented open-string state by its initial and final branes, (i, j), and associate to it the matrix unit E_{ij}. The first index is a row, the second a column. An ordered joining of a j-ending string to a j-starting string has precisely the matrix product

$$(E_{ij})_{ab} = \delta_{ia}\delta_{jb}, \qquad E_{ij}E_{kl} = \delta_{jk}E_{il}. \tag{III.4.1}$$

The Kronecker delta tests whether the intermediate endpoint agrees. It is the physical origin of the index contraction in a matrix interaction. Figure III.4.1 draws that contraction without assigning a distance to an endpoint label.

The rule applies unchanged to more than two branes. For example, a $(1, 2)$ string followed by a $(2, 3)$ string has a matching intermediate endpoint and contributes a $(1, 3)$ matrix component. A $(1, 2)$ string followed by a $(3, 1)$ string cannot be joined in this order:

$$E_{12}E_{23} = E_{13}, \qquad E_{12}E_{31} = 0. \tag{III.4.2}$$

This is why the repeated index is an endpoint condition rather than an arbitrary summation convention. A general matrix field $M = \sum_{i,j} M_{ij}E_{ij}$ retains all allowed ordered pairs. Its product with another field automatically sums only over compatible intermediate branes. The same contraction is what lets a local action use traces of matrix products without separately listing every string joining.

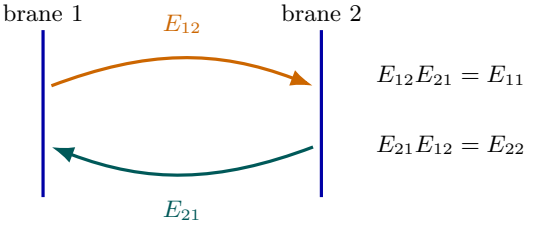


Figure III.4.1: Ordered Chan–Paton labels. The two successive oriented strings $(1, 2)$ and $(2, 1)$ join at endpoint 2 and give $E_{12}E_{21} = E_{11}$. Reversing their order gives E_{22}. The labels identify branes, while their physical separation is specified later by scalar eigenvalues.

For two branes the multiplication is concrete:

$$E_{12} = \begin{pmatrix} 0 & 1 \\ 0 & 0 \end{pmatrix}, \quad E_{21} = \begin{pmatrix} 0 & 0 \\ 1 & 0 \end{pmatrix}, \quad E_{12}E_{21} = E_{11}, \quad E_{21}E_{12} = E_{22}. \tag{III.4.3}$$

The last two answers differ. An interaction that retains the endpoint ordering must therefore retain noncommutative matrix multiplication. The Hermitian combinations $E_{12} + E_{21}$ and $i(E_{12} - E_{21})$, together with E_{11} and E_{22}, span the real vector space of Hermitian 2×2 fields. In general there are N^2 real Hermitian matrix components for each vector or scalar field.

Equivalently, any Hermitian $U(2)$ component may be written

$$H = h_1 E_{11} + h_2 E_{22} + w E_{12} + w^* E_{21}, \qquad h_1, h_2 \in \mathbb{R}, \quad w \in \mathbb{C}. \tag{III.4.4}$$

The two complex-looking off-diagonal entries are conjugates, not two independent complex fields. They carry opposite endpoint orientations while forming one Hermitian matrix. This accounting is useful when a later quadratic action is written using w: a trace contains both orientations and produces a factor of two. At a separated background, the same pair is often called a charged W field. That name describes its relative $U(1)$ charge and mass, not an extra field added by hand.

At coincidence the massless vector states are collected into $A_\mu = A_\mu^\dagger$, $\mu = 0, \ldots, p$. A change of endpoint basis by $U \in U(N)$ acts by conjugation on an adjoint scalar Φ_i, and the corresponding connection transforms inhomogeneously:

$$\Phi_i \longmapsto U \Phi_i U^{-1}, \qquad A_\mu \longmapsto U A_\mu U^{-1} - i(\partial_\mu U) U^{-1}. \tag{III.4.5}$$

For our Hermitian sign convention, this makes $D_\mu \Phi_i = \partial_\mu \Phi_i - i[A_\mu, \Phi_i]$ transform by conjugation. For constant U, the second term in the connection law vanishes. Localizing the endpoint-basis change requires it.

It is useful to test the sign in that local law. Set $U = \mathbf{1}_N + i\vartheta + O(\vartheta^2)$, with Hermitian $\vartheta(x)$. To first order, the field variations read

$$\delta_\vartheta \Phi_i = i[\vartheta, \Phi_i], \qquad \delta_\vartheta A_\mu = \partial_\mu \vartheta + i[\vartheta, A_\mu]. \tag{III.4.6}$$

In $\delta(D_\mu \Phi_i)$, the derivative of the first variation contains $i[\partial_\mu \vartheta, \Phi_i]$. The variation of the connection term contains its negative. The remaining terms combine by the Jacobi identity:

$$\delta_\vartheta (D_\mu \Phi_i) = i[\vartheta, D_\mu \Phi_i]. \tag{III.4.7}$$

Thus the displayed transformation has the sign needed by the covariant derivative that will appear in the action. A source using $D = \partial + i[A, \cdot]$ prints the opposite sign for its matrix connection; its formulas require translation before comparison.

The diagonal subgroup already shows what separation will do. Let U have diagonal entries $e^{i\theta_1}$ and $e^{i\theta_2}$. Then

$$U E_{12} U^{-1} = e^{i(\theta_1 - \theta_2)} E_{12}, \qquad U E_{21} U^{-1} = e^{-i(\theta_1 - \theta_2)} E_{21}. \tag{III.4.8}$$

Thus the two off-diagonal components carry opposite relative $U(1)$ charges. For a common phase $\theta_1 = \theta_2$, both charges vanish: the central $U(1)$ acts trivially on adjoints. This does not erase the center-of-mass scalar coordinates. Conjugation cannot change a matrix trace, and a common physical translation will change that trace.

The product itself gives another useful $U(2)$ check:

$$[E_{12}, E_{21}] = E_{11} - E_{22}, \qquad [E_{11} - E_{22}, E_{12}] = 2E_{12}. \tag{III.4.9}$$

An interaction of the two opposite endpoint orientations therefore returns a diagonal field. Repeating the interaction can produce an off-diagonal field again. The three components close under commutators; one cannot retain only the diagonal fields when

the off-diagonal strings are light. The diagonal sum $E_{11} + E_{22} = \mathbf{1}_2$, on the other hand, commutes with all four matrix units. This finite calculation distinguishes the relative algebra from the central direction without discarding either field from the original $U(2)$ multiplet.

The endpoint algebra alone does not derive which open-string states survive the type-II projections or why their leading interaction has sixteen supercharges. Those are the flat parallel-brane spectrum and low-energy premises. Once supplied, the algebra explains why the fields must be matrix-valued. It also tells us why a stack cannot be described by N independent copies of Chapter 3. The next step is to determine the terms that those matrices inherit from the ten-dimensional field strength.

III.4.3 Reducing the leading ten-dimensional action

Which scalar terms are fixed by the leading gauge action? Use mostly-plus ten-dimensional signature. Capital indices $M, N = 0, \ldots, 9$ split into worldvolume indices $\mu, \nu = 0, \ldots, p$ and transverse indices $i, j = p+1, \ldots, 9$. The starting bosonic term is

$$S_{10,\mathrm{bos}} = -\frac{1}{2g_{10}^2} \int d^{10}x \ \mathrm{Tr}_f(F_{MN}F^{MN}), \qquad \mathrm{Tr}_f(T^a T^b) = \frac{\delta^{ab}}{2}. \tag{III.4.10}$$

For fields independent of the transverse spectator coordinates, write their formal integration volume as $V_\perp = \int d^{9-p}x$ and define the reduced book coupling by $g^2 = g_{10}^2/V_\perp$. Thus integrating the displayed parent term gives $S_{p+1} = \int d^{p+1}x \, \mathcal{L}_{p+1}$ with coefficient $1/g^2$. This volume is a normalization device for the dimensional reduction, not a physical compactification assumption. Since A_M has inverse-length dimension, $[g_{10}^2] = L^6$, $[V_\perp] = L^{9-p}$, and $[g^2] = L^{p-3}$. The half-trace convention makes the component quadratic term $-F^a_{MN}F^{aMN}/(4g^2)$. We do not identify this coefficient with an untranslated coupling printed in a source that uses a different trace or connection sign.

Take Hermitian A_M and define

$$D_M = \partial_M - i[A_M, \cdot], \qquad F_{MN} = \partial_M A_N - \partial_N A_M - i[A_M, A_N]. \tag{III.4.11}$$

Reduction means retaining fields independent of each transverse coordinate: $\partial_i = 0$. Set $A_i = \Phi_i$. The mixed component is then a covariant derivative, while the transverse component is a commutator:

$$F_{\mu i} = \partial_\mu \Phi_i - i[A_\mu, \Phi_i] = D_\mu \Phi_i, \qquad F_{ij} = -i[\Phi_i, \Phi_j]. \tag{III.4.12}$$

The operation is dimensional reduction of a leading gauge theory. It is not a derivation of the D-brane spectrum from a ten-dimensional gauge field.

Count both placements of the mixed indices. With repeated transverse indices an *ordered* sum, antisymmetry of F gives

$$\mathrm{Tr}_f \, F_{MN}F^{MN} = \mathrm{Tr}_f\big(F_{\mu\nu}F^{\mu\nu} + 2D_\mu\Phi_i D^\mu \Phi_i - [\Phi_i, \Phi_j]^2\big). \tag{III.4.13}$$

The factor 2 is the pair (μ, i) and (i, μ). The last minus sign follows from $(-i)^2 = -1$. In particular it is not permissible to replace the ordered (i, j) sum by $i < j$ without changing its coefficient.

For a small matrix test, choose two of the available transverse directions, r and s, and set $\Phi_r = a\sigma_1$, $\Phi_s = b\sigma_2$, with real constants a, b. The Pauli matrices obey $[\sigma_1, \sigma_2] = 2i\sigma_3$. Only the (r, s) and (s, r) entries of the transverse block are nonzero:

$$F_{rs} = -i[\Phi_r, \Phi_s] = 2ab\sigma_3, \qquad F_{sr} = -2ab\sigma_3. \tag{III.4.14}$$

Since $\mathrm{Tr}_f\, \sigma_3^2 = 2$, each ordered square has trace $8a^2b^2$, and both together contribute

$$\mathrm{Tr}_f(F_{rs}^2 + F_{sr}^2) = 16a^2b^2, \qquad \mathcal{L}_{\text{scalar,static}} = -\frac{8a^2b^2}{g^2}. \tag{III.4.15}$$

This explicit pair checks both the ordered factor and the fact that a noncommuting static configuration has a negative Lagrangian potential term. If one counted (r, s) only once while retaining the coefficient in (III.4.16), the energy would be wrong by a factor of two. A diagonal pair has $F_{rs} = 0$, even if its two eigenvalue vectors describe separated branes. Thus the energy measures failure of matrices to commute, rather than spatial separation itself.

Substitution into the parent density produces three terms with fixed relative coefficients:

$$\mathcal{L}_{p+1} = -\frac{1}{2g^2}\,\mathrm{Tr}_f\, F_{\mu\nu}F^{\mu\nu} - \frac{1}{g^2}\,\mathrm{Tr}_f\, D_\mu\Phi_i D^\mu\Phi_i + \frac{1}{2g^2}\,\mathrm{Tr}_f[\Phi_i, \Phi_j]^2. \tag{III.4.16}$$

For a time-dependent single diagonal component, the middle term is positive because $D_0\Phi_i D^0\Phi_i = -\dot{\Phi}_i^2$. The last term is nonpositive as a Lagrangian potential term because a commutator of Hermitian matrices is anti-Hermitian. Both signs are needed in the vacuum argument below.

The temporal block makes the kinetic sign explicit. In a background with $A_0 = 0$, take a diagonal scalar $\Phi_i(t) = \mathrm{diag}(u(t), v(t))$. Then

$$\mathrm{Tr}_f(D_0\Phi_i D^0\Phi_i) = -\dot{u}^{\,2} - \dot{v}^{\,2}, \qquad \mathcal{L}_{\text{kin}} = \frac{\dot{u}^{\,2} + \dot{v}^{\,2}}{g^2}. \tag{III.4.17}$$

Thus the reduced sign gives a positive time kinetic energy before the vacuum matrices are diagonalized. Its relative coefficient to the vector term is fixed by the two mixed blocks of (III.4.13). Changing the overall trace convention would rescale both coefficients; changing only one would break the reduction.

The number of scalars is $9-p$. A D3 stack has six matrices $\Phi_4, \ldots, \Phi_9$; its transverse block contains thirty ordered (i, j) terms with $i \neq j$, or fifteen unordered pairs. More explicitly,

$$\sum_{i,j=4}^{9} \mathrm{Tr}[\Phi_i, \Phi_j]^2 = 2 \sum_{4\le i<j\le 9} \mathrm{Tr}[\Phi_i, \Phi_j]^2. \tag{III.4.18}$$

At $p = 8$ only Φ_9 survives, so its sole commutator $[\Phi_9, \Phi_9]$ vanishes. At $p = 9$ no transverse scalar is present. These small cases are useful checks on any general formula for the potential. Figure III.4.2 records the index split; its two off-diagonal blocks explain the coefficient 2 in (III.4.13).

Another normalization check uses a diagonal $U(2)$ fluctuation. In one transverse direction write $\Phi = \mathrm{diag}(\phi_1, \phi_2)$ and define $\phi_{\mathrm{cm}} = (\phi_1 + \phi_2)/2$, $\delta = \phi_1 - \phi_2$. These are simply linear coordinates on the same two-dimensional space of diagonal matrices. Their kinetic trace splits as

$$\mathrm{Tr}_f(\partial_\mu \Phi \partial^\mu \Phi) = 2\,\partial_\mu \phi_{\mathrm{cm}} \partial^\mu \phi_{\mathrm{cm}} + \frac{1}{2}\,\partial_\mu \delta \partial^\mu \delta. \tag{III.4.19}$$

The cross terms cancel when $\phi_{1,2} = \phi_{\mathrm{cm}} \pm \delta/2$ are substituted. Both the common and the relative position have kinetic energy; the center is not an algebraic redundancy. Multiplying the fields by $\lambda = 2\pi\alpha'$ turns their eigenvalues into physical transverse coordinates. This explicit split will be useful when the relative coordinate enters the off-diagonal mass, while the common coordinate does not.

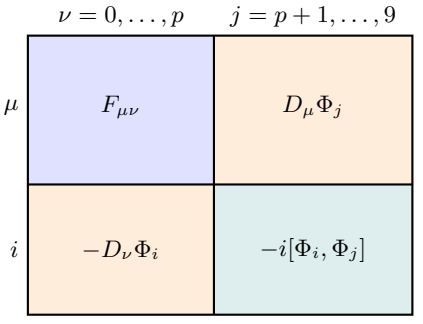


Figure III.4.2: Index blocks of the antisymmetric ten-dimensional field strength. With rows μ, i and columns ν, j, the mixed blocks contain $F_{\mu j} = D_\mu \Phi_j$ and $F_{i\nu} = -D_\nu \Phi_i$, so both contribute to the ordered contraction. The transverse block contains $-i[\Phi_i, \Phi_j]$. The diagram is a counting aid for the explicitly derived action.

Chapter 3's abelian expansion supplies a useful normalization control. For $N = 1$, every commutator in (III.4.16) vanishes and $D_\mu \Phi_i = \partial_\mu \Phi_i$. The resulting quadratic scalar and Maxwell terms are the single-brane terms in the book field coordinate. The endpoint premise and the reduction have different logical roles: string theory supplies the matrix multiplet and its leading interaction; the displayed algebra fixes the signs and coefficients used below.

The transverse index count also tells us which sector a later D-brane construction may use. A D3 stack has six independent scalar directions in which eigenvalues can separate. A D8 stack has one such direction but no two-scalar commutator potential to restrict it. Both cases have worldvolume spatial vector components, so the later quadratic mass argument can still use a separation. The D9 case has neither a transverse scalar nor the corresponding separation mass. Keeping the index domain visible prevents a ten-dimensional parent notation from silently assigning geometry to a direction that was never reduced.

III.4.4 Positive energy and classical positions

Can two separated branes cost no scalar potential energy? Restrict to constant scalar fields, zero worldvolume field strength, and the flat noncompact sector just specified. For any Hermitian pair, $C_{ij} = [\Phi_i, \Phi_j]$ obeys $C_{ij}^\dagger = -C_{ij}$. The potential energy from (III.4.16) is therefore

$$V = -\frac{1}{2g^2}\sum_{i,j} \mathrm{Tr}_f\, C_{ij}^2 = \frac{1}{2g^2}\sum_{i,j} \mathrm{Tr}_f(C_{ij}^\dagger C_{ij}) \geq 0. \tag{III.4.20}$$

For a finite matrix C, $\mathrm{Tr}\, C^\dagger C$ is the sum of squared absolute values of its entries. Thus zero energy forces $C_{ij} = 0$ for every pair, and a commuting tuple conversely has zero scalar potential:

$$V = 0 \quad \Longleftrightarrow \quad [\Phi_i, \Phi_j] = 0 \quad \text{for all available } i, j. \tag{III.4.21}$$

This is a statement about classical constant scalar configurations in the stated sector. It does not classify gauge backgrounds with Wilson lines, fluxes or boundary data.

For two matrices in $U(2)$, the positivity can be resolved into ordinary three-vectors. Write $\Phi_r = a_0 \mathbf{1}_2 + \vec{a}\cdot\vec{\sigma}$ and $\Phi_s = b_0\mathbf{1}_2 + \vec{b}\cdot\vec{\sigma}$, with real vectors $\vec{a}, \vec{b}$. The Pauli product gives

$$[\Phi_r, \Phi_s] = 2i(\vec{a}\times\vec{b})\cdot\vec{\sigma}, \qquad \mathrm{Tr}_f(C_{rs}^\dagger C_{rs}) = 8|\vec{a}\times\vec{b}|^2. \tag{III.4.22}$$

The pair (s, r) contributes the same norm. If these are the only nonzero commutators, their energy is

$$V = \frac{8}{g^2}|\vec{a}\times\vec{b}|^2. \tag{III.4.23}$$

The trace pieces a_0, b_0 disappear from this energy because they commute with everything. Zero energy requires the two traceless vectors to be parallel or one to vanish. A common unitary basis can then align their Pauli directions with σ_3, yielding two diagonal positions. This $U(2)$ calculation is a finite example of the general diagonalization argument, while making the independence of the trace position explicit.

Finite Hermitian commuting matrices can be diagonalized by the same unitary transformation. One can see the required step without assuming nondegenerate eigenvalues. Diagonalize Φ_{p+1}; every commuting Φ_j preserves each of its eigenspaces. Diagonalize the next Hermitian matrix separately inside those invariant subspaces. Continue through the finite tuple. At each step the previous matrices stay scalar on the subspaces being refined. The result is

$$\Phi_i = \mathrm{diag}(\phi_{1i}, \ldots, \phi_{Ni}), \qquad \vec{\phi}_a = (\phi_{a,p+1}, \ldots, \phi_{a9}) \in \mathbb{R}^{9-p}. \tag{III.4.24}$$

The proof also explains why an accidental degeneracy causes no missing vacuum: it increases the freedom to choose a basis within a common eigenspace, while simultaneous diagonalization still exists.

For example, if all N eigenvalue vectors are different, a unitary matrix that preserves every diagonal Φ_i may assign a separate phase to each common eigenvector. If two of those vectors coincide, any $U(2)$ rotation inside their shared eigenspace preserves

the whole tuple. More generally, partition the labels by equality of the full position vectors, not by equality of one coordinate. A block with m_a equal vectors admits an arbitrary $U(m_a)$ change of basis. This gives the stabilizer stated below and explains why eigenvalue crossings are special points of the quotient rather than additional independent positions.

The physical transverse position of brane a is $\vec{X}_a = \lambda\vec{\phi}_a$, with $\lambda = 2\pi\alpha'$. A permutation matrix exchanges diagonal entries without changing the physical gauge orbit. For generic distinct position vectors the residual diagonal conjugations form $U(1)^N$; if m_a positions coincide at each distinct vector, the stabilizer is $\prod_a U(m_a)$. Hence the constant classical scalar vacuum set is

$$\mathcal{M}_{\text{scalar,cl}} = (\mathbb{R}^{9-p})^N/S_N = \text{Sym}^N(\mathbb{R}^{9-p}), \qquad 0 \le p \le 8. \tag{III.4.25}$$

The expression is an unordered set of position vectors. It is not an everywhere free, smooth quotient: coincident vectors have larger stabilizers. Nor is (III.4.25) by itself a theorem about a quantum moduli space.

The center matters even though its gauge action is trivial on adjoints. Decompose each scalar into a trace coordinate and a traceless part:

$$\Phi_i = \phi_{\text{cm},i}\mathbf{1}_N + \widehat{\Phi}_i, \qquad \phi_{\text{cm},i} = \frac{1}{N}\,\text{Tr}_f\,\Phi_i, \qquad \text{Tr}_f\,\widehat{\Phi}_i = 0. \tag{III.4.26}$$

Conjugation leaves $\phi_{\text{cm},i}$ unchanged. A spacetime translation $X_{ai} \mapsto X_{ai} + c_i$, however, changes it by c_i/λ. Quotienting by gauge transformations does not quotient by physical translations. Consequently the center-of-mass coordinates remain in (III.4.25). This distinction will also separate the relative W mass from the common displacement in the next section.

For a concrete $U(2)$ example with two transverse directions, take

$$\Phi_8 = \text{diag}(0,3), \qquad \Phi_9 = \text{diag}(1,2), \qquad [\Phi_8,\Phi_9] = 0. \tag{III.4.27}$$

The two position vectors are $(0,1)\lambda$ and $(3,2)\lambda$. Exchanging both vectors is a single gauge permutation. Exchanging only the entries of Φ_8 while leaving Φ_9 fixed instead changes their pairing and generally describes a different configuration. In a one-matrix comparison, $\text{diag}(0,3)$ and $\text{diag}(3,0)$ are conjugate, whereas $\text{diag}(1,2)$ has the same trace but a different $\text{Tr}\,\Phi^2$:

$$\text{Tr}\,\text{diag}(0,3)^2 = 9, \qquad \text{Tr}\,\text{diag}(1,2)^2 = 5. \tag{III.4.28}$$

Equal traces alone therefore do not determine a conjugacy class. In the two-matrix problem, the paired eigenvalue vectors, rather than two independent unordered eigenvalue lists, are the coordinates of the quotient. Figure III.4.3 shows this pairing and the single simultaneous permutation.

There is an invariant that tests the pairing directly. For the two matrices in (III.4.27), the original paired configuration has $\text{Tr}_f(\Phi_8\Phi_9) = 6$. If we swap the entries of Φ_8 alone, leaving Φ_9 fixed, the trace changes to 3:

$$\text{Tr}_f[\text{diag}(0,3)\,\text{diag}(1,2)] = 6, \quad \text{Tr}_f[\text{diag}(3,0)\,\text{diag}(1,2)] = 3. \tag{III.4.29}$$

The trace of a product is invariant under simultaneous conjugation. Therefore no single gauge transformation relates these two ordered *pairs*, despite the fact that each individual matrix has the same unordered eigenvalues in both descriptions. If instead both matrices are swapped together, the trace stays 6 and the two geometric points are merely relabeled. This test is useful whenever a later brane construction assigns several scalar coordinates to each brane: the gauge quotient permutes complete position vectors, not the coordinates within them independently.

The example also illustrates the role of degeneracy. If the two position vectors become equal, every matrix in the tuple is a scalar multiple of $\mathbf{1}_2$. Conjugation by the entire $U(2)$ then fixes the tuple. At distinct vectors only diagonal phases in the common eigenbasis survive. The change in stabilizer is an algebraic signature of coincidence. It does not, on its own, establish a quantum statement about the local geometry near that coincidence.

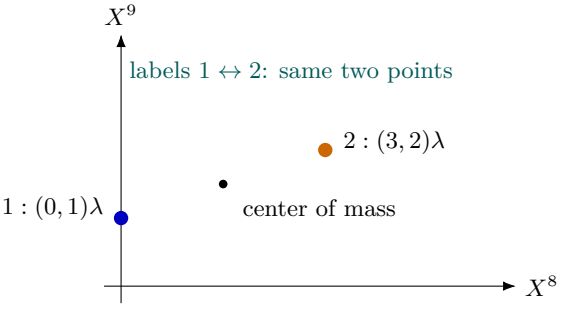


Figure III.4.3: A commuting $U(2)$ pair is two points in the physical (X^8, X^9) plane. The labels 1 and 2 may be exchanged together by one gauge permutation; the two geometric points remain. The average position is a physical translation coordinate, not removed by the central gauge transformation.

At $N = 1$ the potential vanishes without a commutativity condition. At $p = 8$ one scalar also makes it identically zero for any Hermitian matrix, which can then be diagonalized. At $p = 9$ there is no scalar vacuum coordinate of this kind. These limits guard against reading a transverse-position theorem into a system with no transverse direction. The next question is dynamical: when two eigenvalue vectors differ, what does the leading action say about a charged vector fluctuation?

III.4.5 Separation and the massive spatial vector

Take two separated branes with $1 \le p \le 8$. A string stretched from one to the other has a geometric length. The field-theory candidate for its light vector mode is an off-diagonal fluctuation. To compare masses, we must normalize that fluctuation's kinetic term as well as its scalar coupling. Choose the constant background

$$\overline{\Phi}_i = \begin{pmatrix} \phi_{1i} & 0 \\ 0 & \phi_{2i} \end{pmatrix}, \quad \Delta\phi_i = \phi_{1i} - \phi_{2i}, \quad \Delta X_i = \lambda \Delta\phi_i. \tag{III.4.30}$$

For each transverse direction the adjoint operator acts on a matrix unit by

$$[\overline{\Phi}_i, E_{12}] = \Delta\phi_i E_{12}, \qquad [\overline{\Phi}_i, E_{21}] = -\Delta\phi_i E_{21}. \tag{III.4.31}$$

This eigenvalue gives the candidate mass scale, but it alone does not identify a propagating degree of freedom or fix its kinetic normalization.

Choose a spatial worldvolume direction $a \in \{1, \ldots, p\}$ and write its off-diagonal fluctuation as $\delta A_a = w_a E_{12} + w_a^* E_{21}$. In a background gauge suitable for extracting a physical transverse vector polarization, set $\delta A_0 = 0$ for this quadratic calculation and suppress the Goldstone fluctuation along $\Delta\vec{\phi}$. A polarization with $\partial^a w_a = 0$ then has an ordinary electric kinetic term. The trace of that term is

$$\mathrm{Tr}_f(\delta F_{0a}\delta F^{0a}) = -2|\dot{w}_a|^2, \qquad \mathcal{L}_{\mathrm{kin}} = \frac{2}{g^2}|\dot{w}_a|^2. \tag{III.4.32}$$

The full ordered $F_{\mu\nu}F^{\mu\nu}$ sum contains both $(0,a)$ and $(a,0)$, producing the second equality. At nonzero spatial momentum its magnetic partner supplies the usual gradient term. This calculation uses an actual worldvolume spatial component; it is why the domain starts at $p = 1$.

For a D3 vector this gradient can be displayed rather than inferred. Take a wave traveling along x^1 and a polarization in the x^2 direction, so $w_2 = w_2(t, x^1)$ and the other spatial components vanish in this quadratic mode. Then $\delta F_{12} = \partial_1 w_2 E_{12} + \partial_1 w_2^* E_{21}$. Both ordered magnetic placements contribute, and their trace gives

$$\mathcal{L}^{(2)}_{\mathrm{electric+magnetic}} = \frac{2}{g^2}\left(|\partial_0 w_2|^2 - |\partial_1 w_2|^2\right). \tag{III.4.33}$$

Together with the scalar-background term below, a plane wave $w_2 \propto e^{-i\omega t + ikx^1}$ obeys $\omega^2 = k^2 + |\Delta\vec{\phi}|^2$. Thus the ratio computed at rest is the mass in the relativistic dispersion of an actual D3 spatial polarization. The construction also shows exactly where a second spatial direction was used for this convenient nonzero-momentum test; the rest-frame mass argument itself only needs one.

The scalar covariant derivative in the same background is $D_a\overline{\Phi}_i = -i[\delta A_a, \overline{\Phi}_i]$. Its two off-diagonal entries have opposite signs, and the trace is positive:

$$\mathrm{Tr}_f(D_a\overline{\Phi}_i)^2 = 2(\Delta\phi_i)^2|w_a|^2, \qquad \mathcal{L}_{\mathrm{mass}} = -\frac{2}{g^2}\sum_i (\Delta\phi_i)^2|w_a|^2. \tag{III.4.34}$$

The identical prefactors in (III.4.32) and (III.4.34) are decisive. Their ratio gives the physical quadratic mass of this spatial-vector polarization:

$$m_W^2 = \sum_i (\Delta\phi_i)^2 = \frac{|\Delta\vec{X}|^2}{(2\pi\alpha')^2}. \tag{III.4.35}$$

At zero spatial momentum, the quadratic Lagrangian for that component can be read directly from the two traces:

$$\mathcal{L}^{(2)}_w = \frac{2}{g^2}\left(|\dot{w}_a|^2 - |\Delta\vec{\phi}|^2|w_a|^2\right) + \cdots. \tag{III.4.36}$$

Rescaling w_a to a canonical real pair multiplies both displayed terms by the same factor, leaving $m_W^2 = |\Delta\vec{\phi}|^2$. The ellipsis includes the spatial-gradient and constraint terms of the full quadratic action. This ratio is more informative than the adjoint eigenvalue alone: it checks that the field has a time derivative, and it checks the coefficient of the restoring term in the same convention.

The scalar fluctuation in the direction of separation is linked to this vector by the gauge transformation. Write an infinitesimal Hermitian parameter with $\vartheta_{12} = t$. At the diagonal background,

$$(\delta_\vartheta \Phi_i)_{12} = i[\vartheta, \overline{\Phi}_i]_{12} = -i\,\Delta\phi_i\, t. \tag{III.4.37}$$

For $\Delta\vec{\phi} \neq 0$, its component parallel to $\Delta\vec{\phi}$ can be shifted by a broken-generator gauge transformation. A gauge in which that component is removed exposes the massive vector. Scalar components orthogonal to the separation vector do not shift under this particular transformation. Their physical spectrum requires the remaining scalar quadratic terms and constraints; it is not fixed merely by labeling them with the same matrix unit. The mass in (III.4.35) therefore belongs to an isolated physical spatial-vector polarization in the stated p-domain. The background centralizer counts unbroken gauge generators; it does not replace this quadratic physical-mode calculation.

The same formula appears from the leading stretched open-string ground state in the flat supersymmetric setting. With $T_{\mathrm{F1}} = 1/(2\pi\alpha')$, the energy of a straight string of length $|\Delta\vec{X}|$ is

$$m_{\mathrm{stretch}} = T_{\mathrm{F1}}|\Delta\vec{X}| = \frac{|\Delta\vec{X}|}{2\pi\alpha'}, \qquad m_{\mathrm{stretch}}^2 = m_W^2. \tag{III.4.38}$$

The match uses the sourced open-string ground-state premise and the position coordinate inherited from Chapter 1. It does not mean that the Yang–Mills truncation is controlled at arbitrary separation: if the stretched mode is above the low-energy window, the equality is a formal comparison of its leading mass formula rather than a reason to retain it in a low-energy effective theory.

A D3 example fixes all factors. Take $\alpha' = 3/2$ in a common length unit and $|\Delta\vec{X}| = 5$. Then $\lambda = 3\pi$, and

$$|\Delta\vec{\phi}| = \frac{5}{3\pi}, \qquad m_W^2 = \frac{25}{9\pi^2}, \qquad \pi^2 m_W^2 = \frac{25}{9}. \tag{III.4.39}$$

Choose coordinates so that only the ninth transverse scalar differs. After removing a common shift, the same example can be written $\overline{\Phi}_9 = \mathrm{diag}(5/(6\pi), -5/(6\pi))$. For a spatial component w_a, the trace computations now become numbers rather than vector notation:

$$\mathcal{L}_w^{(2)} = \frac{2}{g^2}|\dot{w}_a|^2 - \frac{2}{g^2}\frac{25}{9\pi^2}|w_a|^2 + \cdots . \tag{III.4.40}$$

The coefficient of $|w_a|^2$ alone is not m_W^2; the kinetic coefficient must be divided out. In this coordinate the broken scalar fluctuation is the off-diagonal component of Φ_9, since (III.4.37) is nonzero only for $i = 9$. The other five transverse scalars have different gauge-shift behavior. The example thus checks the ratio and identifies exactly which scalar is the broken-generator direction without claiming a full scalar spectrum.

At rest, a massive spatial vector admits the polarization used in the quadratic calculation whenever $p \geq 1$. A D3 has several spatial directions, making that choice especially transparent. In one spatial dimension the rest-frame component still has a time derivative, but there is no separate transverse spatial polarization at nonzero momentum. The mass ratio remains the rest-frame quadratic result; the constraint analysis organizes the physical mode away from rest.

The D8 limit supplies a useful single-direction control. Its one scalar may have a diagonal background $\overline{\Phi}_9 = \mathrm{diag}(d/2, -d/2)$. There is no commutator potential involving two different scalar directions, but the spatial vector still couples through $D_a\overline{\Phi}_9$. The same trace ratio gives

$$m_W^2 = d^2, \qquad |\Delta X^9| = \lambda|d|. \tag{III.4.41}$$

Thus absence of a scalar commutator potential does not mean that a separated stack has no heavy off-diagonal vector. The potential asks whether scalar matrices commute; the mass term asks whether a charged vector commutes with a chosen scalar background. These are different commutators serving different physical questions. In the D9 limit there is no $\overline{\Phi}_9$ to supply the latter background. For distinct eigenvalue vectors the common centralizer of the background is $U(1)^2$, with Lie algebra dimension 2. At coincidence $\Delta\vec{\phi} = 0$, the mass vanishes and the centralizer grows to $U(2)$. Figure III.4.4 makes the two orientations of the stretched string and the separation vector explicit.

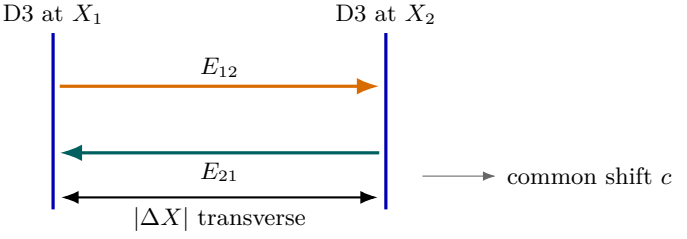


Figure III.4.4: Two parallel D3-branes separated in a transverse direction. The two oriented strings carry E_{12} and E_{21}. Their length is $|\Delta X|$, while a common displacement c moves both branes and leaves that length and the quadratic mass unchanged. The drawing shows the geometry used in the kinetic-to-mass comparison.

Indeed, $\overline{\Phi}_i \mapsto \overline{\Phi}_i + c_i\mathbf{1}_2/\lambda$ changes both positions, but the commutator in (III.4.31) and the difference in (III.4.35) stay fixed. This is another way to see why discarding the trace position from the vacuum set would confuse a physical translation with a gauge identification. The root eigenvalue is relative; the center-of-mass position is absolute up to spacetime translation symmetry, not gauge equivalence.

The limit $p = 0$ requires a separate warning. Its worldvolume has only A_0, with $F_{00} = 0$. In particular,

$$\frac{\partial^2\mathcal{L}}{\partial\dot{A}_0^2} = 0, \qquad A_0 \text{ imposes a gauge constraint rather than a Proca equation.} \tag{III.4.42}$$

One can see the constraint in the leading scalar kinetic term. Here $D_0\Phi_i = \dot{\Phi}_i - i[A_0, \Phi_i]$, so a variation of A_0 has no integration by parts in time. Cyclicity of the trace instead yields the matrix Gauss condition

$$\delta_{A_0}\mathcal{L} \propto \mathrm{Tr}_f\, \delta A_0 \sum_i [\Phi_i, D_0\Phi_i], \qquad \sum_i [\Phi_i, D_0\Phi_i] = 0. \tag{III.4.43}$$

An off-diagonal A_0 can appear algebraically when the scalars are separated, but an algebraic quadratic coefficient is not a particle mass. Solving (III.4.43) and quotienting gauge orbits are necessary before counting physical off-diagonal D0 oscillations. The algebraic centralizer still changes from $U(1)^2$ to $U(2)$ when the D0 positions coincide. Its off-diagonal scalar spectrum, however, needs the constraint and gauge quotient; the spatial-vector derivation cannot be applied to A_0. At $p = 9$ there is no transverse $\Delta\vec{X}$ and hence no separation problem of this kind. These endpoint cases keep a useful mass formula within its actual domain. The next section uses D0-branes for a different purpose: a static matrix energy in a specified RR background.

III.4.6 A dielectric D0 example and its boundary

Can a background favor matrices that do not commute? The flat-background argument in (III.4.20) says no for its own potential. A constant RR four-form adds a cubic coupling, so that conclusion need not survive. We now use a separate leading static D0 example in the source's rescaled RR units. Let $i, j, k = 1, 2, 3$ denote three selected transverse directions and take

$$F^{(4)}_{tijk} = -2f\,\epsilon_{ijk}, \qquad \epsilon_{123} = +1, \qquad \lambda = 2\pi\alpha'. \tag{III.4.44}$$

Here f is a source-local background parameter. The source uses $T_0 = \mu_0$ after its RR potential rescaling. That equality is not a redefinition of the book's general RR charge. The flat stack and its leading Yang–Mills term remain the starting point; only this example adds the specified RR field.

In these units the relevant truncated static potential, relative to the commuting configuration, is

$$\frac{V}{T_0\lambda^2} = -\frac{1}{4}\sum_{i,j=1}^{3} \mathrm{Tr}_f[\Phi_i, \Phi_j]^2 + \frac{2if}{3}\sum_{i,j,k=1}^{3} \epsilon_{ijk}\,\mathrm{Tr}_f(\Phi_i\Phi_j\Phi_k). \tag{III.4.45}$$

The first term is the positive commutator energy of the leading action; the second is the background-induced cubic interaction. The ordered indices and the source's RR sign are essential. Nothing in this calculation asserts an all-order matrix action or stability against every fluctuation.

For $N = 2$, insert the Pauli ansatz $\Phi_i = q\sigma_i$, where $\sigma_i\sigma_j = \delta_{ij}\mathbf{1}_2 + i\epsilon_{ijk}\sigma_k$ and $\mathrm{Tr}_f\,\mathbf{1}_2 = 2$. The commutator and its square for unequal indices are

$$[\Phi_i, \Phi_j] = 2iq^2\epsilon_{ijk}\sigma_k, \qquad \mathrm{Tr}_f[\Phi_i, \Phi_j]^2 = -8q^4 \quad (i \neq j). \tag{III.4.46}$$

There are six ordered unequal pairs, so their sum is

$$\sum_{i,j=1}^{3} \mathrm{Tr}_f[\Phi_i, \Phi_j]^2 = 6(-8q^4) = -48q^4. \tag{III.4.47}$$

For the cubic, the Pauli product gives $\mathrm{Tr}_f(\sigma_i\sigma_j\sigma_k) = 2i\epsilon_{ijk}$. Six nonzero permutations consequently yield

$$\sum_{i,j,k=1}^{3} \epsilon_{ijk}\,\mathrm{Tr}_f(\Phi_i\Phi_j\Phi_k) = 6(2iq^3) = 12iq^3. \tag{III.4.48}$$

Inserting both trace sums produces a one-variable leading potential:

$$\frac{V(q)}{T_0\lambda^2} = -\frac{1}{4}(-48q^4) + \frac{2if}{3}(12iq^3) = 12q^4 - 8fq^3. \tag{III.4.49}$$

The relative minus sign in the cubic comes from $i^2 = -1$. It is the reason the background can lower the energy of a noncommuting ansatz.

Differentiate the actual polynomial rather than inferring a radius from the commutator alone:

$$\frac{1}{T_0\lambda^2}\frac{dV}{dq} = 48q^3 - 24fq^2 = 24q^2(2q - f), \qquad q = 0 \text{ or } q = \frac{f}{2}. \tag{III.4.50}$$

At the nonzero branch, when $f \neq 0$, the energy relative to $q = 0$ is

$$\frac{V(f/2) - V(0)}{T_0\lambda^2} = 12\frac{f^4}{16} - 8f\frac{f^3}{8} = -\frac{f^4}{4}. \tag{III.4.51}$$

For $f = 0$ the two named branches merge at $q = 0$; there is no separate nonzero branch. Lower energy within this ansatz is a precise leading-order comparison, not a full fluctuation or quantum stability theorem.

The one-variable curve gives a slightly sharper statement inside its own ansatz. Its second derivative at the nonzero branch is

$$\frac{1}{T_0\lambda^2}\frac{d^2V}{dq^2}\bigg|_{q=f/2} = (144q^2 - 48fq)\big|_{q=f/2} = 12f^2. \tag{III.4.52}$$

For $f \neq 0$ the branch is thus a local minimum in the single amplitude q that we varied. If f changes sign, the stationary amplitude $q = f/2$ changes sign too, while its energy difference depends on f^4 and its squared radius on f^2. These are direct properties of the displayed polynomial. They do not test matrix fluctuations outside the Pauli ansatz, fermionic effects, higher-order terms or the global conditions required to realize the background.

To interpret the matrices geometrically, define the source's mean-squared radius about a zero center by

$$R^2 = \frac{\lambda^2}{2}\,\mathrm{Tr}_f \sum_{i=1}^{3} \Phi_i^2. \tag{III.4.53}$$

Since each $\sigma_i^2 = \mathbf{1}_2$, the trace sum is $6q^2$, and therefore

$$\frac{R^2}{\lambda^2} = 3q^2, \qquad \left.\frac{R^2}{\lambda^2}\right|_{q=f/2} = \frac{3f^2}{4}. \tag{III.4.54}$$

This radius is a collective second moment of matrices. It is not obtained by assigning three simultaneous eigenvalues to each D0-brane. Each Pauli matrix separately has eigenvalues ± 1, but the eigenvectors of σ_1 do not diagonalize σ_2. The obstruction is already visible in $[\sigma_1, \sigma_2] = 2i\sigma_3$. There is therefore no pair of ordinary points (X^1, X^2, X^3) whose coordinates are the three matrix eigenvalues in the manner of (III.4.24). The positive quantity in (III.4.54) describes the size of this noncommuting ansatz in the source's definition. It does not turn that ansatz into the commuting position quotient of the previous section.

This distinction explains the dielectric interpretation. A background RR coupling changes which matrix configuration is favored by the leading energy. The Pauli matrices respond collectively even though a rank-one scalar has no such cubic coupling. The calculation gives a scale for that response, while its radius definition and energy comparison remain conditional on the chosen background and truncation. The zero-center premise matters. Adding $c_i\mathbf{1}_2$ leaves commutators and the potential invariant but changes the uncentered $\operatorname{Tr}\sum_i \Phi_i^2$. The radius above describes the noncommuting part with the center fixed at the origin. More explicitly,

$$\Phi_i \longmapsto \Phi_i + c_i\mathbf{1}_2 \quad \Longrightarrow \quad \frac{\lambda^2}{2}\operatorname{Tr}_f \sum_i (\Phi_i + c_i\mathbf{1}_2)^2 = R^2 + \lambda^2 \sum_i c_i^2. \tag{III.4.55}$$

The cross term vanishes for the Pauli ansatz because each $\operatorname{Tr}\sigma_i = 0$. The shifted formula is a relation between an uncentered second moment and the radius of the matrix configuration about its chosen center. It does not change the stationary polynomial. Keeping these two geometric quantities separate prevents a free translation from being mistaken for a change in the dielectric configuration.

A useful numerical check sets $f = 3$:

$$q = \frac{3}{2}, \qquad \frac{V}{T_0\lambda^2} = -\frac{81}{4}, \qquad \frac{R^2}{\lambda^2} = \frac{27}{4}. \tag{III.4.56}$$

At $N = 1$, both the commutator and the antisymmetric cubic trace vanish. That limit confirms that the effect is a matrix interaction rather than an abelian scalar displacement.

The same conclusion can be checked term by term. For a one-dimensional matrix representation, all Φ_i are ordinary numbers, so $[\Phi_i, \Phi_j] = 0$. The cubic summand is symmetric under exchanging two factors, while ϵ_{ijk} changes sign. Its complete ordered sum therefore cancels. At $N = 2$, by contrast, the Pauli matrices distinguish the order of the three factors, and the six terms in (III.4.48) add with the same sign. This is the precise matrix feature the RR coupling uses.

The calculation ends where the source's control ends. Higher-order commutator corrections occur beyond a universal symmetrized-trace Born–Infeld prescription. The truncated polynomial cannot certify an exact radius, a full stability spectrum, a general

curved-background solution or a global RR completion. It does exhibit a concrete mechanism: the RR cubic term competes with the positive quartic energy and gives a nonzero stationary matrix configuration at the displayed order. That mechanism will reappear when later chapters discuss matrix and brane-probe constructions, but the present result remains this finite D0 example.

III.4.7 Exercises

The first four tasks have exact submitted answers in the chapter companion. Show the intermediate field-theory or matrix steps on paper. The final task is a written interpretation exercise.

1. **E1, ordered reduction.** Starting with $\mathcal{L} = -\operatorname{Tr}_f F_{MN}F^{MN}/(2g^2)$ and $F_{ij} = -i[\Phi_i, \Phi_j]$, split the ordered contraction. After factoring $1/g^2$, submit the coefficients of $\operatorname{Tr}_f F_{\mu\nu}^2$, $\operatorname{Tr}_f(D_\mu\Phi_i)^2$, and $\operatorname{Tr}_f[\Phi_i, \Phi_j]^2$. Explain the mixed-index factor and the Hermitian commutator sign.

2. **E2, conjugacy and positions.** For one Hermitian $U(2)$ scalar take $A = \operatorname{diag}(0, 3)$, $A_{\text{swap}} = \operatorname{diag}(3, 0)$, and $B = \operatorname{diag}(1, 2)$. All three have trace 3. Submit $\operatorname{Tr} A^2$, $\operatorname{Tr} B^2$, and whether each of A_{swap} and B is separately conjugate to A. Explain why this one-matrix test does not allow independent permutations of different matrices in a commuting tuple.

3. **E3, separated D3-branes.** Two parallel D3-branes have $|\Delta X| = 5$ and $\alpha' = 3/2$, with $X = 2\pi\alpha'\Phi$. Starting from the temporal kinetic and scalar covariant-derivative terms of a spatial off-diagonal vector, compute $\pi^2 m_W^2$ and the dimension of the unbroken $U(1)^2$ Lie algebra. Explain why this formal nonunit-α' mass comparison alone is not a controlled low-energy window at arbitrary separation, and why it supplies no propagating mass for D0 A_0.

4. **E4, the RR Pauli ansatz.** In the leading D0 setup $F^{(4)}_{tijk} = -2f\epsilon_{ijk}$, set $f = 3$ and $\Phi_i = q\sigma_i$. Compute the ordered quartic and cubic traces, then submit the nonzero stationary q, the relative $V/(T_0\lambda^2)$, and R^2/λ^2 using the zero-center radius in (III.4.53).

5. **E5, written interpretation.** A proposed argument says that the symmetrized-trace nonabelian Born–Infeld action is exact at every order because its leading scalar potential agrees with Yang–Mills. Locate the logical gap using the higher-order discussion in Myers, physical PDF p. 25. State which leading-order calculation in this chapter survives and which all-order conclusion does not follow.

Take-home message

Ordered endpoints produce matrix multiplication and a leading $U(N)$ worldvolume multiplet. Reduction of the half-trace ten-dimensional action fixes the scalar kinetic term and positive commutator energy. Its constant flat classical vacua are unordered physical positions, including their center of mass. For separated D3-branes the ratio of a spatial vector's mass and kinetic coefficients equals the squared stretched-string mass; the D0 gauge field instead enforces a constraint. In a specified RR background, a cubic term admits a noncommuting D0 stationary ansatz at leading order. A reader should now be able to multiply endpoint matrices, reduce the ordered field-strength contraction, identify the classical position quotient, calculate a D3 W mass, and evaluate the Pauli ansatz.

Status and sources

Section III.4.2 takes the coincident-stack spectrum as a cited physical premise from Myers (1999, physical PDF p. 3) and Tong (2009, physical PDF pp. 198–199). The sixteen-supercharge leading multiplet is a cited physical premise from Tong (2009, physical PDF pp. 202–203). Ordered endpoint multiplication and relative charges are [MATH] in the stated tension, gauge-group and endpoint conventions.

Section III.4.3 takes the leading matrix action from Tong (2009, physical PDF p. 199, eq. (7.39)) and Myers (1999, physical PDF p. 8, eq. (24)) (cited physical input). The Hermitian block split, ordered coefficients, and rank-one/D8/D9 controls are [MATH]. The book has $D = \partial - i[A, \cdot]$, $-\operatorname{Tr}_f F^2/(2g^2)$, and $\lambda^2\tau_p = 2/g^2$. The source worldvolume connection obeys $A_{\text{source}} = -A_{\text{book}}$; the declared physical scalar dictionary $X = \lambda\Phi$ stays fixed. No disk-amplitude proof is supplied.

Section III.4.4 uses Myers (1999, physical PDF p. 19, eqs. (61)–(64)) and Tong (2009, physical PDF pp. 200–201, eqs. (7.40)–(7.42)) (cited physical input). Positive energy, finite Hermitian diagonalization and the Weyl action, and the classical flat noncompact zero-field scalar quotient are [MATH], as are center preservation, degeneracy stabilizers and the special-rank and dimension checks. No quantum, Wilson-line or flux classification follows.

Section III.4.5 uses the position dictionary in Tong (2009, physical PDF p. 200, eq. (7.42)) and the separated-brane mass frame in Tong (2009, physical PDF p. 201, eq. (7.43)) (cited physical input). The D3 spatial-vector kinetic/mass ratio, centralizer change, D0 velocity-Hessian obstruction, and p9 control are [MATH]. The stretched-string equality is a scoped (cited physical input) match; arbitrary separation does not establish effective-field-theory control or a D0 vector-particle spectrum.

Section III.4.6 uses the specified RR field and leading potential in Myers (1999, physical PDF pp. 20–22, eqs. (65)–(79)) (cited physical input). Pauli traces and the stationary branch, zero-center radius, and rank-one limit are [MATH] within that truncation. Myers' RR units have $T_0 = \mu_0$, with $C_{\text{source}} = g_s C_{\text{book}}$ and $T_{\text{source}} = \mu_{\text{source}} = \mu_{\text{book}}/g_s$; its f remains source-local. The higher-order limitation is Myers (1999, physical PDF p. 25) (cited physical input). The quadratic approximation does not establish exact nonabelian DBI, a quantum vacuum theorem, disk proof or a matrix-theory definition.

The cited physical inputs in this apparatus retain their stated source and regime and are cited physical inputs. The mathematical checks do not establish those physical premises.

References

Myers, R. C. (1999). *Dielectric-Branes*. Version 2. arXiv: `hep-th/9910053`.
Tong, D. (2009). *Lectures on String Theory*. Version 3. arXiv: `0908.0333`.

Chapter III.5

Branes within branes: dissolved charges, instanton numbers, K-theory (light)

III.5.1 A smooth field can carry a lower charge

A D-brane is a source for a Ramond–Ramond (RR) potential. It is tempting to identify every lower-dimensional RR charge with a separate, visibly embedded brane. A gauge field on a higher-dimensional brane gives another possibility. Its flux can couple to the potential that would have coupled to the lower brane. The lower charge is then spread across the parent worldvolume. This is the sense in which one brane can be dissolved in another.

There are three increasingly demanding questions behind this picture. First, which coefficient of a worldvolume field strength has the units and sign of a lower D-brane charge? Second, when two flux configurations give the same integrals, do they describe the same global charge? Third, which charge number is being held fixed when a background B-field changes its representative? The answers require a local Wess–Zumino (WZ) coupling, characteristic classes, a global anomaly example, and a careful distinction among source, Page, and Maxwell charges.

We use the Chapter 3 normalization $\lambda = 2\pi\alpha'$ and a positively oriented parent Dp-brane. The first two calculations set $B = 0$, omit curvature terms, and work in an oriented local charge frame. These assumptions let us calculate the first two flux contributions. They do not say that an arbitrary flux is a stable bound state. Chapter 4 explained how coincident branes supply matrix gauge fields; here their trace controls the lower RR source. The last two sections show why a local source coefficient is only part of a global charge story.

III.5.2 Charge from the WZ exponential

Why does a smooth two-form on a Dp-brane couple to a potential for a D$(p-2)$-brane? Write W_{p+1} for the oriented parent worldvolume and let $C = \sum_q C_q$ be the formal sum of RR potentials. For an ordinary rank-r worldvolume bundle, F is its Hermitian curvature two-form and Tr is the ordinary trace in that bundle. In the local, curvature-omitted WZ term, only the component of total degree (p+1) is integrated:

$$S_{\mathrm{WZ}} = \mu_p \int_{W_{p+1}} \left[C \wedge \operatorname{Tr} \exp(B + \lambda F) \right]_{p+1}, \qquad \lambda = 2\pi\alpha'. \tag{III.5.1}$$

The coupling itself is string-theoretic input. The degree extraction and normalization that follow are calculations within it. A potential C_q has degree q; every factor of F or B has degree two. At $B = 0$,

$$\operatorname{Tr} e^{\lambda F} = r + \lambda \operatorname{Tr} F + \frac{\lambda^2}{2} \operatorname{Tr}(F \wedge F) + O(F^3). \tag{III.5.2}$$

Thus C_{p+1}, $C_{p-1} \wedge F$, and $C_{p-3} \wedge F \wedge F$ are precisely the first three possible degree-$p+1$ pieces. In particular the F^2 term has the factorial $1/2!$; it is not the square of $\operatorname{Tr} F$.

$$S_{\mathrm{WZ}} \supset \mu_p \int_{W_{p+1}} \left[r C_{p+1} + \lambda C_{p-1} \wedge \operatorname{Tr} F + \frac{\lambda^2}{2} C_{p-3} \wedge \operatorname{Tr}(F \wedge F) \right]. \tag{III.5.3}$$

To read the coefficients in lower-brane units, use the book's RR charge normalization $\mu_p = (2\pi)^{-p} (\alpha')^{-(p+1)/2}$. The neighboring charge ratios follow directly, with both powers of 2π and α' visible:

$$\frac{\mu_p \lambda}{\mu_{p-2}} = \frac{(2\pi)^{-p} (\alpha')^{-(p+1)/2} (2\pi\alpha')}{(2\pi)^{-(p-2)} (\alpha')^{-(p-1)/2}} = \frac{1}{2\pi}. \tag{III.5.4}$$

For the next term, the factorial remains part of the comparison:

$$\frac{\mu_p \lambda^2}{2\mu_{p-4}} = \frac{(2\pi)^{-p} (\alpha')^{-(p+1)/2} (2\pi\alpha')^2}{2(2\pi)^{-(p-4)} (\alpha')^{-(p-3)/2}} = \frac{1}{8\pi^2}. \tag{III.5.5}$$

If the parent wraps an oriented two-cycle Σ, the linear term therefore has the charge coefficient

$$q_{p-2}^{\mathrm{gauge}}(\Sigma) = \int_\Sigma \frac{\operatorname{Tr} F}{2\pi}. \tag{III.5.6}$$

The superscript reminds us that this is the gauge contribution in the stated frame. Figure III.5.1 shows the oriented cycle and the RR potential that sees its flux. It depicts a distributed source. It does not assert that a separate small brane exists at any marked point.

For a line bundle L, ordinary Dirac quantization on this $B = 0$ cycle gives $\int_\Sigma F/(2\pi) = n \in \mathbb{Z}$. At $n = 3$, the coupling on the remaining directions is three times the positive D$(p-2)$ coupling. Reversing the orientation of Σ changes the evaluated period to -3, while the local two-form has not changed. At $n = 0$, this gauge-induced component vanishes; the parent still has its C_{p+1} coupling. These controls

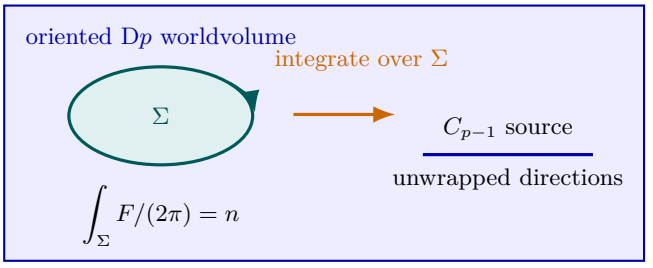


Figure III.5.1: An oriented two-cycle inside a positively oriented Dp-brane. The flux period $\int_\Sigma F/(2\pi) = n$ supplies the coefficient of C_{p-1} on the unwrapped directions. The shaded cycle is a source region, not the location of n separate small branes.

show why both the parent orientation and the integration orientation belong in any statement about the sign of "induced brane number."

A second way to check the factor in (III.5.6) is to keep both the rank and the flux distribution visible. Let the gauge bundle split as $L_1 \oplus L_2$ over the chosen two-cycle. Suppose the two line bundles have periods $n_1 = 2$ and $n_2 = -1$. The two diagonal field strengths are independent, while the trace adds them:

$$\operatorname{Tr} F = F_1 + F_2, \qquad \int_\Sigma \frac{\operatorname{Tr} F}{2\pi} = n_1 + n_2 = 1. \tag{III.5.7}$$

The parent coupling to C_{p+1} has coefficient two, because the bundle has rank two. Its gauge-induced C_{p-1} coefficient is one, not two and not the sum of the absolute values of the periods. Opposite orientations of flux in the two diagonal factors can cancel a lower source without removing either parent brane. This example also explains why the rank term and the linear flux term in (III.5.3) must be read separately.

For an ordinary line bundle the degree-two character component is just its first Chern class. Write $u = c_1(L) = [F/(2\pi)]$. Then the first three terms of the same exponential have a compact cohomological form:

$$\operatorname{ch}(L) = e^u = 1 + u + \frac{u^2}{2} + O(u^3). \tag{III.5.8}$$

The symbol $O(u^3)$ means classes of degree at least six, which cannot contribute when the integration cycle is only four-dimensional. On a two-cycle, only $1 + u$ matters. On a four-cycle the $u^2/2$ term enters. It is the same factorial that appeared before any bundle terminology. This is the route from the worldvolume coupling to the Chern-character language of the next section.

The integration can be written as a simple pushforward when the local geometry factors. Let the wrapped worldvolume be $M_{p-1} \times \Sigma$ with the product orientation. Here M_{p-1} has dimension $p - 1$, and suppose C_{p-1} is pulled back from it while F has legs

only on Σ. Then the linear term of (III.5.3) separates as

$$\begin{aligned}\mu_p\lambda\int_{M_{p-1}\times\Sigma} C_{p-1}\wedge \operatorname{Tr} F &= \mu_p\lambda\left(\int_\Sigma \operatorname{Tr} F\right)\left(\int_{M_{p-1}} C_{p-1}\right)\\ &= \mu_{p-2}\left(\int_\Sigma \frac{\operatorname{Tr} F}{2\pi}\right)\int_{M_{p-1}} C_{p-1}.\end{aligned} \tag{III.5.9}$$

This equality says exactly where the lower-dimensional source lives: on the unwrapped M_{p-1}, with coefficient equal to the oriented flux period. If either the product description or the pullback assumption is absent, the local coupling is still meaningful, but this particular factorization must be replaced by the appropriate fiber integration. The picture of a charge "inside" a brane is shorthand for this coupling, not a claim that the higher-dimensional worldvolume has lost two dimensions.

The integrated period is stable under a smooth deformation of the ordinary bundle connection on a fixed cycle, although the pointwise density changes. The next WZ term asks for a four-cycle and measures a different characteristic component.

III.5.3 Instanton number as dissolved branes

Which four-form does the second flux term count? Let X be a compact oriented four-cycle in the parent worldvolume. In the same $B = 0$, curvature-omitted frame, the coefficient of C_{p-3} is

$$q_{p-4}^{\text{gauge}}(X) = \int_X \frac{\operatorname{Tr}(F\wedge F)}{8\pi^2}. \tag{III.5.10}$$

The denominator is exactly the ratio in (III.5.5). The trace is over the worldvolume bundle; it cannot generally be replaced by $(\operatorname{Tr} F)^2$. We now identify the characteristic class represented by this four-form.

In the chosen Hermitian chart, F is an endomorphism-valued curvature two-form. The trace of its exponential is a closed Chern–Weil form; $\operatorname{ch}(E)$ below denotes its de Rham cohomology class:

$$\operatorname{ch}(E) = \left[\operatorname{Tr}\exp(F/(2\pi))\right] = \operatorname{rk}(E) + \operatorname{ch}_1(E) + \operatorname{ch}_2(E) + \cdots. \tag{III.5.11}$$

Pull E back to a splitting space, where it formally splits into line bundles with degree-two roots $u_1, \ldots, u_r$. Symmetric expressions in these roots descend to characteristic classes on X. Expanding one exponential at a time gives

$$\operatorname{ch}(E) = \sum_{a=1}^{r} e^{u_a}, \qquad \operatorname{ch}_1(E) = \sum_a u_a, \qquad \operatorname{ch}_2(E) = \frac{1}{2}\sum_a u_a^2. \tag{III.5.12}$$

The first two ordinary Chern classes are $c_1 = \sum_a u_a$ and $c_2 = \sum_{a<b} u_a u_b$. Squaring the first and separating the diagonal and off-diagonal terms yields the needed identity:

$$c_1^2 = \sum_a u_a^2 + 2\sum_{a<b} u_a u_b \quad\Longrightarrow\quad \operatorname{ch}_2(E) = \frac{c_1(E)^2 - 2c_2(E)}{2}. \tag{III.5.13}$$

Comparing (III.5.11) with (III.5.10) identifies that WZ coefficient as $\int_X \mathrm{ch}_2(E)$. This is a rational cohomological component. The value can be half-integral even when the bundle's ordinary Chern classes are integral.

For a worked nonunit example, choose a positive degree-two class J on X with $\int_X J^2 = 1$. Let a rank-two bundle have $c_1(E) = 3J$ and $c_2(E) = 4J^2$. The algebra is

$$\mathrm{ch}_0(E) = 2, \qquad \mathrm{ch}_1(E) = 3J, \qquad \mathrm{ch}_2(E) = \frac{9J^2 - 8J^2}{2} = \frac{1}{2}J^2. \tag{III.5.14}$$

Thus the gauge four-form integrates to $1/2$, even though the supplied c_2 integrates to 4. These two numbers answer different questions. The example specifies characteristic data; it does not assert existence of such a bundle on every arbitrary X with that intersection form.

The line-bundle case gives a useful comparison with the rank-two answer. If $c_1(L) = 3J$ on the same oriented four-cycle, the exponential of the single Chern root gives

$$\mathrm{ch}(L) = 1 + 3J + \frac{9}{2}J^2, \qquad \int_X \mathrm{ch}_2(L) = \frac{9}{2}. \tag{III.5.15}$$

The coefficient $9/2$ is exactly half the square of the ordinary first Chern number in this simple one-generator example. It is not the $1/2$ found for the rank-two characteristic data with the same $c_1 = 3J$. The rank-two $c_2 = 4J^2$ contributes a subtractive four units. Thus even if two gauge configurations have the same linear C_{p-1} coefficient, their quadratic C_{p-3} coefficients can differ. The converse also need not hold. This is why lower-charge information is naturally a graded list rather than one integer called "the dissolved charge."

An $SU(2)$ bundle makes the sign issue especially plain. Here $c_1 = 0$, so the same identity reduces to

$$\mathrm{ch}_2(E) = -c_2(E), \qquad \int_X c_2(E) = +1 \quad \Longrightarrow \quad \int_X \mathrm{ch}_2(E) = -1. \tag{III.5.16}$$

The $+1$ is the value of c_2 in the chosen orientation; the WZ degree-four coefficient is -1 in our Hermitian chart. Reversing the orientation of X reverses both evaluated integrals. A statement that a "unit instanton" carries one lower brane must specify whether instanton number denotes c_2, $-c_2$, or a self-duality convention. The orientation and sign are visible in Figure III.5.2.

The sign can be checked directly with two formal Chern roots. For an $SU(2)$ bundle they occur as u and $-u$, since their sum is $c_1 = 0$. The two degree-four expressions are then

$$c_2 = u(-u) = -u^2, \qquad \mathrm{ch}_2 = \frac{u^2 + (-u)^2}{2} = u^2 = -c_2. \tag{III.5.17}$$

The roots live on the splitting space; they need not be Chern classes of global line subbundles on X. Their symmetric square $u^2 = -c_2(E)$ descends to X. It is this descended class that is evaluated there: $\int_X \mathrm{ch}_2(E) = -\int_X c_2(E) = -1$.

The rank-two data used in (III.5.14) make a different point. Their first character component is three, but their second is one half. A naive replacement of the trace by a

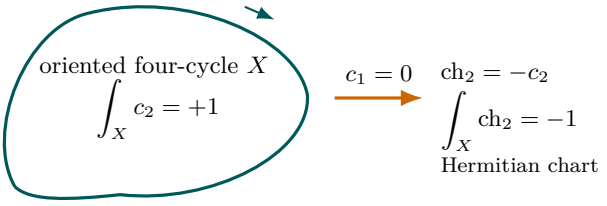


Figure III.5.2: The same oriented four-cycle supports a second Chern class and the degree-four Chern-character component that enters the gauge WZ source. For $c_1 = 0$, the two evaluated numbers have opposite signs. Reversing the integration orientation changes both integrals.

square of its trace would give

$$\frac{1}{2}c_1^2 = \frac{9}{2}J^2, \qquad \text{whereas} \qquad \mathrm{ch}_2 = \frac{1}{2}J^2. \tag{III.5.18}$$

The c_2 term changes the answer by four. This negative control catches the substitution of $\mathrm{Tr}\, F \wedge \mathrm{Tr}\, F$ for $\mathrm{Tr}(F \wedge F)$.

The field need not be concentrated in a tiny region for the integral to be nonzero. Its density $\mathrm{Tr}(F \wedge F)$ can be smooth across the four-cycle. A localized instanton is one useful limit, but the local WZ calculation alone says nothing about an isolated BPS soliton, its size modulus, or the stability of an arbitrary bundle. The distinction becomes more important when we replace a single bundle by a formal brane-antibrane pair: then algebraic additivity is exact, while the physical annihilation step has its own premise.

III.5.4 Bundles and charge bookkeeping

How can two stacks with different visible brane numbers encode the same topological charge? Witten's Type-IIB construction starts with space-filling D9-branes and anti-D9-branes over spacetime. Its tadpole-cancelling pair has equal ranks. On noncompact spacetime, an excitation agrees with the vacuum at infinity, so the difference is represented with compact support. For the mathematical bookkeeping, take complex bundles E and F over a common space X. The formal difference $[E] - [F]$ is a virtual bundle. Direct sum $E \oplus H$ means placing another bundle H alongside E. The stable relation adds the same H to both sides:

$$(E, F) \sim (E \oplus H, F \oplus H), \qquad [E \oplus H] - [F \oplus H] = [E] - [F]. \tag{III.5.19}$$

Mathematically this is the Grothendieck bookkeeping behind $K(X)$. Its physical brane interpretation uses the cited common-pair annihilation premise within the D9 setting just stated. Equation (III.5.19) by itself is not a tachyon-condensation theorem for every configuration.

The Chern character is additive for direct sums. One can see this without an abstract theorem: a block-diagonal curvature has a block-diagonal exponential, and the trace adds. Consequently,

$$\mathrm{ch}(E \oplus H) = \mathrm{ch}(E) + \mathrm{ch}(H), \qquad \mathrm{ch}(E \oplus H) - \mathrm{ch}(F \oplus H) = \mathrm{ch}(E) - \mathrm{ch}(F). \tag{III.5.20}$$

The equality holds separately in degrees zero, two, and four. It is the precise algebra behind the common-H cancellation drawn in Figure III.5.3. The physical interpretation still relies on the setting just stated.

Take a line bundle L with $c_1(L) = J$ on the oriented four-cycle $\int_X J^2 = 1$. For each integer m, its truncated character is

$$\mathrm{ch}(L^m) = e^{mJ} = 1 + mJ + \frac{m^2}{2} J^2 \quad \text{through degree four.} \tag{III.5.21}$$

Now choose $E = L^2 \oplus L^{-1}$ and $F = L$. Their components are calculated term by term:

$$\begin{aligned} \mathrm{ch}(E) &= (1 + 2J + 2J^2) + (1 - J + \tfrac{1}{2}J^2) = 2 + J + \tfrac{5}{2}J^2, \\ \mathrm{ch}(F) &= 1 + J + \tfrac{1}{2}J^2, \\ \mathrm{ch}(E) - \mathrm{ch}(F) &= 1 + 0J + 2J^2. \end{aligned} \tag{III.5.22}$$

The virtual rank is one, the degree-two component vanishes, and the degree-four component is two. This unrestricted virtual-bundle calculation on a four-cycle is not a complete D9–anti-D9 state of the equal-rank, space-filling tadpole-cancelling construction. It also does not prove a stable BPS object exists at a selected modulus.

Add the nontrivial common bundle $H = L^3$. Since $\mathrm{ch}(H) = 1 + 3J + \frac{9}{2}J^2$, the larger pair has

$$\begin{aligned} \mathrm{ch}(E \oplus H) &= 3 + 4J + 7J^2, \\ \mathrm{ch}(F \oplus H) &= 2 + 4J + 5J^2, \\ \mathrm{ch}(E \oplus H) - \mathrm{ch}(F \oplus H) &= 1 + 0J + 2J^2. \end{aligned} \tag{III.5.23}$$

The new stacks have ranks three and two, yet all three displayed components agree with (III.5.22). The cancellation is not merely the observation that adding an empty object changes nothing: H itself carries nonzero first and second character components.

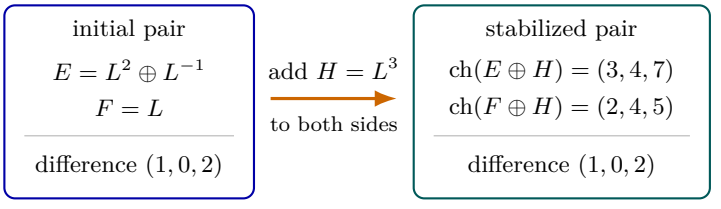


Figure III.5.3: Formal stabilization of a brane-antibrane pair. The common $H = L^3$ contributes $(1, 3, 9/2)$ to each stack, so it cancels in the virtual character. The arrow records mathematical stable bookkeeping; physical annihilation requires the Type-IIB brane-antibrane premise.

Subtracting the antibrane components from the brane components before or after stabilization gives $(1, 0, 2)$. The cancellation is componentwise; even the nonzero degree-four component of H disappears from the formal difference.

The requirement that the same H appear on each side is essential. For instance, keep $H = L^3$ on the brane side but add a trivial line bundle $\mathbf{1}$ on the antibrane side. Their ranks cancel, yet

$$\mathrm{ch}(H) - \mathrm{ch}(\mathbf{1}) = 3J + \frac{9}{2}J^2. \tag{III.5.24}$$

The first and second lower components have changed. A statement that "one extra brane and one extra antibrane cancel" is therefore too coarse. Their bundle data must match in the stable relation. Even when they match, the mathematical equality does not supply a dynamical path that annihilates them in a particular background. The Type-IIB brane-antibrane argument supplies that physical premise in its stated setting; the finite character computation supplies only the visible additive consequence.

A neutral common pair illustrates the limit of interpreting the component vector as a snapshot of a configuration. Take $E = F = L^2$ with no other factors. Both stacks individually have character $1 + 2J + 2J^2$, but their virtual character is zero:

$$\mathrm{ch}(L^2) - \mathrm{ch}(L^2) = 0. \tag{III.5.25}$$

The equality records a vanishing formal charge. It does not say that the two worldvolumes are absent before annihilation, or that the configuration is a vacuum at every point in its field space. Witten's physical construction supplies a tachyonic brane-antibrane process in the appropriate Type-IIB setting; which endpoint is dynamically reached can depend on data outside this Chern-character calculation. This example is also why "rank zero" for a virtual difference should not be read as "no branes were ever present."

There is a loss of information when these components are used as the entire charge label. The Chern character takes an integral K-class to rational cohomology. Torsion classes map to zero because rational cohomology has no torsion. Equality of the displayed rational components therefore need not imply equality of integral K-classes. Nor does a formal virtual rank specify a complete charge lattice, a tadpole-free background, or a BPS state. The limited result is useful: in a setting where the brane-antibrane construction applies, it organizes additive lower-charge data and explains why a common pair is invisible to those data. The next example shows that even the flux period entering this bookkeeping can be shifted by a global anomaly.

III.5.5 Nonspin cycles and half flux

Why can the ordinary integer-period rule fail for a wrapped D-brane? Consider a positively oriented D6 whose spatial compact part is $\mathbb{CP}^2$. Give $\mathbb{CP}^2$ its complex orientation and let $J \in H^2(\mathbb{CP}^2; \mathbb{Z})$ satisfy $\int_{\mathbb{CP}^1} J = 1$ and $\int_{\mathbb{CP}^2} J^2 = 1$. The embedded $\mathbb{CP}^1$ is the positive generator. Its orientation and that of the parent D6 fix the signs of the two gauge-induced coefficients.

Let Q be the D6 worldvolume, with $\mathbb{CP}^2$ as its compact spatial factor. The class $w_2(TQ)$ is the mod-two obstruction to an ordinary spin structure. On $\mathbb{CP}^2$ it is the

nonzero generator J mod 2. A Spin^c structure instead has a determinant line whose integral first Chern class xJ reduces to $w_2(TQ)$, so x must be odd. In the spin ambient, $B = 0$ source convention, the local U(1) factor of the Spin^c connection has half the determinant-line curvature and hence half its period:

$$xJ \bmod 2 = w_2(\mathbb{CP}^2), \qquad x \in 2\mathbb{Z} + 1, \qquad \int_{\mathbb{CP}^1} \frac{F}{2\pi} = \frac{x}{2}. \tag{III.5.26}$$

This F belongs to the Spin^c source frame, not to an ordinary line bundle with unchanged integral $F/(2\pi)$ periods. The integral obstruction $W_3(TQ)$ is the Bockstein of $w_2(TQ)$: it vanishes when that mod-two class has an integral lift. Here $H^3(\mathbb{CP}^2; \mathbb{Z}) = 0$, and the explicit odd lift gives the same conclusion. Freed–Witten states its cohomological anomaly criterion as sufficient; this $B = 0$ specialization is not a universal complete anomaly test. None of this selects a preferred odd integer.

Choose the allowed lift $x = -1$ as a worked sign example. In the positive D6 orientation, the linear gauge WZ term integrates over the positive $\mathbb{CP}^1$ to

$$q_4^{\text{gauge}} = \int_{\mathbb{CP}^1} \frac{F}{2\pi} = -\frac{1}{2}. \tag{III.5.27}$$

For the quadratic term, the cohomological two-form is $[F/(2\pi)] = (x/2)J$. The factorial in the exponential gives

$$q_2^{\text{gauge}} = \frac{1}{2} \int_{\mathbb{CP}^2} \left(\frac{F}{2\pi} \right)^2 = \frac{1}{2} \left(\frac{x}{2} \right)^2 \int_{\mathbb{CP}^2} J^2 = \frac{x^2}{8} = \frac{1}{8} \quad (x = -1). \tag{III.5.28}$$

The two signs behave differently: the linear coefficient changes sign under $x \mapsto -x$, while the quadratic coefficient does not. For $x = +1$, the corresponding gauge values are $+1/2$ and $+1/8$. Figure III.5.4 keeps the cycle orientation and the selected lift visible beside these numbers.

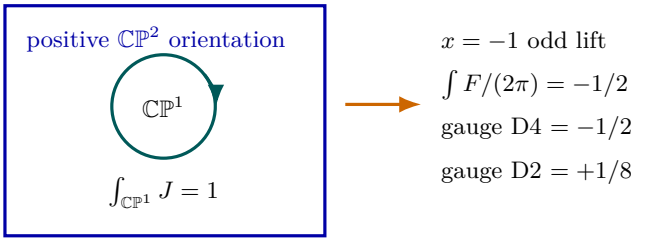


Figure III.5.4: The $B = 0$ Spin^c teaching example on positively oriented $\mathbb{CP}^2$. The positive line has $\int_{\mathbb{CP}^1} J = 1$; the chosen odd lift $x = -1$ gives a negative gauge D4 coefficient and a positive gauge D2 coefficient. These are not total charges. The separate wrapped-D6 wall and wrapped-D4 endpoint statements in the ABJ source use different objects and sign data.

The obstruction can be restated as a failed ordinary-bundle test. An ordinary line bundle on $\mathbb{CP}^2$ would have $c_1(L) = nJ$ and hence an integer period n on the positive

$\mathbb{CP}^1$. The $B = 0$ anomaly example requires instead

$$2\int_{\mathbb{CP}^1} \frac{F}{2\pi} = x, \qquad x \equiv 1 \pmod 2. \tag{III.5.29}$$

No integer period of this F can satisfy that parity equation: its double would be even. The resolution is the local Spin^c U(1) factor: its determinant line has twice its curvature, with odd first Chern class. This is a statement about the allowed worldvolume field in that anomaly frame. It does not turn every half-integral number in an arbitrary background into an allowed D-brane flux.

It is useful to display the full family of allowed lifts, not only its smallest representatives. Write $x = 2m + 1$ with $m \in \mathbb{Z}$. In the same fixed positive orientation, the gauge polynomial becomes

$$q_4^{\text{gauge}} = m + \frac{1}{2}, \qquad q_2^{\text{gauge}} = \frac{(2m+1)^2}{8} = \frac{m(m+1)}{2} + \frac{1}{8}. \tag{III.5.30}$$

Thus every allowed linear coefficient is half-integral. The offset $1/8$ in the quadratic gauge contribution is common modulo an integer, because $m(m+1)/2$ is an integer. Changing to the next odd lift $x + 2$ changes the linear coefficient by one and the quadratic coefficient by $(x + 1)/2$:

$$q_4^{\text{gauge}}(x+2) - q_4^{\text{gauge}}(x) = 1, \qquad q_2^{\text{gauge}}(x+2) - q_2^{\text{gauge}}(x) = \frac{x+1}{2} \in \mathbb{Z}. \tag{III.5.31}$$

This elementary arithmetic separates the fixed parity obstruction from the chosen representative. In particular, $x = -1$ and $x = +1$ differ by one unit of linear gauge charge but have the same quadratic gauge coefficient. One should not infer that their complete physical states are identical; their difference here is only what the displayed gauge polynomial measures.

The number $1/8$ is especially easy to misuse. It is the gauge part of the quadratic WZ expansion in this chart. Curvature couplings contribute to a complete lower charge. The index expression in the Freed–Witten discussion contains an $\widehat{A}$-class factor. Embedding and background conventions also matter when one translates a source coefficient into a Page charge. One cannot call $1/8$ a complete D2 charge in the wrapped-D6 setting merely because it is the output of an exact square. The source's D0 index example is a different brane dimension; it illustrates the same curvature boundary without identifying that D0 number with the D6's gauge D2 contribution.

There are two tempting sign shortcuts to avoid. The anomaly fixes the parity of x, not $x = -1$. Also, the ABJ source describes a half-unit Page contribution from a wrapped D6 wall without fixing a signed wall orientation in that paragraph. Later it chooses a negative half-flux for a wrapped D4 di-baryon endpoint. That D4 choice cannot set the sign of the D6 example here. Reversing the parent D6 orientation would reverse the induced source signs with the same displayed flux. A nonzero B requires a different charge and anomaly frame; the $B = 0$ numbers above do not transfer to it by simply reusing the ordinary bundle formula. This is why the final section first names a charge frame and then changes only its representative.

III.5.6 Page, source and Maxwell charges

Why can a charge label change under a large B-field gauge transformation while the physical flux data stay fixed? A source charge names a localized brane or worldvolume coupling. A Page charge is a localized conserved quantity in a chosen potential representative, and can transform under a large gauge change. A Maxwell charge is read from gauge-invariant flux; in the selected frame below it stays fixed under that representative change. These names refer to distinct measurements. The local WZ coefficients of the preceding sections do not identify them without the background's charge definitions.

Use the selected polynomial frame on $\mathbb{CP}^3$. Let J be the positive generator with $\int_{\mathbb{CP}^j} J^j = 1$, and set $\ell_s^2 = \alpha'$, $R_{11} = g_s\ell_s$. The sourced physical forms are $F_2 = 2\pi k R_{11} J$ and $B_2 = (2\pi\ell_s)^2 bJ$, so $b = \int_{\mathbb{CP}^1} B_2/(2\pi\ell_s)^2$ is a dimensionless representative with integer large-gauge shifts. Divide the D4 and D2 flux integrals by $(2\pi\ell_s)^3 g_s$ and $(2\pi\ell_s)^5 g_s$, respectively. In these units k is the F_2 flux integer, P_4, P_2 are Page flux data, and Q_4, Q_2 are Maxwell flux data. The selected relations are

$$Q_4 = P_4 + kb, \qquad Q_2 = P_2 + bP_4 + \frac{k}{2}b^2. \tag{III.5.32}$$

These are sourced physical definitions for this frame. The equations below are algebra inside it. In particular, the supplied P_2 is flux Page data; it is not automatically a gauge-group rank. Formal numeric examples do not certify a complete quantum charge lattice.

Make a large gauge representative change $b' = b - 1$ at fixed physical background. Holding the first Maxwell component fixed gives

$$P_4' + kb' = P_4 + kb \quad \Longrightarrow \quad P_4' = P_4 + k. \tag{III.5.33}$$

The second equality must be imposed separately. Substitute $b' = b-1$ and $P_4' = P_4 + k$ into its defining polynomial:

$$Q_2' = P_2' + (b-1)(P_4 + k) + \frac{k}{2}(b-1)^2 = P_2' + bP_4 + \frac{k}{2}b^2 - P_4 - \frac{k}{2}. \tag{III.5.34}$$

It follows that the needed Page transformation is

$$P_2' = P_2 + P_4 + \frac{k}{2}, \qquad (Q_4', Q_2') = (Q_4, Q_2). \tag{III.5.35}$$

The half-k term comes from the quadratic part of (III.5.32); dropping it would fail to preserve Q_2. The transformation is a statement about two representatives of one physical background in this polynomial frame, not a claim about all possible charge conventions.

An asymmetric example tests both components. Take $k = 6$, $b = 1/3$, $P_4 = -1$, and $P_2 = 4$. Before the change,

$$Q_4 = -1 + 6\left(\frac{1}{3}\right) = 1, \qquad Q_2 = 4 - \frac{1}{3} + \frac{6}{2}\left(\frac{1}{3}\right)^2 = 4. \tag{III.5.36}$$

The new representative has $b' = -2/3$, $P_4' = 5$, and $P_2' = 6$. Direct substitution, with no appeal to a slogan about gauge invariance, gives

$$Q_4' = 5 + 6\left(-\frac{2}{3}\right) = 1, \qquad Q_2' = 6 + \left(-\frac{2}{3}\right)5 + \frac{6}{2}\left(-\frac{2}{3}\right)^2 = 4. \tag{III.5.37}$$

The two rows in Figure III.5.5 make clear which quantities move. The formal Page inputs are intentionally unequal and nonzero; an identity-normalization example would obscure the cross term bP_4.

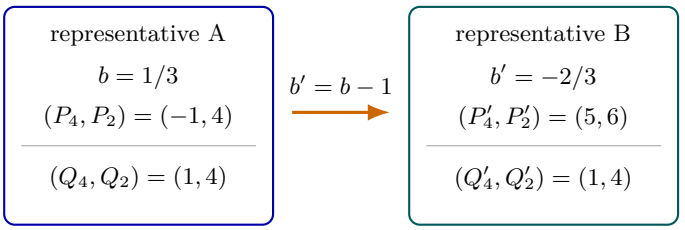


Figure III.5.5: Two potential representatives of the same selected physical background. The arrow is the large gauge change $b' = b - 1$; Page entries transform by (III.5.33) and (III.5.35). Both Maxwell entries agree after direct evaluation. The numbers are formal inputs to this polynomial frame.

The fixed-Maxwell condition can also be checked by solving in the opposite direction. Given Q_4, Q_2, k and a representative b, (III.5.32) determines the Page coordinates:

$$P_4 = Q_4 - kb, \qquad P_2 = Q_2 - bQ_4 + \frac{k}{2}b^2. \tag{III.5.38}$$

Insert $b = 1/3$, $Q_4 = 1$, $Q_2 = 4$, and $k = 6$. The first formula gives $P_4 = -1$; the second gives $P_2 = 4 - 1/3 + 1/3 = 4$. Inserting $b' = -2/3$ instead gives $P_4' = 5$ and $P_2' = 4 + 2/3 + 4/3 = 6$. This inverse calculation recovers the direct transformation without assuming it in advance. It is useful when the invariant fluxes are measured first and a Page representative is chosen afterward.

There is a useful falsification check for the representative rule. Suppose one were to replace b by $b - 1$ while incorrectly leaving both Page values fixed. The first Maxwell polynomial would change by $-k$. The second would change by

$$Q_2(b - 1; P_4, P_2) - Q_2(b; P_4, P_2) = -P_4 - kb + \frac{k}{2}. \tag{III.5.39}$$

At the worked point this would be $1 - 2 + 3 = 2$, while Q_4 would change by -6. Those are not the Maxwell values of the same-background gauge representative used above. The required shifts of both Page components are therefore substantive; there is no single "charge stays fixed" slogan that can replace the two equations. The calculation also exposes why the quadratic coefficient matters: omitting $kb^2/2$ would remove the $k/2$ term and give an inconsistent second transformation.

A continuous physical slide is a different experiment. If b changes by a small real δ while P_4, P_2, k are kept fixed, the polynomial predicts

$$\Delta Q_4 = k\delta, \qquad \Delta Q_2 = \delta(P_4 + kb) + \frac{k}{2}\delta^2. \tag{III.5.40}$$

For the worked point, take $\delta = 1/6$ as a concrete comparison. Then b goes from $1/3$ to $1/2$, and at fixed Page data

$$\Delta Q_4 = 1, \qquad \Delta Q_2 = \frac{1}{6}(-1+2) + 3\left(\frac{1}{6}\right)^2 = \frac{1}{4}. \tag{III.5.41}$$

Thus the new Maxwell pair would be $(2, 17/4)$, not $(1, 4)$. This slide changes physical flux data within the stated model. It is not the large gauge relabeling of the preceding paragraphs. The selected relations do not settle all-order action terms, global K-theory charge, quantum rank identifications, or the dynamics of an ensuing field theory. They do provide a practical rule for Volume VI, Chapter 5, "Fractional branes and the wrapped-brane interpretation," and for the thirteen-chapter Volume VIII revision: Chapter 4, "ABJ theory and fractional M2-branes," and Chapter 5, "From Calabi–Yau fourfolds to Chern–Simons theories." Name the charge definition and its representative before comparing two numbers in those constructions.

III.5.7 Exercises

The first five tasks have exact submissions in the chapter companion. Show the intermediate steps on paper. The final task asks for a written comparison of the physical interpretations.

1. **E1, WZ extraction.** A positively oriented Dp-brane wraps an oriented four-cycle X with $\int_X J^2 = 1$. Choose an oriented two-cycle Σ represented by the Poincaré dual of J, so $\int_\Sigma J = 1$. At $B = 0$, with curvature terms omitted, an ordinary line bundle has $c_1 = 3J$. Expand the WZ exponential through degree four, including the factorial and both μ-ratios. Submit the JSON fields `rank`, `ch1` and `ch2`; the latter two are the induced D$(p-2)$ coefficient on the positive two-cycle and the gauge D$(p-4)$ coefficient on X. Explain why reversing the orientation of the integration cycle changes the evaluated charge.

2. **E2, second Chern character.** A rank-two bundle on the same oriented X has $c_1 = 3J$ and $c_2 = 4J^2$. Derive $\mathrm{ch}_2 = (c_1^2 - 2c_2)/2$ from formal Chern roots. Submit the fields `rank`, `ch1` and `ch2` as the rank and the two character coefficients. Explain why the last answer is neither c_2 nor the universal number of stable dissolved branes.

3. **E3, a common brane-antibrane bundle.** Let $c_1(L) = J$, $E = L^2 \oplus L^{-1}$, and $F = L$. Add $H = L^3$ to both sides. Submit the virtual rank, the coefficients of J and J^2 in $\mathrm{ch}(E) - \mathrm{ch}(F)$, and whether these three components are unchanged after adding H. Submit these as `rank`, `ch1`, `ch2` and `stable_equal`. Compute each direct sum before subtracting. In words, distinguish this character equality from a claim of BPS stability or detection of torsion.

4. **E4, the nonspin four-cycle.** For a positively oriented wrapped D6 on positively oriented $\mathbb{CP}^2$, take $B = 0$, $\int_{\mathbb{CP}^1} J = 1$, and the allowed odd Spin^c lift $x = -1$. Submit the period $\int_{\mathbb{CP}^1} F/(2\pi)$, the gauge D4 coefficient, and the quadratic gauge D2 coefficient as `flux`, `induced_d4` and `gauge_d2`. Explain why the anomaly does not force the negative sign and why the quadratic number is not a total charge.

5. **E5, charge representatives.** In the selected polynomial $Q_4 = P_4 + kb$, $Q_2 = P_2 + bP_4 + kb^2/2$, take $k = 6, b = 1/3, P_4 = -1, P_2 = 4$. Under $b' = b - 1$ at fixed physical background, submit P_2', P_4' and the common Q_4, Q_2 as `shifted_p2`, `shifted_p4`, `maxwell_q4` and `maxwell_q2`. Verify both Maxwell components explicitly. The supplied Page values are formal data in this frame, not rank assignments.

6. **E6, written interpretation.** A student argues: "$\mathbb{CP}^2$ requires half-flux, so it must be negative; its square gives the full lower charge. Likewise $b \mapsto b - 1$ and a slow continuous change of b both leave Maxwell charge fixed." Use the $x = \pm 1$ examples and the two experiments in the final section to identify each false step. State which additional curvature or global data are needed before a complete lower charge can be named.

Take-home message

A worldvolume flux couples a parent brane to lower RR potentials. Its first two gauge coefficients are the first two nontrivial Chern-character components in the stated $B = 0$ frame. Their signs depend on orientation and convention. Stable bundle pairs organize additive charge data, while their rational characters can lose torsion. On a nonspin cycle the allowed connection period can be half-integral, and a Page label can change when the B-field representative changes at fixed Maxwell data. A reader should now be able to extract both WZ coefficients, calculate ch_2, cancel a common bundle explicitly, evaluate the oriented $\mathbb{CP}^2$ example, and distinguish a large gauge change from a physical B-slide.

Status and sources

Section III.5.2: the local WZ exponential is a source-stated physical coupling, subject to the derivative and curvature limits here, from Johnson (2000, physical PDF pp. 112–113, eqs. (284)–(287)). The degree extraction and μ-ratios are [MATH] in the book's normalization. The frame uses the stated tension and trace convention. No all-order or global charge claim is attached to this local coupling.

Section III.5.3: the degree-four WZ source is the same cited physical input. The Chern-root identity, nonunit example, and $SU(2)$ sign are [MATH] in the declared Hermitian and orientation chart. Johnson's instanton statement is source-local; existence, self-duality and BPS stability are not established by the character calculation.

Section III.5.4: the space-filling Type-IIB D9–anti-D9 construction and its physical common-pair annihilation argument are sourced premises from Witten (1998, physical PDF pp. 9–11, section 3). Common-summand character cancellation is [MATH]. The fact

that rational cohomology loses torsion and exact integral data is a cited mathematical boundary from the same source. Formal pairs are not automatically complete tadpole-free backgrounds or stable BPS states.

Section III.5.5: the $B = 0$ Spin^c condition is derived from the source's global anomaly argument; applying its odd-lift period in this local D6 frame is a cited physical input from Freed and Witten (1999, physical PDF pp. 8–9, eqs. (1.12)–(1.13)). Its cohomological criterion is stated there as sufficient. The selected $x = -1$ gauge coefficients are [MATH] under that premise and the WZ term. The curvature boundary follows Freed and Witten (1999, physical PDF p. 10, eq. (1.14)). The distinct unsigned wrapped-D6 wall statement and signed wrapped-D4 endpoint occur respectively in Aharony et al. (2009, physical PDF p. 31 and p. 35, eq. (3.41)). The local convention fixes this scoped sign translation; no total D2 value is inferred.

Section III.5.6: the source/Page/Maxwell distinctions and selected $\mathbb{CP}^3$ polynomial are source-defined physical flux prescriptions from Aharony et al. (2009, physical PDF pp. 18–19, eqs. (2.64)–(2.69), and pp. 30–31, eqs. (3.21)–(3.23)). The representative shift and both invariant Maxwell components are [MATH] within that sourced polynomial. The frame uses the stated tension and orientation conventions. It supplies no all-order action, global lattice, rank identification or field-theory equivalence.

References

Aharony, O. et al. (2009). *D-brane charges in gravitational duals of 2+1 dimensional gauge theories and duality cascades*. Version 2; physical PDF pp. 18–19 and 30–32, eqs. (2.64)–(2.69), (3.18)–(3.23); p. 35, eq. (3.41). arXiv: `0906.2390`.

Freed, D. S. and E. Witten (1999). *Anomalies in String Theory with D-Branes*. Version 2; physical PDF pp. 8–10, eqs. (1.12)–(1.14). arXiv: `hep-th/9907189`.

Johnson, C. V. (2000). *D-Brane Primer*. Version 3; physical PDF pp. 112–113, eqs. (284)–(287). arXiv: `hep-th/0007170`.

Witten, E. (1998). *D-Branes And K-Theory*. Version 2; physical PDF pp. 9–11, section 3. arXiv: `hep-th/9810188`.

Chapter III.6

Branes at angles and magnetized branes: chiral spectra at intersections

III.6.1 A string joining two directions

An open string can end on two branes that meet at an angle. Each endpoint can move along its own brane, but cannot move normally away from it. The same string must satisfy both requirements. This changes its allowed oscillations even when the surrounding spacetime is flat. The relative angle becomes a fractional shift of oscillator frequencies.

This local problem has a useful consequence for constructing field theories. Two D6-branes can fill the same four spacetime directions and wrap different three-cycles internally. A string joining them then supplies matter at an internal intersection. Its orientation fixes its two endpoint charges. The worldsheet fermions and their projection correlate these charges with four-dimensional chirality. On a product of three two-tori, oriented intersection numbers count the resulting signed net contribution in a specified sector.

There is a second description of the endpoint constraint. T-duality along one circle turns a tilted brane into a brane with magnetic flux. A normal position condition becomes a mixed condition on tangential derivatives. The integral wrapping numbers become the rank and first Chern number of a bundle. To see this relation with the correct sign and dimensions, we must derive the endpoint equations from an oriented action before identifying a slope with a field strength.

The three questions have different answers. Boundary conditions determine fractional frequencies. A stated RNS sector and GSO projection determine which excitations describe physical particles. Integral geometry counts their signed net chirality under the appropriate brane and projection premises. We will derive the local boundary and lattice calculations, then reproduce a selected common-spinor argument. The

RNS/GSO prescription, the brane supersymmetry projector and circle T-duality are physical inputs. The elementary calculations below explain their consequences.

The required earlier ingredients are the open strip of Chapter 1, the integer-charge connection and string units of Chapter 3, and the positive circle-duality convention of Chapter II.3. By the end, the reader should be able to solve a rotated strip problem, compute the selected two-plane light tower, evaluate an oriented factorized index, convert a central flux into a dual slope, and test one stated common-spinor branch. These are local ingredients for the compact constructions of the planned treatment of intersecting and magnetized brane models. A nonzero chiral index alone leaves the total compact charge and the other consistency conditions undetermined.

III.6.2 Intersecting boundary conditions

How does one string satisfy two different endpoint directions? Work in a flat physical plane with Euclidean coordinates (x, y). The worldsheet coordinates are dimensionless: $0 \le \sigma \le \pi$ and time τ. An uppercase $X(\tau, \sigma)$ or $Y(\tau, \sigma)$ denotes the embedding coordinate along the corresponding lowercase target axis. Put brane a on the x axis and let brane b pass through the origin with counterclockwise angle θ. In this section choose $0 < \theta < \pi$ and define $\nu = \theta/\pi$. The unit tangent and normal at the second endpoint are

$$t_b = (\cos\theta, \sin\theta), \qquad n_b = (-\sin\theta, \cos\theta), \qquad t_b \cdot n_b = 0. \tag{III.6.1}$$

These two vectors perform different jobs. The normal component of position is fixed, while the tangential component of the spatial derivative vanishes. The first endpoint imposes the same conditions in the unrotated frame:

$$X'(\tau, 0) = 0, \quad Y(\tau, 0) = 0, \qquad n_b \cdot (X, Y)|_\pi = 0, \quad t_b \cdot (X', Y')|_\pi = 0. \tag{III.6.2}$$

A prime means ∂_σ and a dot will mean ∂_τ. Both branes pass through the same target origin, so the normal position constants have been set to zero. Separations in other directions would be additional physical data.

The bulk equations remain free wave equations. For a nonzero frequency ω, take a common time dependence $e^{-i\omega\tau}$ and temporarily allow complex amplitudes. The first endpoint fixes the spatial solutions:

$$(\partial_\tau^2 - \partial_\sigma^2)(X, Y) = 0, \qquad X = A\cos(\omega\sigma)e^{-i\omega\tau}, \quad Y = B\sin(\omega\sigma)e^{-i\omega\tau}. \tag{III.6.3}$$

The physical embedding is the real part. There are still two amplitudes. Identifying them in advance would discard a possible polarization of the endpoint problem. At $\sigma = \pi$, write $u = \pi\omega$. Substitution into the normal position and tangent derivative conditions gives

$$\begin{pmatrix} -\sin\theta\cos u & \cos\theta\sin u \\ -\omega\cos\theta\sin u & \omega\sin\theta\cos u \end{pmatrix} \begin{pmatrix} A \\ B \end{pmatrix} = 0. \tag{III.6.4}$$

The lower row has an explicit ω because it came from a derivative. Its sign matters: the derivative of $\cos(\omega\sigma)$ is negative.

For a nontrivial amplitude vector the full matrix determinant must vanish. Multiplying the two diagonal terms and subtracting the off-diagonal product yields

$$\begin{aligned} D_{\text{full}}(\omega,\theta) &= \omega\big(\cos^2\theta\sin^2 u - \sin^2\theta\cos^2 u\big) \\ &= \omega\big(\sin^2 u - \sin^2\theta\big) = \omega\sin(u-\theta)\sin(u+\theta). \end{aligned} \tag{III.6.5}$$

Only on the branch $\omega \neq 0$ can we divide by this prefactor. The reduced condition then has two factors:

$$D_{\text{red}} = \frac{D_{\text{full}}}{\omega} = \sin\big(\pi(\omega-\nu)\big)\sin\big(\pi(\omega+\nu)\big) = 0, \qquad \omega \neq 0. \tag{III.6.6}$$

Thus the two conjugate frequency towers are

$$\omega \in \mathbb{Z}+\nu \quad \text{or} \quad \omega \in \mathbb{Z}-\nu, \qquad \omega_{+,0} = \nu, \quad \omega_{-,0} = 1-\nu. \tag{III.6.7}$$

The last two entries are the least positive member of each tower. Their order reverses when ν passes through $1/2$. They are not two frequencies that should always be listed in increasing order with the same branch name.

Away from coincident roots, the amplitudes also tell us how the two towers fit the rotated endpoint. For $\omega = k+\nu$, the sine and cosine at $u = k\pi+\theta$ have the same overall sign. The first row of (III.6.4) then gives $B = A$. For the other branch it gives $B = -A$. More directly, these choices reduce the normal condition to

$$\begin{aligned} B = A: &\quad -\sin\theta\cos u + \cos\theta\sin u = \sin(u-\theta), \\ B = -A: &\quad -\sin\theta\cos u - \cos\theta\sin u = -\sin(u+\theta). \end{aligned} \tag{III.6.8}$$

Solving just the first case would produce a single residual sine. It would miss the second tower of the original two-amplitude problem.

For a concrete example take $\theta = \pi/3$. The lowest member of the $B = A$ branch has $\omega = 1/3$, and at a fixed real time phase its endpoint positions are

$$(X(0),Y(0)) = (A,0), \qquad (X(\pi),Y(\pi)) = (A/2,\sqrt{3}A/2). \tag{III.6.9}$$

The second point lies on b. Its normal component is $-(\sqrt{3}/2)(A/2)+(1/2)(\sqrt{3}A/2) = 0$. The tangent derivative vanishes as well: its two contributions are $-\sqrt{3}A/12$ and $+\sqrt{3}A/12$. The other branch begins at $\omega = 2/3$, with $B = -A$. Its second endpoint is $(-A/2,-\sqrt{3}A/2)$, which lies on the same geometric line on its opposite side. Figure III.6.1 shows the first shape. The mode is a shape of one string, not an extra brane connecting the two lines.

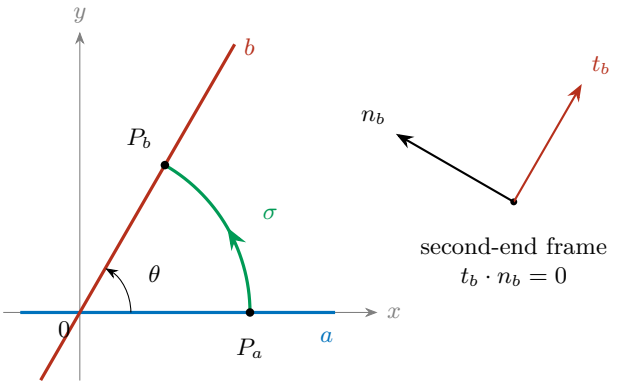


Figure III.6.1: The $\omega = 1/3$, $B = A$, $A = 1$ spatial mode for $\theta = \pi/3$ at a fixed time phase. The curved string runs from $P_a = (1, 0)$ to $P_b = (1/2, \sqrt{3}/2)$. Both brane lines remain continuous. The small tangent and normal vectors at the right show the orthogonal frame used in the two endpoint conditions. The drawing represents the physical (x, y) plane; the string parameter increases from P_a to P_b.

The apparent zero of D_{full} at $\omega = 0$ must be treated separately. The ansatz for Y used a sine that vanishes identically at zero frequency; its amplitude no longer parametrizes the full static solution. Instead solve the zero-frequency spatial equations as linear functions. The first endpoint reduces them to $X = A_0$ and $Y = D_0\sigma$. The remaining equations are

$$-\sin\theta A_0 + \pi\cos\theta D_0 = 0, \qquad \sin\theta D_0 = 0. \tag{III.6.10}$$

For $0 < \theta < \pi$, these imply $D_0 = A_0 = 0$. There is no continuous zero-mode displacement in this intersecting plane. At parallel geometric endpoints, $\theta = 0$, the equations instead allow arbitrary constant X. Its time-dependent free-particle partner is motion along the common brane. These modes have to be restored by the parallel problem itself.

At $\nu = 1/2$ the two positive frequencies in (III.6.7) coincide. In fact, at $\omega = 1/2$ both rows of (III.6.4) vanish, leaving two independent amplitudes. This is a degeneracy of the bosonic boundary problem. It says nothing yet about the ordering of NS fermion modes. Reversing the string exchanges the relative angle and conjugate sectors; the union of frequencies is unchanged. This separation between a geometric frequency calculation and a physical superstring spectrum is the step beyond the NN and DD examples of Chapter 1. We next add the sector and projection data needed to turn frequencies into masses.

III.6.3 Fractional moding and light states

Which of the fractional oscillations become light particles as an angle shrinks? The answer requires the vacuum energy and a projection on states. We now change from

the single bosonic plane to a specific supersymmetric two-plane RNS construction. In two complex planes the relative angles are opposite, so their magnitudes agree. Define the positive twist $\alpha = |\theta_{\rm local}|/\pi$, and restrict throughout the calculation to $0 < \alpha < 1/2$. This restriction fixes which fermionic frequencies are positive. In lightcone gauge the eight transverse real coordinates form four complex boson and fermion pairs. Two pairs are twisted, and the other two are untwisted.

The NS sector means that before the relative rotation the worldsheet fermions are antiperiodic. After the twist, the positive bosonic and fermionic frequencies of one complex pair are respectively

$$\begin{aligned} \text{bosons: } & k+\alpha,\ k+1-\alpha, \\ \text{NS fermions: } & k+\tfrac{1}{2}+\alpha,\ k+\tfrac{1}{2}-\alpha, \qquad k=0,1,2,\ldots. \end{aligned} \tag{III.6.11}$$

The smallest positive fermionic frequency is $1/2-\alpha$. Both sequences in each row are needed in a complex field. The two bosonic sequences are the positive parts of the conjugate towers just derived.

The vacuum energy is a regulated difference of zero-point sums. Use the analytic continuation of the Hurwitz zeta function, defined for $\mathrm{Re}\, s > 1$ by $\zeta(s,q) = \sum_{k\geq 0}(k+q)^{-s}$ and then continued to $s=-1$. The identity needed here is

$$\zeta(-1,q) = -\frac{1}{2}\left(q^2 - q + \frac{1}{6}\right). \tag{III.6.12}$$

This is a regularization prescription for the free-field normal-ordering constant. It does not select the physical states. Bosons contribute plus one half per frequency, giving for one twisted complex boson

$$\begin{aligned} E_B(\alpha) &= \tfrac{1}{2}\big[\zeta(-1,\alpha) + \zeta(-1,1-\alpha)\big] \\ &= -\frac{1}{12} + \frac{1}{2}\alpha(1-\alpha). \end{aligned} \tag{III.6.13}$$

Fermionic oscillators contribute with the opposite sign. Substituting their two positive starting frequencies gives

$$\begin{aligned} E_F(\alpha) &= -\tfrac{1}{2}\big[\zeta(-1,\tfrac{1}{2}+\alpha) + \zeta(-1,\tfrac{1}{2}-\alpha)\big] \\ &= -\frac{1}{24} + \frac{1}{2}\alpha^2. \end{aligned} \tag{III.6.14}$$

Adding these terms cancels the quadratic twist dependence:

$$E_B(\alpha) + E_F(\alpha) = -\frac{1}{8} + \frac{\alpha}{2}. \tag{III.6.15}$$

For an untwisted complex pair, the positive bosonic modes start at one. Its coordinate zero mode has no oscillator zero-point energy. The NS fermionic modes start at 1/2. Directly their two contributions are $\zeta(-1,1) = -1/12$ and $-\zeta(-1,1/2) = -1/24$, so each untwisted pair contributes $-1/8$. This counts the untwisted spectator pairs; it does not extend the selected twisted-sector state ordering to an endpoint. There are

two twisted complex pairs, not one. Therefore the total NS vacuum energy in this construction is

$$E_{\rm NS} = 2\left(-\frac{1}{8}+\frac{\alpha}{2}\right)+2\left(-\frac{1}{8}\right) = -\frac{1}{2}+\alpha. \tag{III.6.16}$$

Using this intercept for a sector with only one twisted complex plane would change the normal-ordering problem. A fractional bosonic frequency by itself cannot fix the intercept.

The GSO projection is now a further physical ingredient. In this two-plane construction it removes the NS vacuum and its purely bosonic descendants. It retains the appropriate first fermion excitation of energy $1/2-\alpha$. Let $\psi^{i\dagger}_{\rm low}$ denote that excitation in one of the two twisted planes, with $i=1,2$. Let $b_1^\dagger, b_2^\dagger$ denote their lowest bosonic creation operators, each of energy α. The selected family of states and its mass shell are

$$|n_1,n_2;i\rangle = (b_1^\dagger)^{n_1}(b_2^\dagger)^{n_2}\psi^{i\dagger}_{\rm low}|0\rangle_{\rm NS}, \qquad N=n_1+n_2\geq 0, \tag{III.6.17}$$

$$\alpha' M_N^2 = \underbrace{\left(-\frac{1}{2}+\alpha\right)}_{\text{vacuum}} + \underbrace{\left(\frac{1}{2}-\alpha\right)}_{\text{surviving fermion}} + \underbrace{N\alpha}_{\text{bosonic excitations}} = N\alpha. \tag{III.6.18}$$

No momentum or extra stretching contribution is included here. We are following the localized states of this specified intersecting configuration. The displayed family is enough to establish the selected sequence of levels; it is not an enumeration of every state or multiplicity of the full string spectrum. In particular, the removed negative-energy vacuum cannot be read as a physical tachyon from this formula.

The distinction between frequency, mass and squared mass is measurable. For positive α' the selected levels obey

$$M_1=\sqrt{\frac{\alpha}{\alpha'}}, \qquad \Delta M^2=\frac{\alpha}{\alpha'}, \qquad M_{N+1}-M_N=\sqrt{\frac{\alpha}{\alpha'}}(\sqrt{N+1}-\sqrt{N}). \tag{III.6.19}$$

The first two quantities even have different dimensions. The physical Regge slope α' has length squared. The mass spacing is nonuniform, whereas the squared-mass spacing is constant. In a numerical example use $\alpha=2/15$ and $\alpha'=7/3$ in a common choice of length unit:

$$M_N^2=\frac{2N}{35}, \qquad (M_0^2,M_1^2,M_2^2,M_3^2)=\left(0,\frac{2}{35},\frac{4}{35},\frac{6}{35}\right). \tag{III.6.20}$$

The corresponding masses are 0, $\sqrt{2/35}$, $2/\sqrt{35}$ and $\sqrt{6/35}$. For example the second positive gap is $(\sqrt{2}-1)\sqrt{2/35}$, smaller than the first positive mass. Figure III.6.2 uses these exact levels in units of M_1.

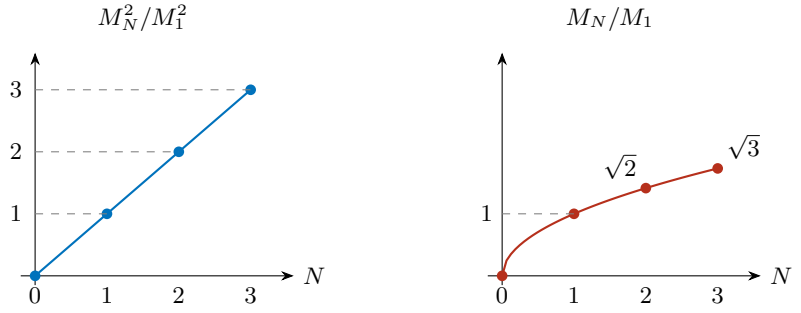


Figure III.6.2: The same four selected levels plotted as squared masses and masses. Left: $M_N^2/(2/35) = N$. Right: $M_N/\sqrt{2/35} = \sqrt{N}$. All horizontal positions label the same integer N. The plotted heights are $0, 1, 2, 3$ and $0, 1, \sqrt{2}, \sqrt{3}$, respectively. Equal increments of N give equal squared-mass intervals and unequal mass intervals. The curves guide the eye; only the marked integer levels are states.

At fixed α', compare twists $\alpha_A = 1/3$ and $\alpha_B = 1/6$. Both lie in the stated open interval. The two directly testable ratios are

$$\frac{(\Delta M^2)_B}{(\Delta M^2)_A} = \frac{1}{2}, \qquad \frac{(M_1)_B}{(M_1)_A} = \frac{1}{\sqrt{2}}. \tag{III.6.21}$$

The same square-root distinction holds as the twist tends to zero. More levels approach zero squared mass, in accord with the weakening confinement of a string near a shallow crossing. The parallel endpoint itself has additional translation and momentum information, as the previous section showed, so a limit of selected levels is not its entire spectrum. At $\alpha = 1/2$, the sequence $k + 1/2 - \alpha$ contains a fermionic zero mode. These NS fermions become periodic, and the creation and annihilation ordering used in the calculation must be replaced. Neither endpoint is included silently in (III.6.18).

The two-plane example teaches how supersymmetric localized light states arise, but it is not yet the four-dimensional D6 intersection problem. For that problem there are three internal planes. The next section uses the Ramond/GSO orientation and chirality relation in its own stated sector, and keeps the topological count distinct from this two-plane mass example.

III.6.4 Chirality from oriented intersections

How can a crossing carry a sign when the number of particles is positive? An oriented open string from stack a to stack b has opposite endpoint charges. For unitary stacks of multiplicities N_a, N_b, its Chan–Paton labels transform in $(\mathbf{N}_a, \overline{\mathbf{N}}_b)$. Reversing the orientation conjugates these labels. In the supersymmetric local Type IIA D6 construction, the Ramond sector and GSO projection correlate string orientation with the four-dimensional fermion chirality. This correlation is the physical premise that turns an oriented crossing into chiral matter. The two orientations supply the particle

and conjugate descriptions of the chiral field; they should not automatically be counted as two independent chiral multiplets.

First isolate the geometric sign. On a rectangular two-torus set the physical periods to $L_1 = 2\pi R_1$ and $L_2 = 2\pi R_2$, with $R_1, R_2 > 0$. Choose the orientation $dx \wedge dy > 0$. Let e_x, e_y be the positively oriented generators of $H_1(T^2, \mathbb{Z})$, with pairing $e_x \cdot e_y = +1$. A closed oriented one-cycle is labelled by its integer wrappings, and a primitive one has relatively prime entries:

$$\begin{gathered}[a] = n_a e_x + m_a e_y, \qquad [b] = n_b e_x + m_b e_y, \\ \gcd(|n_a|, |m_a|) = \gcd(|n_b|, |m_b|) = 1.\end{gathered} \tag{III.6.22}$$

Primitivity removes repeated covering in this elementary example. Stack multiplicity is separate from these two wrapping integers. Negative wrappings reverse a component of the oriented cycle.

The pairing is bilinear and antisymmetric. Since each basis cycle has zero self-pairing, expanding the two classes gives

$$\begin{aligned} I_{ab} = [a] \cdot [b] &= n_a m_b (e_x \cdot e_y) + m_a n_b (e_y \cdot e_x) \\ &= n_a m_b - m_a n_b. \end{aligned} \tag{III.6.23}$$

The same determinant appears in the exterior product of their two lattice vectors:

$$(n_a e_x + m_a e_y) \wedge (n_b e_x + m_b e_y) = (n_a m_b - m_a n_b) e_x \wedge e_y. \tag{III.6.24}$$

Here the wedge is in the oriented rank-two lattice. It is not a claim that an unnormalized physical coordinate differential is the Poincaré dual of a wrapped cycle. This distinction avoids inserting a spurious torus area into an integer pairing.

For straight representatives the physical tangent displacements over one closed traversal are $v_a = (n_a L_1, m_a L_2)$ and $v_b = (n_b L_1, m_b L_2)$. Their determinant shows why positive radii do not alter the local sign:

$$\det(v_a, v_b) = L_1 L_2 I_{ab}, \qquad L_1 L_2 > 0. \tag{III.6.25}$$

A transverse crossing has the sign of this ordered tangent frame. Smooth deformations can create or remove pairs of opposite signs while preserving the algebraic sum. The index counts that sum, rather than the number of all geometric crossings of arbitrary representatives.

Take $a = (2, 1)$ and $b = (1, 2)$. Substitution and reversal of only the first cycle give

$$I_{ab} = 2 \cdot 2 - 1 \cdot 1 = 3, \qquad I_{(-a)b} = (-2) \cdot 2 - (-1) \cdot 1 = -3, \qquad I_{ba} = -3. \tag{III.6.26}$$

The last two operations give the same sign change for different reasons: one reverses a cycle, the other exchanges the order of the pair. For a geometric check use dimensionless coordinates $u = x/L_1$, $v = y/L_2$, each defined modulo one. The straight loops have parametrizations $a(s) = (2s, s)$ and $b(t) = (t, 2t)$ modulo $\mathbb{Z}^2$, with $s, t \in [0, 1)$. For integers k, ℓ representing lattice shifts, intersections satisfy

$$2s - t = k, \quad s - 2t = \ell, \qquad (u, v) = (0, 0),\ (1/3, 2/3),\ (2/3, 1/3) \pmod{\mathbb{Z}^2}. \tag{III.6.27}$$

Indeed, the first equation gives $t = 2s - k$; the second then gives $3s = 2k - \ell$. There are three possible values of s modulo one. All three crossings have positive determinant 3 in the (u, v) coordinate frame. Figure III.6.3 shows the two interior points and the one point represented at the identified corners.

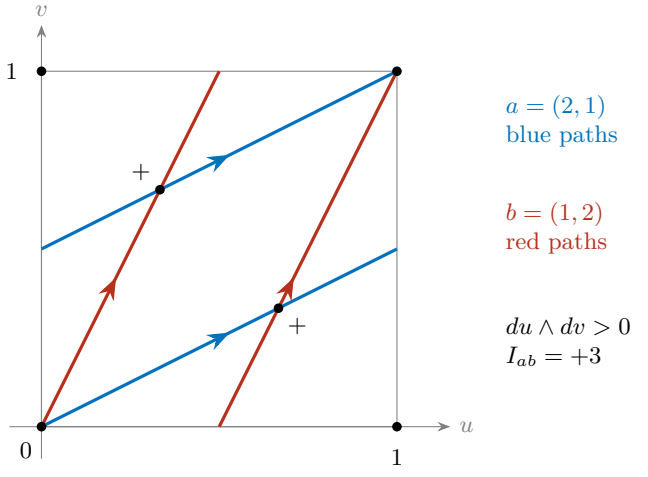


Figure III.6.3: Primitive cycles $a = (2, 1)$ and $b = (1, 2)$ on the periodic (u, v) square. Blue and red arrows give the cycle orientations. Opposite edges are identified without reversing u or v. The two black interior points and the identified corner represent three intersections, each with sign $+$. The four corners represent one point. Labels are placed outside the cycle paths so that their continuity across the square is visible.

Now take $T^6 = T_1^2 \times T_2^2 \times T_3^2$ with the same positive orientation choice on each factor. Consider factorized D6 cycles $\Pi_a = a_1 \times a_2 \times a_3$ and $\Pi_b = b_1 \times b_2 \times b_3$. Require transverse intersections in all three planes. In the distinct, non-invariant ab sector of the stated orientifold/GSO construction, the signed bifundamental index is

$$I_{ab}^{(6)} = \prod_{i=1}^{3} I_{ab}^{(i)} = \prod_{i=1}^{3} (n_a^i m_b^i - m_a^i n_b^i). \tag{III.6.28}$$

This convention multiplies the ordered crossing signs plane by plane. The combinatorics follows because one intersection in each plane specifies one intersection of the product cycles. The identification with a physical chiral index also uses the Ramond/GSO and orientifold-sector premises. It is not a formula for all of $H_3(T^6, \mathbb{Z})$ or for every open-string sector in an orientifold.

A fully explicit product example uses

i	1	2	3
a_i	$(2, 1)$	$(1, 0)$	$(1, 1)$
b_i	$(1, 2)$	$(1, 1)$	$(1, 0)$

$$(I_{ab}^{(1)}, I_{ab}^{(2)}, I_{ab}^{(3)}) = (3, 1, -1). \tag{III.6.29}$$

The second determinant is $1\cdot 1-0\cdot 1=1$, and the third is $1\cdot 0-1\cdot 1=-1$. The product is -3. It describes three net units of the opposite chirality to the chosen positive ab convention. It does not describe a negative number of particles. In terms of numbers n_+ and n_- of the two chirality contributions, the signed count is

$$I_{ab}^{(6)}=n_+-n_-,\qquad n_{\rm total}=n_++n_-\geq|I_{ab}^{(6)}|. \tag{III.6.30}$$

Adding a vectorlike pair changes both n_+ and n_- by one and leaves the index fixed. The equation explains the information that an index loses.

Parallel factors provide another direct limitation. Replace the third pair in (III.6.29) by $a_3=b_3=(1,0)$. Then

$$I_{ab}^{(3)}=1\cdot 0-0\cdot 1=0,\qquad I_{ab}^{(6)}=3\cdot 1\cdot 0=0. \tag{III.6.31}$$

The third plane is now a parallel boundary problem. Its relative displacement and Wilson lines, and its momentum and winding sectors, are extra information. Depending on those data it can retain vectorlike light states or massive towers. The zero signed product neither guarantees masslessness nor proves the absence of states. In particular the transverse localized-sector interpretation used above must be reconsidered when one factor is parallel.

Orientifold images also require their own sectors. In the rectangular reflection example the image sends (n_b^i,m_b^i) to $(n_b^i,-m_b^i)$, but the ab' and aa' strings and invariant stacks have separate projections. The index in (III.6.28) has counted only the specified ab sector. Counting an image as another copy of that sector can change both representations and net multiplicities.

Finally, consider a spectator stack c wrapped on the product of horizontal cycles $(1,0)$ in all three planes. Keep a and b fixed and increase its multiplicity from N_c to N_c+1. In a hypothetical compact completion let Q_c be the RR charge of this spectator together with whatever image contribution that completion requires, in the same charge units as the rest. The change has the form

$$I_{ab}^{(6)\,\rm new}=I_{ab}^{(6)\,\rm old},\qquad Q_{\rm total}^{\rm new}-Q_{\rm total}^{\rm old}=Q_c. \tag{III.6.32}$$

The first equality follows because the pair of cycles entering I_{ab} did not change. The second follows by additivity of the candidate charges. For a nonzero spectator charge, a condition on the total charge can change with no change to this local index. Spectator strings can also change the matter entering anomaly and inflow conditions. This is an information-insufficiency example; it has not constructed a compact vacuum.

To decide compact consistency one must specify the orientifold geometry, all stack and image cycles, their multiplicities, and the O-plane charges. One must then impose the RR charge cancellation conditions in that geometry. The full chiral and vectorlike spectrum and its couplings are needed for the anomaly and inflow analysis. Common supersymmetry of all objects and stability in a stated chamber are further questions. These are the missing inputs to the written exercise at the end. The next section changes from intersection geometry to magnetic bundle data. Chapter 3 supplies its charge normalization, while a treatment of compact intersecting and magnetized brane models will need the complete compact configuration before using these local counts.

III.6.5 Magnetic dual description

Which magnetic field reproduces a brane slope with the correct sign and units? Start with the rectangular physical (x, y) torus, $B = 0$, and constant central fields on the two endpoint branes. Set $\lambda = 2\pi\alpha'$, with $\alpha' > 0$. We use the integer-charge identity connection of Chapter 3. Its local one-form is $a = a_i dX^i$, so a_i has units of inverse length and F_{ij} has units of inverse length squared. These are not the rescaled components along a generator normalized by $\mathrm{Tr}\, T^2 = 1/2$.

Take worldsheet orientation $d\tau \wedge d\sigma$. The induced boundary orientation is positive $d\tau$ at $\sigma = 0$ and negative $d\tau$ at $\sigma = \pi$. For the spacelike plane the bulk and endpoint action is

$$\begin{aligned} S_{\text{bulk}} &= \frac{1}{2\lambda} \int d\tau \int_0^\pi d\sigma \, (\dot{X}^2 - X'^2), \\ S_{\text{end}} &= \int_{\sigma=0} a_i^{(a)}(X) \dot{X}^i d\tau - \int_{\sigma=\pi} a_i^{(b)}(X) \dot{X}^i d\tau. \end{aligned} \tag{III.6.33}$$

The two signs implement the oriented endpoint couplings. Each endpoint uses its own brane field. The use of mostly-plus target signature does not alter this Euclidean spatial-plane calculation.

Integrating the spatial bulk variation by parts gives its endpoint term

$$\delta S_{\text{bulk}}\big|_{\partial\Sigma} = \frac{1}{\lambda} \int d\tau \, \left[X'_k \delta X^k \big|_0 - X'_k \delta X^k \big|_\pi \right]. \tag{III.6.34}$$

For either local connection, integrate its time derivative term by parts and discard variations at the initial and final times. With $F_{ki} = \partial_k a_i - \partial_i a_k$, the connection variation is

$$\begin{aligned} \delta(a_i \dot{X}^i) &= \partial_k a_i \dot{X}^i \delta X^k + a_i \partial_\tau \delta X^i \\ &= F_{ki} \dot{X}^i \delta X^k + \partial_\tau (a_k \delta X^k). \end{aligned} \tag{III.6.35}$$

Thus the full endpoint variation is

$$\begin{aligned} \delta S\big|_{\partial\Sigma} = \int d\tau \Bigg[& \left(\frac{X'_k}{\lambda} + F_{ki}^{(a)} \dot{X}^i \right) \delta X^k \big|_0 \\ & - \left(\frac{X'_k}{\lambda} + F_{ki}^{(b)} \dot{X}^i \right) \delta X^k \big|_\pi \Bigg]. \end{aligned} \tag{III.6.36}$$

The opposite orientation multiplies the entire boundary expression at π, including the bulk term. Consequently the local form of the boundary equation is the same at either end:

$$X'_k + \lambda F_{ki}^{(a)} \dot{X}^i = 0 \quad (\sigma = 0), \qquad X'_k + \lambda F_{ki}^{(b)} \dot{X}^i = 0 \quad (\sigma = \pi). \tag{III.6.37}$$

Changing only one endpoint sign in the action while keeping these equations would instead change the physical charge convention.

For one endpoint suppress the brane label. A local gauge choice for a constant field is $a_x = 0$, $a_y = F_{12} x$. It gives $F = F_{12}\, dx \wedge dy$. Define the dimensionless field $f = \lambda F_{12}$. Then the two ordered equations are

$$x' + f\dot{y} = 0, \qquad y' - f\dot{x} = 0, \qquad F_{ki} = F_{12} \begin{pmatrix} 0 & 1 \\ -1 & 0 \end{pmatrix}_{ki}. \tag{III.6.38}$$

The opposite off-diagonal signs express the antisymmetry of a curvature two-form. There is a physical check on them. The endpoint flow of the worldsheet energy is proportional to

$$\dot{X} \cdot X' = -\lambda \dot{X}^k F_{ki} \dot{X}^i = 0. \tag{III.6.39}$$

A symmetric pair of cross terms would fail this identity for a general endpoint velocity. A scalar tangent or cotangent relation alone cannot determine the ordered matrix signs.

Now perform T-duality on y. In the positive convention of Chapter II.3, write $y = y_L + y_R$ with $y_L = y_L(\tau + \sigma)$ and $y_R = y_R(\tau - \sigma)$, and define $\widetilde{y} = y_L - y_R$. Hence

$$\dot{\widetilde{y}} = y', \qquad \widetilde{y}' = \dot{y}, \qquad R_2' = \frac{\alpha'}{R_2} > 0. \tag{III.6.40}$$

These identities specify the coordinate map, including its sign. Inserting them into (III.6.38) gives

$$x' + f\widetilde{y}' = 0, \qquad \dot{\widetilde{y}} - f\dot{x} = \partial_\tau(\widetilde{y} - fx) = 0. \tag{III.6.41}$$

The second equation fixes a normal position $\widetilde{y} - fx =$ constant along the endpoint worldline. The first is the Neumann condition in the tangent direction. A normalized tangent and normal are therefore

$$t = \frac{(1, f)}{\sqrt{1 + f^2}}, \qquad n = \frac{(-f, 1)}{\sqrt{1 + f^2}}, \qquad \tan\phi = f = \lambda F_{12}. \tag{III.6.42}$$

The angle ϕ is measured counterclockwise from positive x in the physical $(x, \widetilde{y})$ plane. A positive field has positive slope. Reflecting the dual coordinate would reverse this slope and the associated charge chart together. It would be a different convention.

The local gauge potential just used is not periodic as a one-form on the torus. A bundle supplies transition functions between its gauge patches. For an existing rank-n central $U(n)$ bundle, with $n > 0$, its curvature matrix is $F_{12}\mathbf{1}_n\, dx \wedge dy$. The trace is the ordinary fundamental trace, so $\operatorname{Tr} \mathbf{1}_n = n$. In these Hermitian integer-charge units the first Chern number is

$$\begin{aligned} m &= \frac{1}{2\pi} \int_{T^2} \operatorname{Tr} F = \frac{nF_{12}}{2\pi}(2\pi R_1)(2\pi R_2) \in \mathbb{Z}, \\ F_{12} &= \frac{m}{2\pi n R_1 R_2}. \end{aligned} \tag{III.6.43}$$

This is a Chern–Weil evaluation conditional on the genuine global bundle. The bundle's transition data and their compatibility are necessary inputs. A local constant matrix with arbitrary real entries does not establish them. An anti-Hermitian curvature convention would require the corresponding factor of i in this formula.

Substitute the physical dual radius into the flux result:

$$\lambda F_{12} = \frac{m\alpha'}{nR_1R_2} = \frac{mR_2'}{nR_1} = \tan\phi. \tag{III.6.44}$$

The dual cycle winds n times around x and m times around $\widetilde{y}$. Its physical displacement is $(2\pi n R_1, 2\pi m R_2')$, whose ratio is exactly the last expression. This identifies the rank

and degree with the two wrapping integers in the local dictionary. The chart assumes $n > 0$. A vertical cycle $n = 0$ has no finite F_{12} representation in this chart.

For the numerical example take $n = 2$, $m = 3$, $R_1 = 2$, $R_2 = 3$ and $\alpha' = 5$, with all lengths measured in one common unit. Then

$$R_2' = \frac{5}{3}, \qquad F_{12} = \frac{3}{2\pi \cdot 2 \cdot 2 \cdot 3} = \frac{1}{8\pi}, \qquad \lambda F_{12} = 10\pi \frac{1}{8\pi} = \frac{5}{4}. \tag{III.6.45}$$

The original torus has area $(4\pi)(6\pi) = 24\pi^2$. Its integrated trace flux and the dual displacement independently give

$$\frac{1}{2\pi} 2 \frac{1}{8\pi} 24\pi^2 = 3, \qquad \frac{2\pi\, 3(5/3)}{2\pi\, 2(2)} = \frac{10\pi}{8\pi} = \frac{5}{4}. \tag{III.6.46}$$

Both the rank in the trace and the factor λ in the boundary condition are essential. Omitting either changes the answer. Figure III.6.4 keeps the same label and the same rank and degree on both sides of the local duality.

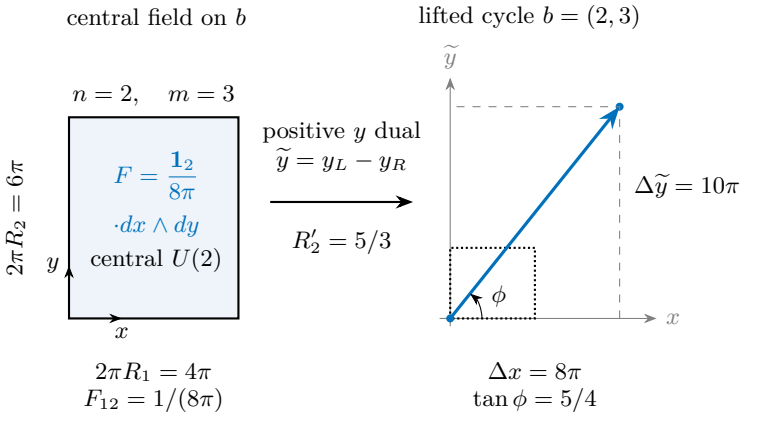


Figure III.6.4: The local flux and angle descriptions for the same object b. Left: a central rank-two field of degree three on physical periods $2\pi R_1 = 4\pi$, $2\pi R_2 = 6\pi$ has $F_{12} = 1/(8\pi)$. Right: the positive y dual has $R_2' = 5/3$, and the lifted $(2, 3)$ cycle has displacement $(8\pi, 10\pi)$ and slope $5/4$. The arrow names the dualized coordinate and its orientation. The central curvature is written inside the left cell. A dotted rectangle on the right marks one dual fundamental cell; the blue line is drawn on its cover to keep its winding unbroken.

There is an important global distinction even in this small example. Although the local curvature is proportional to $\mathbf{1}_2$, the flux per diagonal entry has integral $3/2$ in units of 2π. It cannot define two independent line bundles, each of fractional degree. An ordinary line bundle has integral first Chern number. Rank-two transition functions can mix the local components, so a local diagonal expression is not a global splitting. The calculation assumes such compatible $U(2)$ transition data; it has not constructed them by merely writing the central field.

For two bundles a and b of ranks $n_a, n_b > 0$, the resulting geometric intersection is the same integer combination $n_a m_b - m_a n_b$. This equality follows by substituting their wrapping data into the already established torus pairing. A field-theoretic derivation of a full magnetized compact spectrum would also require the bundle, projections and all other sectors. The local endpoint calculation has related a magnetic boundary constraint to a geometric one. It has not supplied that complete compact equivalence. This is the part of the circle dictionary from Chapter II.3 that the later brane constructions can use together with the WZ units of Chapters 3 and 5.

III.6.6 Supersymmetric angle choices

When do the two branes preserve the same supersymmetry parameter? Being supersymmetric separately is not enough: two branes can impose incompatible relations between the left and right spacetime parameters. We reproduce a sufficient common-spinor branch for flat, equally oriented D6-branes sharing four spacetime directions. Their three internal tangent directions lie in three orthogonal planes. The physical starting point is the D-brane supersymmetry projector. Its common external and Type IIA factors can be suppressed when comparing these two branes. In the source's relative-projector notation the left and right spacetime parameters obey $\widetilde{\varepsilon} = \Gamma_{D_a}\varepsilon = \Gamma_{D_b}\varepsilon$. Each Γ_D is the oriented brane-volume Clifford factor in that condition. The common invertible factors cancel from $\Gamma_{D_a}\varepsilon = \Gamma_{D_b}\varepsilon$. The remaining equation compares their products of internal tangent Clifford matrices.

Define internal coordinates $z^i = x_i + iy_i$, $i = 1, 2, 3$, and six spatial matrices $\Gamma_{x_i}, \Gamma_{y_i}$ with Euclidean Clifford relation $\{\Gamma_A, \Gamma_B\} = 2\delta_{AB}$. This is the spatial part of the mostly-plus spacetime convention. It is useful to realize this algebra on the exterior space $\Lambda^\bullet\mathbb{C}^3$. For an orthonormal basis e^i of $\mathbb{C}^3$, let $a_i^\dagger$ act by exterior multiplication by e^i, and a_i act by contraction with its dual. Then

$$\begin{aligned} a_i &= \frac{\Gamma_{x_i} + i\Gamma_{y_i}}{2}, \qquad & a_i^\dagger &= \frac{\Gamma_{x_i} - i\Gamma_{y_i}}{2}, \\ \{a_i, a_j^\dagger\} &= \delta_{ij}, \qquad & \{a_i, a_j\} &= \{a_i^\dagger, a_j^\dagger\} = 0. \end{aligned} \tag{III.6.47}$$

The scalar 1 in this exterior space is denoted $|0\rangle$, and it is annihilated by every a_i. It is an internal spinor, not the NS vacuum of the earlier section. Define also the ordered top form

$$|\Omega\rangle = a_1^\dagger a_2^\dagger a_3^\dagger |0\rangle, \qquad a_i|0\rangle = 0. \tag{III.6.48}$$

The order fixes the sign of the top form. The two states have opposite internal chirality. The full ten-dimensional spinors include the common external spinor factors and the Type IIA chirality relation.

Put the first brane along the three positive x_i axes. For the second, choose counterclockwise relative angles θ_i from x_i toward y_i. After removing the same common factors from both projectors, the equation for an internal spinor ϵ is

$$P_a\epsilon = P_b\epsilon, \qquad P_a = \Gamma_{x_1}\Gamma_{x_2}\Gamma_{x_3}, \quad P_b = \prod_{i=1}^{3}(\cos\theta_i\Gamma_{x_i} + \sin\theta_i\Gamma_{y_i}). \tag{III.6.49}$$

The product is in increasing i order. These P matrices are the internal volume factors; they are not being normalized here into idempotent projectors on their own. The equation is the relative part of the D-brane condition. The full projector also relates the left and right spacetime parameters.

The exterior representation makes its action transparent. Since $\Gamma_{x_i} = a_i + a_i^\dagger$ and $\Gamma_{y_i} = i(a_i^\dagger - a_i)$, each rotated tangent becomes

$$\cos\theta_i \Gamma_{x_i} + \sin\theta_i \Gamma_{y_i} = e^{-i\theta_i} a_i + e^{i\theta_i} a_i^\dagger. \tag{III.6.50}$$

On $|0\rangle$, every term containing an annihilation operator vanishes. Operators in distinct planes anticommute but have no contraction term. Only the product of three creation operators survives, giving

$$P_a|0\rangle = |\Omega\rangle, \qquad P_b|0\rangle = e^{i(\theta_1+\theta_2+\theta_3)}|\Omega\rangle. \tag{III.6.51}$$

On the top form only the three annihilators survive. Moving them through three creation operators gives $(-1)^{3\cdot 2/2} = -1$, so

$$P_a|\Omega\rangle = -|0\rangle, \qquad P_b|\Omega\rangle = -e^{-i(\theta_1+\theta_2+\theta_3)}|0\rangle. \tag{III.6.52}$$

The shared minus sign does not change the common-spinor equation. Keeping it exhibits the chosen ordering convention rather than concealing it inside a self-overlap.

One can also see the spin lift explicitly. Set $J_i = \Gamma_{x_i}\Gamma_{y_i} = i(1 - 2a_i^\dagger a_i)$, so $J_i^2 = -1$. Different J_i commute. The lift continuous from the identity in the chosen angles is

$$S = \exp\left(\frac{1}{2}\sum_i \theta_i J_i\right), \qquad S^{-1}\Gamma_{x_i} S = \cos\theta_i \Gamma_{x_i} + \sin\theta_i \Gamma_{y_i}, \qquad P_b = S^{-1} P_a S. \tag{III.6.53}$$

Its phases on the two singlet states are

$$S|0\rangle = e^{\frac{i}{2}\sum_i \theta_i}|0\rangle, \qquad S|\Omega\rangle = e^{-\frac{i}{2}\sum_i \theta_i}|\Omega\rangle. \tag{III.6.54}$$

The factors of one half distinguish the spin representation from the vector rotation. They are needed even though a simultaneous projector comparison eventually involves the full-angle phases.

In this fixed complex structure the vector rotation is $R = \mathrm{diag}(e^{i\theta_1}, e^{i\theta_2}, e^{i\theta_3})$. A sufficient branch, continuous with exactly zero signed angle sum, is

$$\theta_1 + \theta_2 + \theta_3 = 0 \quad \Longrightarrow \quad \det R = 1, \qquad P_a|0\rangle = P_b|0\rangle, \quad P_a|\Omega\rangle = P_b|\Omega\rangle. \tag{III.6.55}$$

This is the selected $SU(3)$ common-spinor construction. The D-brane projector premise turns the exhibited internal spinors into compatible supersymmetry parameters with the appropriate external factors. The calculation is a sufficient construction, not a classification of all sign choices, spinors, spin lifts or background projections. Merely specifying the vector determinant would also lose information about the continuous lift and the chosen oriented branes.

For the concrete test take $(\theta_1, \theta_2, \theta_3) = \pi(1/6, 1/3, -1/2)$. The individual rotations and their signed sum are

$$\frac{\theta_1 + \theta_2 + \theta_3}{\pi} = \frac{1}{6} + \frac{1}{3} - \frac{1}{2} = 0, \qquad R = \mathrm{diag}(e^{i\pi/6}, e^{i\pi/3}, e^{-i\pi/2}). \tag{III.6.56}$$

For example, multiplying the first two vector phases gives $e^{i\pi/2}$, which is canceled by the third. The lift phase on $|0\rangle$ is one. Figure III.6.5 displays these three rotations in equally oriented complex planes.

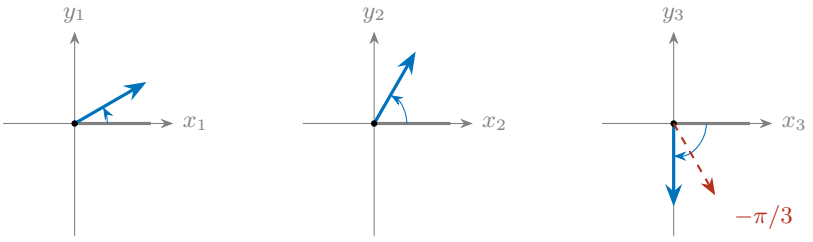


Figure III.6.5: The selected zero-sum relative rotation in three planes, each oriented from positive x_i toward positive y_i. Gray horizontal rays are the first brane's directions. Blue rays are the second brane's directions at $\pi/6$, $\pi/3$ and $-\pi/2$. Signed arcs show the rotation sense. The red dashed ray in the last panel changes only the third angle to $-\pi/3$. The label below each panel states the angle, leaving the directions themselves unobstructed.

Change only the last angle to $-\pi/3$. The new phase calculation gives

$$\frac{\theta_1 + \theta_2 + \theta_3^{\mathrm{new}}}{\pi} = \frac{1}{6} + \frac{1}{3} - \frac{1}{3} = \frac{1}{6}, \qquad P_b^{\mathrm{new}}|0\rangle = e^{i\pi/6}|\Omega\rangle \neq P_a|0\rangle. \tag{III.6.57}$$

The top-form phase is $e^{-i\pi/6}$, so that state also fails the displayed relative equation. This altered configuration fails this selected branch. We have not tested every other internal spinor. Different sign branches and complex-coordinate choices require their own projector calculation.

This angle example is local. To realize it on a compact torus one must choose a lattice and radii admitting the proposed directions. Its third angle is vertical, so the finite-flux chart with $n > 0$ of the preceding section cannot be applied to that factor. No flux value is assigned to it by sending a finite formula through $n = 0$. A globally supersymmetric orientifold would also require compatibility with its image and O-plane projectors. Stability and the existence of all required objects remain separate questions. Chapter 9 develops the broader BPS and projector language. The restricted construction here gives an explicit spinor test that can be used alongside, rather than in place of, the compact charge and spectrum calculations of compact intersecting and magnetized brane models.

III.6.7 Exercises

Exercises E1–E4 have bounded numerical submissions. Give the derivations and interpretation in written work as well. The submitted object has two members, `task` and `answer`. The first is the exercise label and the second contains exactly the fields stated below. Rational fields are exact strings such as `"7/5"` or `"0"`; integer fields are JSON integers and logical fields are JSON booleans. The companion question file specifies the complete public submission format. E5 is a written reasoning problem.

1. **E1, conjugate modes.** The first endpoint lies on the x axis and the second on a line rotated counterclockwise by $\theta = \pi/3$. Use $0 \le \sigma \le \pi$. Derive the full two-amplitude determinant, state where it can be reduced, and submit the least positive frequency from each conjugate tower as rational fields `low_mode` and `next_mode`. Explain why the apparent zero-frequency root needs its own boundary solution. Do not infer an NS vacuum energy from this single-plane calculation.

2. **E2, oriented index.** On $dx \wedge dy > 0$, use primitive cycles $a = (2, 1)$ and $b = (1, 2)$. Submit integer fields `intersection` for I_{ab} and `reversed_intersection` for the result of reversing only a. Locate the crossings on a periodic square. Explain why this local signed count does not decide compact RR charge cancellation or anomaly cancellation.

3. **E3, physical flux units.** A rectangular $B = 0$ torus has $R_1 = 2$, $R_2 = 3$ and $\alpha' = 5$. A central $U(2)$ field has trace Chern number $m = 3$. Dualize y in the positive convention. Submit rational fields `dual_radius`, `lambda_flux`, `slope`, and integer field `flux_quanta`. The middle two rationals mean λF_{12} and the physical $(2, 3)$ dual-cycle slope, respectively. Show the trace-flux integral and both endpoint signs in written work. Explain why local central curvature does not define two independent fractional-degree line bundles.

4. **E4, a selected common spinor.** In the fixed complex coordinates and spin lift of the preceding section, use $\theta_i/\pi = (1/6, 1/3, -1/2)$. Then change only the last entry to $-1/3$. Submit rational fields `phase_sum` and `changed_phase_sum` for the signed sums in units of π. Submit logical fields `common_spinor` and `changed_common_spinor` for satisfaction of the selected zero-sum condition. Reconstruct the action on $|0\rangle$ and $|\Omega\rangle$. State which other spinors and compact conditions this particular calculation has left untested.

5. **E5, written interpretation.** A product of three transverse T^2 intersections has nonzero signed ab index and an oriented chiral bifundamental under the stated GSO and orientifold-sector premises. Explain which additional geometry, stack and image charge classes, O-plane contributions, RR cancellation conditions, full spectrum, anomaly and inflow information, common supersymmetry and stability data are needed before claiming a consistent compact four-dimensional vacuum. Use the horizontal spectator c to explain how the local I_{ab} can stay fixed while a total candidate charge changes. Then use the parallel third factor

$a_3 = b_3 = (1, 0)$ to explain how a zero signed product can coexist with vectorlike states or momentum and winding towers. Distinguish possible light states from guaranteed masslessness. This exercise asks for a physical argument, not a numerical certification of a compact model.

III.6.8 Take-home message

A relative brane angle changes both endpoint projectors of a single open string. The nonzero-frequency two-amplitude determinant produces two conjugate towers. The two-plane NS calculation then shows how its vacuum constant and surviving fermion combine into a selected equally spaced sequence of squared masses. The GSO projection is essential to this physical interpretation. It is not supplied by the bosonic determinant.

On an oriented torus, the determinant of two wrapping vectors gives a signed intersection. In the stated transverse factorized ab sector, three such determinants multiply to a chiral index. The sign records chirality. The index loses vectorlike information and leaves other stack and image sectors uncounted. A parallel factor illustrates why a zero index need not mean no states.

The flux description follows from varying the two oriented endpoint actions. Its antisymmetric matrix contains λF, and the positive dual-coordinate map turns it into a slope. With a genuine central $U(n)$ bundle, the trace Chern integral supplies the integer degree and the dual cycle has wrappings (n, m). The selected $SU(3)$ projector construction then exhibits compatible local supersymmetry parameters. Together these calculations provide usable boundary, spectrum, index, flux and spinor inputs. A compact construction still has to assemble all of them with its global charge, projection, anomaly and stability data.

Status and sources

Boundary conditions. Section III.6.2 uses the flat rotated-endpoint premise of Berkooz et al. (1996, physical PDF p. 6, eq. (3.1)). The local strip realization and two-amplitude spectrum are worldsheet results [WS], with its determinant factorization as a mathematical consequence. The local spectrum calculation [MATH] gives the least positive member of each conjugate tower. The full determinant has the factor ω; its reduction is restricted to $\omega \neq 0$. The zero-frequency solution is a separate boundary calculation. The source's $e^{+i\theta_{\mathrm{BDL}}} Z$ boundary condition has physical line angle $\theta_{\mathrm{local}} = -\theta_{\mathrm{BDL}}$ relative to the positive x axis. This sign conversion precedes use of its mode notation. The free-strip convention is the one used in Chapter 1.

Two-plane light tower. Section III.6.3: the light towers are [WS] results under the two-plane RNS/GSO construction of Berkooz et al. (1996, physical PDF pp. 7–8, eqs. (3.2)–(3.6)). The zeta normal-ordering arithmetic and the distinction between ΔM^2 and M_1 are calculated under these premises. The Hurwitz zeta value is the analytic-continuation identity used to evaluate the free-field sum, not a derivation of GSO. The source visibly prints the empty interval $0 \geq \theta \geq \pi/2$ on physical p. 7 after taking $\alpha > 0$. Our working branch $0 < \alpha < 1/2$ is independently stated. Neither a

corrected edition nor a published erratum is asserted. The endpoints require different mode ordering or zero-mode data.

Oriented chirality and its limits. Section III.6.4: the relevant [WS] input is the orientation/GSO chirality premise in the local D6 system of Berkooz et al. (1996, physical PDF pp. 8–9, eqs. (3.7)–(3.8)). The displayed fermion vertices on physical p. 9 omit the half factor present in that page's explanatory spacetime spin-field sentence. They are not used here as normalized vertex operators. The oriented torus determinant is a mathematical calculation [MATH]. The index calculation [WS] uses Ibáñez et al. (2001, physical PDF p. 13, eq. (3.5)) for the distinct non-invariant ab sector, with the factorized index also anchored by Blumenhagen et al. (2000, physical PDF p. 11, eq. (2.25)). Image, self-image and parallel sectors retain their separate conditions. The local insufficiency result [MATH] is the conditional argument obtained by varying a spectator at fixed a, b. The local assignments and separate anomaly condition in Ibáñez et al. (2001, physical PDF pp. 7–8, eqs. (2.3)–(2.4)) illustrate the need for more data. No compact tadpole, anomaly polynomial or stable vacuum is computed by that argument.

Flux and angle. Section III.6.5: the signed endpoint variation and its dual are [WS], with the radius arithmetic given explicitly. The Chern–Weil trace integral is a mathematical calculation [MATH], conditional on a genuine rank-n bundle. The local isometric duality uses the rectangular $B = 0$ central-field chart, with $n > 0$, positive physical radii, integer degree and compatible global transitions. It transfers no QFT claim between frames and asserts no global orientifold equivalence. The ordered magnetic signs agree with Blumenhagen et al. (2000, physical PDF p. 5, eq. (2.2)). That source's physical pp. 7–8, eqs. (2.12)–(2.15), give radius inversion and positive slope in its radius units. No explicit declaration $\alpha' = 1$ was located there; it retains explicit α' in (2.10)–(2.11). The chapter restores physical units from the endpoint action and the inherited positive dual radius, rather than attributing such a declaration to the source.

The rank and Chern-number prose of Ibáñez et al. (2001, physical PDF p. 12, before eq. (3.3)) is used separately from its printed mixed boundary rows. Its two (3.3) derivative directions have dot product $-\sin(2\vartheta)$, and its (3.4) mixed matrix has symmetric off-diagonal entries. Measuring the angle from the dualized axis explains a scalar cotangent relation but cannot repair those ordered signs. The signed derivation here does not claim to be a published correction. Bachas (1995, physical PDF pp. 7–8, eqs. (3.1)–(3.3)) explicitly uses $\alpha' = 1/2$ and endpoint charges. Its charge chart translates to $F_a = -q_L H$, $F_b = +q_R H$ in our oriented action. It is not silently identified with the book's integer-charge connection at both ends. The connection uses the integer-charge normalization and the dual coordinate uses the physical circle convention.

Selected spinor and scope. Section III.6.6: the spinor calculation [WS] uses the D-brane projector premise and sufficient $SU(3)$ construction of Berkooz et al. (1996, physical PDF pp. 3–5, eqs. (2.1)–(2.9)). The exterior-algebra action reproduces that selected construction, with Clifford normalization and spin phases defined before use. The pair of exact signed sums and their consequence are mathematical results [MATH] for that spinor branch. No all-sign necessity, lattice realization, chamber stability or full compact supersymmetry theorem is inferred.

Exercises 1–4 ask for bounded calculations and Exercise 5 for written interpretation. A nonlinear flux modification can agree on finitely many samples and still violate the general Chern–Weil relation.

References

Bachas, C. (1995). “A Way to Break Supersymmetry”. In: *arXiv preprint*. Source edition: arXiv v1, 20 physical PDF pages; boundary mode check only. arXiv: `hep-th/9503030`.

Berkooz, M., M. R. Douglas, and R. G. Leigh (1996). “Branes Intersecting at Angles”. In: *Nuclear Physics B* 480. Source edition: arXiv v2, 18 physical PDF pages, pp. 265–278. DOI: `10.1016/S0550-3213(96)00452-X`. arXiv: `hep-th/9606139`.

Blumenhagen, R. et al. (2000). “Noncommutative Compactifications of Type I Strings on Tori with Magnetic Background Flux”. In: *Journal of High Energy Physics* 2000.10. Source edition: arXiv v1, 26 physical PDF pages, p. 006. arXiv: `hep-th/0007024`.

Ibáñez, L. E., F. Marchesano, and R. Rabadán (2001). “Getting Just the Standard Model at Intersecting Branes”. In: *Journal of High Energy Physics* 2001.11. Source edition: arXiv v2, 45 physical PDF pages; only local index and global-consistency distinctions are reused, p. 002. arXiv: `hep-th/0105155`.

Chapter III.7

Branes ending on branes: boundary conditions and BIons

III.7.1 What an endpoint asks of a field

A string ending on a D-brane is an electric source for the brane gauge field. It also pulls on the brane. A description that keeps the electric field but fixes every transverse displacement misses this second effect. The simplest useful picture is a charged spike: electric flux spreads over the D3 worldvolume, while a transverse scalar bends the brane into a long throat. The relation between the flux and the throat length turns its energy into a string tension times a length.

There are several different meanings of an endpoint in this picture. The open-string boundary condition specifies where the string can end. The worldvolume variational problem specifies which field values or derivatives can be prescribed there. An electric source specifies a flux. For several D3-branes, the endpoint can instead require singular noncommuting scalar fields. Finally, a field allowed locally at an endpoint need not give a normalizable mode on the entire brane segment. These are related questions, but each needs its own calculation.

We begin with the surface term of a quadratic action. We then retain the full electric and scalar dependence of the derivative-truncated abelian DBI action. Its Legendre transform gives a pair of energy squares without requiring the two vectors to be parallel. The radial solution is a specialization of that result. Only after naming the physical charge identification do we calculate the energy of its regulated shell. A finite matrix pole and an interval eigenvalue problem supply the corresponding local tools for suspended D3-branes.

Chapter 3 supplies the abelian action and its derivative regime. Chapter 4 supplies the leading matrix fields and their physical position dictionary. Here the scalar endpoint problem is deliberately simpler than the coupled supersymmetric boundary theory. The boundary supersymmetry and fivebrane identifications are cited physical inputs. The calculations below establish surface signs, an abelian energy relation, a finite pole, and scalar modes under those inputs. The broader projector tools belong to Chapter 9.

III.7.2 Boundary variation of a gauge theory

What must be fixed at an endpoint so that a field equation follows from an action? The bulk Euler–Lagrange equation is only part of the answer. Integration by parts leaves a surface term. A valid variational problem must say which boundary variations are allowed, or must supply a boundary action that cancels their coefficients. This is the field-theory version of the endpoint question in Chapter 1.

Let s increase from left to right on $0 \le s \le L$, with $L > 0$. The remaining coordinates x^a are tangent to the boundary; one of them is time. Use mostly-plus signature, a real scalar ϕ, and a positive constant κ. With variations of compact support in the tangential directions, the action and its first variation are

$$S_\phi = -\frac{\kappa}{2}\int d^d x\, \partial_\mu\phi\partial^\mu\phi, \qquad \delta S_\phi = -\kappa\int d^d x\, \partial^\mu\phi\partial_\mu\delta\phi. \tag{III.7.1}$$

The boundary is spatial, so raising its normal index does not change its sign. Integrating the last derivative gives the bulk wave equation and a separate spatial boundary term:

$$\delta S_\phi = \kappa\int d^d x\, (\Box\phi)\delta\phi - \kappa\int_{\partial M} d^{d-1}x\, n^s\phi'\delta\phi, \qquad \phi' = \partial_s\phi. \tag{III.7.2}$$

The outward direction points toward decreasing s at the left end and toward increasing s at the right end. Thus the two coefficients have opposite signs:

$$n^s(0) = -1, \qquad n^s(L) = +1, \qquad \delta S_\phi\big|_{\partial M} = \int d^{d-1}x\, [\kappa\phi'(0)\delta\phi(0) - \kappa\phi'(L)\delta\phi(L)]. \tag{III.7.3}$$

Figure III.7.1 keeps the coordinate arrow and the two normal arrows separate. Reversing the normal at only one end changes the variational problem rather than changing a harmless drawing convention.

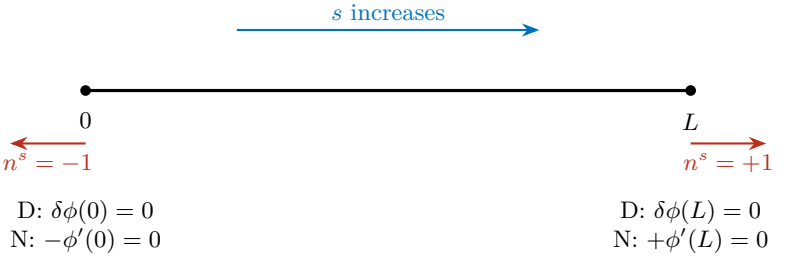


Figure III.7.1: One oriented interval. The coordinate s increases rightward; the outward normal at 0 points left, and the outward normal at L points right. A fixed scalar value removes its variation. A freely varied scalar instead requires the displayed outward derivative to vanish when there is no boundary action. These local choices will be imposed on the same interval in the spectral problem.

Dirichlet data fix the value of ϕ, so that $\delta\phi = 0$ at that end. Neumann data allow

arbitrary $\delta\phi$ and set its coefficient to zero. In this problem the alternatives are

$$\mathrm{D}: \quad \phi\big|_{\partial M} = \phi_b, \quad \delta\phi\big|_{\partial M} = 0; \qquad \mathrm{N}: \quad n^s\phi'\big|_{\partial M} = 0. \tag{III.7.4}$$

The Dirichlet value ϕ_b need not be zero. The homogeneous Dirichlet condition used for fluctuations later is a condition on the fluctuation about a fixed background. The choices at the two ends are independent for this free scalar. In particular, imposing Dirichlet data at the right end does not require Dirichlet data at the left.

For a concrete variation take $\kappa = 3/2$, $L = 2$, and the trial profile $\phi(s) = s^2 + s$. The derivatives at the ends are 1 and 5, hence

$$\delta S_\phi\big|_{\partial M} = \int d^{d-1}x \left[\frac{3}{2}\delta\phi(0) - \frac{15}{2}\delta\phi(2)\right]. \tag{III.7.5}$$

This profile is useful for testing the surface signs; it is not a static source-free solution of the bulk equation. Fixing both values kills its surface variation. Allowing arbitrary variation at either end does not, since the corresponding derivative is nonzero. For an NN solution the constant profile $\phi = \phi_0$ satisfies both derivative conditions. For ND data with a prescribed right value, the same constant can satisfy the static bulk problem only if its value is that right boundary value. Whether its fluctuation is a zero mode is a later, homogeneous problem.

A gauge field illustrates why an endpoint source must also be specified. To avoid confusion with the dimensionless DBI electric vector below, denote the Maxwell coupling by g_{M}. For an abelian connection A_μ, put $F_{\mu\nu} = \partial_\mu A_\nu - \partial_\nu A_\mu$. Antisymmetry combines the two differentiated variations:

$$\begin{aligned} S_A &= -\frac{1}{4g_{\mathrm{M}}^2}\int d^dx\, F_{\mu\nu}F^{\mu\nu}, \\ \delta S_A &= \frac{1}{g_{\mathrm{M}}^2}\int d^dx\, (\partial_\mu F^{\mu\nu})\delta A_\nu - \frac{1}{g_{\mathrm{M}}^2}\int_{\partial M} d^{d-1}x\, n_\mu F^{\mu a}\delta A_a. \end{aligned} \tag{III.7.6}$$

The index a is tangent to the boundary. The coefficient of a normal variation vanishes by antisymmetry. Fixing the tangential connection, with the corresponding restriction on gauge transformations, removes the surface variation. If it is varied freely, the source-free natural condition is $n_\mu F^{\mu a} = 0$.

Define a boundary current by the convention $\delta S_B = \int_{\partial M} j^a \delta A_a$. Its sign is part of the definition, not an implicit charge choice. The coefficient of an arbitrary tangential variation is then

$$\delta(S_A + S_B)\big|_{\partial M} = \int_{\partial M}\left(j^a - \frac{n_\mu F^{\mu a}}{g_{\mathrm{M}}^2}\right)\delta A_a, \qquad \frac{n_\mu F^{\mu a}}{g_{\mathrm{M}}^2} = j^a. \tag{III.7.7}$$

For example, a specified component $j^a = 2$ and $g_{\mathrm{M}}^2 = 3$ requires outward flux component 6. In the same coordinate basis this means $F^{sa} = -6$ at the left end and $F^{sa} = 6$ at the right end if both outward currents have that value. The normal, not a universal coordinate sign, relates the source to the field.

This calculation explains what an endpoint asks of the action. It does not yet select a supersymmetric boundary condition. That requires the other fields and their

variations, a preserved supercharge, and possibly boundary degrees of freedom. It also does not decide which allowed profiles are normalizable. Chapter 4 identifies the fields to which these choices apply; the final section of this chapter performs the separate global scalar-mode test. The charged spike next replaces the linear Maxwell constitutive law by the nonlinear abelian DBI law.

III.7.3 Electric spikes

How can the gauge field and the shape of a brane support the same endpoint? Work with a flat static abelian D3 in static gauge. Let $\mathbf{x} = (x^1, x^2, x^3)$ be orthonormal spatial worldvolume coordinates and let $X(\mathbf{x})$ be one physical transverse displacement, measured in length. There is no background two-form and no magnetic field. The electric field is $E_i = F_{0i}$. Inherited from Chapter 3 are the tension $\tau_3 > 0$ and $\lambda = 2\pi\alpha' > 0$. Define the dimensionless vectors

$$u_i = \partial_i X, \qquad e_i = \lambda E_i, \qquad D_i = \frac{\partial \mathcal{L}}{\partial E_i}, \qquad q_i = \frac{D_i}{\tau_3 \lambda}. \tag{III.7.8}$$

Here $\mathbf{D}$ is the canonical electric displacement, not the electric field. All dot products in this section use the Euclidean spatial worldvolume metric. No alignment between $\mathbf{e}$ and $\mathbf{u}$ is imposed. DBI keeps their full algebraic dependence, but neglects higher derivatives of the field strength and second derivatives of the embedding. A large allowed slope is not by itself a promise that those neglected derivatives are small.

The determinant makes the general domain visible. The static induced metric has spatial block $S = I + \mathbf{u}\mathbf{u}^T$. The matrix in the DBI square root and the elementary rank-one inverse are

$$M = \begin{pmatrix} -1 & \mathbf{e}^T \\ -\mathbf{e} & S \end{pmatrix}, \qquad A = 1 + \mathbf{u}^2, \qquad \det S = A, \qquad S^{-1} = I - \frac{\mathbf{u}\mathbf{u}^T}{A}. \tag{III.7.9}$$

Taking the Schur complement of S gives

$$\begin{aligned} \Delta = -\det M &= A(1 - \mathbf{e}^T S^{-1} \mathbf{e}) \\ &= (1 + \mathbf{u}^2)(1 - \mathbf{e}^2) + (\mathbf{e} \cdot \mathbf{u})^2 = A - \mathbf{e}^T K \mathbf{e}, \qquad K = AI - \mathbf{u}\mathbf{u}^T. \end{aligned} \tag{III.7.10}$$

The Lagrangian is $\mathcal{L} = -\tau_3 \sqrt{\Delta}$ on the real branch $\Delta > 0$. Along $\mathbf{u}$, K has eigenvalue 1; in the two orthogonal directions its eigenvalue is A. At $\mathbf{u} = 0$ all three eigenvalues are 1. In particular K is positive definite. If $\mathbf{u} \neq 0$ and $\mathbf{e} = e_\parallel \hat{\mathbf{u}} + \mathbf{e}_\perp$, the domain reads

$$e_\parallel^2 + A\, \mathbf{e}_\perp^2 < A. \tag{III.7.11}$$

This is an ellipsoid in electric-field coordinates. The condition $|\mathbf{e}| < 1$ is sufficient, but it is not the general real domain. At $\Delta = 0$ the finite-displacement Legendre transformation below is singular. We remain on the strict branch.

Differentiate the Lagrangian at fixed scalar slope. The factor λ comes from $\mathbf{e} = \lambda \mathbf{E}$:

$$\mathbf{D} = \tau_3 \lambda \frac{K\mathbf{e}}{\sqrt{\Delta}}, \qquad \mathbf{q} = \frac{K\mathbf{e}}{\sqrt{\Delta}}, \qquad K^{-1} = \frac{I + \mathbf{u}\mathbf{u}^T}{A}. \tag{III.7.12}$$

The inverse follows by multiplying $K(I+\mathbf{u}\mathbf{u}^T)=AI$. Writing $w=\mathbf{q}^TK^{-1}\mathbf{q}\geq 0$ first eliminates $\mathbf{e}$ from the determinant:

$$\mathbf{e}=\sqrt{\Delta}K^{-1}\mathbf{q},\qquad \Delta(1+w)=A,\qquad \Delta=\frac{A}{1+w},\qquad w=\frac{\mathbf{q}^2+(\mathbf{u}\cdot\mathbf{q})^2}{A}. \tag{III.7.13}$$

Every finite $\mathbf{q}$ gives a positive Δ at fixed finite $\mathbf{u}$. This also shows why fixing the displacement is a convenient way to describe the charged source.

The energy density is $\mathcal{H}=\mathbf{D}\cdot\mathbf{E}-\mathcal{L}$. Because the configuration is static, the scalar has zero canonical momentum. Using $\Delta+\mathbf{e}^TK\mathbf{e}=A$ yields

$$\begin{aligned} h\equiv\frac{\mathcal{H}}{\tau_3}&=\mathbf{q}\cdot\mathbf{e}+\sqrt{\Delta}=\frac{A}{\sqrt{\Delta}}\\ &=\sqrt{1+\mathbf{u}^2+\mathbf{q}^2+(\mathbf{u}\cdot\mathbf{q})^2},\qquad \mathbf{e}=\frac{\mathbf{q}+\mathbf{u}(\mathbf{u}\cdot\mathbf{q})}{h}. \end{aligned} \tag{III.7.14}$$

The last equation reconstructs the original electric field. It is an inverse constitutive relation, not the assertion $\mathbf{e}=\mathbf{q}$ for arbitrary fields.

For an actual nonparallel example take $\mathbf{u}=(1,0,0)$ and $\mathbf{e}=(1,1/2,0)$. Direct substitution gives

$$\begin{gathered} A=2,\quad K=\operatorname{diag}(1,2,2),\quad \Delta=2-1-\tfrac{1}{2}=\tfrac{1}{2},\quad \mathbf{e}^2=\tfrac{5}{4},\\ \mathbf{q}=(\sqrt{2},\sqrt{2},0),\quad h=\sqrt{1+1+4+2}=2\sqrt{2}. \end{gathered} \tag{III.7.15}$$

This is real even though $|\mathbf{e}|>1$. The inverse relation gives $(2\sqrt{2},\sqrt{2},0)/(2\sqrt{2})=(1,1/2,0)$, as required. Neither electric displacement nor electric field is parallel to the slope. Figure III.7.2 shows its position in a section of the real domain. Restricting the derivation to radial parallel vectors would have lost this example and obscured the domain.

To find the special balance between electric flux and bending, rearrange the full Hamiltonian, rather than dropping the nonparallel terms. Expansion of either right-hand side gives precisely the same h^2:

$$h^2=(1+\mathbf{u}\cdot\mathbf{q})^2+|\mathbf{u}-\mathbf{q}|^2,\qquad h\geq 1+\mathbf{u}\cdot\mathbf{q}. \tag{III.7.16}$$

$$h^2=(1-\mathbf{u}\cdot\mathbf{q})^2+|\mathbf{u}+\mathbf{q}|^2,\qquad h\geq 1-\mathbf{u}\cdot\mathbf{q}. \tag{III.7.17}$$

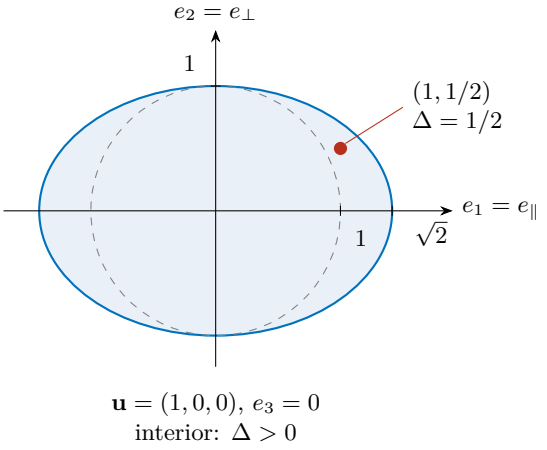


Figure III.7.2: Electric domain for $\mathbf{u} = (1, 0, 0)$ and $e_3 = 0$. The real branch is the interior of $e_1^2 + 2e_2^2 = 2$. The open disk inside the dashed unit circle is a sufficient subdomain; the two points where the circle touches the ellipse are excluded. The marked point $(1, 1/2)$ lies outside that circle and inside the ellipse. Both axes are dimensionless components of $\lambda\mathbf{E}$; the vertical component is perpendicular to the scalar slope.

The stronger intermediate bounds contain the absolute values of the first terms. The displayed weaker versions are useful for integration. Equality in the first displayed bound occurs at $\mathbf{u} = \mathbf{q}$, where $1 + \mathbf{u} \cdot \mathbf{q} = 1 + \mathbf{u}^2 > 0$. The second is saturated at $\mathbf{u} = -\mathbf{q}$, where $1 - \mathbf{u} \cdot \mathbf{q} = 1 + \mathbf{u}^2 > 0$. No negative-energy choice of square-root branch is involved.

For a source-free spatial region Ω, Gauss law gives $\nabla \cdot \mathbf{q} = 0$. Therefore the term bounding the excess energy is a boundary quantity:

$$\int_\Omega \nabla X \cdot \mathbf{q}\, d^3x = \int_{\partial\Omega} X\, \mathbf{q} \cdot \mathbf{n}\, dS, \qquad E_{\text{exc}} \geq \pm\tau_3 \int_{\partial\Omega} X\, \mathbf{q} \cdot \mathbf{n}\, dS. \tag{III.7.18}$$

The two signs come from the two completions. They have a variational energy interpretation when the scalar boundary values and normal fluxes are fixed consistently. Altering those boundary data changes the quantity being bounded. A pointwise algebraic inequality alone is not a proof of stability against every possible change of endpoint or core.

For the parallel branch $\mathbf{q} = \mathbf{u}$ the constitutive relation and determinant simplify substantially:

$$h = 1 + \mathbf{u}^2, \qquad \mathbf{e} = \mathbf{u}, \qquad \Delta = 1. \tag{III.7.19}$$

Thus the dimensionless electric field on this branch can have magnitude greater than one without leaving the real domain. The slope changes the induced spatial metric at the same time. For $\mathbf{q} = -\mathbf{u}$, one instead has $\mathbf{e} = -\mathbf{u}$, the same h, and again $\Delta = 1$. These are statements inside the truncated abelian action. Calling the corresponding string configuration BPS also uses the physical supersymmetry input discussed in the next section.

At radius $r = 2$ in the radial branch with $c = 3/4$, the slope and normalized displacement are 3/16. Hence

$$q_r = u_r = \frac{c}{r^2} = \frac{3}{16}, \qquad h = 1 + \frac{9}{256} = \frac{265}{256}, \qquad \frac{\mathcal{H} - \tau_3}{\tau_3} = \frac{9}{256}. \tag{III.7.20}$$

A flat uncharged brane has $\mathbf{u} = \mathbf{q} = 0$ and zero excess energy. Reversing both vectors leaves this positive excess unchanged. Reversing only $\mathbf{q}$ selects the opposite completion when the slope is held fixed. Confusing these two operations loses the distinction between electric orientation and the side toward which the brane bends. The next calculation imposes the field equations and integrates the energy, with the factors inherited from Chapter 3 restored.

III.7.4 Flux measures string charge

Which source does the radial spike describe? We take as physical input that an F1 endpoint couples electrically to the integer-charge brane connection, that its oriented displacement flux is an integer n, and that a fundamental string has tension $T_{\mathrm{F1}} = 1/\lambda$. The protected string interpretation of the electric/scalar branch is also inherited from the physical string construction. It is not inferred from a completed square. With these identifications stated first, the worldvolume calculation can test the precise relation between energy, flux, and geometric length. This is the endpoint object of Chapter 1 expressed in the field normalization of Chapter 3.

First check that the proposed shape is a solution on the region where there is no source. The constraint from the gauge field is Gauss law. The scalar equation follows by varying the Hamiltonian at fixed $\mathbf{q}$; X appears only through its gradient:

$$\nabla \cdot \mathbf{q} = 0, \qquad \nabla \cdot \left(\frac{\mathbf{u} + \mathbf{q}(\mathbf{u} \cdot \mathbf{q})}{h} \right) = 0. \tag{III.7.21}$$

The static gauge field must also obey the electric Bianchi identity $\nabla \times \mathbf{e} = 0$. On $\mathbf{q} = \mathbf{u}$, the vector in parentheses is $\mathbf{u}$ and $\mathbf{e} = \nabla X$. Both scalar and gauge requirements reduce to a harmonic scalar away from its endpoint:

$$\nabla^2 X = 0, \qquad \nabla \times \nabla X = 0 \quad (r > 0). \tag{III.7.22}$$

The reduction uses the full Hamiltonian in the previous section. It does not replace a general stationary equation by an unmotivated Coulomb guess.

Let $r = |\mathbf{x}|$ and let $\widehat{\mathbf{r}}$ point toward increasing r. A radial divergence is $r^{-2}\partial_r(r^2 q_r)$. The source-free solution with positive constant c and $X(\infty) = 0$ is therefore

$$r^2 q_r = c, \qquad X' = q_r = \frac{c}{r^2}, \qquad X(r) = -\frac{c}{r}, \qquad c \geq 0. \tag{III.7.23}$$

For $c > 0$ the spike extends toward negative X near the origin, while its gradient and its electric displacement point outward. There is no contradiction: the gradient measures the increase of X as one moves away from its negative tip. A closed sphere detects flux even though the divergence vanishes on every punctured neighborhood. The excluded

source is precisely why the divergence theorem cannot be applied through $r = 0$ without an additional source term.

Keep only a shell $\delta \le r \le R$, where $0 < \delta < R$. Both the charge-measuring sphere and the inner boundary of the shell need orientations. With the sphere oriented by $+\hat{\mathbf{r}}$, its flux is independent of its radius:

$$n = \int_{S_r^2} \mathbf{D} \cdot \hat{\mathbf{r}}\, dS = \tau_3 \lambda \int_{S_r^2} \frac{c}{r^2}\, dS = 4\pi\tau_3 \lambda c. \tag{III.7.24}$$

The inner boundary of the shell has outward normal $-\hat{\mathbf{r}}$. Its outward flux relative to the shell is therefore $-n$. The two shell boundary fluxes sum to zero, as required by Gauss law. Figure III.7.3 distinguishes the enclosed-source orientation from the shell orientation and marks the two values of X.

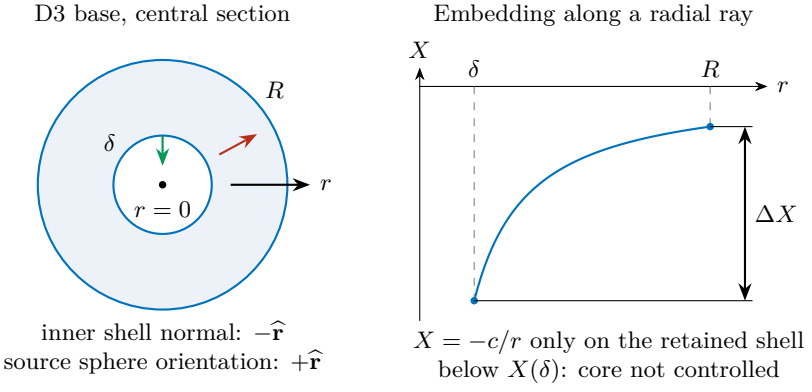


Figure III.7.3: A meridional section of the derivative-truncated spike $X = -c/r$ and its regulated shell. The left panel is a central section of the D3 base; its two circles represent cuts through the bounding spheres. The right panel gives one radial ray of the embedding. Radial arrows represent positive displacement flux in the base. The inner shell boundary normal points toward decreasing r, opposite to the enclosed-source sphere orientation. Only $\delta \le r \le R$ contributes to the highlighted length. The unresolved region below the inner cutoff is excluded; no smooth core is depicted.

Subtract the energy of the flat brane on the same shell. The remaining density is $\tau_3 c^2/r^4$, and the volume measure is $4\pi r^2 dr$. The radial integral has one remaining inverse square:

$$\begin{aligned} \Delta E_{\delta,R} &= 4\pi\tau_3 c^2 \int_\delta^R \frac{dr}{r^2} \\ &= 4\pi\tau_3 c^2 \left(\frac{1}{\delta} - \frac{1}{R}\right), \qquad \Delta X = X(R) - X(\delta) = c\left(\frac{1}{\delta} - \frac{1}{R}\right). \end{aligned} \tag{III.7.25}$$

The length ΔX is positive. It is a difference of transverse positions, not the radial width $R - \delta$ and not the induced arc length of a curve on the brane. Eliminating c

using the flux yields

$$\Delta E_{\delta,R} = \frac{n}{\lambda}\,\Delta X = nT_{\mathrm{F1}}\Delta X \qquad (c \geq 0). \tag{III.7.26}$$

This is the conditional energy calculation. Flux quantization and the F1 identification supplied the meaning of n; the integral supplied the coefficient multiplying the actual length.

The same result follows directly from the boundary form of the energy bound. Inserting both shell normals gives

$$\tau_3 \int_{\partial\Omega} X\mathbf{q}\cdot\mathbf{n}\,dS = 4\pi\tau_3 c\,[X(R) - X(\delta)] = 4\pi\tau_3 c^2\left(\frac{1}{\delta} - \frac{1}{R}\right). \tag{III.7.27}$$

Retaining only the outer surface would have produced a negative term for this negative-X spike. The positive energy requires the inner surface with its correct orientation.

Units are a useful check on every factor. Let ℓ denote a length unit and use $\hbar = c_{\mathrm{light}} = 1$. Since the connection is normalized so that its line integral is dimensionless, the dimensions are

$$\begin{gathered}[X] = [r] = \ell, \quad [\lambda] = \ell^2, \quad [\tau_3] = \ell^{-4}, \quad [E_i] = [D_i] = \ell^{-2}, \\ [u_i] = [e_i] = [q_i] = 1, \quad [c] = \ell^2, \quad [n] = 1, \quad [T_{\mathrm{F1}}] = \ell^{-2}, \quad [\Delta E] = \ell^{-1}.\end{gathered} \tag{III.7.28}$$

Thus λ cannot simply be dropped from the flux or the energy. The source's $\alpha' = 1$ field convention also needs a conversion. At those fixed units its electric field is $\mathbf{E}_{\mathrm{CM}} = 2\pi\mathbf{E}_{\mathrm{book}}$, and the chain rule gives

$$\mathbf{D}_{\mathrm{book}} = 2\pi\mathbf{\Pi}_{\mathrm{CM}}, \qquad \int_{S^2}\mathbf{\Pi}_{\mathrm{CM}}\cdot d\mathbf{S} = \frac{n}{2\pi}, \qquad \int_{S^2}\mathbf{D}_{\mathrm{book}}\cdot d\mathbf{S} = n \quad (\alpha' = 1). \tag{III.7.29}$$

In general units the local dimensionless DBI field is $\lambda\mathbf{E}_{\mathrm{book}}$ and $\mathbf{D} = \tau_3\lambda\mathbf{q}$. Restoring physical coordinates as well as λ gives (III.7.24). Equating dimensionful coordinates to the source's numerical $\alpha' = 1$ coordinates without a unit conversion would not do so.

Here is a nonunit-λ example that also reconstructs a whole shell. Choose $\lambda = 5/2$, $n = 2$, $c = 1$, and $\tau_3 = 1/(5\pi)$ in consistent length units. Take $\delta = 3/8$ and $R = 3$. The flux and length are

$$4\pi\tau_3\lambda c = 2, \qquad \Delta X = \frac{8}{3} - \frac{1}{3} = \frac{7}{3}, \qquad T_{\mathrm{F1}} = \frac{2}{5}, \qquad \Delta E = \frac{4}{5}\frac{7}{3} = \frac{28}{15}. \tag{III.7.30}$$

For these choices the integral and tension-times-length calculation agree with every normalization explicit. If both $\mathbf{q}$ and $\mathbf{u}$ reverse, the profile is $+c/r$, the oriented charge is -2, and the geometric length remains $7/3$. The general statement is

$$n \longmapsto -n, \qquad X \longmapsto -X, \qquad \Delta X_{\mathrm{geom}} = |X(R) - X(\delta)|, \qquad \Delta E = \frac{|n|}{\lambda}\Delta X_{\mathrm{geom}}. \tag{III.7.31}$$

Holding the spike shape fixed while reversing only the flux gives $\mathbf{q} = -\mathbf{u}$ and saturates the other energy bound. It is a different relative sign choice. In both cases the

Hamiltonian is positive. For $c = 0$ the shape is flat, the flux and excess vanish, and no length can be inferred by dividing by the zero charge.

Energy on this fixed solution is additive under a subdivision of the shell. For any $\delta < \rho < R$, the two integrals have the same c:

$$\Delta E_{\delta,\rho} + \Delta E_{\rho,R} = 4\pi\tau_3 c^2 \left[\left(\frac{1}{\delta} - \frac{1}{\rho} \right) + \left(\frac{1}{\rho} - \frac{1}{R} \right) \right] = \Delta E_{\delta,R}. \tag{III.7.32}$$

For the numerical shell above, $\rho = 3/4$ gives energies $16/15$ and $4/5$, whose sum is $28/15$. This checks the integral as a function of the boundaries, rather than merely one value of the total energy.

Finally, the limit $\delta \to 0$ is not a core solution. It gives $\Delta X \sim c/\delta$ and $\Delta E \sim 4\pi\tau_3 c^2/\delta$. In the same limit derivatives of the embedding grow without bound. The action used here omits precisely the higher-derivative information needed to justify an extrapolation there. Saturation within this action neither supplies a source-independent nonlinear supersymmetry proof nor resolves the endpoint microscopically. This distinction is essential before using endpoint data in the suspended brane constructions of Volume VII-A. Brane creation and the quantum s-rule require their own physical inputs.

III.7.5 Nonabelian endpoint data

A scalar Dirichlet or Neumann label cannot describe every endpoint of several coincident D3-branes. The scalars are matrices, and an endpoint can prescribe a singular noncommuting triple. We now take the physical half-BPS D3/D5 boundary assignment as an input from the supersymmetric boundary construction. Its D3 bulk theory has sixteen real supercharges; the boundary preserves eight. The D5-type boundary admits a Nahm pole. The purpose of the calculation is to translate its sign and verify one finite residue. Neither the translation nor that residue establishes the physical assignment.

The source frame must be fixed before writing the equation. Denote its spacetime coordinates by $u^0, \ldots, u^9$. We use the frame after the source's exchange of its two scalar triples in section 2.3. In that frame its D3 is 0123, its D5 is 012456, its NS5 is 012789, and the pole triple is its 456. The book uses the passive relabeling

$$(x^0, x^1, x^2, x^3, x^4, x^5, x^6, x^7, x^8, x^9) = (u^0, u^1, u^2, u^7, u^8, u^9, u^3, u^4, u^5, u^6). \tag{III.7.33}$$

This moves the ordered three-block 789 past the four-block 3456. It has $3 \cdot 4 = 12$ transpositions and determinant $+1$. The ordered pole directions become 789 and the inward coordinate is $s = x^6 = u^3 = y \geq 0$. No coordinate is actively rotated through a brane.

Object	Source frame after exchange	Book frame
D3	0123	0126
D5	012456	012789
NS5	012789	012345
Inward direction	$+u^3$	$+x^6$
Ordered pole triple	(u^4, u^5, u^6)	(x^7, x^8, x^9)

Table III.7.1: The passive source-to-book conversion. Directions 012 are common. The last row specifies an ordered triple, so its orientation is part of the sign convention. The NS5 label belongs to the same final source frame as the D5 and the pole.

Figure III.7.4 shows the correspondence of directions with explicit arrow endpoints. An earlier source discussion uses a different assignment of its X and Y triples before their exchange. Taking that assignment while retaining the later Figure 1 brane labels would combine two frames. The passive permutation in Table III.7.1 converts the final frame as a whole.

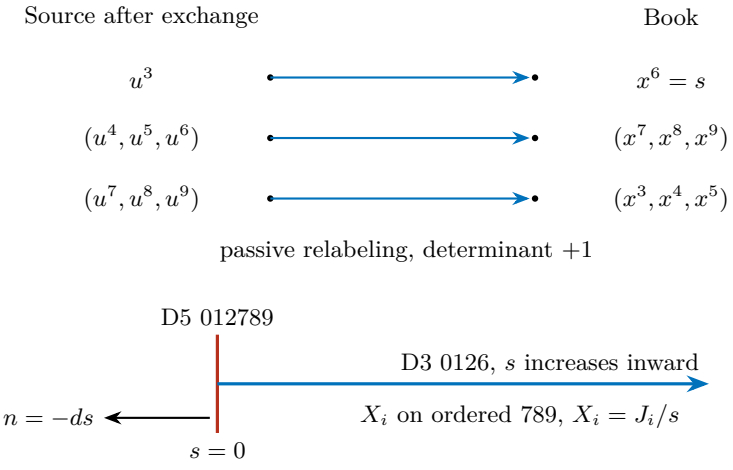


Figure III.7.4: Direction correspondence and the local D5 endpoint. The three arrows connect ordered source direction groups to their book counterparts; they are coordinate identifications, not motions of a brane. Below, the D5 is at $s = 0$ and the D3 extends toward increasing $s = x^6$. The boundary normal points toward decreasing s. The pole fields refer to book 789, whereas 012 is common to both objects.

Here X_i, $i = 1, 2, 3$, denotes the Hermitian Yang–Mills scalar triple associated with those ordered 789 directions. Unlike the single physical-length displacement X in the abelian DBI calculation, these fields have dimension inverse length. In the leading position dictionary of Chapter 4, physical matrix displacements are λX_i. The pole is a statement about the field boundary behavior, not a reliable picture of separated

position eigenvalues at its singularity. Write $D_s = \partial_s - i[A_s, \cdot\,]$ in the Hermitian book connection and $\epsilon_{123} = +1$.

Let $\mathcal{X}_i$ denote the source's anti-Hermitian fields, with its connection translated as $\mathcal{A}_s = -iA_s$. The source equation and its field translation are

$$D_y\mathcal{X}_1 + [\mathcal{X}_2, \mathcal{X}_3] = 0, \qquad \mathcal{X}_i = -iX_i, \qquad y = s, \tag{III.7.34}$$

with two cyclic equations. Substitution gives $-iD_sX_1 - [X_2, X_3] = 0$. Multiplication by i therefore yields

$$D_sX_1 - i[X_2, X_3] = 0, \qquad D_sX_i - \frac{i}{2}\epsilon_{ijk}[X_j, X_k] = 0. \tag{III.7.35}$$

For $i = 1$, the 23 and 32 terms in the sum are equal, which accounts for the factor $1/2$. This sign uses both the anti-Hermitian-to-Hermitian conversion and an inward s. Reversing the coordinate without converting the equation would reverse the derivative term only.

Choose the local gauge $A_s = 0$ on $s > 0$. Let σ_i be the Pauli matrices and $J_i = \sigma_i/2$. Explicitly,

$$J_1 = \frac{1}{2}\begin{pmatrix} 0 & 1 \\ 1 & 0 \end{pmatrix}, \qquad J_2 = \frac{1}{2}\begin{pmatrix} 0 & -i \\ i & 0 \end{pmatrix}, \qquad J_3 = \frac{1}{2}\begin{pmatrix} 1 & 0 \\ 0 & -1 \end{pmatrix}. \tag{III.7.36}$$

These matrices are Hermitian, traceless, and noncommuting. For example, $J_1J_2 = i\sigma_3/4$ and $J_2J_1 = -i\sigma_3/4$; all cyclic products give

$$[J_1, J_2] = iJ_3, \qquad [J_2, J_3] = iJ_1, \qquad [J_3, J_1] = iJ_2. \tag{III.7.37}$$

The factor multiplying $i\sigma_3$ in the first commutator is $1/2$, not 1 or $1/4$. The derivative and the commutator must be evaluated in the same normalization.

For a real constant a try $X_i = aJ_i/s$. Its derivative and quadratic term are

$$\partial_sX_i = -\frac{a}{s^2}J_i, \qquad -\frac{i}{2}\epsilon_{ijk}[X_j, X_k] = \frac{a^2}{2s^2}\epsilon_{ijk}\epsilon_{jk\ell}J_\ell = \frac{a^2}{s^2}J_i. \tag{III.7.38}$$

The last equality uses $\epsilon_{ijk}\epsilon_{jk\ell} = 2\delta_{i\ell}$. Thus the full residual and its three explicit matrices are

$$\begin{aligned} \mathcal{R}_i &= \frac{a(a-1)}{s^2}J_i, \\ (\mathcal{R}_1, \mathcal{R}_2, \mathcal{R}_3) &= \frac{a(a-1)}{2s^2}\left(\begin{pmatrix} 0 & 1 \\ 1 & 0 \end{pmatrix}, \begin{pmatrix} 0 & -i \\ i & 0 \end{pmatrix}, \begin{pmatrix} 1 & 0 \\ 0 & -1 \end{pmatrix}\right). \end{aligned} \tag{III.7.39}$$

The nontrivial pole is $a = 1$; $a = 0$ is the trivial solution. At $a = 2$ the coefficient of every J_i/s^2 is 2, so doubling the residue does not produce another solution. At $s = 2$ for $a = 1$, the two terms in each equation are $-J_i/4$ and $+J_i/4$. At the same point for $a = 2$, their sum is $J_i/2$. These finite matrices test the sign as well as the size of the residue.

The pole has no finite boundary value at $s = 0$. It specifies an asymptotic singularity, whereas ordinary Dirichlet data specify a value. The source relates such residues to Lie

algebra homomorphisms $\rho : \mathfrak{su}(2) \to \mathfrak{g}$ and to D5-type boundary conditions. Here $\mathfrak{g}$ is the gauge Lie algebra and ρ sends the three standard generators to the residue matrices. That general physical and moduli-space construction is cited, not proved by the rank-two example. We have verified one local solution on $s > 0$, not all representations, allowed perturbations, or a global moduli space. The local gauge choice also says nothing about interval holonomies or their endpoint quotient.

Chapter 4 explains why the fields can fail to commute. IX, Chapter 4 uses the oriented pole when discussing nonabelian endpoints. The scalar-mode calculation next instead linearizes about the regular flat scalar problem. It is not the fluctuation operator about this singular triple, and it must not be used as its complete spectrum.

III.7.6 Interval zero modes

When does a field allowed by an endpoint become a massless field on a suspended segment? There are two global questions after the local variation has been settled. The same profile must satisfy the condition at the other endpoint, and its kinetic norm over the actual domain must be finite. The elementary scalar problem makes both tests explicit before gauge constraints or interacting boundary fields are introduced.

Let $\varphi(x^a, s)$ be a real free fluctuation with the positive kinetic coefficient of the first derivation. Take a product metric and a flat measure on $0 \le s \le L$. Separate a profile by $\varphi = \chi(x^a) f(s)$ and define the nonnegative mass parameter k when the eigenvalue is nonnegative. The wave equation separates as

$$(\Box_{\parallel} + \partial_s^2)\varphi = 0, \qquad (\Box_{\parallel} - k^2)\chi = 0, \qquad -f'' = k^2 f. \tag{III.7.40}$$

The sign of the mass term uses mostly-plus signature. The induced kinetic coefficient of χ is proportional to $\int_0^L |f|^2 ds$. Thus a solution of the differential equation and a finite kinetic coefficient are different requirements.

We first justify the nonnegative eigenvalue rather than assume it. For a smooth eigenfunction satisfying homogeneous N or D data at each end, integration by parts gives

$$k^2 \int_0^L |f|^2 ds = \int_0^L |f'|^2 ds - [\overline{f} f']_0^L = \int_0^L |f'|^2 ds \ge 0. \tag{III.7.41}$$

Each endpoint term vanishes because either f or f' vanishes there. For two such functions f, g, the corresponding boundary difference $[\overline{f} g' - \overline{f}' g]_0^L$ also vanishes. These separated conditions give the usual symmetric scalar boundary problem. The displayed positive quadratic form suffices to exclude negative mass-squared eigenfunctions here. No claim about the stability of a coupled brane theory follows from this free scalar form.

The case $k = 0$ must be solved before dividing by k. Its complete local solution and endpoint equations are

$$f(s) = A + Bs, \qquad \text{N at } 0: \ B = 0, \qquad \text{D at } 0: \ A = 0. \tag{III.7.42}$$

For NN, $B = 0$ satisfies both ends and A remains free. For DD, the right value gives $A + BL = 0$ in addition to $A = 0$, hence $B = 0$. For ND, the left derivative gives $B = 0$

and the right value then gives $A = 0$:

conditions	right-end equation after the left end	zero-eigenvalue profiles
NN	$B = 0$	A arbitrary
DD	$BL = 0$	$f = 0$
ND	$A = 0$	$f = 0$

(III.7.43)

Only a nonzero eigenfunction counts as a mode. The zero function at DD or ND is not an additional zero mode. The positivity identity gives an alternative quick check: a zero eigenvalue forces $f' = 0$, and any Dirichlet end then kills that constant.

For $k > 0$ use independent sine and cosine solutions:

$$f(s) = A\cos(ks) + B\sin(ks), \qquad f'(s) = k[-A\sin(ks) + B\cos(ks)]. \tag{III.7.44}$$

At the left NN endpoint, $f'(0) = kB = 0$ sets $B = 0$. At the right end, $f'(L) = -Ak\sin(kL) = 0$. For a nonzero profile $A \neq 0$, so the positive spectrum is

$$\text{NN}, \quad k_n = \frac{n\pi}{L}\ (n = 1, 2, \ldots), \qquad f_n(s) = A\cos\frac{n\pi s}{L}, \qquad f_0(s) = A_0. \tag{III.7.45}$$

The last constant is the separately solved $k = 0$ mode. It is not obtained by dividing a positive-k endpoint equation by k and then setting $k = 0$ afterward.

For DD, $f(0) = A = 0$ and $f(L) = B\sin(kL) = 0$. This time the sine solution gives

$$\text{DD}, \quad k_n = \frac{n\pi}{L}\ (n = 1, 2, \ldots), \qquad f_n(s) = B\sin\frac{n\pi s}{L}. \tag{III.7.46}$$

The apparent $n = 0$ sine is identically zero. A constant nonzero profile would fail both Dirichlet values. These are two ways to see the same absence, but solving $A + Bs$ was needed to exclude every possible zero-eigenvalue profile.

For ND, N is at $s = 0$ and D at $s = L$. The left derivative again sets $B = 0$, while the right value requires $A\cos(kL) = 0$. Therefore

$$\text{ND}, \quad k_n = \frac{(n + 1/2)\pi}{L}\ (n = 0, 1, \ldots), \qquad f_n(s) = A\cos\frac{(n + 1/2)\pi s}{L}. \tag{III.7.47}$$

The lowest profile travels from an extremum to a zero, using a quarter of a wavelength. The DD profile must travel from a zero to a zero and uses half a wavelength. This explains the relative factor of two in the first positive values. The labels are scalar boundary conditions; they are not the ND oscillator directions of an entire open-string worldsheet spectrum from Chapter 1.

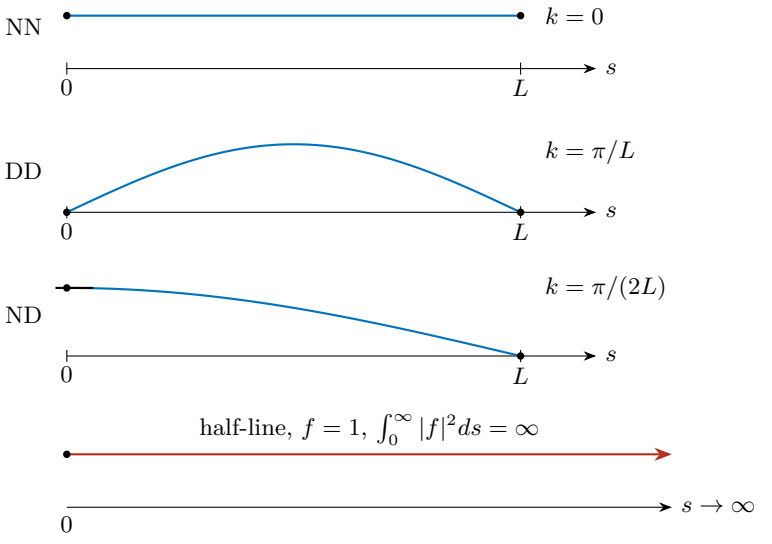


Figure III.7.5: The lowest nonzero profiles on the same finite interval and the separate constant on a half-line. The NN constant has $k = 0$; the DD sine has $k = \pi/L$; the ND cosine has $k = \pi/(2L)$, with N at the left. Dots mark boundary values and short horizontal ticks mark Neumann slopes. The bottom domain continues to infinity, so its locally allowed constant has an infinite flat-measure norm. Amplitudes in the drawing are chosen for visibility rather than unit normalization.

For $L = 3/2$, the first allowed k/π in the three problems and the lowest positive NN value are

$$(k/\pi)^{\mathrm{NN}}_{\mathrm{first}} = 0, \qquad (k/\pi)^{\mathrm{DD}}_{\mathrm{first}} = \frac{2}{3}, \qquad (k/\pi)^{\mathrm{ND}}_{\mathrm{first}} = \frac{1}{3}, \qquad (k/\pi)^{\mathrm{NN}}_{\mathrm{first\ positive}} = \frac{2}{3}. \tag{III.7.48}$$

For instance the ND function is $\cos(\pi s/3)$. Its derivative vanishes at $s = 0$, and its value at $s = 3/2$ is $\cos(\pi/2) = 0$. The DD function is $\sin(2\pi s/3)$ and vanishes at both endpoints. Replacing its first eigenvalue by zero while leaving a nonzero constant profile would immediately violate $f(0) = 0$. Figure III.7.5 shows the endpoint behavior that these equations test.

Normalization completes the finite-interval calculation. The raw constant $f = 1$ has norm squared L. For the positive modes, integrating the squared trigonometric functions gives

$$\begin{aligned} \int_0^L \cos^2(ks)\, ds &= \frac{L}{2} + \frac{\sin(2kL)}{4k}, \\ \int_0^L \sin^2(ks)\, ds &= \frac{L}{2} - \frac{\sin(2kL)}{4k}. \end{aligned} \tag{III.7.49}$$

For each allowed positive NN, DD, or ND value, the final sine term is zero. Normalized

representatives can therefore be chosen as

$$f_0^{\mathrm{NN}} = \frac{1}{\sqrt{L}}, \qquad f_n^{\mathrm{NN}} = \sqrt{\frac{2}{L}} \cos \frac{n\pi s}{L}, \qquad f_n^{\mathrm{DD}} = \sqrt{\frac{2}{L}} \sin \frac{n\pi s}{L}, \qquad f_n^{\mathrm{ND}} = \sqrt{\frac{2}{L}} \cos \frac{(n+1/2)\pi s}{L}. \tag{III.7.50}$$

The index ranges are those already stated. At $L = 3/2$ the raw constant norm squared is $3/2$, the normalized constant is $\sqrt{2/3}$, and the positive-mode normalization factor is $2/\sqrt{3}$. A local derivative condition does not supply any of these normalization factors.

Now change the actual domain to $0 \le s < \infty$, retaining the flat measure and N at the origin. At zero eigenvalue the solution is again $A + Bs$, and N again sets $B = 0$. The remaining constant is not square integrable unless it vanishes:

$$\|A\|^2_{[0,L]} = |A|^2 L < \infty, \qquad \|A\|^2_{[0,\infty)} = \lim_{S\to\infty} |A|^2 S = \infty \quad (A \neq 0). \tag{III.7.51}$$

There is no right endpoint condition on the half-line to impose at a finite L. The global test has changed to the behavior at infinity. Nor does taking $L \to \infty$ preserve a fixed normalized constant: $L^{-1/2}$ tends to zero at each fixed s, while its integral norm over the growing interval remains one. This sequence does not produce a nonzero square-integrable constant on the half-line.

A useful worked reasoning route for the written exercise starts with $f = 1$. First evaluate $f'(0) = 0$, a local statement. Next put the same function on a finite interval with N at its other end; it solves the zero-eigenvalue problem and has norm squared L. Then put it on the half-line; it still solves the same local equation and left condition, but its norm diverges. Finally ask what establishes the D5 or NS5 identification in the first place. That requires the sourced half-BPS brane and field dictionary, including its scalar triples and other fields. None of the three scalar computations supplies it. This route uses an explicit function to separate four different statements. The physical dictionary enters only in the final step.

The common misconception is that a Neumann endpoint automatically yields a dynamical massless field. The missing questions are the other endpoint, the domain measure, and the actual coupled and gauge-reduced field content. IX.1 uses endpoint filtering to identify candidate fields on finite segments. The scalar results here explain that first filter. They do not determine an interacting boundary-SCFT spectrum, fluctuations about the Nahm pole, or all supersymmetric brane boundary conditions.

III.7.7 Exercises

The first five exercises have bounded numerical submissions. Write the intermediate derivation as well; the submitted numbers test only the specified consequences. The final exercise is a written explanation. The public question file specifies exact rational strings and Boolean fields for the numerical submissions.

1. **E1. Surface signs.** For $S = -\kappa \int (\partial\phi)^2/2$ on $0 \le s \le L$, take $\kappa = 3/2$ and no boundary action. Find the coefficients multiplying $\phi'(0)\delta\phi(0)$ and $\phi'(L)\delta\phi(L)$ in

the spatial surface variation. Derive both outward normals and state the allowed D or N data. Submit the two coefficients.

2. **E2. A radial density.** In the static abelian D3 model set $\mathbf{q} = \mathbf{u} = c\widehat{\mathbf{r}}/r^2$, with $c = 3/4$ and $r = 2$. Starting from the general nonparallel Hamiltonian, obtain the positive-branch energy square. Find q_r and $(\mathcal{H} - \tau_3)/\tau_3$ at that point. Find the same excess for the uncharged flat brane. Submit these three quantities.

3. **E3. Flux and units.** Assume the sourced F1 endpoint identification. Let $n = 2$, $\lambda = 5/2$, and let the regulated spike segment have physical length $\Delta X = 7/3$. Show how $n = \int_{S^2} \mathbf{D} \cdot d\mathbf{S}$ enters the shell integral. Submit the F1 tension, the positive excess energy, the oriented flux after reversing F1 orientation, and the positive energy after reversal. Distinguish a simultaneous reversal of flux and spike side from a reversal at fixed scalar profile.

4. **E4. A finite pole.** Use $D_s X_i - i\epsilon_{ijk}[X_j, X_k]/2 = 0$, $\epsilon_{123} = +1$, $J_i = \sigma_i/2$, and $X_i = aJ_i/s$ in $A_s = 0$ gauge. Find the coefficient of $i\sigma_3$ in $[J_1, J_2]$ and the coefficient of J_i/s^2 in the residual for $a = 1$ and $a = 2$. Verify all cyclic components and submit the three coefficients. Explain why the failed $a = 2$ substitution tests the normalization as well as the sign.

5. **E5. Modes and norms.** Solve $-f'' = k^2 f$ on a flat interval of length $L = 3/2$ with NN, DD, and ND conditions. Here ND means N at $s = 0$ and D at $s = L$. Solve $k = 0$ separately. Submit the first allowed k/π for each case. Also submit whether a nonzero constant NN profile has finite norm on this interval and on a half-line with flat measure. Show the endpoint equations and the two integrals.

6. **E6. Written interpretation.** Explain why a local Neumann condition, a finite-interval zero mode, noncompact normalizability, and a half-BPS fivebrane boundary dictionary are four distinct statements. Use one explicit profile. State which physical premise supplies the brane identification. Follow the reasoning route of testing the local derivative, solving on the specified domain, integrating the kinetic norm, and then identifying the source of the physical dictionary. This exercise is written and is not machine-certified.

Take-home message

An endpoint first specifies a variational problem. Its electric flux and the brane's transverse slope can then balance in the abelian DBI energy. On a regulated radial shell the excess energy equals the supplied F1 charge magnitude times its tension and transverse length. A matrix pole specifies different local endpoint data, while a finite-interval mode requires two endpoint conditions and a finite norm. A reader should now be able to derive the two surface signs, reconstruct the DBI Hamiltonian and its real branch, calculate the shell energy with nonunit λ, verify the spin-half pole in the stated frame, and distinguish a finite scalar zero mode from a locally allowed half-line profile.

Status and sources

The calculation uses the stated metric, tension, axis and trace conventions. The body uses the cited physical premises and displays the conditional calculations.

Section III.7.2 uses the endpoint definition in Polchinski (1995, physical PDF p. 3, eq. (4)) as a worldsheet premise [WS]. The scalar surface variation is [MATH], derived for a smooth real scalar, $\kappa > 0$, no boundary action, and the two stated outward normals. The gauge-current extension is the corresponding direct variation with the explicitly defined $\delta S_B = \int j\delta A$. The physical half-BPS boundary context is in Gaiotto and Witten (2009, physical PDF pp. 10–12, eqs. (2.13)–(2.15)); that context is not derived from the scalar variation.

Section III.7.3 uses the derivative-truncated static abelian DBI premise of Chapter 3 and Callan and Maldacena (1998, physical PDF p. 6, eqs. (3.2)–(3.4)). The electric-field calculation is mathematical [MATH] and conditional on that action, flat background, one physical-length scalar, and zero magnetic field. The displayed determinant, inverse Legendre map, nonparallel example and two squares establish only this conditional algebra. The domain is $\Delta > 0$; $|\mathbf{e}| < 1$ is not its general definition.

Section III.7.4 follows the harmonic branch and nonlinear energy in Callan and Maldacena (1998, physical PDF pp. 6–7, eqs. (3.5)–(3.7)). The source-free radial solution and finite shell integral are [MATH] within the stated action, with $0 < \delta < R$ and the endpoint excluded. The charge and string-mass input is Callan and Maldacena (1998, physical PDF pp. 3–4, eqs. (2.5)–(2.6)). The conversion of its $\alpha' = 1$ connection gives $D_{\text{book}} = 2\pi\Pi_{\text{CM}}$ in those units; physical units restore $\lambda = 2\pi\alpha'$. One conditional mathematical consequence [MATH] is, $\Delta E = |n|\Delta X/\lambda$. Its integral F1 charge and protected/BPS physical interpretation are separate inputs. The paragraph after the source's eq. (3.7), physical PDF p. 7, explicitly leaves its full Born–Infeld supersymmetry-variation check undone. No such proof or core completion is supplied here.

Section III.7.5 uses Gaiotto and Witten (2009, physical PDF pp. 25–26, eqs. (2.40)–(2.43)) and the source's post-section-2.3 frame in Gaiotto and Witten (2009, physical PDF pp. 28–29, section 2.5.1 and Figure 1). The orientation convention translates the anti-Hermitian source fields by $\mathcal{X}_i = -iX_i$ and fixes the inward s and ordered book 789. The rank-two local substitution on $s > 0$ and the coordinate conversion with determinant $+1$ are conditional calculations [MATH]. The half-BPS D3/D5/NS5 assignment and D5-pole identification are separate physical inputs. The general homomorphism and Nahm-moduli construction is cited source material, not a theorem proved in this chapter.

Section III.7.6 derives the spectral results [MATH] for the flat free scalar operator on the stated finite interval or half-line. Its zero-mode, positivity and norm conclusions use those actual domains. The brane motivation retains the separate physical premise in the source's section 2.5.1 and Figure 1. No complete gauge/fermion spectrum, interacting boundary-SCFT spectrum, or fluctuation spectrum of the singular pole is inferred. Exercises E1–E5 consume these bounded calculations; E6 is written interpretation. Finite numerical controls do not establish completeness. In particular the independently derived shell-additivity relation checks boundary dependence beyond the fixed charge examples. The physical boundary inputs remain conditional.

References

Callan Jr., C. G. and J. M. Maldacena (1998). “Brane Dynamics From the Born-Infeld Action”. In: *Nucl. Phys. B* 513. Source edition: arXiv v3, physical PDF pages 2–4 and 6–7, pp. 198–212. DOI: 10.1016/S0550-3213(97)00700-1. arXiv: hep-th/9708147.

Gaiotto, D. and E. Witten (2009). “Supersymmetric Boundary Conditions in N=4 Super Yang-Mills Theory”. In: *J. Statist. Phys.* 135. Source edition: arXiv v2, physical PDF pages 8–12, 24–26 and 28–29, pp. 789–855. DOI: 10.1007/s10955-009-9687-3. arXiv: 0804.2902 [hep-th].

Polchinski, J. (1995). “Dirichlet-Branes and Ramond-Ramond Charges”. In: *Phys. Rev. Lett.* 75. Source edition: arXiv v3, physical PDF page 3, pp. 4724–4727. DOI: 10.1103/PhysRevLett.75.4724. arXiv: hep-th/9510017.

Chapter III.8

T-duality on D-branes: the brane dictionary

III.8.1 An endpoint loses a direction

An open string can carry momentum around a circle even though it has no conserved winding number there. Its endpoints can move, allowing a loop of string to unwind. When the circle becomes small, nonzero momentum costs a large energy. The light open-string states then seem to lose a spatial direction. Closed strings in the same theory have the circle duality of Chapter II.3, so their description still includes that direction. Where has the open string gone?

The endpoints supply the answer. In the dual coordinate they sit at fixed positions, while the interior still vibrates. A direction available to the bulk string has become transverse to its endpoint brane. A gauge holonomy around the original circle determines the dual brane's position. This is why a Wilson line, which changes the masses of charged fields without producing a local field strength, can turn into an actual separation between branes.

This chapter derives that dictionary on a free open strip. We keep a physical spacelike circle, its orientation and its radius visible through the calculation. We then compare absolute energies, follow two separately labelled transverse dualities, and ask which parts of that reasoning can be used for a circle fiber that degenerates. The last question separates three useful constructions: the flat D3/D5 boundary map, the curved NS5 of a brane tiling, and the isometric approximation to a localized five-brane background.

We use the endpoint conditions of Chapter 1, the tension normalization of Chapter 3, and the circle units of Chapter II.3. After this chapter, the reader can exchange complete NN and DD modes and obtain positions and vector masses from holonomy. The same conventions allow wrapped-energy and gauge-coupling comparisons. They also allow a labelled two-circle brane table to be completed and reversed. The final test is to identify the isometry and global conditions of a proposed five-brane duality. A correct dimension count does not construct a curved background.

III.8.2 Boundary conditions and oscillators

How can the endpoints become fixed without freezing the string? The answer requires both worldsheet derivatives. Use Lorentzian strip coordinates τ, σ, with $0 \le \sigma \le \pi$. A dot and a prime denote ∂_τ and ∂_σ. The target coordinate X has length units and period $2\pi R$; α' has length squared. On a flat circle with vanishing B field the free equation is

$$(\partial_\tau^2 - \partial_\sigma^2)X = 0, \qquad X \sim X + 2\pi R. \tag{III.8.1}$$

The local solution splits into left and right movers. We choose the positive dual coordinate of Chapter II.3:

$$X = X_L(\tau+\sigma) + X_R(\tau-\sigma), \qquad \widetilde{X} = X_L(\tau+\sigma) - X_R(\tau-\sigma). \tag{III.8.2}$$

If the derivatives of the two one-variable functions are X_L' and X_R', then $\dot{X} = X_L' + X_R'$ and $X' = X_L' - X_R'$. Applying the same chain rule to the difference gives the operative identities

$$\dot{\widetilde{X}} = X', \qquad \widetilde{X}' = \dot{X}. \tag{III.8.3}$$

There is no minus sign in the first identity with these Lorentzian strip and positive-coordinate conventions. The difference also solves the wave equation, so the map changes the boundary data while preserving free bulk propagation.

At each endpoint, Neumann means that the normal derivative vanishes. Dirichlet means that the coordinate is fixed in time, although the two endpoint values can be different. Equation (III.8.3) gives

$$X'|_{0,\pi} = 0 \implies \dot{\widetilde{X}}|_{0,\pi} = 0, \qquad \dot{X}|_{0,\pi} = 0 \implies \widetilde{X}'|_{0,\pi} = 0. \tag{III.8.4}$$

Thus NN becomes DD and DD becomes NN. Here DD describes a pair of fixed endpoint values, not an instruction to set the entire coordinate to zero. Figure III.8.1 distinguishes the worldsheet strip from the physical target circle.

First follow the zero mode. In the absence of a holonomy, single-valued NN states have momentum $k = n/R$, $n \in \mathbb{Z}$. The strip normalization fixes its coefficient and its dual:

$$X_0 = x + 2\alpha' \frac{n}{R}\tau, \qquad \widetilde{X}_0 = \widetilde{x} + 2\alpha' \frac{n}{R}\sigma. \tag{III.8.5}$$

The original constant velocity becomes a constant slope. Integrating that slope over the actual strip width gives

$$\widetilde{X}(\pi) - \widetilde{X}(0) = \frac{2\pi\alpha' n}{R} = 2\pi n \widetilde{R}, \qquad \widetilde{R} = \frac{\alpha'}{R}. \tag{III.8.6}$$

The endpoints agree on the dual circle and differ on its covering line. The integer n is now the image of one fixed endpoint relative to the other. It was a momentum number, not a topological winding number of the unconstrained original NN string. Using the closed-string spatial period 2π in this integration would insert an erroneous factor of two.

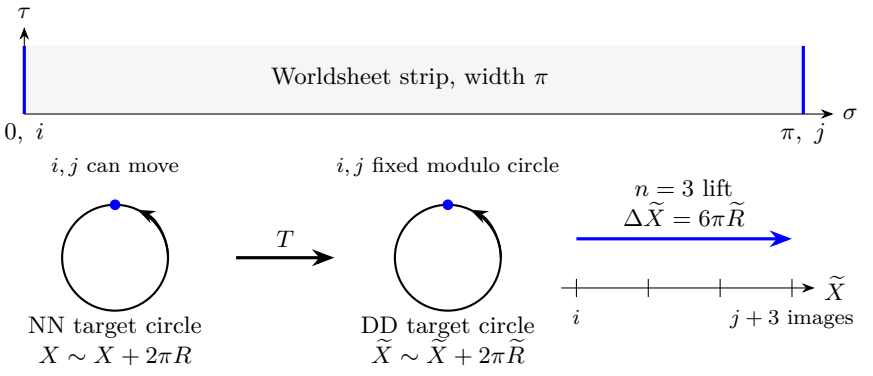


Figure III.8.1: The same oriented string, with endpoint i at $\sigma = 0$ and j at $\sigma = \pi$. The upper panel is the worldsheet strip; its width is π, independently of the target radius. The lower panels show positive target circles before and after duality. Without a Wilson line, the two fixed dual endpoints coincide modulo $2\pi\widetilde{R}$. The covering-line arrow depicts the $n = 3$ zero mode, whose lifted endpoint difference is three dual circumferences. Oscillations of the interior do not move those endpoints.

The oscillator map is equally necessary. For a real NN solution the complete nonzero-frequency part can be written with independent real coefficients A_m, B_m of length dimension:

$$X = x + 2\alpha' k\tau + \sum_{m=1}^{\infty} \cos(m\sigma)[A_m \cos(m\tau) + B_m \sin(m\tau)]. \tag{III.8.7}$$

The cosine in σ enforces Neumann at both boundaries because m is integral. Integrate $\widetilde{X}' = \dot{X}$ term by term for a smooth solution, or first for a finite mode sum. The integration constant is fixed by $\dot{\widetilde{X}} = X'$ up to a constant position. The result is

$$\widetilde{X} = \widetilde{x} + 2\alpha' k\sigma + \sum_{m=1}^{\infty} \sin(m\sigma)[-A_m \sin(m\tau) + B_m \cos(m\tau)]. \tag{III.8.8}$$

Both independent temporal phases matter. Keeping only the A_m term would illustrate one phase of each mode but would not give the full real solution. For one frequency, differentiating the two expressions yields

$$X'_m = -m \sin(m\sigma)[A_m \cos(m\tau) + B_m \sin(m\tau)] = \dot{\widetilde{X}}_m, \tag{III.8.9}$$

$$\dot{X}_m = m \cos(m\sigma)[-A_m \sin(m\tau) + B_m \cos(m\tau)] = \widetilde{X}'_m. \tag{III.8.10}$$

The sine oscillators vanish at 0 and π, so only the affine slope contributes to the endpoint difference. At $\sigma = \pi/2$, an odd-m oscillator can be nonzero. This gives a direct counterexample to the idea that fixed endpoints imply a motionless string.

For completeness, start instead with DD values y_i and $y_j + 2\pi wR$ on a covering line. Define the oriented difference $d = y_j - y_i + 2\pi wR$. A general real free solution with

those endpoint values is

$$X = y_i + \frac{d}{\pi}\sigma + \sum_{m=1}^{\infty} \sin(m\sigma)[C_m \cos(m\tau) + D_m \sin(m\tau)]. \tag{III.8.11}$$

The same derivative identities now integrate to an NN coordinate:

$$\widetilde{X} = \widetilde{x} + \frac{d}{\pi}\tau + \sum_{m=1}^{\infty} \cos(m\sigma)[C_m \sin(m\tau) - D_m \cos(m\tau)]. \tag{III.8.12}$$

For example, differentiating one term of the last cosine sum gives

$$\widetilde{X}'_m = m \sin(m\sigma)[-C_m \sin(m\tau) + D_m \cos(m\tau)] = \dot{X}_m. \tag{III.8.13}$$

This is precisely the time derivative of the previous sine mode. The new endpoint normal derivative vanishes, including the zero mode. Its momentum is

$$\widetilde{k} = \frac{d}{2\pi\alpha'}. \tag{III.8.14}$$

When the original endpoints coincide modulo $2\pi R$, $d = 2\pi w R$ and $\widetilde{k} = w/\widetilde{R}$. For distinct endpoints the shifted momentum will be explained by a Wilson line in the inverse description. This is the full zero-mode and oscillator inverse, not just a reversal of the endpoint name.

Consider the nonunit example $\alpha' = 7/3$, $R = 5/2$, $n = 3$, with all lengths expressed in one chosen unit. Direct substitution gives

$$k = \frac{6}{5}, \qquad 2\alpha' k = \frac{28}{5}, \qquad \widetilde{R} = \frac{14}{15}, \qquad \frac{\Delta\widetilde{X}}{2\pi} = \frac{14}{5}. \tag{III.8.15}$$

Indeed $(14/5)/(14/15) = 3$. An additional NN mode $A\cos\sigma\cos\tau + B\cos\sigma\sin\tau$ becomes $-A\sin\sigma\sin\tau + B\sin\sigma\cos\tau$ and leaves these numbers unchanged. Conversely, choosing DD separation $d = \pi R$ with $w = 0$ gives $\widetilde{k} = R/(2\alpha') = 15/28$, halfway between two unshifted momentum levels. The inverse description therefore needs a nontrivial relative holonomy rather than an integer momentum assertion.

A Dp spans p spatial Neumann directions. Dualizing a tangent circle removes one; dualizing a transverse circle adds one:

$$T_{\parallel} : Dp \longrightarrow D(p-1), \qquad T_{\perp} : Dp \longrightarrow D(p+1). \tag{III.8.16}$$

This boundary calculation is bosonic. For type-II strings the associated reflection of the right-moving fermion reverses one spacetime chirality. That separate worldsheet input exchanges IIA and IIB; the allowed even IIA and odd IIB D-branes are consistent with the dimension rule. A scalar wave equation alone does not establish the GSO projection or the Ramond–Ramond charge of the endpoint brane. Chapter 9 will use the supersymmetry information that is not contained in this scalar map. The next section uses the zero-mode slope to make the endpoint position measurable.

III.8.3 Wilson lines become positions

Where is a dual brane if the original field strength is zero? A flat connection can still have holonomy around a circle. A charged open string measures that holonomy, and its shifted momentum determines a displaced endpoint after duality. The question is global even in a locally free background.

Use a constant Hermitian matrix connection a_X on a flat wrapped $U(N)$ stack, with no other separation or flux. It is the connection for integer endpoint charges. Diagonalize its holonomy, and define real fractions u_i modulo integers by

$$\begin{aligned} a_X &= \frac{1}{R}\,\mathrm{diag}(u_1,\dots,u_N), \\ U &= \exp\left(i\int_0^{2\pi R} a_X\,dX\right) = \mathrm{diag}(e^{2\pi i u_1},\dots,e^{2\pi i u_N}). \end{aligned} \tag{III.8.17}$$

This a_X is a matrix connection, not a coefficient along a half-normalized central generator. Let $E_{ij} = |i\rangle\langle j|$ be the Chan–Paton matrix of a string whose endpoint at $\sigma = 0$ is i and whose endpoint at $\sigma = \pi$ is j. Choose the Fourier factor $e^{inX/R}$ and the covariant derivative

$$D_X = \partial_X - i[a_X,\,\cdot\,], \qquad [a_X, E_{ij}] = \frac{u_i - u_j}{R}E_{ij}. \tag{III.8.18}$$

Applying this operator, rather than guessing an endpoint sign, gives

$$D_X\left(e^{inX/R}E_{ij}\right) = i\frac{n - u_i + u_j}{R}e^{inX/R}E_{ij}, \qquad k_{ij,n} = \frac{n - u_i + u_j}{R}. \tag{III.8.19}$$

The Fourier label n is an integer, while the covariant momentum k need not be an integer multiple of $1/R$. A gauge transformation that removes a_X locally transfers the same information to a twisted periodicity of the charged field. Removing a local connection therefore does not remove its observable phase around the full circle.

The position convention consistent with the positive dual coordinate is

$$Y_i = 2\pi\alpha'(a_X)_{ii} = 2\pi\widetilde{R}u_i, \qquad Y_i \sim Y_i + 2\pi\widetilde{R}, \qquad \widetilde{R} = \frac{\alpha'}{R}. \tag{III.8.20}$$

A common additive position is free. Once an origin and a lift are chosen, the string from i to the nth image of j has the oriented displacement

$$\Delta Y_{ij,n} = Y_j - Y_i + 2\pi n\widetilde{R} = 2\pi\widetilde{R}(n - u_i + u_j) = 2\pi\alpha' k_{ij,n}. \tag{III.8.21}$$

This follows from the same strip integration as (III.8.6). It also fixes which ordering of the two eigenvalues belongs to E_{ij}. The actual length and its classical stretching energy are positive quantities:

$$\ell_{ij,n} = |\Delta Y_{ij,n}|, \qquad T_{\mathrm{F1}} = \frac{1}{2\pi\alpha'}, \qquad T_{\mathrm{F1}}\ell_{ij,n} = |k_{ij,n}|. \tag{III.8.22}$$

Calling the signed ΔY a length would lose the distinction between orientation and mass. For a chosen image the straight segment on the covering line has that length;

the shortest string between the two circle positions requires an additional minimization over images.

The superstring mass formula is a further physical input. In the NS sector write $N_{\rm NS}$ for the oscillator level and $a_{\rm NS}$ for the intercept that is subtracted. With all other separations and momenta suppressed, the mass measured in the common noncompact worldvolume directions is

$$M_{ij,n}^2 = k_{ij,n}^2 + \frac{N_{\rm NS} - a_{\rm NS}}{\alpha'}, \qquad a_{\rm NS} = \frac{1}{2}. \tag{III.8.23}$$

The vacuum energy is $-1/2$. It is not the subtractive intercept. The GSO projection removes the NS ground state, and the first surviving vector has $N_{\rm NS} = 1/2$. Thus the oscillator contribution cancels:

$$M_{\rm vector,ij,n}^2 = \left(\frac{n - u_i + u_j}{R}\right)^2 = \left(\frac{\ell_{ij,n}}{2\pi\alpha'}\right)^2. \tag{III.8.24}$$

The agreement is an equality of the free vector masses under the stated spectrum and tension inputs. It does not ensure that a state with large ℓ lies within a low-energy Yang–Mills truncation. That truncation also requires energies well below the massive string levels, whose spacing is set by $1/\sqrt{\alpha'}$.

Now take $\alpha' = 7/3$, $R = 5/2$, $(u_1, u_2) = (1/6, 2/3)$, and fix E_{12} with $n = 1$. First find the radius and ordered positions:

$$\widetilde{R} = \frac{7/3}{5/2} = \frac{14}{15}, \qquad \frac{Y_1}{2\pi} = \frac{14}{15}\frac{1}{6} = \frac{7}{45}, \qquad \frac{Y_2}{2\pi} = \frac{14}{15}\frac{2}{3} = \frac{28}{45}. \tag{III.8.25}$$

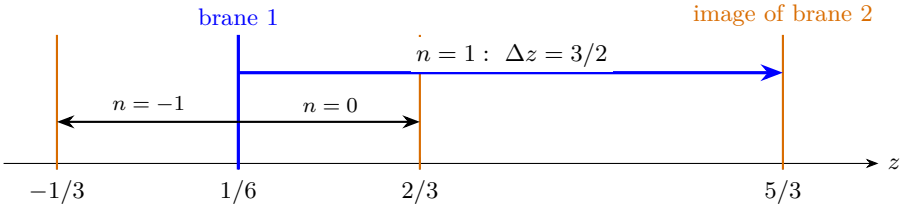
The commutator and Fourier derivative combine to give

$$Rk_{12,1} = 1 - \frac{1}{6} + \frac{2}{3} = \frac{3}{2}, \qquad k_{12,1} = \frac{3/2}{5/2} = \frac{3}{5}. \tag{III.8.26}$$

The endpoint computation reaches the same answer with its image shown:

$$\frac{\Delta Y_{12,1}}{2\pi} = \frac{28}{45} - \frac{7}{45} + \frac{14}{15} = \frac{7}{5}, \qquad \ell_{12,1} = \frac{14\pi}{5}. \tag{III.8.27}$$

Multiplying by the F1 tension gives $\ell/(2\pi\alpha') = 3/5$ and hence $M^2 = 9/25$. Figure III.8.2 shows why this particular state goes beyond the closest image. The image label specifies which string has been calculated. Selecting the lightest state is a further step.



$z = Y/(2\pi\widetilde{R})$, positive to the right
$\widetilde{R} = 14/15, \quad \ell_{n=1} = 14\pi/5, \quad \ell_{\min} = 14\pi/15$

Figure III.8.2: The E_{12} string on a covering line in the dimensionless coordinate $z = Y/(2\pi\widetilde{R})$. Brane 1 is at $1/6$; images of brane 2 are at $-1/3, 2/3, 5/3$. The long upper arrow is the specified $n = 1$ string. The two lower arrows are the equally short $n = -1, 0$ strings. Positive orientation is rightward. For $\widetilde{R} = 14/15$ the physical positions obey $(Y_1, Y_2)/(2\pi) = (7/45, 28/45)$. Moving brane 1 to its next image by a large gauge transformation requires relabelling the upper string $n' = 2$.

For arbitrary relative fraction $\delta = u_j - u_i$, the shortest-image vector obeys

$$M^2_{\min} = \frac{1}{R^2} \min_{n\in\mathbb{Z}} (n+\delta)^2, \qquad \ell_{\min} = 2\pi\widetilde{R} \min_{n\in\mathbb{Z}} |n+\delta|. \tag{III.8.28}$$

In the example $\delta = 1/2$, the two minimizing integers are $n = 0, -1$. They give opposite oriented displacements and the same mass:

$$k_{12,0} = \frac{1}{5}, \quad k_{12,-1} = -\frac{1}{5}, \qquad \ell_{\min} = \frac{14\pi}{15}, \qquad M^2_{\min} = \frac{1}{25}. \tag{III.8.29}$$

The degeneracy is geometric: the endpoints are antipodal, so the two shortest arcs have equal length. It is not gauge enhancement, since neither has zero length. At coincidence modulo the circle, instead, $\delta \in \mathbb{Z}$ and $n = -\delta$ gives

$$\Delta Y = 0, \qquad k = 0, \qquad M^2_{\text{vector}} = 0. \tag{III.8.30}$$

For the flat $U(2)$ stack the holonomy centralizer is generically $U(1) \times U(1)$ and becomes $U(2)$ at coincidence. The off-diagonal vectors then join the two diagonal vectors. This is a statement about this Chan–Paton system, not a determination of a global gauge group in a compact construction with additional projections or fixed data.

A large gauge transformation shifts u_i by an integer ℓ_i. The holonomy is unchanged, while a chosen lift of the position moves by an integer circumference. Spectrum invariance requires transforming the Fourier label as well:

$$u_i' = u_i + \ell_i, \qquad Y_i' = Y_i + 2\pi\widetilde{R}\ell_i, \qquad n' = n + \ell_i - \ell_j. \tag{III.8.31}$$

Substitution checks both the momentum and the lifted displacement:

$$n' - u_i' + u_j' = n - u_i + u_j, \qquad \Delta Y'_{ij,n'} = \Delta Y_{ij,n}. \tag{III.8.32}$$

For $u_1 \mapsto u_1 + 1$ in the example, $n = 1$ must become $n' = 2$. Then $2 - 7/6 + 2/3 = 3/2$ as before. Keeping $n = 1$ instead gives $1/2$, a different string of the same full spectrum. The gauge invariant object is the set of states with their relabelled images, not a fixed integer label detached from the connection.

Reversing the oriented string gives E_{ji} and $-n$. Its displacement and momentum change sign:

$$k_{ji,-n} = -k_{ij,n}, \qquad \Delta Y_{ji,-n} = -\Delta Y_{ij,n}, \qquad M^2_{ji,-n} = M^2_{ij,n}. \tag{III.8.33}$$

The squared mass alone therefore cannot resolve an inconsistent endpoint order. The covariant derivative in (III.8.19) can. This is also why a common shift of all u_i translates the branes but leaves the adjoint masses unchanged, although the full holonomy can retain a common central phase.

Chapter 6 uses the same positive dual coordinate for a nonzero constant central magnetic field. Its already fixed local chart has tangent $(1, f)$ and normal $(-f, 1)$, where $f = 2\pi\alpha' F_{12}$. For a genuine central $U(n)$ bundle of positive rank on circles of physical radii R_1, R_2, its trace degree m gives the relation

$$m = 2\pi n R_1 R_2 F_{12}, \qquad \tan\phi = f = \frac{m\widetilde{R}_2}{nR_1}, \qquad \widetilde{R}_2 = \frac{\alpha'}{R_2}. \tag{III.8.34}$$

That chart extends the connection-to-position idea to a slope. It does not replace a rank-n bundle by n independent fractional-degree line bundles. The present flat-holonomy derivation neither proves a global magnetized-brane equivalence nor supplies its chiral spectrum. Those questions remain in Chapter 6. We now need a different comparison: if a brane gains or loses a circle, why is its total energy unchanged?

III.8.4 Wrapped brane energies and gauge couplings

Which energy should agree when a brane loses a circle? A wrapped brane loses a worldvolume direction under tangent duality. The two resulting tensions have different dimensions, so comparing their numerical values would not compare the same observable. The appropriate observable is the energy per common spectator spatial volume, including the wrapped circumference once.

Work in a flat, unwarped product, with constant dilaton, vanishing flux, and physical spacelike radius R. Let g_s be the asymptotic string coupling, and τ_p the physical energy per spatial p-volume. The absolute type-II D-brane tension and the circle/dilaton map are inputs:

$$\tau_p(g_s) = \frac{1}{(2\pi)^p \alpha'^{(p+1)/2} g_s}, \qquad \widetilde{R} = \frac{\alpha'}{R}, \qquad \widetilde{g}_s = g_s \frac{\sqrt{\alpha'}}{R}. \tag{III.8.35}$$

Equivalently $\tau_p = \mu_p / g_s$ in the inherited charge units. Since τ_p already contains the inverse coupling, no additional factor g_s^{-1} multiplies its static energy. The dilaton transformation comes from the worldsheet measure; it will not be derived by requiring an energy equality.

For a spatially wrapped Dp, $p \geq 1$, write V_{p-1} for the common spectator volume. Its induced metric is the flat product metric, so the spatial volume integral factors:

$$E = \tau_p \int_{V_{p-1}} d^{p-1}x \int_0^{2\pi R} dX, \qquad \frac{E}{V_{p-1}} = (2\pi R)\tau_p. \tag{III.8.36}$$

The circumference is $2\pi R$, not R and not an angular integral with a dimensionless metric omitted. Evaluating it gives

$$(2\pi R)\tau_p = \frac{R}{(2\pi)^{p-1}\alpha'^{(p+1)/2} g_s}. \tag{III.8.37}$$

In the dual frame the D$(p-1)$ has no wrapped direction in this comparison. Its tension is

$$\tau_{p-1}(\widetilde{g}_s) = \frac{1}{(2\pi)^{p-1}\alpha'^{p/2}(g_s\sqrt{\alpha'}/R)} = \frac{R}{(2\pi)^{p-1}\alpha'^{(p+1)/2} g_s}. \tag{III.8.38}$$

Hence

$$\frac{E}{V_{p-1}} = (2\pi R)\tau_p(g_s) = \tau_{p-1}(\widetilde{g}_s). \tag{III.8.39}$$

The dimensions are length to the power $-p$ on both sides. This is an algebraic consistency check of two physical inputs, the absolute tension and the measure map. An unknown common tension normalization would cancel from a ratio check, so the equality alone could not determine the absolute D-brane tension.

The inverse, transverse operation is the same equality in the other direction. A localized D$(p-1)$ gains a circle of radius R; its new Dp coupling is $\widetilde{g}_s\sqrt{\alpha'}/\widetilde{R} = g_s$. Its energy includes $2\pi R$. Both operations require an allowed type-II brane and a physical spatial circle. A D0 has no spatial worldvolume circle to wrap; the formula with a tangent D0 is not a new physical example.

Take the D4 example $\alpha' = 9/4$, $R = 5/3$, $g_s = 2/5$. A tangent duality gives an IIB D3 with

$$\sqrt{\alpha'} = \frac{3}{2}, \qquad \widetilde{R} = \frac{9/4}{5/3} = \frac{27}{20}, \qquad \widetilde{g}_s = \frac{2}{5}\frac{3/2}{5/3} = \frac{9}{25}. \tag{III.8.40}$$

The energy comparison can be made without hiding factors of 2π. Multiplying the common E/V_3 by $(2\pi)^3\alpha'^2$ gives, on the wrapped side,

$$(2\pi)^3\alpha'^2\frac{E}{V_3} = \frac{R}{\sqrt{\alpha'}g_s} = \frac{5/3}{(3/2)(2/5)} = \frac{25}{9}. \tag{III.8.41}$$

On the D3 side the same expression is $1/\widetilde{g}_s = 25/9$. The original D4 tension and the final D3 tension are not equal; their integrated energies are. Changing units rescales both energies with the same dimensions and leaves this normalized comparison intact.

An odd-p example tests a different power of α'. Wrap a type-IIB D3 at the same radius and coupling, giving an IIA D2. Before duality,

$$\frac{E}{V_2} = \frac{R}{(2\pi)^2\alpha'^2 g_s} = \frac{1}{(2\pi)^2}\frac{5/3}{(81/16)(2/5)} = \frac{200}{243(2\pi)^2}. \tag{III.8.42}$$

After duality the absolute D2 tension gives independently

$$\tau_2(9/25) = \frac{1}{(2\pi)^2(9/4)^{3/2}(9/25)} = \frac{200}{243(2\pi)^2}. \tag{III.8.43}$$

The same general derivation works for every allowed wrapped p, rather than depending on the D4 example or setting $\alpha' = 1$. These two numerical cases illustrate the identity; they do not prove its physical inputs for arbitrary curved or fluxed branes.

Energy matching must also be kept separate from gauge-coupling normalization. Put $\lambda = 2\pi\alpha'$. Expanding the flat DBI action to quadratic order in a weak field strength gives, for the fundamental matrix trace,

$$S_{F^2} = -\frac{\tau_p\lambda^2}{4}\int d^{p+1}x\ \mathrm{Tr}_f(F_{\mu\nu}F^{\mu\nu}). \tag{III.8.44}$$

Here the connection entering F is the same integer-charge connection that enters a holonomy. The book uses Hermitian generators with $\mathrm{Tr}_f(T^aT^b) = \delta^{ab}/2$ and the component coupling g_{book}. In this convention

$$-\frac{1}{2g^2_{\mathrm{book}}}\mathrm{Tr}_f\, F^2 = -\frac{1}{4g^2_{\mathrm{book}}}F^a_{\mu\nu}F^{a\mu\nu}, \qquad \frac{1}{2g^2_{\mathrm{book}}} = \frac{\tau_p\lambda^2}{4}. \tag{III.8.45}$$

Matching coefficients therefore determines

$$g^2_{\mathrm{book}} = \frac{2}{\tau_p\lambda^2} = 2(2\pi)^{p-2}g_s\alpha'^{(p-3)/2}. \tag{III.8.46}$$

For an identity $U(1)$ connection of charge one, instead, the action is $-f^2/(4g^2_{U(1)})$. Its coefficient in DBI gives

$$g^2_{U(1)} = \frac{1}{\tau_p\lambda^2} = (2\pi)^{p-2}g_s\alpha'^{(p-3)/2} = \frac{1}{2}g^2_{\mathrm{book}}. \tag{III.8.47}$$

For a single brane the normalized generator is $1/\sqrt{2}$. Writing its matrix connection in that basis changes the component, not the matrix holonomy: $a = A^0/\sqrt{2}$ and $F^0 = \sqrt{2}f$. The component action then has $-f^2/(2g^2_{\mathrm{book}})$, exactly the identity-connection expression above. Inserting $\sqrt{2}$ into $Y_i = \lambda(a_X)_{ii}$ would change the integer-charge phase and spoil the endpoint spectrum.

For the dual D3 in the example, the book coupling is

$$g^2_{D3,\mathrm{book}} = 4\pi\widetilde{g}_s = \frac{36\pi}{25}, \qquad \frac{g^2_{D3,\mathrm{book}}}{4\pi} = \frac{9}{25}, \qquad g^2_{U(1)} = \frac{18\pi}{25}. \tag{III.8.48}$$

The ratio two is a trace normalization, whereas the change from g_s to $\widetilde{g}_s$ is a physical duality transformation. They perform different jobs. Chapter 3 derives the DBI approximation and its regime; here its leading coefficient provides a consistent normalization across circle frames. The next figure follows both wrapped circles and the unchanged stack through the complete D3/D5 example.

III.8.5 Two dualities and a tiling

How does a D3 acquire the two worldvolume directions of a D5 in a brane tiling? Start with N identical D3-branes along 0123 in type IIB, transverse to two flat rectangular circles X^4 and X^6. Keep their physical radii R_4, R_6 labelled even after duality. There is no NS5 in this starting flat product. We hold α' fixed, set $B = 0$, and use a constant asymptotic coupling g_s.

Dualizing X^4 changes a DD direction into NN and exchanges IIB with IIA. The first step is

$$\begin{aligned} D3_{0123} \xrightarrow{T_4} D4_{0123\widetilde{4}}, \qquad & (R_4, R_6) \longmapsto (\widetilde{R}_4, R_6), \\ \widetilde{R}_4 = \frac{\alpha'}{R_4}, \qquad & g_s^{(1)} = g_s \frac{\sqrt{\alpha'}}{R_4}. \end{aligned} \tag{III.8.49}$$

The superscript on g_s labels the duality step. It is not a power. The X^6 circle remains transverse to the D4, so a second transverse duality gives

$$\begin{aligned} D4_{0123\widetilde{4}} \xrightarrow{T_6} D5_{0123\widetilde{4}\widetilde{6}}, \qquad & \widetilde{R}_6 = \frac{\alpha'}{R_6}, \\ g_s^{(2)} = g_s^{(1)} \frac{\sqrt{\alpha'}}{R_6} = g_s \frac{\alpha'}{R_4 R_6}. & \end{aligned} \tag{III.8.50}$$

The final theory is IIB. The number N is unchanged at both steps. Each endpoint stack is being redescribed, not supplemented by a newly created brane. Figure III.8.3 retains the same two labelled circles and illustrates how point support becomes a wrapped cycle and then a wrapped torus.

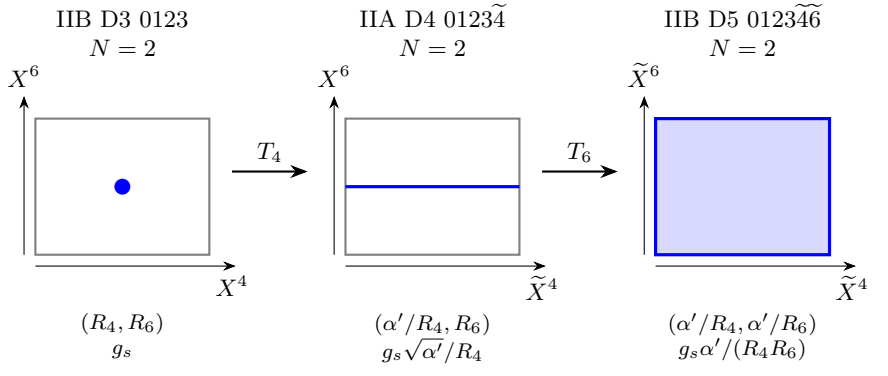


Figure III.8.3: The transverse torus support of the same $N = 2$ stack through T_4 then T_6. The horizontal direction is labelled 4 and the vertical direction 6 in every panel; a tilde denotes the dual physical coordinate. The D3 is a point on the torus, the D4 wraps its horizontal circle, and the D5 wraps both circles. Common 0123 directions are suppressed. Opposite sides of each square are identified. The support of the two coincident branes is drawn once and its multiplicity is stated explicitly. There is no NS5 in any panel.

Let V_3 be the original spatial volume along 123. Define E_a/V_3 for the three frames, including every newly wrapped circumference. The three directly computed expressions are

$$\frac{E_0}{V_3} = N\tau_3(g_s) = \frac{N}{(2\pi)^3\alpha'^2 g_s}, \tag{III.8.51}$$

$$\frac{E_1}{V_3} = N(2\pi\widetilde{R}_4)\tau_4(g_s^{(1)}) = \frac{N\widetilde{R}_4}{(2\pi)^3\alpha'^{5/2} g_s^{(1)}}, \tag{III.8.52}$$

$$\frac{E_2}{V_3} = N(2\pi\widetilde{R}_4)(2\pi\widetilde{R}_6)\tau_5(g_s^{(2)}) = \frac{N\widetilde{R}_4\widetilde{R}_6}{(2\pi)^3\alpha'^3 g_s^{(2)}}. \tag{III.8.53}$$

The wrapped volumes are essential. Substitute the first-step radius and coupling into the middle expression:

$$\frac{\widetilde{R}_4}{\alpha'^{5/2} g_s^{(1)}} = \frac{\alpha'/R_4}{\alpha'^{5/2} g_s\sqrt{\alpha'}/R_4} = \frac{1}{\alpha'^2 g_s}. \tag{III.8.54}$$

For the D5 the separate two-circle cancellation is

$$\frac{\widetilde{R}_4\widetilde{R}_6}{\alpha'^3 g_s^{(2)}} = \frac{\alpha'^2/(R_4R_6)}{\alpha'^3 g_s\alpha'/(R_4R_6)} = \frac{1}{\alpha'^2 g_s}. \tag{III.8.55}$$

Consequently $E_0 = E_1 = E_2$ per the same spectator volume. This is the transverse version of the wrapped-energy relation, applied twice with labels retained. It checks the coupling map at both steps and would fail if one left the second coupling unchanged.

For a concrete table choose $\alpha' = 9/4$, $R_4 = 5/3$, $R_6 = 7/2$, $g_s = 2/5$ and $N = 2$. The newly created radii and couplings are

$$\widetilde{R}_4 = \frac{27}{20}, \qquad \widetilde{R}_6 = \frac{9}{14}, \qquad g_s^{(1)} = \frac{9}{25}, \qquad g_s^{(2)} = \frac{9}{25}\frac{3/2}{7/2} = \frac{27}{175}. \tag{III.8.56}$$

It is useful to normalize by the initial brane multiplicity:

$$\mathcal{E}_a = \frac{(2\pi)^3\alpha'^2 E_a}{NV_3}, \qquad \mathcal{E}_0 = \frac{1}{g_s}, \quad \mathcal{E}_1 = \frac{\widetilde{R}_4}{\sqrt{\alpha'}\, g_s^{(1)}}, \quad \mathcal{E}_2 = \frac{\widetilde{R}_4\widetilde{R}_6}{\alpha' g_s^{(2)}}. \tag{III.8.57}$$

The two wrapped rows evaluate to

$$\mathcal{E}_1 = \frac{27/20}{(3/2)(9/25)} = \frac{5}{2}, \qquad \mathcal{E}_2 = \frac{(27/20)(9/14)}{(9/4)(27/175)} = \frac{5}{2}. \tag{III.8.58}$$

Table III.8.1 collects all three frames.

Frame and brane	Worldvolume	Labelled radii $(4,6)$	Coupling	$\mathcal{E}$
IIB D3	0123	$(5/3, 7/2)$	2/5	5/2
IIA D4	$0123\widetilde{4}$	$(27/20, 7/2)$	9/25	5/2
IIB D5	$0123\widetilde{4}\widetilde{6}$	$(27/20, 9/14)$	27/175	5/2

Table III.8.1: Two labelled transverse dualities in a flat product, with the same $N = 2$ throughout. Radii are physical lengths in the chosen common unit. The energy uses the entire wrapped dual-circle volume in each frame. The type alternates at each step.

The return path is a useful physical check. Starting from the final D5, dualize the now tangent $\widetilde{X}^6$ circle. Its radius returns to R_6 and the coupling becomes

$$R_6^{\text{back}} = \frac{\alpha'}{\widetilde{R}_6} = \frac{7}{2}, \qquad g_s^{\text{back},1} = \frac{27}{175}\frac{3/2}{9/14} = \frac{9}{25}. \tag{III.8.59}$$

The brane is the IIA D4 along $0123\widetilde{4}$. Dualizing its tangent $\widetilde{X}^4$ circle then gives

$$R_4^{\text{back}} = \frac{\alpha'}{\widetilde{R}_4} = \frac{5}{3}, \qquad g_s^{\text{back},2} = \frac{9}{25}\frac{3/2}{27/20} = \frac{2}{5}. \tag{III.8.60}$$

The result is the original IIB D3 along 0123, with both transverse circles restored. A reversal must recover the axes and coupling as well as the brane dimension. Merely toggling p would miss the content of these checks.

The energy argument does not depend on $N = 2$. At the level of the sum of probe tensions used here, each identical brane contributes the same energy, so

$$\frac{E_a(N)}{V_3} = \frac{N}{(2\pi)^3\alpha'^2 g_s}, \qquad E_a(N+M) = E_a(N)+E_a(M), \qquad \mathcal{E}_a(N) = \frac{1}{g_s}. \tag{III.8.61}$$

For $N = 3$ in the numerical example the energy normalized without dividing by N is 15/2, while the per-brane normalized value remains 5/2. This distinguishes total energy from a normalized value that hides the multiplicity. The finite-stack calculation does not address backreaction, compact tadpole cancellation or an interacting bound-state spectrum.

Now compare this flat result with the toric brane-tiling construction. In that construction the relevant compact directions are also 46, and the D5 spans 012346. An NS5 spans 0123 and a holomorphic curve Σ in the four real directions 4567. After identifying the dual coordinates as those of the construction, the worldvolumes read

$$D5:\ 012346, \qquad NS5:\ 0123 \times \Sigma_{4567}, \qquad X^4, X^6 \text{ compact.} \tag{III.8.62}$$

The curved NS5 and the singular circle-fibration construction are sourced geometric input. They are not additional rows generated by dualizing a featureless flat torus. Figure III.8.4 shows their worldvolume roles separately from Figure III.8.3.

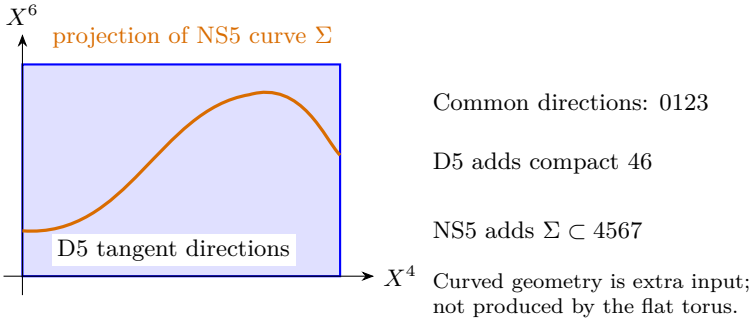


Figure III.8.4: The separately sourced NS5/D5 geometry. The coordinate plane 46 is compact, with positive 4 rightward and positive 6 upward; $5, 7$ are the other two real curve directions. The shaded rectangle identifies the compact D5 tangent directions, with 0123 suppressed. In the actual construction D5 regions are bounded by the NS5 in this plane; the shading does not specify their shapes. The curved line is a schematic projection of $\Sigma \subset 4567$, not an equation for a specific toric curve or a calculated coamoeba. The direction table states the full worldvolumes and makes explicit the extra NS5 absent from the flat two-duality calculation.

This comparison explains the useful part of the dictionary for Chapter VII.4: the D3-to-D5 dimension, axes, radius and coupling data are calculable before discussing a tiling. The source's selected phase uses equal face multiplicities for its D5 regions. Its interacting $SU(N)$ language does not remove the local $U(N)$ Chan–Paton connection used above; the treatment of central modes needs the actual construction. A flat boundary map also does not determine the quiver superpotential or prove a statement about the coamoeba of every holomorphic curve. Chapter II.10 introduces the NS5-curve interface, and the geometry and mirror tools in Volumes IV and V supply the further background.

The circles must keep their identities in applications. X^6 here is a full transverse circle before duality, not a finite interval between two NS5-branes. Nor is it a spacetime X^3 circle used in a different compactification. Reusing the symbol T without stating the circle can turn an energy-preserving dictionary into an unsupported chain. The next section gives a quantitative example of the missing condition: an angular dependence that no isometric field transformation can retain.

III.8.6 Circle fibrations and localization

When is a circle direction available for an elementary geometric T-duality? The flat examples have a continuous shift symmetry of the background fields. A circle fiber can still have that symmetry even when it is globally nontrivial. A localized source, however, can break it. To distinguish these situations we first keep track of the fiber's period and patches, then calculate exactly what circle averaging loses.

For this section only, r_T, g_T are Tong's dimensionless radial coordinate and parameter. They are not a physical radius R or the string coupling g_s. Let ϑ, φ be usual polar

angles on the base $\mathbb{R}^3$, with $0 \le \vartheta \le \pi$ and φ of period 2π. The cited coincident charge-N ALF metric has a fiber coordinate ψ of period 4π:

$$ds^2 = H_N\, d\mathbf{r}_T \cdot d\mathbf{r}_T + \frac{1}{4} H_N^{-1} (d\psi + \omega)^2, \qquad H_N = \frac{1}{g_T^2} + \frac{N}{2r_T}, \qquad \omega = N \cos\vartheta\, d\varphi. \tag{III.8.63}$$

This is a sourced metric on its appropriate punctured-base chart. The period and the factor $1/4$ are part of its geometry. Put $\chi = \psi/2$ and $A = \omega/2$. Then

$$\chi \sim \chi + 2\pi, \qquad ds^2 = H_N\, d\mathbf{r}_T \cdot d\mathbf{r}_T + H_N^{-1} (d\chi + A)^2, \qquad A = \frac{N}{2} \cos\vartheta\, d\varphi. \tag{III.8.64}$$

At large r_T the fiber coefficient tends to g_T^2, so its radius in these source units is g_T. This observation does not identify g_T with g_s, or supply a conversion to an arbitrary physical target-circle radius. In particular, the physical circle formula of the previous sections cannot be used by simply renaming these parameters.

A local mixed metric component does not determine the bundle on the whole sphere. With increasing χ as fiber orientation, choose the usual base orientation $\sin\vartheta\, d\vartheta \wedge d\varphi$. The curvature is

$$F_A = dA = -\frac{N}{2} \sin\vartheta\, d\vartheta \wedge d\varphi. \tag{III.8.65}$$

Its Chern number includes both angular ranges and the fiber's 2π normalization:

$$c_1 = \frac{1}{2\pi} \int_{S^2} F_A = -\frac{N}{4\pi} \int_0^{2\pi} d\varphi \int_0^{\pi} \sin\vartheta\, d\vartheta = -N. \tag{III.8.66}$$

For the concrete choice $N = 3$, this is -3. Reversing the base orientation alone changes the integral to $+3$, with the fiber still oriented by increasing χ. This orientation is separate from an NS5 linking-three-sphere orientation. Equating the two without defining the map would make the charge sign ambiguous.

The polar singularities of A are removed in separate patches. Choose

$$A_N = \frac{N}{2} (\cos\vartheta - 1) d\varphi, \qquad A_S = \frac{N}{2} (\cos\vartheta + 1) d\varphi. \tag{III.8.67}$$

The first is regular at the north pole and the second at the south pole. They have the same curvature and obey

$$A_N - A_S = -N\, d\varphi, \qquad \chi_N = \chi_S + N\varphi, \qquad d\chi_N + A_N = d\chi_S + A_S. \tag{III.8.68}$$

As φ increases by 2π on the overlap, the two fiber coordinates differ by $2\pi N$, an allowed period precisely for integral N. The transition is therefore real global information, not a singular choice of vector potential. Figure III.8.5 fixes the orientation and patch sign used in this computation.

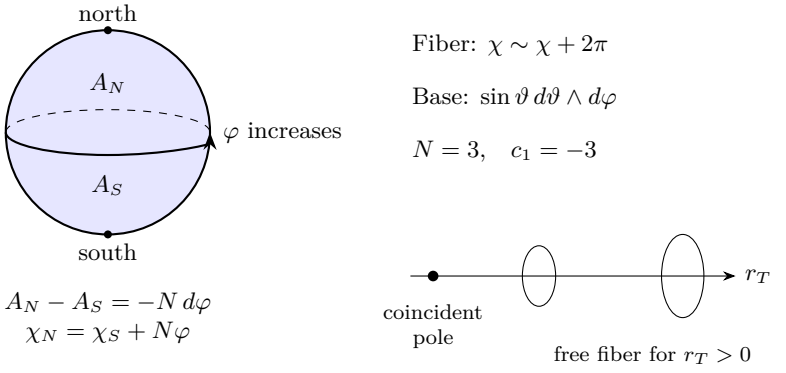


Figure III.8.5: A base sphere at fixed $r_T > 0$ with north and south connection patches. The overlap is parametrized by increasing φ; its transition preserves $d\chi + A$ with χ of period 2π. The base uses the usual polar orientation $\sin\vartheta\,d\vartheta \wedge d\varphi$. Thus $N = 3$ gives $c_1 = -3$, although the fiber-coordinate transition is $+3\varphi$. The inset marks the collapsing fiber at the coincident pole; the sphere-patch calculation alone does not prove a smooth core.

Indeed the free-fiber chart fails at $r_T = 0$. Dropping the constant term in H_N and setting $r_T = \rho^2/(2N)$ gives the leading core metric

$$ds^2 \simeq d\rho^2 + \frac{\rho^2}{4}\left[d\vartheta^2 + \sin^2\vartheta\,d\varphi^2 + \left(d\frac{\psi}{N} + \cos\vartheta\,d\varphi\right)^2\right]. \tag{III.8.69}$$

To see the radial coefficient, use $H_N \simeq N^2/\rho^2$ and $dr_T = (\rho/N)d\rho$; the product $H_N dr_T^2$ is $d\rho^2$. The fiber angle ψ/N has period $4\pi/N$. Thus $N = 1$ has the usual smooth $\mathbb{R}^4$ core, while coincident $N > 1$ gives $\mathbb{C}^2/\mathbb{Z}_N$. The $N = 3$ example above cannot be described as a smooth single-center core. Separated centers require the corresponding multi-center geometry rather than changing the period by hand.

For $N = 1$ the circle isometry in (III.8.63) permits the ordinary Buscher construction. In the classical dual description it produces an NS5 smeared around the dual angle θ, of period 2π, with harmonic function

$$H_0(r_T) = \frac{1}{g_T^2} + \frac{1}{2r_T}. \tag{III.8.70}$$

The isometric NS5/KK field dictionary is the one introduced in Chapter II.10. The localized supergravity solution on $\mathbb{R}^3 \times S^1$ has, for $r_T > 0$, the different function

$$H_{\rm loc}(r_T, \theta) = \frac{1}{g_T^2} + \frac{1}{2r_T}\frac{\sinh r_T}{\cosh r_T - \cos\theta}. \tag{III.8.71}$$

The elementary obstruction is directly calculable:

$$\partial_\theta H_{\rm loc} = -\frac{\sinh r_T \sin\theta}{2r_T(\cosh r_T - \cos\theta)^2}. \tag{III.8.72}$$

For example, at $r_T = 1$, $\theta = \pi/2$ it is $-\sinh(1)/(2\cosh^2(1)) \simeq -0.2468$. The derivative vanishes at $\theta = 0, \pi$, but a stationary value of a function at two angles is not a continuous circle symmetry. The localized field is therefore outside the ordinary isometric Buscher hypothesis. Applying that hypothesis to H_0 remains possible; it supplies information about H_0.

What, exactly, was discarded by replacing $H_{\rm loc}$ with H_0? Set $q = e^{-r_T}$, so $0 < q < 1$, and denote the dimensionless source profile by $K(r_T, \theta) = 2r_T(H_{\rm loc} - g_T^{-2})$. Using $\sinh r_T = (q^{-1} - q)/2$ and $\cosh r_T = (q^{-1} + q)/2$ gives

$$K = \frac{1 - q^2}{1 - 2q\cos\theta + q^2} = \frac{1}{1 - qe^{i\theta}} + \frac{1}{1 - qe^{-i\theta}} - 1. \tag{III.8.73}$$

Expand each denominator as a geometric series. Pairing conjugate terms makes the Fourier content real:

$$K = 1 + \sum_{k=1}^{\infty} q^k (e^{ik\theta} + e^{-ik\theta}) = 1 + 2\sum_{k=1}^{\infty} e^{-kr_T}\cos(k\theta). \tag{III.8.74}$$

This identity includes all harmonics. A finite expansion through q^2 can illustrate the first terms but cannot by itself justify an exact angular average.

The justification is uniform convergence away from the core. On any region $r_T \geq r_0 > 0$, put $q_0 = e^{-r_0} < 1$. Each absolute harmonic is at most $2q_0^k$, whose sum is finite. The uniform tail bound is

$$\sup_{\substack{r_T \geq r_0 \\ \theta \in [0, 2\pi]}} \left| K - 1 - 2\sum_{k=1}^{m} e^{-kr_T}\cos(k\theta) \right| \leq \frac{2q_0^{m+1}}{1 - q_0}. \tag{III.8.75}$$

Consequently the continuous partial sums converge uniformly and can be integrated term by term over the compact angle. Each nonconstant cosine has zero integral, so the full, not truncated, average is

$$\frac{1}{2\pi}\int_0^{2\pi} K\, d\theta = 1, \qquad \frac{1}{2\pi}\int_0^{2\pi} H_{\rm loc}\, d\theta = \frac{1}{g_T^2} + \frac{1}{2r_T} = H_0. \tag{III.8.76}$$

This argument uses the stated positive radial lower bound. It makes no uniform claim on a region containing $r_T = 0$.

The first two discarded terms of H are

$$\delta H_1 = \frac{e^{-r_T}}{r_T}\cos\theta, \qquad \delta H_2 = \frac{e^{-2r_T}}{r_T}\cos(2\theta). \tag{III.8.77}$$

Relative to the smeared pole term $1/(2r_T)$, the leading correction is $2e^{-r_T}\cos\theta$. More quantitatively, keeping m harmonics gives

$$|H_{\rm loc} - H^{(m)}| \leq \frac{e^{-(m+1)r_T}}{r_T(1 - e^{-r_T})}, \quad H^{(m)} = H_0 + \frac{1}{r_T}\sum_{k=1}^{m} e^{-kr_T}\cos(k\theta). \tag{III.8.78}$$

For the zero-mode approximation specifically,

$$\frac{|H_{\rm loc} - H_0|}{1/(2r_T)} = |K - 1| \le \frac{2e^{-r_T}}{1 - e^{-r_T}}. \tag{III.8.79}$$

The denominator of the left side is the sourced pole contribution, not the full H_0. The full relative error additionally depends on g_T and is no greater than this bound for positive g_T^2. Thus $r_T \gg 1$ controls the angular approximation, independently of whether other conditions make supergravity reliable.

Figure III.8.6 plots the exact source profile. At $r_T = 3$, $q \simeq 0.04979$ and the uniform zero-mode relative bound is about 0.1048. Keeping two harmonics reduces the profile error to at most $2e^{-9}/(1 - e^{-3}) \simeq 0.000260$. At $r_T = 1$ the zero-mode bound is about 1.164, so no comparably small uniform angular error is promised. These are bounds from the complete series, not fits at a few angles.

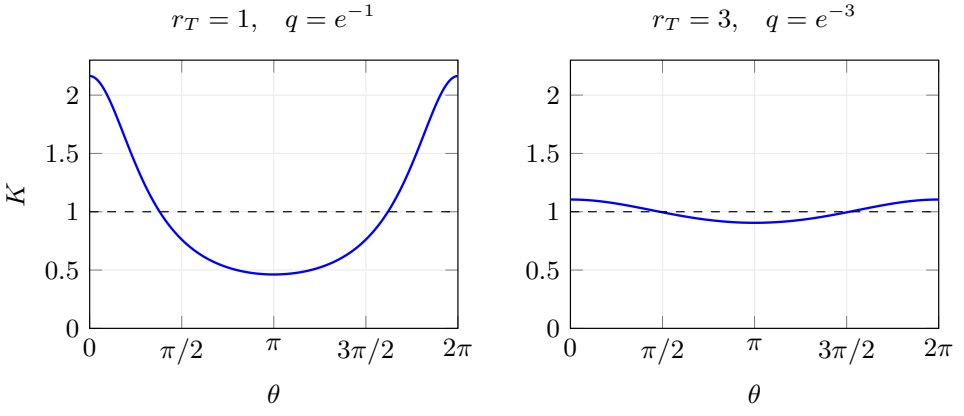


Figure III.8.6: Exact normalized localized profile $K = 2r_T(H_{\rm loc} - g_T^{-2})$ against the dual angle of period 2π, in the source's dimensionless units. Both panels have the same vertical scale and zero-mode average $K_0 = 1$. The blue curves use $r_T = 1$ and $r_T = 3$; the dashed line is the exact angular average, not a fitted constant. The first and second omitted harmonics are respectively $2e^{-r_T}\cos\theta$ and $2e^{-2r_T}\cos 2\theta$. The radial exponential suppresses angular contrast far from the core.

The core exposes the failure without any numerical sampling. At the source angle and at the antipodal angle the exact expressions are

$$K(r_T, 0) = \coth(r_T/2), \qquad K(r_T, \pi) = \tanh(r_T/2). \tag{III.8.80}$$

As $r_T \to 0^+$ these behave as $2/r_T$ and $r_T/2$, respectively. The corresponding source contributions to the harmonic function obey

$$H_{\rm loc}(r_T, 0) - g_T^{-2} \sim \frac{1}{r_T^2}, \qquad H_{\rm loc}(r_T, \pi) - g_T^{-2} \longrightarrow \frac{1}{4}, \qquad H_0 - g_T^{-2} = \frac{1}{2r_T}. \tag{III.8.81}$$

The average diverges, but it describes neither angular behavior near the core. The error bound also grows without limit as $r_T \to 0$. This is why a large-radius Fourier truncation cannot be extended uniformly into the localized source.

Averaging is mathematically noninvertible: adding any multiple of $\cos\theta$ to an integrable profile leaves its average unchanged. Even exact knowledge of H_0 cannot recover the erased Fourier coefficients. Tong's specified two-dimensional $\mathcal{N} = (4, 4)$ gauged linear sigma model supplies an additional worldsheet mechanism. Its vortex instantons, including multiple topological sectors, correct the target metric with angular dependence and account for localization. That is a cited physical result for that model. We have derived the Fourier identity and its approximation bounds here; we have not derived the instanton measure or its all-sector coefficients. A quantum worldsheet mechanism can add information absent from classical isometric Buscher fields, but this is not an arbitrary nonisometric Buscher rule.

Finally, a proposed NS5-to-KK-to-IIA/M chain needs more than a local harmonic function. The elementary T step uses invariant metric and dilaton and compatible B/H patches, with specified circle periods and holonomies. Flux quantization, the fiber transition and any fixed points or degeneration must agree globally. The transition (III.8.68) is an example of such required data. At a localized angle the elementary isometry has already failed; it cannot be restored by renaming the averaged background as the localized one. A toric D3/D5 direction table and this localized-circle problem ask different questions.

The later IIA/M step is restricted to a massless IIA background admitting the specified isometric circle reduction and the corresponding metric frame and global data. In the common physical asymptotic length convention of Chapter II.9 its radius is $R_{10} = g_{s,\mathrm{IIA}}\sqrt{\alpha'}$, with X^{10} of period $2\pi R_{10}$ and angular coordinate of period 2π. Identifying the IIA description with an M-theory completion uses a nonperturbative premise. No arithmetic comparison above proves that premise, and an arbitrary Romans-mass background has no assumed ordinary circle lift. Chapter 10 takes up NS5 worldvolume physics, rather than obtaining it from the dimension count or the Fourier average.

III.8.7 Exercises

Use the physical-radius and positive-dual-coordinate conventions of the chapter. E1–E4 have bounded numerical submissions through the companion; the accompanying derivations and interpretation questions are written work. E5 is entirely written. Rational answer fields are exact strings, such as `"5/7"`; integer fields such as a winding or an axis label are JSON integers. Every bounded submission has top-level fields `task` and `answer`. The public question file gives the full required field types and ordering of arrays.

1. **E1. Momentum becomes an image.** On the open strip $0 \le \sigma \le \pi$, take $\alpha' = 7/3$, $R = 5/2$ and $n = 3$, with no Wilson line. Starting from $X = x + 2\alpha'(n/R)\tau$, determine the dual radius, the coefficients in $\widetilde{X} = \widetilde{x} + c_\tau\tau + c_\sigma\sigma$, the lifted endpoint difference divided by 2π, and the winding. Submit `dual_radius`, `tau_slope`,

`sigma_slope`, `endpoint_difference_over_2pi`, and `winding` in `answer`, with `task` equal to `"E1"`. In written work derive both derivative identities for both temporal oscillator phases, check the endpoint conditions, and give the inverse DD-to-NN zero mode. Explain why the interior need not be fixed.

2. **E2. A holonomy and a selected string.** Take a flat wrapped $U(2)$ stack with $\alpha' = 7/3$, $R = 5/2$, $a_X = \mathrm{diag}(1/6, 2/3)/R$ and $B = 0$. Choose E_{12}, $D_X = \partial_X - i[a_X, \cdot]$, Fourier label $n = 1$, endpoint 1 at $\sigma = 0$ and endpoint 2 at $\sigma = \pi$. Submit `dual_radius`, `positions_over_2pi` as the ordered two-entry array with common origin zero, `kinetic_momentum`, `separation_over_2pi`, and `mass_squared` of the first GSO-surviving NS vector. Use `task` equal to `"E2"`. In written work obtain the sign from the commutator, distinguish signed displacement from length, and show how $u_1 \mapsto u_1 + 1$ must relabel n. Determine the shortest images and explain why their degeneracy differs from coincidence enhancement. Those last reasoning tasks are not assessed by the numerical submission.

3. **E3. Wrapped energy and the factor of two.** A single type-IIA D4 spans $0123X$, with $R = 5/3$, $\alpha' = 9/4$, $g_s = 2/5$ and no flux. Dualize X. Submit `dual_radius`, `dual_gs`, `normalized_energy` defined as $(2\pi)^3\alpha'^2 E/V_3$, and `book_gym_squared_over_4pi` for the resulting IIB D3; use `task` equal to `"E3"`. Start from the absolute τ_p in (III.8.35). In written work carry out the general-p wrapped integral and the trace matching. Explain why the identity-abelian coupling is different while the connection holonomy and dual positions are unchanged. Repeat the absolute energy comparison for a wrapped IIB D3 to test an odd-p case.

4. **E4. Keep the circles labelled.** Start with $N = 2$ IIB D3-branes along 0123, transverse to a rectangular torus with $(R_4, R_6) = (5/3, 7/2)$, $\alpha' = 9/4$, $g_s = 2/5$, and $B = 0$. Apply T_4 then T_6. Submit `task` equal to `"E4"` and `answer` containing a `steps` array with three rows: initial, after T_4, after T_6. Each row has `p`, `type`, `worldvolume`, `count`, `gs`, `radii`, and `normalized_energy`. The worldvolume lists all integer coordinate labels including 0; retain labels 4 and 6 for the dual coordinates. The radii array is always ordered $(4, 6)$. Energy is $(2\pi)^3\alpha'^2 E/(NV_3)$ with all wrapped dual volumes included. In written work reverse T_6 then T_4, prove the energy identity for general positive N, and explain why this table neither produces the curved NS5 nor proves a general toric coamoeba statement.

5. **E5. What an average cannot recover.** Use the sourced H_{loc} in (III.8.71) for $r_T > 0$. Derive its isometry test, its first two nonconstant Fourier harmonics, and its exact circle average. Justify exchanging sum and integral on $r_T \geq r_0 > 0$, give an error bound, and explain the angular contrast at the core. For a proposed NS5-to-KK-to-IIA/M chain, identify the isometric T step, the missing patch/flux/fixed-point data, and the nonperturbative M-lift premise. Explain how Tong's specific instanton mechanism differs from an arbitrary nonisometric duality, and why the flat toric brane-dimension count cannot discharge this localization question. Specify a massless isometric IIA reduction whenever discussing the M step. This task is assessed by written reasoning.

III.8.8 Take-home message

Take-home message

Circle duality exchanges the endpoint derivatives as well as the bulk coordinate. An NN momentum becomes a DD image, and an integer-charge holonomy becomes a brane position. With endpoint order fixed, the same covariant momentum gives the signed separation and the positive vector mass. The wrapped energy agrees only after including the actual circle volume and the dilaton shift; the book's trace factor is a separate normalization. Two labelled transverse dualities explain the flat D3/D4/D5 map. A curved NS5 needs additional geometry. For a localized five-brane, the exact Fourier average is the smeared profile, but the lost angular modes and global fiber data cannot be reconstructed from that average. The IIA/M identification adds its own nonperturbative premise.

Status and sources

§III.8.1–III.8.2. The open-circle boundary map follows Johnson (2000, physical PDF pp. 61–62, eqs. (161)–(164)), using the exact arXiv:hep-th/0007170v3 edition. The derivative identities, real oscillator exchange and lifted zero-mode difference are derived here for a free strip [MATH]; their physical circle-duality use is the local isometric worldsheet dictionary [WS]. The tangent/transverse brane identification and separate type-II chirality input follow that source's physical pp. 66–67 and 104–105, Section 5.6 [WS]. The type-II parity and RR-consistency statement is also sourced in Polchinski (1995, physical PDF pp. 3–4, eqs. (4)–(7)), arXiv:hep-th/9510017v3 [WS]. The scalar calculation does not derive a GSO or RR-charge theorem. The calculation uses the metric, tension, strip and physical circle conventions stated above.

§III.8.3. The Wilson-line and position inputs are in Johnson (2000, physical PDF pp. 62–67, eqs. (165)–(175)) [WS]. Given these inputs, the commutator sign, large-gauge relabelling, nearest-image masses and flat $U(2)$ centralizers are conditional algebra [MATH]. The first GSO-surviving NS vector is sourced on physical pp. 87–88, eqs. (231)–(234) [WS]. We use vacuum energy $-1/2$ and subtractive intercept $+1/2$: the nearby source prose uses a negative a while (233) subtracts it. Equation (171) prints $\theta_j - \theta_i$, whereas (174) prints $\theta_i - \theta_j$. The fixed E_{ij} convention and explicit covariant derivative determine the orientation here; reversing both endpoints and image reverses the displacement while preserving its square. No source erratum is assumed. The original Figure 17 correctly has primed radii; only its text extraction loses the primes. The connection uses the integer-charge normalization inherited from Chapters 3 and 4. The magnetic-slope comparison uses the restricted rectangular central-field chart of Chapter 6; no new compact magnetic equivalence is inferred.

§III.8.4. The measure/dilaton shift is sourced in Johnson (2000, physical PDF p. 54, eq. (139)) [WS]. The tension recursion and absolute physical tension use physical pp. 71 and 109, eqs. (182)–(183), (274)–(275) of the same exact edition [WS]. Their input is separate from the displayed energy and trace-normalization checks [MATH].

The quadratic action and the book half-trace translation use the tension and trace conventions of Chapter 3. Johnson's (276) has a final equality without g_s; its preceding τ_p expression and (275) retain it, as does the chapter. No new normalization ratification is made. The general-p identity, D4 and odd-p D3 examples are conditional checks, not a derivation of the dilaton measure or an extension to arbitrary flux or curvature.

§III.8.5. The flat D3/D4/D5 boundary and chirality map uses the local worldsheet dictionary [WS] for the stated labelled axes. Given that map and the tension input, the radius/coupling entries and general-N energy additivity are conditional calculations [MATH]. The separately cited toric NS5/D5 construction is Franco et al. (2006, physical PDF pp. 8–10, introduction end and Section 2), arXiv:hep-th/0504110v2 [GEO-E]. It has compact 46, D5 along 012346, and NS5 along $0123 \times \Sigma_{4567}$. The curved NS5, selected face multiplicities and interacting-sector interpretation are source input, not outputs of the flat energy table. No coamoeba theorem, quiver dynamics or new QFT-transfer claim is established. The downstream pointer is VII.4; II.3 forward-route consistency remains a whole-volume integration check.

§III.8.6. The ALF metric, ψ period 4π, factor $1/4$, and coincident charge-N pole follow Tong (2002, physical PDF p. 20, eqs. (A.32)–(A.34)), arXiv:hep-th/0204186v3 [SUGRA]. The $\chi = \psi/2$ conversion, patch transition and signed c_1 are derived here with the stated sphere orientation [MATH], reusing Volume II, Chapter 10. The elementary isometric NS5/KK map uses the source's physical pp. 2–3, eqs. (1.1)–(1.3), in the same isometric domain [WS]. Its localized profile, eq. (1.4), is sourced supergravity input [SUGRA]. The angular derivative, uniformly convergent Poisson series, exact average, error bound and core angular contrast are derived for $r_T > 0$ [MATH]. The multi-instanton GLSM localization mechanism is cited from the same exact source, physical pp. 1–3 [WS]; no all-sector instanton calculation is supplied here. Ordinary Buscher requires the declared isometry and compatible global and measure data. The physical-radius and massless IIA/M discussion uses the units of Volume II, Chapter 9 and is conditional on the nonperturbative IIA/M lift. A finite radius or tension match does not establish that premise. No arbitrary nonisometric map or massive-IIA circle lift is assumed.

§III.8.7–III.8.8. E1–E4 assess bounded submitted circle, position, mass, coupling and energy values. The oscillator arguments, shortest-image interpretation, general-p and general-N reasoning, reverse route and NS5 limits also have written components. E5 is written only. The chapter derives its free-mode, finite-matrix and convergent-series statements under explicit hypotheses; it cites rather than proves the superstring spectrum, absolute tension, curved toric construction, GLSM instanton mechanism and nonperturbative IIA/M identification. No full QFT equivalence is inferred from these local dictionaries.

References

Franco, S. et al. (2006). "Brane dimers and quiver gauge theories". In: *JHEP* 01, p. 096. DOI: 10.1088/1126-6708/2006/01/096. arXiv: hep-th/0504110.

Johnson, C. V. (July 2000). “D-brane primer”. In: *Theoretical Advanced Study Institute in Elementary Particle Physics (TASI 99): Strings, Branes, and Gravity*. Exact source edition: arXiv v3, pp. 129–350. DOI: 10.1142/9789812799630_0002. arXiv: hep-th/0007170.

Polchinski, J. (1995). “Dirichlet Branes and Ramond-Ramond charges”. In: *Phys. Rev. Lett.* 75. Exact source edition: arXiv v3, pp. 4724–4727. DOI: 10.1103/PhysRevLett.75.4724. arXiv: hep-th/9510017.

Tong, D. (2002). “NS5-branes, T duality and world sheet instantons”. In: *JHEP* 07. Exact source edition: arXiv v3, p. 013. DOI: 10.1088/1126-6708/2002/07/013. arXiv: hep-th/0204186.

Chapter III.9

Kappa symmetry and supersymmetric branes

III.9.1 A supersymmetric brane is a compatible object

A D2-brane stretched along two spatial axes is an extended object in a supersymmetric spacetime. The spacetime may have thirty-two supersymmetries, but the chosen brane preserves only those that leave its configuration unchanged. Adding a second brane asks a compatibility question: can the same supersymmetry preserve both objects? Their individual fractions do not answer it. Two branes can impose the same condition, impose independent compatible conditions, or impose inconsistent conditions.

The missing link between an embedding and a condition on supersymmetry is kappa symmetry. The brane action contains fermionic superspace coordinates with a local redundancy. A spacetime supersymmetry can move those coordinates and still preserve the brane if a local kappa transformation compensates the movement. This mechanism turns the geometric question into an eigenspace problem. The eigenspace must be taken inside the actual space of background Killing spinors. A projector cannot manufacture a supersymmetric background.

We develop the calculation on a single abelian D2 probe in flat massless type IIA spacetime, first without a gauge field and then with constant magnetic flux. The magnetic example is useful because its flux also couples to the D0 potential. It shows why a brane carrying two kinds of charge need not impose two independent projections. A short membrane calculation then separates a cited superspace action from the algebraic consequences of its projector. Finally, a sheared tangent plane makes the relation to calibration explicit.

The required background is the real type-II spinor space from Volume II, Chapter 4 and the DBI/WZ action from Chapter 3. Chapter 5 supplies the global charge questions; Chapters 6 and 8 give the separate flux-angle and T-duality dictionaries. The calibration geometry belongs to Volume IV, Chapter 6. Here we derive selected Clifford, determinant

and norm identities. The local invariance of the full superspace actions and the global calibrated-cycle theorem are cited physical and mathematical inputs, respectively.

III.9.2 A local fermionic redundancy

Why can a bosonic brane preserve a spacetime supersymmetry that shifts its fermionic coordinate? The answer requires keeping a gauge transformation separate from a physical change. Let σ^a, $a = 0, 1, 2$, be D2 worldvolume coordinates and let its superspace embedding be

$$Z^M(\sigma) = (X^\mu(\sigma), \theta^\alpha(\sigma)), \qquad \mu = 0, \ldots, 9, \quad \alpha = 1, \ldots, 32. \tag{III.9.1}$$

The X^μ are bosonic coordinates. The real Grassmann coordinate θ is a spacetime Majorana spinor and a worldvolume scalar. In flat superspace the invariant vector pullback and induced metric have the form

$$\Pi_a^\mu = \partial_a X^\mu - \bar{\theta}\Gamma^\mu \partial_a \theta, \qquad G_{ab} = \eta_{\mu\nu}\Pi_a^\mu \Pi_b^\nu, \qquad \bar{\theta} = \theta^T C_{\text{charge}}. \tag{III.9.2}$$

We use mostly-plus signature and upper-index spacetime gamma matrices. C_{charge} denotes charge conjugation. It will never denote an RR potential or the local three-gamma matrix introduced below.

The superspace DBI and WZ terms work together. In the source normalization with the overall constants suppressed, their flat-space structure is

$$S_{\text{super}} = -\int d^3\sigma \sqrt{-\det(G + \mathcal{F})} + \int \Omega_3, \qquad \mathcal{F} = dV - b. \tag{III.9.3}$$

Here b is the pulled-back superspace NS two-form and Ω_3 is the superspace WZ form. The source connection V absorbs the flux units. For our bosonic example, $dV = \lambda F$ with $\lambda = 2\pi\alpha'$ and $B_{\text{NS}} = 0$. The book combination $P[B_{\text{NS}}] + \lambda F$ then agrees with the source combination. Setting the bosonic NS two-form to zero does not set b to zero as a superspace form. Its fermionic components participate in local invariance.

The full local invariance of this action is a sourced premise. It uses on-shell superspace torsion, NS and RR constraints. It is stronger than the statement that a matrix squares to one. The latter only identifies a candidate half-rank transformation. The cancellation of the DBI and WZ variations is an additional physical statement. We use the D2 case for which the cited construction supplies that statement, and do not attempt a full superspace proof.

In a native column-spinor convention the transformation at a bosonic configuration takes the form

$$\delta\theta = (1 + K)\kappa + \epsilon, \qquad K^2 = 1, \qquad \theta = 0. \tag{III.9.4}$$

The parameter ϵ is a background supersymmetry parameter and $\kappa(\sigma)$ is local. In flat spacetime the background Killing spinors are constant. In a curved background ϵ must already satisfy the background Killing-spinor equations and their global conditions. The brane test acts on that solution space.

To preserve the bosonic configuration we require $\delta\theta = 0$. Multiplication by $1 - K$ removes the kappa term:

$$0 = (1 - K)\delta\theta = (1 - K)(1 + K)\kappa + (1 - K)\epsilon = (1 - K)\epsilon. \tag{III.9.5}$$

Conversely, when $K\epsilon = \epsilon$, the choice

$$\kappa = -\frac{\epsilon}{2}, \qquad (1 + K)\kappa + \epsilon = -\frac{\epsilon + K\epsilon}{2} + \epsilon = 0 \tag{III.9.6}$$

supplies a compensator. One may add a kappa parameter in $\ker(1 + K)$ without changing the transformation. Thus compensation and the positive eigenspace condition are equivalent within this sourced transformation law. This is the origin of the familiar brane projection.

A source can state the same mechanism with a row spinor and a differently signed operator. The Aganagic–Popescu–Schwarz formula restricts the row variation by $\delta\bar{\theta}(1 + \gamma_{\mathrm{APS}}) = 0$. An unrestricted row parameter $\bar{\zeta}$ therefore gives

$$\delta\bar{\theta} = \bar{\zeta}(1 - \gamma_{\mathrm{APS}}), \qquad \gamma_{\mathrm{APS}}^2 = 1. \tag{III.9.7}$$

Transposing this equation and using the Majorana conjugation rule gives

$$\delta\theta = (1 + K)\zeta, \qquad K = -C_{\mathrm{charge}}^{-1}\gamma_{\mathrm{APS}}^{T}C_{\mathrm{charge}}. \tag{III.9.8}$$

The sign belongs to this row-to-column conversion. The positive barred projector in the Bergshoeff–Townsend transformation has its own operator; it is not a reason to replace γ_{APS} by that operator. Section III.9.5 will perform the conversion with a magnetic field and keep its relative sign.

For a concrete example choose $X^0 = \sigma^0$, $X^1 = \sigma^1$, $X^2 = \sigma^2$, with other coordinates constant, and choose the ordered orientation $d\sigma^0 \wedge d\sigma^1 \wedge d\sigma^2 > 0$. The induced lower time gamma is $\gamma_0 = -\Gamma^0$. At zero flux the source row operator is $-\Gamma^0\Gamma^1\Gamma^2$. The rank-three Majorana transpose sign is positive, so the column operator is

$$A = \Gamma^{012} = \Gamma^0\Gamma^1\Gamma^2, \qquad \gamma_{\mathrm{APS}} = -A, \qquad K = A. \tag{III.9.9}$$

For any A-positive background spinor, substituting $\kappa = -\epsilon/2$ into (III.9.4) cancels the variation. For an A-negative spinor the residual projection $(1 - A)\epsilon = 2\epsilon$ cannot vanish. This example identifies which half is preserved before counting it.

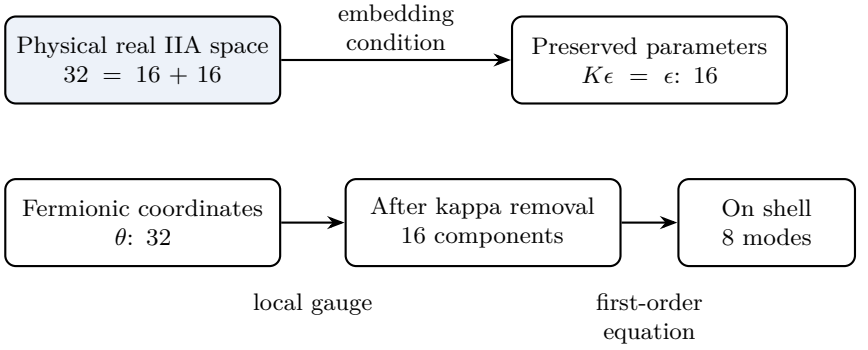


Figure III.9.1: Three distinct counts for the flat D2. The upper branch tests background supersymmetry parameters against an embedding. The lower branch removes a local redundancy from fermionic fields and then uses their first-order equations. The two occurrences of sixteen count different objects. The diagram assumes the physical real IIA space, not an unrestricted doubled spinor space.

Figure III.9.1 also prevents a common misreading of kappa symmetry. Removing sixteen redundant fermionic field components and preserving sixteen spacetime supercharges are different operations. For the flat D2, the seven transverse scalars and the one propagating abelian vector mode give eight bosonic on-shell modes. The fermionic count runs from thirty-two components to sixteen after local gauge removal, and to eight on shell. The first-order equation is responsible for the last reduction. Chapter 3's bosonic DBI action does not prove this fermionic structure; the superspace action supplies the premise. We next count the background eigenspace without confusing it with those field components.

III.9.3 The real spinor space

Half of which space survives a D2 projection? In type IIA the parameter has two real Majorana–Weyl components of opposite chirality. With the chirality operator and space written explicitly,

$$\chi = \Gamma^0\Gamma^1\cdots\Gamma^9, \qquad \chi^2 = 1, \qquad S = S_+ \oplus S_-, \qquad \dim_{\mathbb{R}} S_+ = \dim_{\mathbb{R}} S_- = 16. \tag{III.9.10}$$

Thus $\dim_{\mathbb{R}} S = 32$. These are real counts. Neither replacing S by one fixed chiral summand nor treating an unrestricted sixty-four-component doublet as physical is the IIA calculation. The physical type-II distinction was established in Volume II, Chapter 4.

There is no need to print a 32×32 matrix to determine its projection rank. We use a real static representation with $(\Gamma^0)^T = -\Gamma^0$ and $(\Gamma^i)^T = \Gamma^i$ for spatial i. For an ordered product of r distinct mutually orthogonal indices, moving the second copy back

through the first gives

$$(\Gamma^{\mu_1}\cdots\Gamma^{\mu_r})^2 = (-1)^{r(r-1)/2}\prod_{a=1}^{r}\eta^{\mu_a\mu_a}. \tag{III.9.11}$$

For A, there are three exchanges and one negative metric factor. Transposition also reverses the product and introduces one time sign:

$$A^2 = (-1)^3(-1)\,1 = 1, \qquad A^T = -\Gamma^2\Gamma^1\Gamma^0 = A. \tag{III.9.12}$$

The reversal of three different gammas contributes the second minus in the transpose calculation. This is why no additional i belongs in A. Multiplying it by i would instead give square -1 and destroy a real positive/negative eigenspace interpretation.

A useful trace argument is conjugation by an invertible gamma that anticommutes with the blade. For example a spatial direction outside 012 gives

$$\Gamma^3 A(\Gamma^3)^{-1} = -A \quad\Longrightarrow\quad \operatorname{tr} A = -\operatorname{tr} A = 0. \tag{III.9.13}$$

Since $A^2 = 1$, its minimal polynomial divides $(x-1)(x+1)$, whose roots are distinct over the reals. There are no Jordan blocks. If n_+ and n_- are the multiplicities, the dimension and trace equations are

$$n_+ + n_- = 32, \qquad n_+ - n_- = 0, \qquad n_+ = n_- = 16. \tag{III.9.14}$$

The actual projection matrices and their ranks follow:

$$P_A = \frac{1+A}{2}, \qquad P_{-A} = \frac{1-A}{2}, \qquad P_A^2 = P_A, \qquad \operatorname{rank} P_A = \operatorname{tr} P_A = 16. \tag{III.9.15}$$

The equality between rank and trace holds because the matrix is an idempotent. That condition will matter for intersecting branes.

Chirality does not provide another harmless label on this positive space. Each individual ten-dimensional gamma anticommutes with χ; an odd product therefore does as well:

$$A\chi = -\chi A, \qquad A : S_+ \longrightarrow S_-, \qquad A : S_- \longrightarrow S_+. \tag{III.9.16}$$

Suppose both $A\epsilon = \epsilon$ and $\chi\epsilon = \epsilon$ held. Applying their product in two orders would give

$$A\chi\epsilon = \epsilon, \qquad A\chi\epsilon = -\chi A\epsilon = -\epsilon, \qquad \epsilon = 0. \tag{III.9.17}$$

This vanishing is not an absence of IIA supersymmetry. It says that a preserved spinor cannot lie entirely in one of the two summands.

One can exhibit all sixteen preserved components without choosing a matrix basis. Choose any $\xi \in S_+$ and form

$$\epsilon = \xi + A\xi, \qquad A\epsilon = A\xi + \xi = \epsilon, \qquad \frac{1+\chi}{2}\epsilon = \xi. \tag{III.9.18}$$

The last equation makes this map injective. Conversely the positive chiral part of any A-positive ϵ determines its negative part as $A\xi$. Thus the positive eigenspace is the

graph of an isomorphism between two real sixteen-component spaces. For a unit ξ the two summands are orthogonal in the static component norm; dividing $\xi + A\xi$ by $\sqrt{2}$ gives a unit preserved spinor. This is a complete worked description of the real eigenspace, rather than a count inferred from a formal fraction.

An eleven-dimensional algebraic extension will be useful for the membrane. Define $\widehat{\Gamma}^{\mu} = \Gamma^{\mu}$ for $\mu = 0, \ldots, 9$ and $\widehat{\Gamma}^{10} = \chi$. The inherited relations imply

$$\begin{gathered} \{\widehat{\Gamma}^{10}, \widehat{\Gamma}^{\mu}\} = 0, \qquad (\widehat{\Gamma}^{10})^2 = 1, \\ \{\widehat{\Gamma}^{\hat{\mu}}, \widehat{\Gamma}^{\hat{\nu}}\} = 2\eta^{\hat{\mu}\hat{\nu}} 1. \end{gathered} \tag{III.9.19}$$

No extra spinor components have been added. The planar triple $\widehat{\Gamma}^{012}$ is the same A, so its positive space again has real dimension sixteen. The physical membrane interpretation requires the action premise in Section III.9.7; the algebra alone is not an IIA/M-theory duality argument. The practical lesson for later brane constructions is to specify the physical spinor space before counting eigenvectors. Figure III.9.1 should be read with precisely that space at its starting point.

III.9.4 Compatible intersections

When does a second half-projection halve the first one's solutions? Keep the first brane along 012 and introduce local matrix names

$$A = \Gamma^{012}, \qquad B = \Gamma^{034}, \qquad C = \Gamma^{013}. \tag{III.9.20}$$

Here B is a matrix, distinct from B_{NS}, and C is a matrix, distinct from both C_q and C_{charge}. Each ordered triple is a real symmetric traceless involution. Time 0 is common to all the static branes. Spatial common directions must be read separately, as in Figure III.9.2.

Start with the branes along 012 and 034. Moving the second Γ^0 through two spatial factors and then using $(\Gamma^0)^2 = -1$ gives

$$AB = -\Gamma^1\Gamma^2\Gamma^3\Gamma^4 = BA, \qquad (AB)^2 = 1. \tag{III.9.21}$$

The four-spatial-gamma blade has zero trace. For instance conjugating it by Γ^1 changes its sign, because three other spatial factors must be crossed. Therefore all three traces needed for the intersection calculation vanish:

$$\operatorname{tr} A = \operatorname{tr} B = \operatorname{tr}(AB) = 0. \tag{III.9.22}$$

The product of the two positive projectors is an idempotent because they commute. Its image is exactly the common positive eigenspace:

$$Q = P_A P_B = \frac{1 + A + B + AB}{4}, \qquad Q^2 = Q, \qquad AQ = BQ = Q. \tag{III.9.23}$$

If a vector is already positive under both operators, Q fixes it; this proves the reverse inclusion of images. Taking a trace now counts the intersection:

$$\dim_{\mathbb{R}}(S_{A+} \cap S_{B+}) = \frac{32 + \operatorname{tr} A + \operatorname{tr} B + \operatorname{tr} AB}{4} = 8. \tag{III.9.24}$$

In particular, zero trace of the product is a hypothesis used in the last step, not a consequence of the statement that the two branes differ.

For comparison, the 012 and 013 branes share the spatial 1 axis. The sign calculation is short enough to do in full:

$$AC = -\Gamma^1\Gamma^2\Gamma^1\Gamma^3 = +\Gamma^2\Gamma^3, \qquad CA = \Gamma^3\Gamma^2 = -\Gamma^2\Gamma^3. \tag{III.9.25}$$

Thus $\{A, C\} = 0$. A common positive vector would satisfy both $AC\epsilon = \epsilon$ and $CA\epsilon = \epsilon$, whereas the operators are negatives of one another. It follows that

$$S_{A+} \cap S_{C+} = \{0\}. \tag{III.9.26}$$

Sharing a spatial axis is not a sufficient compatibility criterion. The Clifford signs, including the time direction, do the work.

Multiplying two projector matrices without checking compatibility gives a particularly instructive wrong answer. Let $Q' = P_A P_C$. From $P_A C P_A = 0$, one obtains

$$P_A P_C P_A = \frac{1}{2} P_A, \qquad (Q')^2 = \frac{1}{2} Q' \neq Q'. \tag{III.9.27}$$

The image of Q' lies inside S_{A+}. On that subspace, the preceding formula shows that its restriction is one half of the identity, so it already reaches every vector of S_{A+}. Consequently

$$\operatorname{rank}(P_A P_C) = 16, \qquad \dim(S_{A+} \cap S_{C+}) = 0. \tag{III.9.28}$$

The rank sixteen is not a supersymmetry count. The product maps vectors without being the projection onto their simultaneous solutions.

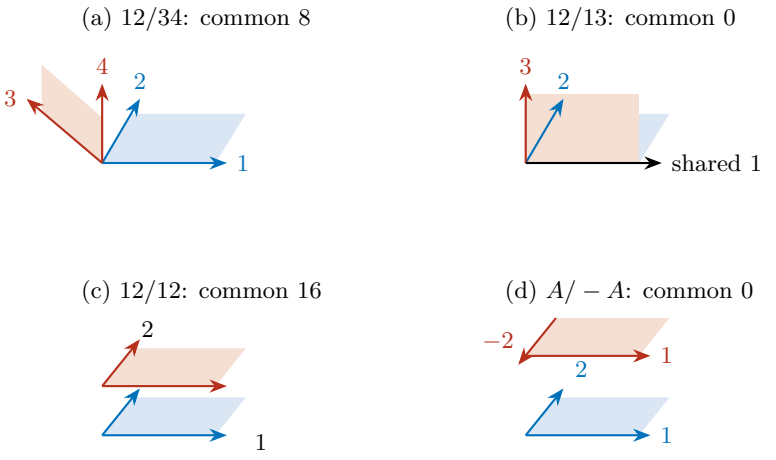


Figure III.9.2: Four local flat probe comparisons, with the first oriented D2 always along spatial 12 and time 0 suppressed. The second plane is 34, 13, 12, or the same 12 plane with reversed orientation. A pair of arrows specifies each ordered spatial plane. The last two panels use a small separation only to make the two copies legible. Numbers are dimensions of common real spinors, not intersection-state multiplicities.

Dependence supplies the other two cases in Figure III.9.2. A repeated brane imposes A a second time. Reversing its orientation instead imposes $-A$. Both pairs commute, but their product traces differ:

$$\operatorname{tr}(AA) = 32, \quad P_A P_A = P_A; \qquad \operatorname{tr}(A(-A)) = -32, \quad P_A P_{-A} = 0. \tag{III.9.29}$$

Putting these values into the general trace formula gives sixteen and zero, respectively. Opposite projectors are unequal commuting operators whose product is not traceless. Thus inequality of the matrices does not justify a universal quarter-supersymmetry rule.

There is also a direct method that works for every pair above. Stack the two linear conditions instead of guessing a product projector:

$$\dim\{\epsilon : K_1\epsilon = K_2\epsilon = \epsilon\} = 32 - \operatorname{rank}\begin{pmatrix} K_1 - 1 \\ K_2 - 1 \end{pmatrix}. \tag{III.9.30}$$

For the four pairs (A, B), (A, C), (A, A) and $(A, -A)$, the stacked ranks are $24, 32, 16, 32$, giving $8, 0, 16, 0$. The trace and anticommutator derivations explain these numbers before any particular matrix realization is chosen.

The eight common spinors for 012/034 mean one quarter of the flat background supersymmetries obey these two probe conditions. This is a statement about compatible parameters. It does not determine the localized matter spectrum, a backreacted global solution, or whether a particular quantum bound state is populated. The Hanany–Witten configurations in IX use the same method with their own IIB spinor space and

oriented projectors. Their separate source-sign translation is still required. Likewise Chapter 7's boundary equations cannot be justified by counting this D2 pair. The transferable procedure is to identify the physical space, establish the operator relations, and only then count common solutions.

III.9.5 The signed magnetic projector

A magnetic field on the D2 carries a coupling to the D0 potential. Why can the resulting configuration still preserve sixteen supersymmetries? The answer is one rotated projection. Deriving its signed coefficients requires more information than checking that it is an involution. Assume a single flat abelian D2 in massless IIA with constant dilaton, $B_{\mathrm{NS}} = 0$, no electric field and constant real magnetic field in an orthonormal chart. Define

$$f = \lambda F_{12}, \qquad \lambda = 2\pi\alpha', \qquad D = \Gamma^0\chi = -\Gamma^1\Gamma^2\cdots\Gamma^9. \tag{III.9.31}$$

The last equality uses $(\Gamma^0)^2 = -1$. The matrix D is an ordered rank-nine spatial blade with an overall minus sign, even though its first expression contains both a gamma and χ.

We first evaluate the source row formula. In the chosen static chart $\gamma_0 = -\Gamma^0$, $\gamma_1 = \Gamma^1$ and $\gamma_2 = \Gamma^2$. Let $\psi = \gamma_a d\sigma^a$ and identify the source Γ_{11} with χ through the chiral labels. The Aganagic–Popescu–Schwarz three-form is

$$\rho_3 = \frac{\psi^3}{3!} + \mathcal{F}\,\chi\psi, \qquad \mathcal{F} = f\,d\sigma^1\wedge d\sigma^2. \tag{III.9.32}$$

Wedge multiplication antisymmetrizes the three distinct gammas. Its 3! permutations cancel the displayed 3!. The first coefficient is $\gamma_0\gamma_1\gamma_2 = -A$. For the magnetic term, $d\sigma^1\wedge d\sigma^2\wedge d\sigma^0$ has the positive 012 orientation. Since $\chi\gamma_0 = -\chi\Gamma^0 = \Gamma^0\chi = D$, the coefficient of the full source volume form is

$$\rho_{\mathrm{row}} = -A + fD, \qquad \gamma_{\mathrm{APS}} = \frac{-A + fD}{\sqrt{1+f^2}}. \tag{III.9.33}$$

The square root is positive. The determinant giving it will be evaluated independently in Section III.9.6.

To convert this row operator, start with the Majorana rule $C_{\mathrm{charge}}\Gamma^\mu C_{\mathrm{charge}}^{-1} = -(\Gamma^\mu)^T$. For a rank-$r$ antisymmetrized product, the r individual minus signs and the $r(r-1)/2$ reversal exchanges combine into

$$C_{\mathrm{charge}}^{-1}(\Gamma^{[r]})^T C_{\mathrm{charge}} = (-1)^{r(r+1)/2}\Gamma^{[r]}. \tag{III.9.34}$$

The exponent is 6 for $r = 3$ and 45 for $r = 9$. Thus A is even under this conjugated transpose and D is odd. Substitution into (III.9.8) gives

$$K(f) = -C_{\mathrm{charge}}^{-1}\gamma_{\mathrm{APS}}^T C_{\mathrm{charge}} = \frac{A + fD}{\sqrt{1+f^2}}. \tag{III.9.35}$$

At $p = 0$ the source one-form $\rho_1 = \chi\psi$ similarly has row coefficient D and column coefficient D for the selected D0 orientation. This fixes the relative sign used in the D2/D0 example. An involution test alone would accept the wrong replacement $f \mapsto -f$.

Now determine why this is one half-projection. The needed Clifford identities, including the vanishing mixed term, are

$$A^2 = D^2 = 1, \qquad AD = -DA, \qquad (A + fD)^2 = (1 + f^2)1. \tag{III.9.36}$$

For example $AD = -\Gamma^{12}\chi$ while $DA = +\Gamma^{12}\chi$. Both A and D are traceless; the latter trace vanishes by conjugation with Γ^0. Hence $K^2 = 1$ and $\operatorname{tr} K = 0$, giving sixteen positive eigenvalues at every finite real f. Imposing $A\epsilon = \epsilon$ and $D\epsilon = \epsilon$ separately would instead give no nonzero solution because they anticommute. Dissolved charge changes the operator; it does not append that second independent constraint.

The rotation is useful both for interpreting the result and for checking its branch. Let

$$\tan\beta = f, \qquad -\frac{\pi}{2} < \beta < \frac{\pi}{2}, \qquad \cos\beta = \frac{1}{\sqrt{1+f^2}}, \quad \sin\beta = \frac{f}{\sqrt{1+f^2}}. \tag{III.9.37}$$

The condition $\cos\beta > 0$ fixes the oriented finite-field branch. For $J = DA$, the same algebra gives $J^2 = -1$, $JA = D$ and $AJ = -D$. Define

$$R = \cos\frac{\beta}{2} + J\sin\frac{\beta}{2}, \qquad R^{-1} = \cos\frac{\beta}{2} - J\sin\frac{\beta}{2}. \tag{III.9.38}$$

Writing the two half-angle coefficients temporarily as a, b, direct multiplication gives

$$RAR^{-1} = (a^2 - b^2)A + 2abD = \cos\beta\, A + \sin\beta\, D = K(f). \tag{III.9.39}$$

In the multiplication, $JAJ = A$ accounts for the $-b^2A$ term. The half-angle is required because conjugation contains both R and R^{-1}. It is not a guess from the final coefficient circle.

For an explicit positive field take $f = 3/4$. The hypotenuse is $5/4$, so $K = (4A + 3D)/5$. Here $a = 3/\sqrt{10}$ and $b = 1/\sqrt{10}$: $a^2 - b^2 = 4/5$ and $2ab = 3/5$. For $f = -5/12$, the hypotenuse is $13/12$, and the coefficients are instead

$$K(3/4) = \frac{4}{5}A + \frac{3}{5}D, \qquad K(-5/12) = \frac{12}{13}A - \frac{5}{13}D. \tag{III.9.40}$$

In the second case $a = 5/\sqrt{26}$, $b = -1/\sqrt{26}$, which reproduce both coefficients through (III.9.39). The sign of the flux survives the rotation calculation.

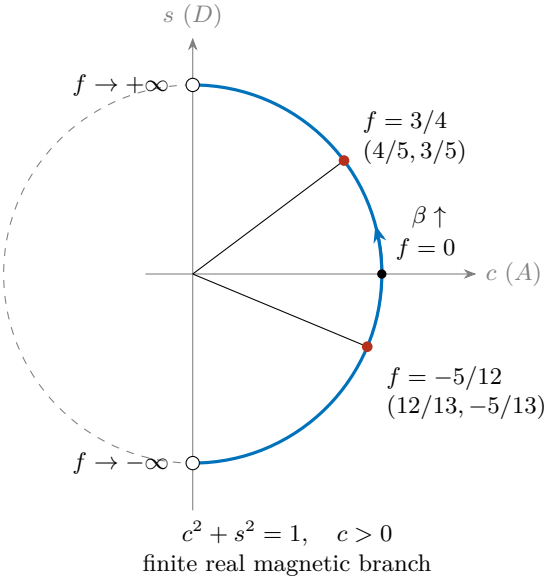


Figure III.9.3: The coefficients $c = \cos\beta$, $s = \sin\beta$ in $K = cA + sD$. Finite real magnetic flux occupies the right semicircle $c > 0$, oriented toward increasing β. The points $(4/5, 3/5)$ and $(12/13, -5/13)$ are the two worked examples. The endpoint D0 directions are limits, not finite-f points. This is a circle of operator coefficients; a geometric brane angle needs its separate T-duality identification.

Figure III.9.3 makes the limiting tests visible:

$$K(0) = A, \qquad \lim_{f\to+\infty} K(f) = D, \qquad \lim_{f\to-\infty} K(f) = -D. \tag{III.9.41}$$

A reversal of the entire brane orientation would send K to $-K$; it is different from changing only f. The endpoints describe normalized charge directions at arbitrarily large flux density. They do not create an isolated finite-energy D0 state from a noncompact D2. Chapters 6 and 8 explain when the coefficient angle is also a geometric angle in a specified dual description. The calculation here requires neither that dictionary nor a general electric-field branch, whose determinant and reality conditions differ.

III.9.6 Local energy and dissolved charge

What do the two signed projector coefficients mean for an energy and a charge measurement? First retain the normalization of the local action. Let $\tau_2 > 0$ be the physical D2 tension, including the asymptotic inverse string coupling once. In an orthonormal static chart the full bosonic DBI matrix is

$$G + \lambda F = \begin{pmatrix} -1 & 0 & 0 \\ 0 & 1 & f \\ 0 & -f & 1 \end{pmatrix}, \qquad \det(G + \lambda F) = -(1 + f^2). \tag{III.9.42}$$

Expansion along the time row reduces the determinant to $-(1+f^2)$, with a plus from the two antisymmetric magnetic entries. There are no electric components, so the static Hamiltonian density is the negative of the Lagrangian density:

$$\mathcal{L}_{\rm DBI} = -\tau_2\sqrt{1+f^2}, \qquad \mathcal{E}_{\rm proper} = \tau_2\sqrt{1+f^2} > 0. \tag{III.9.43}$$

This is energy per physical area measured with proper time. The branch is fixed by positive tension and the positive real square root.

The two rational examples provide a normalization check with no tension set to one. At $\tau_2 = 7/3$ their proper densities are

$$\mathcal{E}_{\rm proper}(3/4) = \frac{7}{3}\frac{5}{4} = \frac{35}{12}, \qquad \mathcal{E}_{\rm proper}(-5/12) = \frac{7}{3}\frac{13}{12} = \frac{91}{36}. \tag{III.9.44}$$

For fixed $|f|$ the energy is even, although the coefficient multiplying D is odd. Thus measuring only the energy would miss a magnetic sign error. The signed coefficients in Figure III.9.3 distinguish charge direction from this even energy. The positive branch has its minimum at $f = 0$; its weak-field expansion begins with the Maxwell magnetic energy,

$$\mathcal{E}_{\rm proper} = \tau_2 + \frac{\tau_2}{2}f^2 + O(f^4). \tag{III.9.45}$$

The expansion is a local small-$|f|$ statement. The unexpanded magnetic determinant above still belongs to the abelian action without higher derivatives; it is not a nonabelian or arbitrary rapidly varying action.

Coordinate changes can conceal this normalization. To see how, let the static induced metric have lapse $N > 0$ and a positive spatial Gram matrix g_{ij}, $i, j = 1, 2$, with no shift. Write

$$G_{ab} = \begin{pmatrix} -N^2 & 0 & 0 \\ 0 & g_{11} & g_{12} \\ 0 & g_{12} & g_{22} \end{pmatrix}, \qquad \Delta = g_{11}g_{22} - g_{12}^2 > 0, \qquad h = \lambda F_{12}. \tag{III.9.46}$$

The spatial off-diagonal entries of $G + \lambda F$ are $g_{12} + h$ and $g_{12} - h$. Their product is $g_{12}^2 - h^2$, so

$$-\det(G + \lambda F) = N^2(\Delta + h^2), \qquad f = \frac{h}{\sqrt{\Delta}}. \tag{III.9.47}$$

The second equation is the orthonormal magnetic field obtained by dividing the two-form coefficient by the physical area Jacobian. The coordinate static energy and proper local energy are therefore

$$\mathcal{E}_{\rm coordinate} = N\tau_2\sqrt{\Delta + h^2}, \qquad \frac{\mathcal{E}_{\rm coordinate}}{N\sqrt{\Delta}} = \tau_2\sqrt{1+f^2}. \tag{III.9.48}$$

The lapse is retained in energy conjugate to coordinate time. Dividing only by the area Jacobian would leave that lapse in the answer.

For a full nonunit example choose $N = 2$, spatial lengths 3 and 5, and the same physical field $f = 3/4$. Then $g_{11} = 9$, $g_{22} = 25$, $g_{12} = 0$, $\sqrt{\Delta} = 15$ and $h = 15f$. Direct substitution gives

$$-\det(G + \lambda F) = 900(1+f^2), \qquad \mathcal{E}_{\rm coordinate} = 30\tau_2\sqrt{1+f^2}. \tag{III.9.49}$$

With $\tau_2 = 7/3$ this is $175/2$ per coordinate area. Dividing by $N\sqrt{\Delta} = 30$ returns $35/12$. Using $h = f$ in this chart would change the physical field; setting $N = 1$ midway would confuse proper and coordinate time. These are normalization questions even in a flat background.

Now consider the WZ term in the book's inherited RR normalization. For $B_{\mathrm{NS}} = 0$ and the positive ordered orientation it contains

$$S_{\mathrm{WZ}} = \mu_2 \int_{W_3} \big(P[C_3] + \lambda F \wedge P[C_1]\big), \qquad \frac{\mu_2 \lambda}{\mu_0} = \frac{1}{2\pi}. \tag{III.9.50}$$

μ_p denotes the RR charge coefficient, not τ_p with its inverse coupling. The source tensions suppressed in superspace formulas must not be silently restored as either coefficient. Positive magnetic flux gives a positive local coefficient for the D0 coupling in this chart. If a compact oriented spatial surface Σ and a globally valid integer-charge abelian connection are additionally supplied, the coefficient in D0 units is

$$\frac{\mu_2 \lambda}{\mu_0} \int_\Sigma F = \frac{1}{2\pi} \int_\Sigma F = n. \tag{III.9.51}$$

Integrality of n is an extra global premise, treated in Chapter 5; the local determinant does not impose it. Likewise the WZ term is a sourced physical coupling, whereas the ratio and integral in (III.9.51) are its consequences in the stated units.

This explains the complementary roles of the projector and energy. The normalized pair of D2/D0 directions rotates with signed flux, while the local DBI energy remains positive. On an infinite plane the constant densities integrate to an infinite total energy. Neither a finite matrix rank nor a positive local density asserts a stable quantum state of prescribed global charge. The relevant pitfalls are to count two anticommuting conditions as independent halves, to equate coordinate and proper energies, and to infer global charge quantization from a local field value. Each mistake discards an assumption that the calculation has kept explicit.

III.9.7 The membrane action

What additional input is needed to call the same triple-gamma algebra a membrane supersymmetry calculation? It is the eleven-dimensional superspace action and its local fermionic transformation. Write $\widehat{Z}$ for a membrane superspace embedding and $\widehat{E}_a{}^{\hat{\mu}}$ for the pulled-back supervielbein. Its induced metric is

$$\widehat{g}_{ab} = \widehat{E}_a{}^{\hat{\mu}} \widehat{E}_b{}^{\hat{\nu}} \eta_{\hat{\mu}\hat{\nu}}, \qquad V = \sqrt{-\det \widehat{g}} > 0. \tag{III.9.52}$$

V here is a scalar volume density, not the source D-brane connection used earlier. For positive tension $T = T_{\mathrm{M2}}$, an auxiliary positive density $\widehat{v}$ writes the scalar part of the cited membrane action as

$$\mathcal{L}_{\mathrm{scalar}} = T \left(\frac{\det \widehat{g}}{2\widehat{v}} - \frac{\widehat{v}}{2} \right) = -\frac{T}{2} \left(\frac{V^2}{\widehat{v}} + \widehat{v} \right). \tag{III.9.53}$$

The full action also has a super-three-form term. It is not removed by choosing a background with zero bosonic C_3: that choice specifies the lowest bosonic component, not every superspace component.

Eliminating $\widehat{v}$ is a calculation we can do completely. Vary it while holding the embedding fixed:

$$\frac{\partial \mathcal{L}_{\text{scalar}}}{\partial \widehat{v}} = \frac{T}{2}\left(\frac{V^2}{\widehat{v}^2} - 1\right) = 0, \qquad \widehat{v} > 0 \quad \Longrightarrow \quad \widehat{v} = V. \tag{III.9.54}$$

The negative algebraic root lies outside this branch. There is only one positive stationary value for nondegenerate Lorentzian $\widehat{g}$. A useful off-shell identity also fixes the sign:

$$\mathcal{L}_{\text{scalar}} + TV = -\frac{T}{2\widehat{v}}(\widehat{v} - V)^2 \leq 0. \tag{III.9.55}$$

Thus the stationary scalar Lagrangian is a maximum with respect to this auxiliary variable. It is not a negative physical energy: after elimination the scalar Lagrangian is $-TV$, the familiar Lorentzian Nambu–Goto sign. In the inherited book orientation the action takes the separate form

$$S_{\text{M2}} = -T_{\text{M2}} \int d^3\sigma \sqrt{-\det \widehat{g}} + T_{\text{M2}} \int P[C_3]. \tag{III.9.56}$$

Its superspace meaning remains the sourced one. This scalar elimination has not tested the fermionic variation.

For a numerical example use the determinant and tension in E5: $\det \widehat{g} = -36/25$ and $T = 11/7$. The positive volume is $V = 6/5$, so direct substitution gives

$$\widehat{v} = \frac{6}{5}, \qquad \mathcal{L}_{\text{scalar}} = \frac{11}{7}\left(-\frac{3}{5} - \frac{3}{5}\right) = -\frac{66}{35}. \tag{III.9.57}$$

Both terms contribute; dropping either would give a factor-of-two error. The example also keeps the tension separate from the density.

The sourced kappa matrix is the normalized induced three-gamma product. With the source's barred convention it is written

$$\widehat{\Gamma}_{\text{BT}} = \frac{\varepsilon^{abc}\widehat{E}_a{}^{\hat{\mu}}\widehat{E}_b{}^{\hat{\nu}}\widehat{E}_c{}^{\hat{\rho}}\Gamma_{\hat{\mu}\hat{\nu}\hat{\rho}}}{3!\sqrt{-\det \widehat{g}}}, \qquad \delta_\kappa \widehat{E}^\alpha = [\bar{\kappa}(1 + \widehat{\Gamma}_{\text{BT}})]^\alpha. \tag{III.9.58}$$

On a static 012 plane with source $\varepsilon^{012} = +1$, the lower time gamma makes this barred representative $-A$. We choose the native oriented sector with column condition $A\epsilon = \epsilon$; reversing the source volume orientation exchanges the eigenspace labels. This choice is sufficient for the finite ranks below. It is not a conversion of the full signed source super-three-form coupling into the signed book C_3 charge. The inherited WZ normalization in (III.9.56) and this selected projector sector are separate statements.

Using the real extension $\widehat{\Gamma}^{10} = \chi$ from (III.9.19), the selected planar conditions give

$$\dim S_{012,+} = 16, \qquad \dim(S_{012,+} \cap S_{034,+}) = 8, \qquad \dim(S_{012,+} \cap S_{013,+}) = 0. \tag{III.9.59}$$

The plane comparisons in Figure III.9.2 apply to these selected M2 operators as well. These numbers follow from the same trace and anticommutator derivations as the D2 examples. Thirty-two is still the real spinor dimension; introducing the eleventh gamma does not double it.

Volume II, Chapter 8 fixes the physical membrane tension and circle units. Volume VIII's quadratic bosonic membrane fluctuation calculation uses the bosonic truncation of such an action. That fluctuation calculation cannot certify the full fermionic completion or its superspace constraints. Nor does the algebraic extension above establish a nonperturbative M-theory completion. The useful result here is narrower: under the cited membrane action and projection premise, we can eliminate the positive auxiliary density and count the selected local supersymmetry parameters. The next section turns the triple-gamma condition into a geometric measurement without extending that physical premise.

III.9.8 Tangent planes and calibration

How can a local spinor condition recognize an oriented area? A wrapped brane presents a family of tangent planes, so both the actual area and the spinor used to test it must be kept. Work in a flat static frame with Euclidean spatial metric. Let u, v be independent tangent vectors and define their full Gram area

$$\begin{aligned} g(u,v) &= \begin{pmatrix} u\cdot u & u\cdot v \\ u\cdot v & v\cdot v \end{pmatrix}, \\ a(u,v) &= \sqrt{(u\cdot u)(v\cdot v)-(u\cdot v)^2} > 0. \end{aligned} \tag{III.9.60}$$

The area is positive and independent of an orientation reversal. Orientation instead enters the wedge numerator. The associated static plane operator is

$$K_{uv} = \frac{\sum_{i<j}(u^i v^j - u^j v^i)\Gamma^{0ij}}{a(u,v)}. \tag{III.9.61}$$

Spatial indices are Cartesian. This is an ordered-product formula; there is no extra 2! in the sum over $i<j$.

To check its normalization for arbitrary independent u, v, choose an oriented orthonormal pair e, e' spanning them by Gram–Schmidt. Their oriented wedge is $u\wedge v = a\, e\wedge e'$. If $\Gamma(e) = e^i\Gamma^i$, the numerator reduces to $a\Gamma^0\Gamma(e)\Gamma(e')$. The three factors anticommute and have squares $-1, 1, 1$. Therefore

$$K_{uv} = \Gamma^0\Gamma(e)\Gamma(e'), \qquad K_{uv}^2 = (-1)^3(-1)1 = 1, \qquad K_{uv}^T = K_{uv}. \tag{III.9.62}$$

The transpose proof is the same three-factor reversal as for A. A degenerate plane has $a = 0$, so this normalization is undefined. One must not assign a projection to a collapsed pair of tangent vectors by dividing by its vanishing area.

Now fix a unit real spinor ϵ in the same static representation. Define a spatial two-form through its ordered components,

$$\phi = \sum_{i<j} \phi_{ij}\, dx^i \wedge dx^j, \qquad \phi_{ij} = \epsilon^T\Gamma^{0ij}\epsilon, \qquad \epsilon^T\epsilon = 1. \tag{III.9.63}$$

This is a positive component norm in a fixed frame, not a proposed Lorentz-invariant positive spinor norm. Evaluation on the tangent pair relates the geometric two-form to the projector:

$$\phi(u,v) = a(u,v)\,\epsilon^T K_{uv}\epsilon. \tag{III.9.64}$$

The form depends on the chosen spinor. Changing the spinor separately at each point would change the object being tested.

The central norm identity can be derived for any real vector η, before imposing unit length. Symmetry and the involution give

$$\begin{aligned}\|(1-K)\eta\|^2 &= \eta^T(1-K)^T(1-K)\eta \\ &= \eta^T(2-2K)\eta = 2\big(\|\eta\|^2 - \eta^T K\eta\big).\end{aligned} \tag{III.9.65}$$

For our unit spinor this yields the one-sided oriented bound and its precise equality condition:

$$a - \phi(u,v) = \frac{a}{2}\|(1-K_{uv})\epsilon\|^2 \geq 0, \qquad \phi(u,v) = a \iff K_{uv}\epsilon = \epsilon. \tag{III.9.66}$$

Applying the same argument to $-K$ also gives $\phi \geq -a$. The upper bound is the calibration condition for the chosen orientation. An oppositely oriented plane can saturate the lower bound instead. The physical use is that a positive spinor eigenspace is detected by saturation of an oriented area inequality, rather than by the smallness of an unoriented angle alone.

We can compute a nonorthogonal example completely. Select any unit A-positive spinor and restrict the tangent vectors to spatial $\mathbb{R}^4$, with

$$u = (2,0,0,0), \qquad v = (1,3/5,4/5,0). \tag{III.9.67}$$

The anticommutator of A and C proves the needed second bilinear: $\epsilon^T C\epsilon = \epsilon^T ACA\epsilon = -\epsilon^T C\epsilon$. Thus $\phi_{12} = 1$ and $\phi_{13} = 0$ for every such spinor. All dot products, including the shear, enter the area calculation:

$$u\cdot u = 4, \quad u\cdot v = 2, \quad v\cdot v = 1 + \frac{9}{25} + \frac{16}{25} = 2, \qquad g = \begin{pmatrix} 4 & 2 \\ 2 & 2 \end{pmatrix}. \tag{III.9.68}$$

Consequently $\det g = 8 - 4 = 4$ and $a = 2$, rather than $\|u\|\|v\| = \sqrt{8}$. In the oriented wedge, the longitudinal component of v drops out:

$$u \wedge v = \frac{6}{5}e_1 \wedge e_2 + \frac{8}{5}e_1 \wedge e_3, \qquad K_{uv} = \frac{3A + 4C}{5}, \qquad \phi(u,v) = \frac{6}{5}. \tag{III.9.69}$$

The norm residual and area deficit now agree through two calculations:

$$\|(1-K_{uv})\epsilon\|^2 = 2\left(1 - \frac{3}{5}\right) = \frac{4}{5}, \qquad a - \phi = 2 - \frac{6}{5} = \frac{4}{5}. \tag{III.9.70}$$

Here $a/2 = 1$, so the two numerical values happen to coincide. Their units and general relation are different. The plane is not calibrated by this spinor. Its 12 projection has signed area $6/5$, whereas its full area is 2.

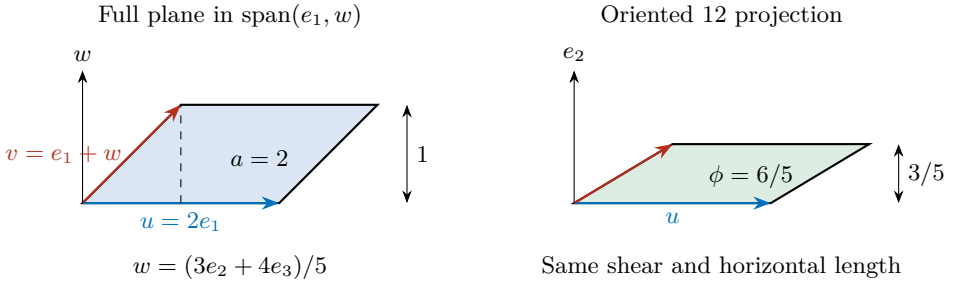


Figure III.9.4: The actual sheared parallelogram of (III.9.67). The horizontal direction is e_1 and the vertical screen direction is the unit vector $w = (3e_2 + 4e_3)/5$. Thus $u = 2e_1$ and $v = e_1 + w$ have full area 2. Its 12 projection, drawn at right with the same horizontal scale, replaces w by $3e_2/5$ and has area $6/5$. The orientation is the ordered pair (u, v) in both panels. The Gram off-diagonal entry is 2; the drawing does not replace the full Gram determinant by the product of side lengths.

Figure III.9.4 distinguishes a shear from a change of area. Subtracting e_1 from v removes the shear without changing $u \wedge v$, a or K. In contrast, altering the length of u changes both the wedge and the area. An independent example that varies this length is

$$u' = (3, 0, 0, 0), \qquad v' = (4, 5, 12, 0),$$
$$g' = \begin{pmatrix} 9 & 12 \\ 12 & 185 \end{pmatrix}, \qquad \det g' = 1665 - 144 = 1521. \tag{III.9.71}$$

The positive area is 39, the wedge coefficients are 15 and 36, and the bilinear is 15. Hence

$$K_{u'v'} = \frac{5A + 12C}{13}, \qquad \|(1 - K_{u'v'})\epsilon\|^2 = 2\left(1 - \frac{5}{13}\right) = \frac{16}{13}. \tag{III.9.72}$$

In particular $(5/13)^2 + (12/13)^2 = 1$ still normalizes the projector. This second example prevents the special value $u^1 = 2$ from masquerading as part of a general area formula.

For an aligned comparison use $u = 2e_1$, $v = 3e_2$. Then $a = 6$, $K = A$, $\phi = 6$ and the residual vanishes. Replacing v by $-3e_2$ keeps the positive area 6 but gives $K = -A$, $\phi = -6$ and residual squared 4. Replacing it by a multiple of e_1 instead makes the Gram determinant zero. These three cases distinguish saturation, orientation reversal and degeneration. None requires a negative area.

Finally, a constant spinor and constant Cartesian gamma matrices make the coefficients of ϕ constant. In this flat patch,

$$d\phi = \sum_{k,i<j} (\partial_k \phi_{ij}) dx^k \wedge dx^i \wedge dx^j = 0. \tag{III.9.73}$$

Closure and the plane inequality supply an ordinary calibration form. For a surface, however, the same ϵ must solve $K(x)\epsilon = \epsilon$ at every tangent plane. The existence of a sixteen-component positive space at each separate point does not establish a nonzero

intersection of those spaces over the surface. Volume IV, Chapter 6 uses this local-to-global distinction when stating volume minimization. We now identify the further physical premises needed before turning it into a wrapped-brane state.

III.9.9 From local planes to global states

A local projector solves a compatibility problem at a point. A wrapped brane is a global object, and a physical BPS state requires still more information. Figure III.9.5 separates these statements so that an area inequality is not asked to establish a spectrum.

The ordinary calibrated-cycle theorem applies to an already realized compact smooth oriented boundaryless cycle in an oriented Riemannian manifold with a globally defined closed calibration. The cycle must saturate the calibration at all its oriented tangent planes. Under the usual smooth homologous-competitor hypotheses, the integral of the closed form is the same on the cycle and its competitors, while the pointwise bound puts that integral below each competitor's volume. Thus the realized calibrated cycle minimizes ordinary volume in that class. This is the cited theorem stated in Volume IV, Chapter 6; it is not an existence theorem for a representative of an arbitrary homology class. In a noncompact problem or one with boundaries, boundary conditions and the allowed class of deformations must be specified before transferring that conclusion.

For the spinorial application there must also be one global background Killing spinor. A spin structure or quotient lift may obstruct it even when each local metric patch admits the same Clifford matrices. The constant spinor of our flat example is part of that example's background; it is not a prescription for extending an arbitrary patch spinor around a compact space. If the spinor does extend, its local plane conditions still have to agree everywhere on the realized embedding.

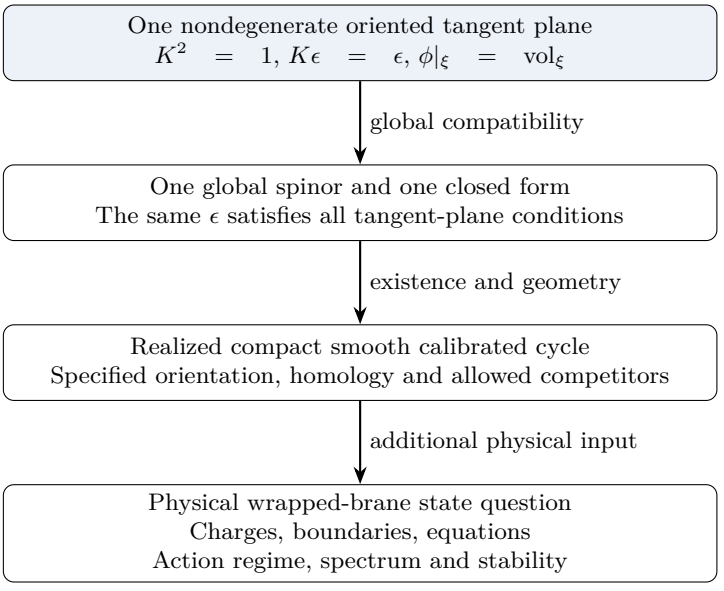


Figure III.9.5: Logical requirements for using the flat spinor-plane bound in a wrapped-brane problem. Each downward step adds premises; no reverse implication or existence assertion is drawn. The ordinary-volume statement belongs to a realized calibrated cycle. The final physical state question also depends on charges, boundary conditions, the action regime and quantum stability. General redshift and electrostatic energies require their own analysis.

The action regime matters independently. Our D2 calculation uses a single abelian derivative-truncated probe with fixed flat background, constant dilaton and constant magnetic field. A coupled source must satisfy the background equations as well as its worldvolume equations. A curved flux background can have redshift-weighted volume and an electrostatic contribution to static energy. Ordinary volume alone then is not the relevant energy functional. The generalized calibration discussion in the cited source treats this distinction; the flat norm identity derived here does not prove its curved-flux theorems.

Finally the global charge sector must support the proposed physical state, with appropriate spectrum and stability or chamber assumptions. A supersymmetry fraction is not a multiplet-shortening argument for a protected observable, and it supplies no index calculation. The local rank counts in this chapter therefore do not determine BPS multiplicities. They provide necessary compatibility information for constructions that must separately address these questions.

Chapter 7 offers a related warning. In its Hermitian convention with inward $s = x^6$ and ordered transverse 789, the Nahm equation is $D_s X_i - (i/2)\epsilon_{ijk}[X_j, X_k] = 0$. A finite rank-two residue can test that equation in its stated ansatz. It is not a proof of kappa invariance or a classification of all supersymmetric boundaries. The same separation applies to Volume VIII's bosonic membrane fluctuations and the full superspace premise

used here. A useful construction argument specifies which local equation it has solved, which global object exists, and which state question remains.

III.9.10 Exercises

E1–E5 have bounded numerical submissions. Written derivations and interpretations are separate parts of the work and are not certified by those numerical submissions. The public `questions.json` gives each exact JSON schema. An answer has precisely the top-level fields `task` and `answer`; the task string is the exercise ID. Within `answer`, use exactly the field names listed below. E1 and E2 use integers, E3 and E4 use exact rational strings, and E5 mixes these as specified. A rational string has an optional minus sign, a decimal integer numerator and, optionally, a slash followed by a positive integer denominator; use no decimal point, leading plus or spaces. For example `"7/11"` illustrates the syntax only. Follow `benchmark/PROTOCOL.md` for the public submission envelope. E6 is written and ungraded.

E1. In the physical real type-IIA space, use $A = \Gamma^{012}$ and $\chi = \Gamma^0 \cdots \Gamma^9$. Calculate the real spinor dimension, the ranks of $(1 + A)/2$ and $(1 - A)/2$, and the dimension of the common A-positive and χ-positive space. Under task `E1`, submit the integer fields `real_dimension`, `rank_plus` and `rank_minus`. The chirality intersection goes in the integer field `common_with_positive_chirality`. Explain why a physical IIA pair is not an unrestricted sixty-four-component doublet, and why its positive brane spinors need not have definite ten-dimensional chirality.

E2. For $A = \Gamma^{012}$, $B = \Gamma^{034}$ and $C = \Gamma^{013}$, compute common positive dimensions for (A, B), (A, C), (A, A) and $(A, -A)$. Submit integer fields `independent`, `anticommuting`, `duplicate`, and `opposite` under task `E2`. Derive the compatibility or dependence of each pair before counting. Explain why the rank of $P_A P_C$ is not a count of its simultaneous solutions.

E3. In the selected flat, constant-dilaton abelian D2 with $B_{\mathrm{NS}} = 0$ and no electric field, write $K = cA + sD$ with $c > 0$, $s/c = f$, $D = \Gamma^0\chi$ and $f = \lambda F_{12}$ in an orthonormal chart. Determine the coefficients at $f = 3/4$ and $f = -5/12$, and the positive proper DBI energy density at $\tau_2 = 7/3$, $f = 3/4$. Submit rational-string fields `positive_c`, `positive_s`, `negative_c`, `negative_s`, and `energy_density` under task `E3`. Recover the relative flux sign from the APS row-to-column map. Explain why the two charge directions are not two simultaneous half-projections.

E4. In Euclidean spatial $\mathbb{R}^4$, take $u = (2, 0, 0, 0)$, $v = (1, 3/5, 4/5, 0)$ and a unit real A-positive spinor. Use $\phi_{12} = 1$, $\phi_{13} = 0$ and $K_{uv} = (u^1v^2A + u^1v^3C)/a$. Calculate every independent Gram entry, the positive area, $\phi(u, v)$ and $\|(1 - K_{uv})\epsilon\|^2$. Submit rational-string fields `gram11`, `gram12`, `gram22`, `area`, `phi`, and `residual_norm_squared` under task `E4`. Discuss why local saturation, if it occurred, would not guarantee a populated global BPS state. Repeat the geometric calculation in written work with $u = (3, 0, 0, 0)$ and $v = (4, 5, 12, 0)$ to test the dependence on u^1.

E5. For the sourced flat M2 probe, use the real extension $\widehat{\Gamma}^{10} = \chi$ and the chosen oriented planar condition $A\epsilon = \epsilon$. Find the real spinor dimension, the single rank and common positive dimensions for 012/034 and 012/013. Also eliminate the positive auxiliary density in $\mathcal{L} = T[\det \widehat{g}/(2\widehat{v}) - \widehat{v}/2]$ with $\det \widehat{g} = -36/25$, $T = 11/7$ and zero pulled-back bosonic C_3. Under task `E5`, submit integer fields `real_dimension`, `rank_single`, `common_012_034`, and `common_012_013`, together with rational-string fields `auxiliary_density` and `nambu_goto_density`. Explain which parts follow from scalar stationarity and finite algebra, and which require the cited superspace action.

E6. *Written, ungraded.* Explain why simultaneous local projector solutions do not establish a global supersymmetric wrapped-brane state. Address background Killing spinors and spin structure, a realized smooth calibrated representative, charge and boundary conditions, equations of motion and the backreaction regime, and spectrum/stability or chamber assumptions. Distinguish the full sourced M2 superspace action from a bosonic quadratic fluctuation calculation. State the Chapter 7 Nahm sign with inward x^6 and ordered 789, and explain why its rank-two residue proves neither kappa invariance nor general boundary classification.

III.9.11 Take-home message

Take-home message

A brane preserves a background supersymmetry when a local kappa transformation compensates it. In the selected real IIA space this becomes $K\epsilon = \epsilon$ on thirty-two real components. One flat D2 leaves sixteen; the four pairs studied here leave $8, 0, 16, 0$. Constant magnetic flux gives one signed rotated projector, $K = (A + fD)/\sqrt{1+f^2}$, together with a positive proper DBI density. The membrane action supplies a separate superspace premise; eliminating its positive auxiliary density is a scalar calculation. A static spinor bilinear translates the plane projection into oriented area saturation. Global geometry and physical state existence require their own additional hypotheses.

After this chapter the reader should be able to convert the selected APS row formula to the column condition, count compatible constraints in the physical real space, derive the signed magnetic coefficients and distinguish proper from coordinate energy, and evaluate a sheared plane with its full Gram determinant and norm residual. These are the local calculations needed before applying the separate charge, wrapped-cycle and brane-engine constructions.

Status and sources

§III.9.2 Local action. The full superspace D2 action and its local invariance are cited physical premises. Their sources are Aganagic et al. (1997, physical PDF pp. 3–4, 6–8, eqs. (1)–(8), (21)–(39)), Bergshoeff and Townsend (1997, physical PDF pp. 4–5, 13–16, 25, eqs. (2.1)–(2.8), (4.17)–(4.30)), and the compensating transformation in Bergshoeff, Kallosh, et al. (1997, physical PDF pp. 3, 10, eqs. (5), (38)–(40)). The

APS letter omits full proofs of its three key identities, as its conclusion states. BT reports full verification in bosonic backgrounds for $p \leq 6$, and in general backgrounds for $p = 0, 2$; the present D2 lies within those ranges. The standard on-shell superspace constraints remain hypotheses, not conclusions of a bosonic determinant. The restricted row/column translation is [MATH] under the stated Majorana and source conventions. It does not certify the physical premises.

§III.9.3 Real ranks. The involution, trace, chiral-graph and real rank calculations [MATH] use the physical IIA space inherited from Volume II, Chapter 4. The algebraic eleven-dimensional extension is independent of the membrane action premise.

§III.9.4 Intersections. The intersection calculations for the four specified flat pairs are mathematical results [MATH]. The physical probe method and constant-field solutions come from Bergshoeff, Kallosh, et al. (1997, physical PDF pp. 13–14, eqs. (53)–(57)). The zero product-trace condition is kept explicit: opposite matrices are an exception to the source's unequal-commuting shorthand.

§III.9.5 Magnetic operator. The operator calculations for the finite real magnetic branch are mathematical results [MATH], with the source coefficient sign fixed by APS pp. 6–7.

§III.9.6 Energy and charge. The energy calculation [MATH] assumes the abelian DBI action and inherited physical units. The physical WZ interpretation uses the local D0 coupling supported by Johnson (2000, physical PDF pp. 112–113, eqs. (285)–(286)) and BT pp. 4–5. Chapter 5 owns global flux quantization.

§III.9.7 Membrane. The full superspace membrane action is a physical premise from Bergshoeff and Townsend (1997, physical PDF pp. 20, 23, eqs. (6.1), (6.20)–(6.24)) and Bergshoeff, Kallosh, et al. (1997, physical PDF pp. 20–21, eqs. (92)–(94)). The selected eleven-dimensional ranks and positive auxiliary-branch elimination are [MATH] conditional on it. No unconverted signed M2/C_3 dictionary, fermionic completion proof or M-theory duality proof is inferred.

§III.9.8 Calibration. The symmetric-involution norm identity, full Gram examples and flat constant-form closure are mathematical results [MATH]. Their spinorial geometric interface follows Gutowski et al. (1999, physical PDF pp. 1–2, eqs. (2)–(7)), with the lower-time-index sign paired with the chosen native orientation.

§III.9.9 Global interface. The ordinary-volume theorem is the already scoped [MATH] result of Volume IV, Chapter 6 for a realized compact smooth oriented calibrated cycle and suitable homologous competitors. The existence of a physical state is a separate question. The redshift and electrostatic qualification is explicit in GPT physical p. 1, eq. (1).

Conventions and scope. The calculations use the stated metric, Clifford, tension and charge conventions. The cited physical premises are inputs to the mathematical deductions. A preserved fraction alone does not establish a short BPS representation.

The supplied calculations cover the real ten- and eleven-dimensional Clifford relations, selected common kernels, the APS transpose sign, magnetic rotations and determinants, auxiliary stationarity, and the sheared-plane components. The variable-u^1 shear shows the dependence on the plane directly. These finite calculations do not establish a compact cycle, a stable spectrum, or a general curved-flux theorem.

References

Aganagic, M., C. Popescu, and J. H. Schwarz (1997). "D-brane actions with local kappa symmetry". In: *Phys. Lett. B* 393. Source edition hep-th/9610249v2; physical PDF pages 3, 4, 6, 7, 8, pp. 311–315. DOI: 10.1016/S0370-2693(96)01643-7. arXiv: hep-th/9610249.

Bergshoeff, E., R. Kallosh, et al. (1997). "Kappa symmetry, supersymmetry and intersecting branes". In: *Nucl. Phys. B* 502. Source edition hep-th/9705040v2; physical PDF pages 2, 3, 5, 6, 7, 8, 10, 12, 13, 14, 20, 21, pp. 149–169. DOI: 10.1016/S0550-3213(97)00470-7. arXiv: hep-th/9705040.

Bergshoeff, E. and P. K. Townsend (1997). "Super D-branes". In: *Nucl. Phys. B* 490. Source edition hep-th/9611173v3; physical PDF pages 4, 5, 13, 14, 15, 16, 20, 23, 24, 25, pp. 145–162. DOI: 10.1016/S0550-3213(97)00072-2. arXiv: hep-th/9611173.

Gutowski, J., G. Papadopoulos, and P. K. Townsend (1999). "Supersymmetry and generalized calibrations". In: *Phys. Rev. D* 60. Source edition hep-th/9905156v3; physical PDF pages 1, 2, p. 106006. DOI: 10.1103/PhysRevD.60.106006. arXiv: hep-th/9905156.

Johnson, C. V. (July 2000). "D-brane primer". In: *Theoretical Advanced Study Institute in Elementary Particle Physics (TASI 99): Strings, Branes, and Gravity*. Source edition hep-th/0007170v3; physical PDF pages 112, 113, pp. 129–350. DOI: 10.1142/9789812799630_0002. arXiv: hep-th/0007170.

Chapter III.10

NS5-brane worldvolume theories and little strings

III.10.1 The worldvolume question

A fivebrane can carry a theory even when its coupling to bulk gravity is removed. The degrees of freedom that remain need not all be point particles. A membrane ending on a fivebrane has a string as its boundary, and the energy of that string measures the separation from another fivebrane. This gives a concrete way to study a worldvolume theory: identify its light fields, find the objects charged under those fields, and ask which of their energy scales survive a limit.

For an NS5-brane, this route also explains why a low-energy field theory and a finite-string-scale theory are different descriptions. Type IIA and type IIB fivebranes have different free multiplets. Both preserve sixteen real supercharges, but the IIA multiplet contains a chiral two-form, whereas the IIB multiplet contains a vector. The extended objects they couple to have different dimensions. Removing gravity does not erase that distinction, and it does not by itself remove the intrinsic string scale.

We work with flat parallel positively oriented NS5-branes along 012345, with no orientifold, additional projection, RR deformation or Romans-mass region. The separated branch means that the branes occupy distinct transverse positions and that we observe them below the scales of the stretched objects connecting them. Each isolated brane then has a free infrared multiplet. The identification of that multiplet and the existence of the charged stretched states are physical inputs. We will derive their polarization counts, tensions, scale dependence and selected compactification masses. These calculations do not construct the interacting theory at coincidence.

The prerequisites are the six-dimensional supersymmetry grammar of Volume I, Chapter 8, the bulk NS5 geometry of Volume II, Chapter 10, and the endpoint and brane-energy methods of Chapters 7 and 9. The present chapter supplies the tension and scale calculations used in suspended fivebrane constructions. XVI treats the interacting $(2, 0)$ theory; the planned discussion of composite constructions and little string theories treat the finite-string-scale dynamics beyond this preview.

After working through the chapter, the reader should be able to count the tensor and vector multiplets without multiplying the supersymmetry algebra by the number of branes; distinguish a stretched-string tension from a stretched-particle mass; choose a limit that keeps a finite tensor string tension; and match separate winding and momentum masses on a worldvolume circle. A further goal is to identify the physical premises that none of this arithmetic can establish.

III.10.2 Fields on separated fivebranes

Why do fivebranes with the same six worldvolume directions carry different fields in IIA and IIB? Begin with a slowly moving isolated brane. Its transverse position can vary from point to point along the worldvolume. Such a displacement is a scalar field from the six-dimensional viewpoint. The four visible transverse directions in either ten-dimensional theory are 6789. These account for four real scalar fields before we say anything about supersymmetry.

For the IIA brane there is another local displacement in its M-theory description. Under the IIA/M-theory identification, the NS5 becomes an M5 localized on the transverse x^{10} circle. Its position on that circle is a fifth scalar locally. It is periodic globally, rather than an additional noncompact IIA coordinate. With the common physical length convention, its period is

$$X^{10} \sim X^{10} + 2\pi R_{10}, \qquad R_{10} = g_s \ell_s. \tag{III.10.1}$$

Here g_s is the asymptotic string coupling, ℓ_s is the string length, and $\alpha' = \ell_s^2$. The use of the M circle is a conditional physical identification, with the same massless-IIA domain as in Volume II, Chapter 9. It is not a new local supergravity argument for an extra coordinate in every IIA background.

The other bosonic field on an isolated IIA NS5 is a worldvolume two-form. Its three-form field strength is self-dual in the book's $(2,0)$ convention. Denote the worldvolume potential by $B_{\rm wv}$ and its free field strength by $H_{\rm wv}$ to distinguish them from the bulk NS two-form. In a flat patch,

$$H_{\rm wv} = dB_{\rm wv}, \qquad H_{\rm wv} = *_6 H_{\rm wv}. \tag{III.10.2}$$

The IIA infrared multiplet is the $(2,0)$ tensor multiplet. The self-duality condition is part of its field content. It halves the physical two-form polarizations, rather than adding another independent field to an unconstrained two-form.

The IIB NS5 instead has a $(1,1)$ vector multiplet. Its four scalars describe the visible transverse displacements, and its gauge potential is a one-form $A_{\rm wv}$, with free field strength

$$F_{\rm wv} = dA_{\rm wv}. \tag{III.10.3}$$

One way to understand the assignment is the conditional IIB S-duality identification with a D5-brane, whose massless fields are a vector and four displacement scalars. The physical identification relates the theories; it does not make a weakly coupled open-D-string description available at small NS5-frame g_s. The tensor and vector

assignments are sourced facts about fivebranes. Counting their components will test their consequences, rather than derive the assignments from the metric.

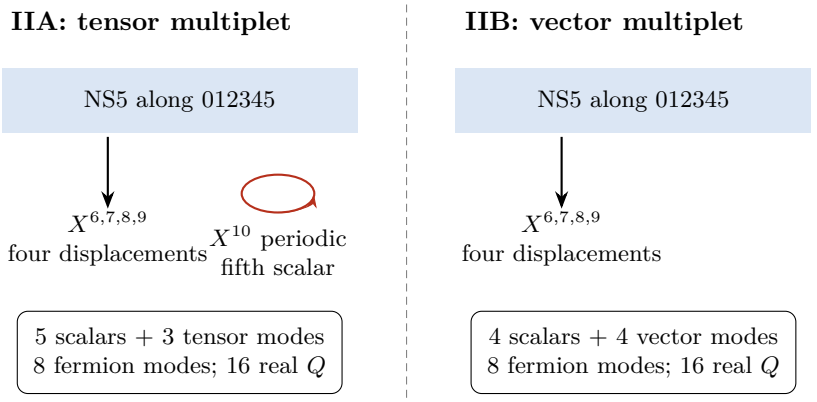


Figure III.10.1: The free fields of isolated IIA and IIB NS5-branes. The common worldvolume is 012345 and the visible transverse space is 6789. Only the IIA column uses the transverse M circle to describe a fifth local displacement. The field and fermion entries count physical on-shell polarizations; the Q entries count preserved real supersymmetry generators.

To count a massless field, fix a null worldvolume momentum. Gauge constraints remove the two light-cone directions, leaving a Euclidean four-dimensional transverse space for its physical polarizations. This is the vector space on which the massless little group $SO(4)$ acts. A vector therefore has

$$n_{\text{vector}} = 6 - 2 = 4 \tag{III.10.4}$$

physical polarizations. For a two-form, the remaining antisymmetric indices can be chosen from four directions. Before imposing chirality, the count is

$$n_{\text{two-form}} = \binom{4}{2} = \frac{4 \cdot 3}{2} = 6. \tag{III.10.5}$$

The Euclidean Hodge operator on this polarization space realizes the chirality restriction. It should not be confused with applying a Euclidean six-dimensional self-duality condition to the spacetime field strength. We have already fixed a null momentum and retained only physical transverse components.

Choose an oriented orthonormal basis e^1, e^2, e^3, e^4 for this polarization space, and write $e^{ij} = e^i \wedge e^j$. The three complementary pairs transform as

$$\begin{aligned} *_4 e^{12} &= e^{34}, & *_4 e^{13} &= -e^{24}, & *_4 e^{14} &= e^{23}, \\ *_4 e^{34} &= e^{12}, & *_4 e^{24} &= -e^{13}, & *_4 e^{23} &= e^{14}. \end{aligned} \tag{III.10.6}$$

In each pair, one linear combination has Hodge eigenvalue $+1$ and one has eigenvalue -1. For example, $e^{12}+e^{34}$ has eigenvalue $+1$, whereas $e^{12}-e^{34}$ has eigenvalue -1. A basis for the positive subspace is

$$e^{12}+e^{34}, \qquad e^{13}-e^{24}, \qquad e^{14}+e^{23}. \tag{III.10.7}$$

Thus either chiral choice has three polarizations:

$$\dim\ker(*_4-1)=3, \qquad \dim\ker(*_4+1)=3. \tag{III.10.8}$$

An overall opposite chirality convention would exchange these subspaces. It would not change the count. We keep the book's positive $(1,0)$ supercharge convention and its $(2,0)$ self-dual tensor.

The complete bosonic count can now be made field by field:

$$\begin{aligned} &\text{IIA}: \quad 5 \text{ scalar modes} + 3 \text{ tensor modes} + 0 \text{ vector modes} = 8,\\ &\text{IIB}: \quad 4 \text{ scalar modes} + 0 \text{ tensor modes} + 4 \text{ vector modes} = 8. \end{aligned} \tag{III.10.9}$$

Equal totals do not erase the distinction between the fields. A one-form gauge potential couples electrically to a particle worldline; a two-form couples electrically to a string worldsheet. This is why the change from vector to tensor will become visible in the dimensions of the endpoints in the next section.

Fermion polarizations and supercharges are different counts. In the six-dimensional multiplet grammar of Volume I, a symplectic-Majorana–Weyl fermion unit has eight real components before imposing its massless equation; the equation leaves four real on-shell polarizations. The $(2,0)$ tensor multiplet has two such chiral units, and the $(1,1)$ vector multiplet has two units of opposite chirality. For both,

$$n_{\text{fermions}} = 2\left(\frac{8}{2}\right) = 8. \tag{III.10.10}$$

This is the sourced free supermultiplet content. No physical fermion has been counted twice by treating a symplectic reality partner as an independent complex field. By contrast, (p,q) records real supersymmetry generators of the two chiralities:

$$\begin{aligned} &\text{IIA}: \quad (Q_+,Q_-)=(16,0), \qquad 8(2+0)=16,\\ &\text{IIB}: \quad (Q_+,Q_-)=(8,8), \qquad 8(1+1)=16. \end{aligned} \tag{III.10.11}$$

The massless Dirac equation halves the fermion modes. It does not halve the number of generators in this algebra.

As a complete separated-brane example, take three parallel branes of one type, and remain below all nonzero stretched-object scales. The field species are three free copies of the corresponding multiplet:

	scalars	tensor modes	vector modes	bosons	fermions
IIA, $N=3$	15	9	0	24	24
IIB, $N=3$	12	0	12	24	24

(III.10.12)

For general separated N, the corresponding totals are $8N$ bosonic and $8N$ fermionic modes. The same sixteen ambient generators act on every parallel brane; there are not $16N$ independently preserved spacetime supercharges. Rotating one brane relative to the others would change the shared supersymmetry problem, rather than this multiplicity rule.

For one brane the complete inventory is already the $8 + 8$ pair in Figure III.10.1, with the charge splits in (III.10.11). For several branes, diagonal displacements describe the separated branch, but these free fields cannot predict all extra states that become light at coincidence. In particular, counting five scalars does not derive a nonabelian tensor action. The adjacent endpoint calculation tells us which scale signals the failure of the separated description. The interacting $(2, 0)$ construction in XVI starts where that description ceases to be sufficient.

III.10.3 Strings between fivebranes

What becomes light as two parallel fivebranes approach, and why is its energy a tension in one theory and a mass in the other? Fix two IIA NS5-branes along 012345 at $x^6 = 0, L$, with $L > 0$. An M2, or its IIA D2 description, can stretch along 016. At each end of its x^6 interval its boundary extends along 01. The boundary is therefore a string on the fivebrane. The appropriate charge couples to the worldvolume two-form introduced above.

This statement uses the sourced existence of a straight supersymmetric stretched configuration. The leading brane analysis identifies the boundary and its charge; extending that analysis to an actual protected state is a physical premise. With that premise supplied, the energy of a static strip follows from area. If its length along x^1 is Δx^1, then

$$E = T_{\mathrm{M2}} L\, \Delta x^1, \qquad T_{\mathrm{string}} = \frac{E}{\Delta x^1} = T_{\mathrm{M2}} L. \tag{III.10.13}$$

All lengths and tensions in this comparison use one common asymptotic length convention. The minimal membrane tension and the IIA/M units are

$$T_{\mathrm{M2}} = \frac{1}{(2\pi)^2 \ell_p^3}, \qquad \ell_p^3 = g_s \ell_s^3. \tag{III.10.14}$$

The separation-dependent string tension is consequently

$$T_{\mathrm{string}} = \frac{L}{(2\pi)^2 g_s \ell_s^3}. \tag{III.10.15}$$

This is a string tension measured by a worldvolume observer, not the bulk NS5 tension. It has mass dimension two because a membrane tension has mass dimension three and is multiplied by a length.

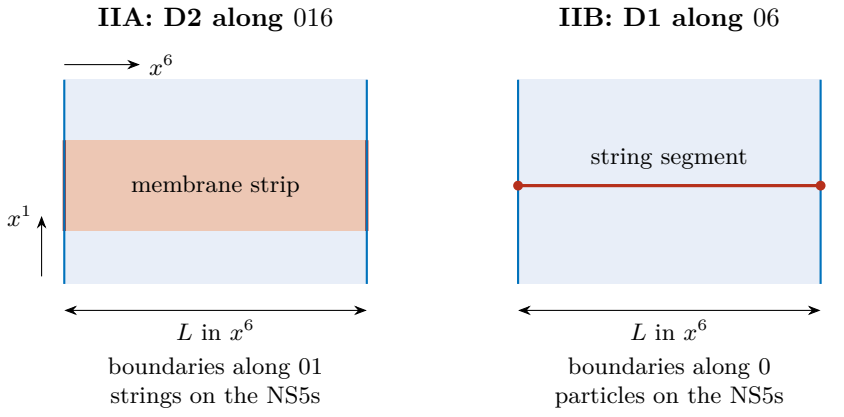


Figure III.10.2: The dimensions of stretched-brane boundaries. In the IIA panel, a D2 strip along 016 has string boundaries along 01. In the separate IIB configuration, a D1 along 06 has particle boundaries along 0. Both panels keep the same two parallel fivebrane positions $0, L$ in x^6. The type change labels two configurations, rather than a motion within one theory.

The common-frame formula deserves a check in the leading NS5 background. Let Z_5 be its harmonic function. Away from its singular centers the string-frame metric and dilaton have the form

$$ds_s^2 = \eta_{\mu\nu}dx^\mu dx^\nu + Z_5\delta_{ij}dx^i dx^j, \qquad e^\Phi = g_s\sqrt{Z_5}, \\ \mu = 0,\dots,5, \qquad i = 6,\dots,9. \tag{III.10.16}$$

Denote the string-frame metric by G. For a static straight D2 with no worldvolume flux and no RR potential term in this background, the leading DBI energy density contains the unshifted dilaton factor $e^{-\Phi}$. Its coefficient without that factor is $1/[(2\pi)^2\ell_s^3]$. The pullback along 016 gives

$$e^{-\Phi}\sqrt{-\det P[G]_{016}} = \frac{1}{g_s\sqrt{Z_5}}\sqrt{Z_5} = \frac{1}{g_s}. \tag{III.10.17}$$

Thus the static density per coordinate dx^1dx^6 has no residual Z_5 factor. Integrating it yields

$$\frac{E}{\Delta x^1} = \frac{1}{(2\pi)^2\ell_s^3}\int_0^L \frac{dx^6}{g_s} = \frac{L}{(2\pi)^2 g_s\ell_s^3}. \tag{III.10.18}$$

The coordinate interval here agrees with the separation measured by the asymptotic string metric. It is not the divergent transverse proper distance down an NS5 throat. The cancellation explains why an extra transverse proper-length factor should not be appended to (III.10.15).

The cancellation is a leading probe calculation outside the singular cores. Near a core the local dilaton becomes large, and higher-order effects or backreaction invalidate a literal DBI derivation across the endpoint. The sourced BPS interpretation is additional input; an algebraically finite integrand does not repair singular-core control. Likewise $L \to 0$ is a formal zero of the displayed tension, at precisely the locus where the separated free-field description fails.

The IIB comparison makes the role of the boundary dimension explicit. A D1 along 06 stretches between IIB fivebranes, so its boundary at each end is a worldline along 0. Its energy is a particle mass on the NS5. The same leading background has

$$e^{-\Phi}\sqrt{-\det P[G]_{06}} = \frac{1}{g_s\sqrt{Z_5}}\sqrt{Z_5} = \frac{1}{g_s}. \tag{III.10.19}$$

With the D1 coefficient $1/(2\pi\ell_s^2)$, integration gives

$$M_{\text{particle}} = \frac{1}{2\pi\ell_s^2}\int_0^L \frac{dx^6}{g_s} = \frac{L}{2\pi g_s\ell_s^2}. \tag{III.10.20}$$

Its mass dimension is one. The D2 and D1 formulas involve different powers of ℓ_s because the parent branes have different dimensions. Their endpoint charges are compatible with tensor and vector fields, respectively, as Figure III.10.2 shows. Charge compatibility alone does not establish that every allowed state exists.

For a nonunit example, take $g_s = 3/5$, $\ell_s = 2$ and $L = 7/3$ in the common length unit. Removing only the displayed factors of 2π, we obtain

$$\begin{aligned}(2\pi)^2 T_{\text{string}} &= \frac{7/3}{(3/5)\,2^3} = \frac{7}{3}\frac{5}{24} = \frac{35}{72},\\ 2\pi M_{\text{particle}} &= \frac{7/3}{(3/5)\,2^2} = \frac{7}{3}\frac{5}{12} = \frac{35}{36}.\end{aligned} \tag{III.10.21}$$

These reduced quantities are still dimensionful in the chosen length unit. They are not redefinitions of the physical tensions or masses. At fixed L, ℓ_s, decreasing g_s sends the tensor tension to infinity. Keeping it finite instead requires $L \propto g_s$ when ℓ_s is fixed. The zero-separation formula gives zero tension, but says nothing by itself about the interacting spectrum at that point.

A useful local comparison comes from adding a D6 along 0123456 on this interval. For this comparison only, assume a flat unwarped constant-dilaton patch and a gauge zero mode constant in x^6. In the book's half-trace normalization,

$$S_7 = -\frac{1}{2g_7^2}\int \mathrm{Tr_f}\, F_{MN}F^{MN}, \qquad \mathrm{Tr_f}(T^aT^b) = \frac{1}{2}\delta^{ab}, \qquad g_7^2 = 2(2\pi)^4 g_s\ell_s^3. \tag{III.10.22}$$

Integrating the constant zero mode over x^6 gives

$$\frac{1}{g_6^2} = \frac{L}{g_7^2}, \qquad g_6^2 = \frac{2(2\pi)^4 g_s\ell_s^3}{L}. \tag{III.10.23}$$

Multiplying by the stretched D2 tension cancels the geometric and coupling factors:

$$T_{\text{string}}g_6^2 = \frac{L}{(2\pi)^2 g_s\ell_s^3}\frac{2(2\pi)^4 g_s\ell_s^3}{L} = 2(2\pi)^2 = 8\pi^2. \tag{III.10.24}$$

For the numerical example, $g_6^2 = 2(2\pi)^4(72/35)$, so $(35/72)(2\pi)^{-2}\,2(2\pi)^4(72/35) = 8\pi^2$ again. The product is dimensionless since g_6^2 has length dimension two. Dropping the factor of two in g_7^2 would change the product by two; it would silently change the trace convention.

This interval interpretation is used in X.4. It is an auxiliary local gauge-theory comparison, rather than a claim that every pair of isolated NS5-branes contains a D6 gauge interval. Warped or massive-IIA regions require their own reduction. In particular the presence of D8-branes or nonzero Romans mass does not permit an automatic lift to the simple M circle used here.

There is a second use of the membrane tension that does not require adding a D6. The transverse x^{10} circle has the full physical circumference $2\pi R_{10}$. A membrane wrapped once around it has string tension

$$T_{\mathrm{M2}}(2\pi R_{10}) = \frac{2\pi g_s \ell_s}{(2\pi)^2 g_s \ell_s^3} = \frac{1}{2\pi \ell_s^2} = T_{\mathrm{F1}}. \tag{III.10.25}$$

The cancellation of g_s matters. Although the physical transverse circle shrinks at fixed ℓ_s as $g_s \to 0$, its membrane-weighted period remains finite. In particular,

$$\Delta\big(T_{\mathrm{M2}} X^{10}\big) = T_{\mathrm{M2}}(2\pi R_{10}) = T_{\mathrm{F1}}. \tag{III.10.26}$$

The combination on the left is a tension coordinate with mass dimension two. No scalar kinetic term has been derived, so its period must not be called a canonically normalized scalar circumference. Nor should it be identified with g_6^{-2} from the separate interval model merely because both quantities have mass dimension two.

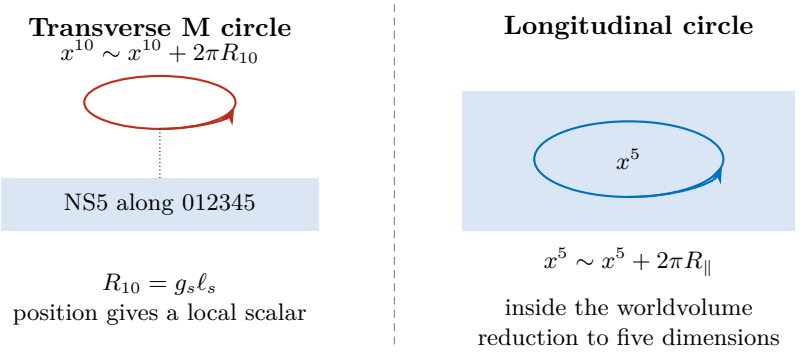


Figure III.10.3: Two physically different circles. The transverse x^{10} circle belongs to the IIA/M description and supplies a local scalar position. A longitudinal x^5 circle is a compact direction within the fivebrane and is available for worldvolume reduction in either type-II description. Each stated period is a full circumference.

Figure III.10.3 separates the two circles before we take any limit. The fifth scalar uses a transverse circle, whereas the later five-dimensional particle masses will use a longitudinal circle. At fixed string length the former has a shrinking geometric radius and a finite tension-coordinate period. These two facts can coexist because T_{M2} diverges.

The same reasoning suggests the next question: which other scales remain finite when gravity is removed?

III.10.4 Keeping a finite string scale

How can bulk gravitational interactions vanish while strings with finite tension remain on the fivebrane? We must distinguish three measurements: the strength of bulk gravity, the intrinsic string tension, and the separation-dependent tensor-string tension. A limit can remove the first without removing the second or the third. Keeping track of all three prevents a low-energy approximation from being mistaken for the entire decoupled theory.

First fix the gravitational units. With the full physical transverse circumference, dimensional reduction of the Einstein term in the common asymptotic length convention gives

$$\frac{1}{2\kappa_{10}^2} = \frac{2\pi R_{10}}{2\kappa_{11}^2}, \qquad 2\kappa_{11}^2 = (2\pi)^8 \ell_p^9. \tag{III.10.27}$$

Substituting $\ell_p^3 = g_s \ell_s^3$ and $R_{10} = g_s \ell_s$ yields

$$2\kappa_{10}^2 = \frac{(2\pi)^8 (g_s \ell_s^3)^3}{2\pi g_s \ell_s} = (2\pi)^7 g_s^2 \ell_s^8. \tag{III.10.28}$$

The factor 2π in the circumference is needed for the exact normalization. Both expressions have the correct length dimension: κ_{11}^2 has dimension nine, while κ_{10}^2 has dimension eight. Using a source radius measured in a differently rescaled metric without translating its units would spoil this check.

Let $E > 0$ be a finite fixed observation energy. A dimensionless measure of bulk gravitational interactions and a measure of string corrections at that energy are, respectively,

$$\kappa_{10}^2 E^8 = \frac{(2\pi)^7}{2} g_s^2 (E\ell_s)^8, \qquad \alpha' E^2 = (E\ell_s)^2. \tag{III.10.29}$$

Vanishing of the first quantity suppresses this bulk gravitational parameter. Vanishing of the second sends the intrinsic string scale above the observation energy. These conditions constrain different combinations of g_s and ℓ_s. The finite-string-scale fivebrane limit keeps ℓ_s fixed while sending g_s to zero. The assertion that an autonomous worldvolume sector survives is a physical premise about the NS5 system, beyond the displayed gravitational estimate.

To distinguish paths precisely, introduce a positive parameter $\epsilon \to 0^+$ and fixed positive prefactors g_0, ℓ_0, L_0:

$$g_s = g_0 \epsilon^a, \qquad \ell_s = \ell_0 \epsilon^b, \qquad L = L_0 \epsilon^c. \tag{III.10.30}$$

The powers of ϵ follow by substitution into the already derived formulas. For the intrinsic length and gravitational scales,

$$\alpha' = \ell_0^2 \epsilon^{2b}, \qquad 2\kappa_{10}^2 = (2\pi)^7 g_0^2 \ell_0^8 \epsilon^{2a+8b}. \tag{III.10.31}$$

For the intrinsic string tension and observation scale,

$$T_{\rm F1} = \frac{\epsilon^{-2b}}{2\pi\ell_0^2}, \qquad E\ell_s = E\ell_0\epsilon^b. \tag{III.10.32}$$

Finally, the transverse-circle radius and stretched-string tension give

$$R_{10} = g_0\ell_0\epsilon^{a+b}, \qquad T_{\rm string} = \frac{L_0}{(2\pi)^2 g_0\ell_0^3}\epsilon^{c-a-3b}. \tag{III.10.33}$$

These are six different quantities. In the fixed order $(\alpha', 2\kappa_{10}^2, T_{\rm F1}, E\ell_s, R_{10}, T_{\rm string})$, their exponents are

$$\big(2b,\ 2a+8b,\ -2b,\ b,\ a+b,\ c-a-3b\big). \tag{III.10.34}$$

A positive exponent means the corresponding quantity vanishes, a negative exponent means it diverges, and zero means its fixed prefactor survives. This reading must be attached to the quantity: a diverging tension means a disappearing low-energy excitation, whereas a vanishing Newton coefficient suppresses gravitational interactions.

Keeping the tensor-string tension finite and nonzero fixes a relation between the path exponents,

$$c = a + 3b, \qquad T_{\rm string} = \frac{L_0}{(2\pi)^2 g_0\ell_0^3}. \tag{III.10.35}$$

It is the scaled separation, rather than the unscaled coordinate L, that measures a finite tensor-branch tension. Sending the branes close together in bulk coordinates can therefore leave a nonzero physical worldvolume scale.

On the finite-string-scale path choose $a > 0$, $b = 0$ and $c = a$. Equations (III.10.31)–(III.10.33) then give

$$\begin{aligned} \kappa_{10}^2 E^8 \longrightarrow 0, \qquad \alpha' = \ell_0^2, \qquad T_{\rm F1} = \frac{1}{2\pi\ell_0^2}, \\ R_{10} \longrightarrow 0, \qquad T_{\rm string} = \frac{L_0}{(2\pi)^2 g_0\ell_0^3}. \end{aligned} \tag{III.10.36}$$

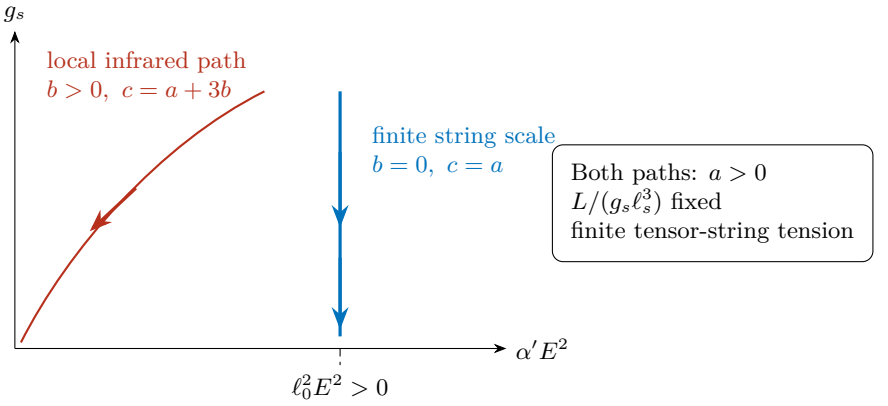
The fivebrane theory that retains an intrinsic string scale in this limit is called little-string theory. Its existence and decoupling are cited physical inputs here. Bulk massive string excitations still have finite string-scale masses when ℓ_s is fixed. They were not sent to infinite mass by reducing g_s; the physical decoupling statement concerns their coupling to the retained sector.

An isolated IIA brane has its free tensor theory far below the surviving string scale, and the IIB description has its infrared vector theory. The full finite-scale theory contains additional degrees of freedom. In particular the little-string tension $T_{\rm F1}$ does not equal every separation-dependent tension $T_{\rm string}$. The latter can vary with the tensor-branch position while the former fixes the intrinsic scale.

There is also a further local infrared path. Choose $a > 0$, $b > 0$ and $c = a + 3b$. Now

$$\begin{aligned} \kappa_{10}^2 E^8 \longrightarrow 0, \qquad E\ell_s \longrightarrow 0, \qquad T_{\rm F1} \longrightarrow \infty, \\ T_{\rm string} = \frac{L_0}{(2\pi)^2 g_0\ell_0^3}. \end{aligned} \tag{III.10.37}$$

This path removes the intrinsic string scale from observations at fixed E, while retaining a chosen finite tensor-string tension. It is a scale separation appropriate to the sourced low-energy description on the branch. It does not produce a nonabelian $(2,0)$ Lagrangian. For IIB, the $(1,1)$ gauge theory is an effective infrared description whose interaction scale depends on ℓ_s. Removing ℓ_s at fixed energy need not leave nonzero interactions. No universal interacting IIB local limit is implied.



Arrows denote $\epsilon \to 0^+$. Endpoints on $g_s = 0$ are limits; the diagram does not establish existence of a decoupled interacting theory.

Figure III.10.4: Two paths with vanishing bulk coupling at a fixed observation energy. The vertical path keeps $\alpha' E^2$ positive and finite; the curved path sends it to zero as well. In both cases the separation is scaled so that $c = a + 3b$ and the tensor-string tension stays finite. The axes show parameters, not a phase diagram or a proof of factorization.

For an explicit calculation use the same nonunit prefactors as before, $g_0 = 3/5$, $\ell_0 = 2$, $L_0 = 7/3$. The finite-string-scale choice $(a,b,c) = (2,0,2)$ gives, in the order of (III.10.34),

$$(2\cdot 0,\ 2\cdot 2 + 8\cdot 0,\ -2\cdot 0,\ 0,\ 2+0,\ 2-2-3\cdot 0) = (0,4,0,0,2,0). \tag{III.10.38}$$

The local infrared choice $(a,b,c) = (1,1,4)$ instead gives

$$(2,\ 2+8,\ -2,\ 1,\ 1+1,\ 4-1-3) = (2,10,-2,1,2,0). \tag{III.10.39}$$

Both retain the same tensor tension, but only the second sends T_{F1} to infinity. The actual prefactors provide a separate normalization check:

$$\begin{aligned} \frac{2\kappa_{10}^2}{(2\pi)^7\epsilon^{2a+8b}} &= \left(\frac{3}{5}\right)^2 2^8 = \frac{9}{25}\,256 = \frac{2304}{25}, \\ \frac{2\pi T_{\mathrm{F1}}}{\epsilon^{-2b}} &= \frac{1}{2^2} = \frac{1}{4}, \qquad (2\pi)^2 T_{\mathrm{string}} = \frac{35}{72}. \end{aligned} \tag{III.10.40}$$

The path powers alone cannot recover these prefactors. Conversely, checking the prefactors at one finite ϵ cannot establish an asymptotic limit without the powers.

Several boundary choices reveal what the conditions do. If $a = b = 0$, the gravitational coefficient is constant; there is no parametric gravitational decoupling. If $b = 0$, $a > 0$ and $c = 0$, the unscaled separation gives $T_{\text{string}} \propto \epsilon^{-a}$, which diverges. If instead $c > a$ at $b = 0$, the tension vanishes. These last two paths reach different worldvolume scales despite both having $g_s \to 0$. Figure III.10.4 keeps the finite tension condition explicit precisely to exclude that ambiguity.

The bulk NS5 throat of Volume II, Chapter 10 supplies a different kind of control: a small-curvature and weak-local-dilaton region for selected supergravity calculations. Such a region is not a definition of the entire worldvolume theory. A vanishing Newton coefficient also does not prove Hilbert-space factorization, the existence of a proposed state, or the survival of a particular interacting amplitude. The next section probes the finite intrinsic scale through masses after circle reduction, keeping these physical premises separate from the algebra.

III.10.5 A circle along the fivebrane

How does a string on a six-dimensional fivebrane produce a particle after compactification? Compactify the worldvolume direction x^5 on a physical circle of radius $R_\parallel > 0$, with periodic fermion spin structure. We will compare two separate pure sectors from the start. In the first, an existing string wraps the circle statically, with no additional excitation energy. In the second, a pure KK mode descends from a massless six-dimensional field and has zero momentum in the noncompact spatial directions. These conditions are needed for the masses below; they do not describe a state simultaneously carrying winding and momentum.

The circle is longitudinal because it lies within 012345:

$$x^5 \sim x^5 + 2\pi R_\parallel. \tag{III.10.41}$$

It is distinct from the transverse x^{10} circle in Figure III.10.3. Periodic spin structure allows the six-dimensional supersymmetry generators to have constant zero modes around x^5. Antiperiodic fermions would change this reduction and cannot be included under the same supersymmetric assumptions.

For a pure static string of tension T and winding $w \in \mathbb{Z}$, the wrapped length is $2\pi|w|R_\parallel$. Its rest energy follows by integrating the tension:

$$M_w = \int_0^{2\pi|w|R_\parallel} T\, ds = 2\pi|w|R_\parallel T. \tag{III.10.42}$$

This uses an existing purely wrapped configuration. Oscillator excitations, waves, other charges or additional kinetic energy would change its energy. Reversing w reverses orientation but leaves the positive rest mass unchanged. When $T = T_{\text{F1}}$, the intrinsic little-string winding mass is

$$M_w^{\text{little}} = 2\pi|w|R_\parallel \frac{1}{2\pi\alpha'} = \frac{|w|R_\parallel}{\alpha'}. \tag{III.10.43}$$

The full circumference is what removes the 2π in the fundamental string tension. A formula $|w|R_\parallel T$ would miss this factor.

For the separate KK sector, periodicity quantizes the circle momentum. A massless six-dimensional parent has the Fourier dependence

$$\phi(x, x^5) = \phi_n(x) e^{inx^5/R_\parallel}, \qquad p_5 = \frac{n}{R_\parallel}, \qquad n \in \mathbb{Z}. \tag{III.10.44}$$

Here x contains the five noncompact spacetime coordinates. For that massless parent, its six-dimensional dispersion relation becomes

$$E^2 - \boldsymbol{p}^2 = p_5^2 = \frac{n^2}{R_\parallel^2}, \qquad M_n^{\mathrm{KK}} = \frac{|n|}{R_\parallel}. \tag{III.10.45}$$

At $\boldsymbol{p} = 0$, the energy is the five-dimensional rest mass shown on the right. Nonzero noncompact momentum increases E rather than the invariant rest mass M_n^{KK}. The parent being massless is essential. Merely assigning an integer momentum to an existing state does not remove its six-dimensional rest mass.

For comparison, a free six-dimensional parent of mass m_0 obeys

$$E^2 - \boldsymbol{p}^2 = m_0^2 + \frac{n^2}{R_\parallel^2}, \qquad M_5^2 = m_0^2 + \frac{n^2}{R_\parallel^2}. \tag{III.10.46}$$

The choice $m_0 = 1$, $n = 2$, $R_\parallel = 3/2$ gives

$$M_5 = \sqrt{1 + \left(\frac{2}{3/2}\right)^2} = \sqrt{1 + \frac{16}{9}} = \frac{5}{3}, \qquad \frac{|n|}{R_\parallel} = \frac{4}{3}. \tag{III.10.47}$$

The difference is the retained parent mass. This free-particle comparison introduces no joint winding-and-momentum dispersion relation for little strings.

Longitudinal T-duality relates the IIA and IIB NS5 descriptions on these circles. In the inherited physical units its radius and asymptotic-coupling relations are

$$R'_\parallel = \frac{\alpha'}{R_\parallel}, \qquad g'_s = \frac{g_s \ell_s}{R_\parallel}. \tag{III.10.48}$$

The fivebrane remains wrapped on the longitudinal circle. This is not the transverse NS5/KK-monopole transformation, which has different geometry and isometry requirements. The physical identification of the worldvolume sectors under longitudinal T-duality is sourced; inverting a radius alone cannot establish it.

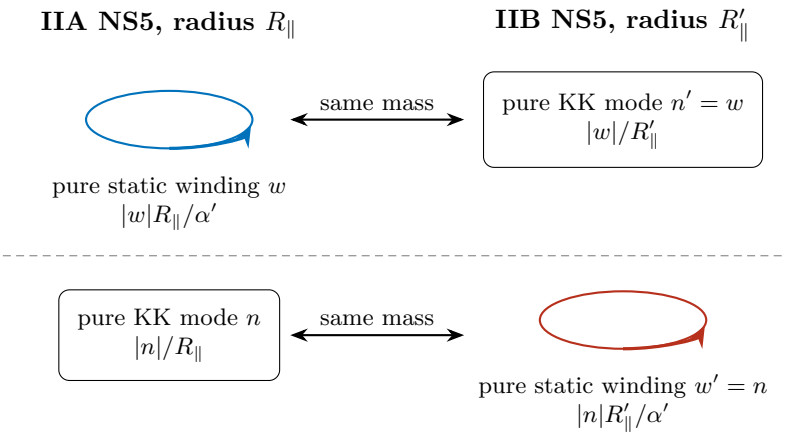
Conditional on that identification, the pure winding sector is mapped to a pure massless-parent momentum sector in the dual description. Its mass agrees because

$$\frac{|w| R_\parallel}{\alpha'} = \frac{|w|}{R'_\parallel}. \tag{III.10.49}$$

Separately, original KK momentum is mapped to pure winding in the dual description:

$$\frac{|n|}{R_\parallel} = \frac{|n| R'_\parallel}{\alpha'}. \tag{III.10.50}$$

Each equality compares the same mass in two descriptions of one pure sector. Adding the two entries would assert information about a different state. Neither the existence of such a joint state nor its interactions have been derived here.



$R'_\parallel = \alpha'/R_\parallel$. Each row is a separate pure sector.
Wrapped strings have no extra excitation; KK parents are massless, with zero noncompact momentum. Neither circle is the transverse x^{10} circle.

Figure III.10.5: Two separate pure-sector identifications under longitudinal IIA/IIB T-duality. The upper row maps a statically wound little string with no extra excitation into pure KK momentum of a massless parent; the lower row makes the reverse comparison for the other original sector. The circles lie along x^5 within the NS5. No vertex or formula combines the rows into a joint state.

The nonunit example makes all four masses explicit. Use $\ell_s = 2$, $R_\parallel = 3/2$, winding $w = -3$ in the pure winding sector and $n = 2$ in the separate massless-parent KK sector, at zero noncompact momentum. The dual radius is

$$\alpha' = 4, \qquad R'_\parallel = \frac{4}{3/2} = \frac{8}{3}. \tag{III.10.51}$$

The two original masses are

$$M_w^{\text{little}} = \frac{3(3/2)}{4} = \frac{9}{8}, \qquad M_n^{\text{KK}} = \frac{2}{3/2} = \frac{4}{3}. \tag{III.10.52}$$

In the dual description, the original winding gives momentum $n' = w$, and the original momentum gives winding $w' = n$. Therefore

$$M_{n'=w}^{\text{KK}} = \frac{3}{8/3} = \frac{9}{8}, \qquad M_{w'=n}^{\text{little}} = \frac{2(8/3)}{4} = \frac{4}{3}. \tag{III.10.53}$$

The four masses in order are $9/8, 4/3, 9/8, 4/3$. The minus sign of the original winding is visible as an orientation label, but absolute values enter its mass. Figure III.10.5 keeps the two calculations on different rows for this reason.

There is another wrapped string on a separated IIA tensor branch. It has $T = T_{\text{string}}$, rather than the intrinsic T_{F1}. For a pure static once-wrapped configuration with no extra excitation energy,

$$M_{\text{tensor}} = 2\pi R_{\|} T_{\text{string}}, \qquad 2\pi M_{\text{tensor}} = R_{\|}\big[(2\pi)^2 T_{\text{string}}\big]. \tag{III.10.54}$$

Using the tension from (III.10.21),

$$2\pi M_{\text{tensor}} = \frac{3}{2}\frac{35}{72} = \frac{105}{144} = \frac{35}{48}. \tag{III.10.55}$$

Thus the reduced tensor wrapping mass is $35/48$, while the physical mass is $35/(96\pi)$ in the chosen unit. Replacing the tensor tension by $1/(2\pi\alpha')$ would change the object being wrapped. A mass depending on separation and a mass set by the intrinsic string scale answer different questions.

The finite-radius condition also matters for the decoupling limit. At fixed finite $R_{\|}$ and fixed ℓ_s, taking $g_s \to 0$ gives $g_s' \to 0$. Thus the same bulk weak-coupling path exists in both circle descriptions. A simultaneous scaling $R_{\|} = R_0\epsilon^d$ would instead give

$$R_{\|}' = \frac{\ell_0^2}{R_0}\epsilon^{2b-d}, \qquad g_s' = \frac{g_0\ell_0}{R_0}\epsilon^{a+b-d}. \tag{III.10.56}$$

For example, along the finite-string-scale path with $b = 0$, a radius shrinking as ϵ^d requires $a - d > 0$ for dual coupling to vanish. If $d = a$, the dual coupling stays finite; if $d > a$, it diverges. These are algebraic checks of a changed path, rather than an extension of the fixed-radius claim. The dual radius and the momentum and winding scales must be rechecked at the same time.

At fixed tension, sending $R_{\|} \to \infty$ makes every nonzero pure winding mass diverge while the KK gap tends to zero. Setting $w = 0$ or $n = 0$ gives zero for the corresponding pure-sector contribution, but does not create a physical massless particle for every formal label. State existence, protection and global gauge group information remain physical questions. XVI uses circle reduction in its interacting $(2, 0)$ and five-dimensional applications; the free masses derived here supply units and checks, rather than that interacting construction.

III.10.6 Beyond the local description

The preceding calculations distinguish two meanings of a theory on a fivebrane. Its infrared field theory describes the light local fields on the chosen branch. Its finite-string-scale limit can retain additional string excitations after bulk gravity decouples. The second description is the little-string theory in the cited NS5 construction. Its existence is a physical input; the six scale exponents show which energies that input allows us to retain.

The presence of strings, even tensionless strings, is not by itself a test of nonlocality. The local $(2, 0)$ theory also has stringlike excitations whose tensions vanish at its singular point. In the little-string discussion, longitudinal T-duality supplies the cited reason that one ordinary local-QFT spacetime description is insufficient: two different worldvolume

circle radii describe the same physics with momentum and winding exchanged. The mass matches above illustrate that identification; they do not prove the complete duality or determine the stress tensor and interacting spectrum.

As a comparison, the two paths in Figure III.10.4 have identical finite tensor-string tension and the same free infrared multiplet assignment. One retains finite intrinsic little-string tension, while the other sends it above the fixed observation energy. The equality of their free polarization counts cannot distinguish these theories. The finite-scale spectrum and its physical identifications are additional information. A harmonic function or a weak-coupling region in a bulk metric cannot supply that information on its own.

The useful continuation to suspended branes is correspondingly specific. X.4 uses the local D6 interval and $8\pi^2$ tension-coupling product, with its own additional matter and anomaly analysis. Chapter 5 of that volume uses a local massless-IIA M-circle frame with no local D8/O8/M9 objects. The interacting $(2,0)$ construction belongs to XVI, beginning with its Chapter 1 and continuing to compactification applications. The full little-string discussion belongs to the planned treatment of little string theories across construction engines and the roadmap beyond it. None of these continuations is fixed by the four free calculations in this chapter.

III.10.7 Exercises

The first four exercises have bounded numerical or representation answers. The fifth asks for written physical reasoning. The public companion gives the exact JSON submission structure for each bounded task, including which entries are integers and which are rational strings. A reduced quantity removes only the stated powers of 2π; it never changes the physical normalization.

1. **Free multiplets (II10-E1).** For one flat isolated positively oriented NS5 along 012345, with no extra projection or background deformation, use the sourced IIA tensor and IIB vector identifications. For each type give the real scalar, self-dual tensor and vector polarization counts, the total bosonic and fermionic on-shell counts, and the two real supercharge counts (Q_+, Q_-). Derive the tensor count using the complementary Hodge pairs. Explain in writing why three separated parallel branes multiply the species but not the sixteen common spacetime supercharges. The bounded submission concerns the single brane inventories only.

2. **Stretched objects and the interval (II10-E2).** Take $g_s = 3/5$, $\ell_s = 2$ and $L = 7/3$ in the common asymptotic length frame. For the existing straight IIA D2 boundary string and the separate IIB D1 boundary particle, compute $(2\pi)^2 T_{\mathrm{string}}$ and $2\pi M_{\mathrm{particle}}$. Give their mass dimensions, the g_s power of the tension at fixed L, ℓ_s, the exponent c in $L \propto g_s^c$ needed for a finite nonzero tension at fixed ℓ_s, and the formal coincident reduced tension. In the separate flat constant-zero-mode D6 interval model with $g_7^2 = 2(2\pi)^4 g_s \ell_s^3$ and $g_6^{-2} = L/g_7^2$, compute $T_{\mathrm{string}} g_6^2/\pi^2$. State in writing why the formal zero at coincidence and the leading background cancellation do not prove singular-core control or state existence.

3. **Two scale paths (II10-E3).** At fixed finite E, set $g_s = (3/5)\epsilon^a$, $\ell_s = 2\epsilon^b$ and $L = (7/3)\epsilon^c$, with $\epsilon \to 0^+$. For $(a, b, c) = (2, 0, 2)$ and $(1, 1, 4)$ give the six exponents in the exact order $(\alpha', 2\kappa_{10}^2, T_{\mathrm{F1}}, E\ell_s, R_{10}, T_{\mathrm{string}})$. Also give the two common prefactors $[2\kappa_{10}^2/(2\pi)^7]/\epsilon^{2a+8b}$ and $[2\pi T_{\mathrm{F1}}]/\epsilon^{-2b}$. Explain in writing which scale survives on each path and why the vanishing Newton parameter is not a factorization theorem.

4. **Separate pure sectors on a circle (II10-E4).** Use a periodic-spin longitudinal x^5 circle with $R_\parallel = 3/2$ and $\ell_s = 2$. Assume an existing pure statically wrapped little string with $w = -3$ and no extra excitation energy. In a separate sector take KK momentum $n = 2$ from a massless six-dimensional parent at zero noncompact momentum. Compute $R'_\parallel$, the original pure winding mass, the original KK mass, and their respective dual KK and winding masses. These are four separate entries, not contributions to a joint-state mass. Then wrap an existing pure static tensor string once, with no extra excitation and $(2\pi)^2 T_{\mathrm{string}} = 35/72$, and give $2\pi M_{\mathrm{tensor}}$. All six bounded answers are rational strings. As a written diagnostic, replace the massless parent by a free parent with $m_0 = 1$ and compare its rest mass with the original KK entry.

5. **Physical premises (II10-E5, written).** Explain which physical premises the four calculations do not establish. Address the IIA $(2, 0)$ and IIB $(1, 1)$ infrared assignments; the fifth IIA scalar and its finite tension-coordinate period; separation-dependent tensionless strings versus intrinsic finite-tension little strings; gravity decoupling versus eliminating α' at fixed energy; and why a dilaton or curvature window does not define the entire theory. Include the periodic spin structure and the failure of an automatic simple M lift through a D8/Romans-mass region. Route the interacting $(2, 0)$ construction and full little-string dynamics to their later homes. In particular, explain why equal $8 + 8$ free counts do not identify the finite-scale theories. This written task is not certified by a numerical grader.

III.10.8 Take-home message

The field living on a brane determines what sort of charged object we should look for. The IIA tensor couples to a boundary string of a stretched membrane; the IIB vector couples to the particle boundary of a stretched D1. Once those physical objects are identified, their tensions, masses and scale dependence follow in one common frame. The finite tension-coordinate period of the transverse circle and the winding masses of a longitudinal circle are two different consequences of using full physical circumferences.

Removing gravity and removing the string scale are separate operations. A finite-string-scale NS5 limit can retain little strings, whereas a further infrared path sends that intrinsic tension to infinity at fixed observation energy. The distinction is visible in circle masses, provided pure static winding and massless-parent KK sectors are kept separate. The existence of the retained theory, its protected states and its interacting dynamics remain physical inputs beyond these conditional calculations.

Status and sources

Scope and conventions. The conventions use the six-dimensional multiplets of Volume I and the dimensional-reduction, trace, membrane, circle and supergravity normalizations stated above. The local notation distinguishes R_{10} from $R_{\|}$, physical tensions from reduced exercise quantities, and worldvolume potentials from bulk potentials. The IIA/M lift and IIB S-duality are nonperturbative physical premises.

§10.2. The free IIA tensor and IIB vector identifications are cited physical premises. Strominger (1995), exact arXiv v1, physical PDF pp. 2–5, equations (1)–(8) and the longitudinal T-duality paragraph, supplies the endpoint and tensor/vector identifications. Its $(0,2)$ chirality naming is translated to the book's $(2,0)$ convention without importing a projector sign. Seiberg (1997), exact v2, physical PDF pp. 3–4, §2.1 and equations (2.1)–(2.3), supplies the infrared distinction and periodic fifth scalar. The conditional free counting is a mathematical calculation [MATH], including the explicit transverse Hodge decomposition. Fermionic representation content is a multiplet premise; counting is not a derivation of the brane assignment. For $N > 1$, a total count alone does not fix the individual species counts.

§10.3. The conditional tension, interval product and period computations assume the stretched states and inherited units. Strominger v1, physical PDF pp. 3–5, equations (6)–(8), distinguishes leading-order supersymmetry from the presumed corrected BPS configuration. The singular-core completion is not derived here. Its stronger global-group and moduli assertions on physical PDF p. 6 are excluded from this free-branch use. Myers (1999), exact v2, physical PDF p. 2, equations (1)–(3), and p. 7, equations (21)–(23), supplies the leading DBI domain and physical D-brane tension. Its shifted dilaton and rescaled RR normalization are source-local; the physical tension is not multiplied by a second asymptotic g_s^{-1}. The local interval match uses the stated dimensional-reduction and half-trace conventions, not a warped massive-IIA reduction.

§10.4. The conditional Newton normalization and six exact power laws are mathematical calculations [MATH]. They do not establish factorization or an interacting limit. Witten (1995), exact v2, physical PDF pp. 11–12, §2.3, equations (2.9)–(2.14), supplies the frame comparison. The radius prose on physical p. 11 conflicts with the scaling of equations (2.13)–(2.14) on p. 12. We use the equations with an explicit frame translation, not the conflicting sentence. The source-metric $r \sim g_s^{2/3}$ is not directly identified with physical $R_{10} = g_s \ell_s$. Lu (1997), exact v1, physical PDF pp. 3–4, equations (1.5)–(1.6) and the subsequent minimum-charge discussion, cross-checks the membrane and Newton units under its charge-quantization premises. It does not independently prove M-theory or minimal-state existence. For little-string existence, decoupling and nonlocality at finite scale, Seiberg v2, physical PDF pp. 2–4, introduction and §2.1, is the physical source. Its schematic M_s, scalar and gauge-coupling units are not used as exact book normalization constants.

§10.5. The separate pure static winding and massless-parent KK kinematics and the rational example are mathematical calculations [MATH]. The pure static/no-extra-excitation condition and massless six-dimensional parent/zero noncompact momentum

condition are essential. The massive-parent diagnostic gives 5/3, whereas the massless-parent KK entry gives 4/3; the reduced tensor wrapping mass is 35/48. These are not joint-state energies. The physical longitudinal IIA/IIB sector identification uses Seiberg v2, physical PDF pp. 4–5, §2.1, equation (2.4) and its wrapped-state paragraph, and Strominger v1, physical PDF p. 5, longitudinal T-duality paragraph. Fixed finite radius is part of the limit; scaling the radius requires the displayed dual-coupling and hierarchy recheck.

§10.6 and limits. A weak-dilaton/small-curvature region describes selected bulk observables; it does not define the full theory. The lift and supergravity statements retain their local domains. D8/Romans-mass extensions and the interacting $(2, 0)$ and little-string constructions remain outside this chapter.

Calculations and exercises. Exercises 1–4 cover free field counts, nonunit stretched tensions and the interval product, six scale exponents with nonunit prefactors, and six separate circle quantities. Exercise 5 asks for written interpretation. The calculations require the stated physical premises. The bibliography records the exact preprint editions used. The published Seiberg title has a metadata variant; the title below follows the v2 PDF. No claim depends on silently substituting a later edition.

References

Lu, J. X. (1997). *Remarks on M-Theory Coupling Constants and M-Brane Tension Quantizations*. Primary PDF edition v1. arXiv: `hep-th/9711014`.

Myers, R. C. (1999). *Dielectric-Branes*. Primary PDF edition v2. arXiv: `hep-th/9910053`.

Seiberg, N. (1997). *New Theories in Six Dimensions and Matrix Description of M-theory on T^5 and $T^5/\mathbb{Z}_2$*. Primary PDF edition v2, 3 June 1997; title follows the PDF title page. arXiv: `hep-th/9705221`.

Strominger, A. (1995). *Open P-Branes*. Primary PDF edition v1, 10 December 1995. arXiv: `hep-th/9512059`.

Witten, E. (1995). *String Theory Dynamics in Various Dimensions*. Primary PDF edition v2. arXiv: `hep-th/9503124`.